CHARACTERIZING THE NUCLEAR LOCALIZATION OF ADENOMATOUS POLYPOSIS COLI PROTEIN

By

©2008
Jamie R.Z. Cunningham

B.S., University of Kansas, 2002

Submitted to the Department of Molecular Biosciences and the
Faculty of the Graduate School of the University of Kansas
In partial fulfillment of the requirements for the degree of
Doctor of Philosophy

_____
Chairperson – Kristi Neufeld

_____
Committee members: Kathy Suprenant

_____
Audrey Lamb

_____
Steve Benedict

_____
Jeff Staudinger

Date defended: 4/25/2008

The Dissertation Committee for Jamie Cunningham certifies
that this is the approved version of the following dissertation:

CHARACTERIZING THE NUCLEAR LOCALIZATION OF ADENOMATOUS POLYPOSIS COLI PROTEIN

Committee:

_____
Chairperson – Kristi Neufeld

_____
Kathy Suprenant

_____
Audrey Lamb

_____
Steve Benedict

_____
Jeff Staudinger

Date approved: 4/25/2008

Abstract

Mutation of tumor suppressor protein Adenomatous Polyposis Coli (APC) has been shown to be an early, if not rate limiting step in the progression of both hereditary and sporadic colorectal cancers. The observation that APC can shuttle in and out of the nucleus, and the identification of two highly conserved nuclear localization sequences (NLSs) strongly support a role for APC in the nuclear compartment. Little is currently known about the function(s) of nuclear APC or how nuclear functions contribute to tumor suppression.

To further evaluate the role of APC in the nucleus we generated the APC mNLS mouse. The APC mNLS mice carry amino acid changes in both APC NLSs designed to inhibit interaction with importin-α without disrupting APC's other cellular functions. Generation of the mNLS mice is ongoing, with fully congenic animals expected in early 2009. In the interim, I have conducted a preliminary analysis of the phenotype of the non-congenic APC mNLS animals. Evaluation of the subcellular localization of APC in the intestinal epithelium of the APC mNLS animals revealed that APC retains its ability to shuttle in and out of the nucleus, even in the homozygous mutant mice. While a mild defect in nuclear import could be detected in the differentiated cells at the colonic luminal surface, the more undifferentiated cells in the lower regions of the intestinal crypts displayed a normal localization of APC. The APC mNLS$^{-/-}$ mice were viable and did not display intestinal polyposis. However, subtle differences were detected between mice that carry the APC mNLS mutations and their wild type (WT) littermates. These

differences included higher levels of β-catenin in the intestinal epithelium of the APC mNLS mutant mice and an increased incidence of lymphoid nodules compared to their littermates with WT APC.

To further evaluate the need for APC in the nuclear compartment, I exposed cultured cells expressing WT APC or APC with mutant NLSs to ultraviolet (UV) light. UV-irradiated cells displayed a nuclear accumulation of both the mutant and WT forms of APC with implications for an importin-α independent mechanism of nuclear import. Further characterization of the nuclear accumulation of APC revealed that nuclear translocation was transient and cell cycle dependent. Finally, the nuclear localization of APC could be partially suppressed using inhibitors of G_2/M checkpoint kinases.

Acknowledgements

I would like to thank my husband, Loren Cunningham, for supporting me and for putting up with me while I was writing this dissertation. I would also like to thank my parents, Steven and Claire Zerbe, for their endless patience and encouragement. They instilled in me the strong belief that I am capable of anything. Without that kind of confidence an achievement like this would not have been possible.

I would like to express my tremendous gratitude to my mentor Dr Kristi Neufeld. I am extremely fortunate to have had the opportunity to work in her lab. I would also like to acknowledge the members of my graduate committee, Dr. Kathy Suprenant, Dr. Audrey Lamb, Dr. Steve Benedict and Dr. Jeffery Staudinger for all the advice and assistance they have given me. I want to thank Dr. David Moore and Dr. Yoshiaki Azuma for helping me collect the best possible data.

I want to thank all of my lab mates for the help they have given me and for discussions we have had. They have made the lab a great place to work every day and I always knew that someone would have my back if I accidentally set my bench on fire. I would also like to specifically thank Preston Alltizer for figuring out how to use the cryotome and for being a super-undergrad. His assistance on this project went above and beyond the call of duty and the data presented here is better because of it.

Table of Contents

List of Figures

List of Tables

CHAPTER 1

INTRODUCTION: APC AND THE INTESTINAL EPITHELIUM

The Architecture of the Intestine

The alimentary canal is the tube that extends through the body from the mouth to the anus, the lumen of which is considered open to the external environment (1). The function of the alimentary canal is to facilitate the physical and chemical breakdown of food and absorb nutrients into the body. The small intestine and the large intestine, or colon, make up the distal region of the alimentary canal. Absorption of nutrients takes place primarily in the small intestine while the colon reabsorbs valuable water and electrolytes from the undigested material and waste products before they are expelled from the body (1).

The structural organization of tissues making up the alimentary canal is largely conserved along its entire length and can be classified into four distinct layers (1). The innermost layer that lines the lumen is called the *mucosa* and consists of the epithelium and underlying connective tissue, the lamina propria. Below the mucosa is the dense irregular connective tissue of the *submucosa* followed by two layers of smooth muscle known as the *muscularis externa*. The final layer is a membrane of simple squamous epithelium and associated connective tissue that marks the boundary between the gastrointestinal tract and the organs of the body (1). The primary focus of this project is on the structure and maintenance of the epithelial layer of the mucosa. Over 80% of life-threatening human cancers are carcinomas,

which, by definition, arise from cells of epithelial origin (2). The epithelial layer lining the lumen of the intestine is a highly proliferative tissue that is continuously exposed to physical, chemical and pathogenic stresses. When considering these factors it is no surprise that the intestinal epithelium is one of the most common sites for cancer development in the human body (3).

The intestinal epithelium and its normal functions

The mucosal layer of the intestine serves three main functions. First, the mucosa forms a protective barrier between the external environment of the lumen and the organs and tissues of the body. Second, the epithelial surface is where the absorption of nutrients, water and electrolytes from digested food occurs. Finally, a great deal of secretion takes place along the length of the intestine. Specialized cells within the epithelium secrete antibacterial enzymes, hormones and mucus important for the continued maintenance and function of the intestine (1). The evidence of these functions is apparent in both the architecture of the mucosal layer and the cell types contained therein.

The mucosa of both the small intestine and the colon are lined with a single layer of columnar epithelial cells and contain numerous straight, tubular glands known as the *crypts of Lieberkühn* (1) (Figure 1.1A). These invaginations of the colonic epithelium are arranged in an orderly fashion and extend the full thickness of the mucosa. The crypts of the small intestine are slightly shallower than those found in the colon (Figure 1.1B). In addition the small intestinal mucosa also projects

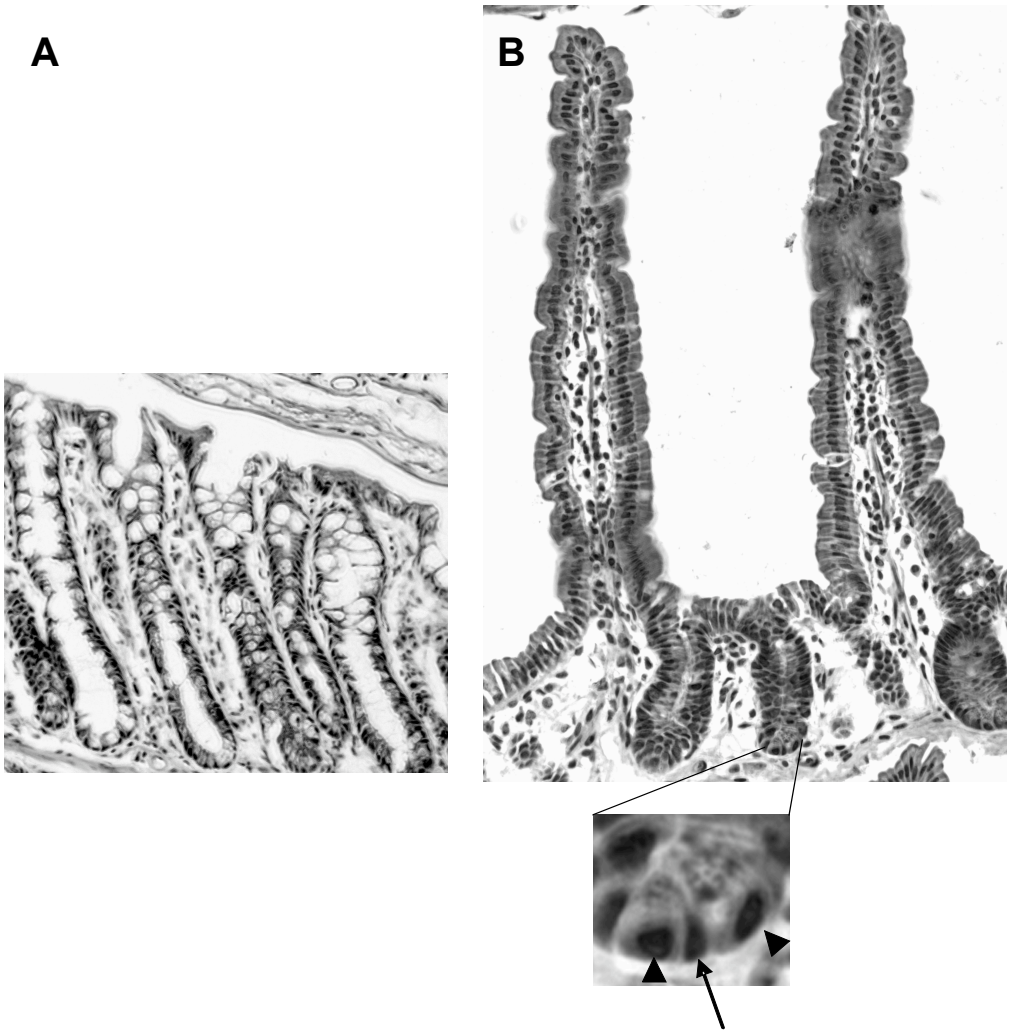

Figure 1.1
Longitudinal slices of frozen intestinal tissue. Tissue was stained with Hematoxylin and Eosin dyes to visualize the cells. Hematoxylin dye carries a net positive charge giving it a high affinity for nucleic acids. The nuclei therefore appear as dark ovals in the image above. Eosin carries a negative charge and shows a high affinity for the enzymes in the granules of the Paneth cells as well as a lesser affinity for proteins of the cytoplasm. (A) Crypts of Lieberkühn from the colon with vesicles of non-staining mucin in the goblet cells visible in the upper half of the crypts. (B) Crypt-villus structure from the small intestine. The inset from the base of the crypt shows the Paneth cells (arrow heads) two large oval nuclei with dark staining granules in the apical space above. Also visible is a Crypt Base Columnar cell (CBC), the wedge shaped nucleus between the two Paneth cells (arrow). The CBC cells are hypothesized to be the stem cells.

outward into the lumen to form villi. These villi greatly increase the surface area available for the absorption of nutrients.

There are five main cell types found in the intestinal epithelium; the enterocytes, goblet cells, paneth cells, enteroendocrine cells and microfold cells (Table1.1). The enterocytes are the absorptive cells. Because the main function of the intestine is the absorption of water, salts and nutrients, enterocytes are the primary cell type in the intestine. Goblet cells are each independent mucus secreting glands that function to lubricate the intestine and provide a protective barrier against pathogens (4). Goblet cells become increasingly necessary as more and more moisture is removed from the undigested material as it continues through the intestine. Therefore, while there are relatively few goblet cells in the small intestine, the ratio of goblet cells to enterocytes can approach 1:1 in the distal region of the colon (1). Paneth, enteroendocrine and microfold cells have specialized functions and are found in lower abundance in the intestine. Paneth cells are found primarily in the small intestine, though they can occasionally be seen in the colon. They reside at the base of the crypts of Lieberkühn and secrete antibacterial enzymes to stabilize the appropriate levels of bacterial flora in the gut (5). Enteroendocrine cells secrete peptide hormones that regulate secretion by the pancreas, gallbladder and stomach (6). Microfold cells, also known as M-cells are found associated with nodules of lymph tissue and facilitate the uptake of microorganisms for presentation to the immune system (7).

Table 1.1 The cell types of the intestinal epithelium.
Adapted from Ross, M. H., and Pawlina, W. (2005) *Histology: A text and atlas*, Lippincott Williams & Wilkins, Baltimore, MD

Cell type	Function	Location	Appearance
Enterocytes	Absorbtion of water and nutrients.	The primary cell type in the intestine. Found all along the crypt-villus structures.	Columnar epithelia. Apical surface is covered with microvilli
Goblet cells	Secretion of mucus for the protection and lubrication of the intestine	Interspersed with the enterocytes at an increasing ratio moving distally	Large apical surface filled with mucous. The nucleus and organells are in the narrow basal region. Goblet-shaped
Paneth cells	Secretion of antibacterial enzymes	Primarily in the small intestine at the base of the crypts	Oval base with a large nucleus. Apical portion is filled with refractile acidophilic granuals
Enteroendocrine cells	Secretion of peptide hormones	Interspersed throughout the intestine	Difficult to distinguish without special preperation of the tissue
Microfold cells	Endocytosis of antigens for presentation to the immune system	Associated with lymphoid nodules along the length of the intestine	Relativly flat with apical folds rather than microvilli

The entire epithelial layer of the intestine is in a constant cycle of cell death and renewal. Cells of the intestinal epithelium arise from adult stem cell progenitors. Although the exact number and location of the intestinal stem cells has been a source of controversy in the past (8), recent evidence from the Clevers lab (9) has demonstrated rather convincingly that there are a 4-6 stem cells at the base of each crypt of Lieberkühn. In the small intestine, the stem cells are interspersed amongst the paneth cells which also reside at the base of the crypt (9) (Figure 1.1B). These stem cells give rise to the precursors of all five cell types. These precursors, also known as transit amplifying cells, divide several times as they migrate upward along the walls of the crypts where they cease division and undergo differentiation. The differentiated cell types continue to migrate to the luminal surface of the colon or to the tops of the villi in the small intestine, then undergo apoptosis and are shed into the lumen. In the mouse, the cells of the intestinal epithelium are completely replaced in approximately a week's time (10). Tight control over this system is maintained through a complex coordination of external and internal cell signaling events (11). The processes of proliferation, migration, differentiation and apoptosis must be in perfect balance. The loss of control over any part of the system can result in the formation of tumors.

Cancer and the intestine

Colorectal cancer was responsible for an estimated 52,180 deaths in 2007 and accounts for almost 10% of all cancer deaths making it second only to lung cancer as

a leading cause of cancer related mortality in the United States (3). The lifetime risk of developing colorectal cancer for men and women is 1:17 and 1:19, respectively (3). Unlike a bacterial or viral infection that can be traced to a distinct external source, cancer is a disease in which an organism is overcome by rogue cells of its own body (2). Because cancer cells are unique to each host, there are, in essence, as many types of cancer as there are patients that develop the disease. There are attributes, however, that seem to be shared by a vast majority if not all cancers (12). These attributes, conferred through the mutation of regulatory proteins, allow the tumor cells to grow and invade the surrounding tissues. In a 2000 review, Weinberg and Hannan outlined six molecular, biochemical and cellular traits which they designated the "Hallmarks of Cancer" (12). This set of traits, outlined below, is currently the best biological descriptions of what constitutes cancer.

Cells forming a tumor must be able to produce their own proliferative signals and ignore or overcome inhibitory signals from the body. This allows for the abnormal growth of individual cells to create a tumor mass within an otherwise properly functioning tissue. With each cell division, the telomeres at the ends of the chromosomes are shortened; creating a built-in "fuse" that when finally exhausted causes either senescence or cell death (reviewed in 13). Therefore, the increased proliferation of dysplastic cells must eventually be accompanied by an immortalization of the cell, usually through an aberrant lengthening of the telomeres, as well as an insensitivity to intracellular and exogenous apoptotic signals. Any cell cluster is limited in its size by the ability of oxygen and nutrients to reach the

innermost cells. Cells become hypoxic and will begin to undergo necrosis if they are not within a fraction of a millimeter from a blood supply (2). Consequently tumor progression must be accompanied by the ability to stimulate capillary growth to supply the dysplastic cells with blood. A tumor that has obtained these attributes has the potential to grow very large but is still isolated within its tissue of origin and therefore considered benign. To be considered cancerous, the cells must be able to migrate outward from the site of the primary tumor, invading the surrounding tissues and metastasizing to distant sites in the body. With the acquisition of malignancy, the tumor has become a cancer.

A cell of the intestinal epithelium does not convert immediately from a normal, healthy cell to a carcinoma in one step. The development of a malignant carcinoma is a multi-step process that begins with an initial mutation in a vital area of the genome resulting in an abnormal or dysplastic cell. Through continued cell divisions and mutational events this cell's progeny must advance through various stages of polyposis beginning as an early benign adenoma and progressing to an invasive cancer by continuing to acquire genetic mutations that will confer the necessary attributes on the cells (2). The high number of mutations that must occur within a single population of cells to result in a carcinoma strongly supports the conclusion that there is a certain amount of genetic instability required for cancer development as well (14).

Because the colon is one of the more common sites of tumor development and the polyps are relatively accessible, colorectal cancer is currently one of the best

characterized forms of human cancer. In 1990 Fearon and Vogelstein published a review outlining the types of mutations typically seen in human intestinal polyps and the stage at which those mutations were most commonly observed, compiling a tentative time line of cancer development in the intestine. This and subsequence genetic models of colorectal tumorigenesis place the mutation of the *Adenomatous Polyposis Coli* (*APC*) gene as one of the initiating steps in the progression of colon cancer (11, 15). Though very little was known about the *APC* gene at the time, it was clear that understanding its function in the cell could be a valuable tool in both the detection of early benign tumors and the prevention of cancer development in the intestine.

Adenomatous Polyposis Coli

Adenomatous Polyposis Coli (APC) is a 312 kDa multifunctional protein that is expressed in a wide variety of epithelial tissues (16, 17). The loss of functional APC through inactivating mutations has been closely linked to carcinogenesis and led to the initial identification of the *APC* gene in the early 1990s by several labs searching for a genetic cause to hereditary colon cancer (17-19). The hereditary syndrome, Familial Adenomatous Polyposis (FAP), results from germline mutation of *APC*, and is characterized by the development of hundreds to thousands of polyps in the colon and rectum. Polyposis begins, on average, at 16 years of age in a person who has inherited a mutant copy of *APC,* and if left untreated the average age for the detection of a colorectal carcinoma in a FAP patient is 39 years (20). This disease,

while rather rare in the population, is a dominant, autosomal condition that is nearly 100% penetrant.

In addition to being the causative agent of a familial syndrome, sporadic loss of APC in somatic cells was identified in over 80% of human colon carcinomas (21). Furthermore, investigation into early adenomas found *APC* mutations in a majority of precancerous lesions (polyps) as well (22). It is now widely accepted that *APC* mutation is an initiating, and possibly rate-limiting, step in the development of most colon carcinomas.

Like a majority of tumor suppressor proteins, it appears that a single copy of *APC* is sufficient to prevent polyposis at the tissue level. This is supported by the observation that in both humans and in animal models a loss of both copies of *APC* is detected in nearly all tumors tested (21, 22). Cells that have lost both copies of *APC* initially develop benign polyps. These early adenomas, however, contain the potential to progress to malignant carcinomas, making our understanding of APC's function as a tumor suppressor vitally important in the pursuit of better methods of diagnosis and treatment for patients with colon cancer (15).

More than 700 different disease causing mutations of the *APC* gene have been described, nearly all of which cause a truncation of the protein product through frame shift mutations or point mutations leading to premature stop codons (23). These mutations take place, primarily, within the mutation cluster region of *APC* which lies in exon 15 between codons 1000 and 1600 (Figure 1.2). The most common disease-causing mutation of *APC* results in a protein truncation at amino acid 1309, closely

Figure 1.2
A scale diagram of APC exons (intron locations are indicated; however, the amount of sequence removed is not shown to scale). Exon 15 makes up over 75% of the 2843 amino acid APC protein and contains the APC "mutation cluster region" (indicated in red). The three most common human mutations associated with disease result in an alteration of amino acids 1309, 1061 or 1465 (indicated in blue).

followed by truncations at amino acids 1061 and 1465. Together, mutations at these three sites are responsible for approximately 33% of the recorded tumors (24). In both humans and in mouse models, the exact location of the APC truncation greatly affects the severity of the phenotype. For example patients who have truncating mutations between codons 1250 and 1330 typically develop over 5000 polyps, while patients with mutations beyond codon 1578 may develop fewer than 100 polyps and have an average age of onset that is 10-15 years later than patients with the more severe form of the disease (25). Different APC truncations are also associated with different extra-intestinal manifestations of the disease. For example 70% of all FAP patients develop dental abnormalities such as extra or missing teeth. Other common benign manifestations include epidermoid cysts, desmoid tumors and hamartomas of the pigmented retinal epithelium (25). This diversity of symptoms originally supported the belief that FAP was, in fact, several different syndromes. It is now known that characteristic forms of congenital hypertrophy of the retinal pigment epithelium (CHRPE), Gardner Syndrome, Turcot Syndrome and hereditary desmoid disease are all caused by different mutations resulting in various truncations of the APC protein, (reviewed in 23). The variation in phenotypes caused by different mutations of the *APC* gene supports the idea that APC has a multifunctional role in tumor suppression and makes the understanding of APC's various cellular roles all the more important.

APC protein structure

The functional domains of APC were originally estimated based on amino acid sequence (17, 19) and were later confirmed with *in vitro* biochemical methods and in cultured cells (26). The conventional APC protein contains 2843 amino acids and is approximately 312kDa (Figure 1.3). APC has 15 exons, the last of which encodes over 75% of the total protein (Figure 1.2). The structure and binding partners of the APC protein have been extensively reviewed (26, 27). Briefly, the extreme N-terminal portion of APC is made up of heptad repeats that have been predicted to form a coiled-coil domain and facilitate oligomerziation of the APC protein (17, 19). However, a function for APC as an oligomer has yet to be revealed. The N-terminal region also contains two nuclear export sequences (NES) which directly interact with Crm-1/Exportin and play a role in nuclear/cytoplasmic shuttling of the protein (28, 29). One of the primary motifs in the N-terminal region of the APC protein is the ARM or armadillo domain. This region, made up of seven copies of a 42 amino acid motif, is named because of similarity to a region of repeats in the protein β-catenin (armadillo in fruit flies) (30). The armadillo repeats have been shown to interact with a number of other protein partners including the B56α regulatory subunit of phosphatase 2a (PP2A) (31), APC-stimulated guanine nucleotide exchange factor (Asef) (32), and the Rac1 and Cdc42 effector protein IQGAP1 (33). The APC Arm domain has also been shown to interact with kinesin superfamily-associatied protein 3A (KAP3A) in both yeast-two hybrid analysis and by co-immunoprecipitation from cell lysate (34). Staining of full length APC and

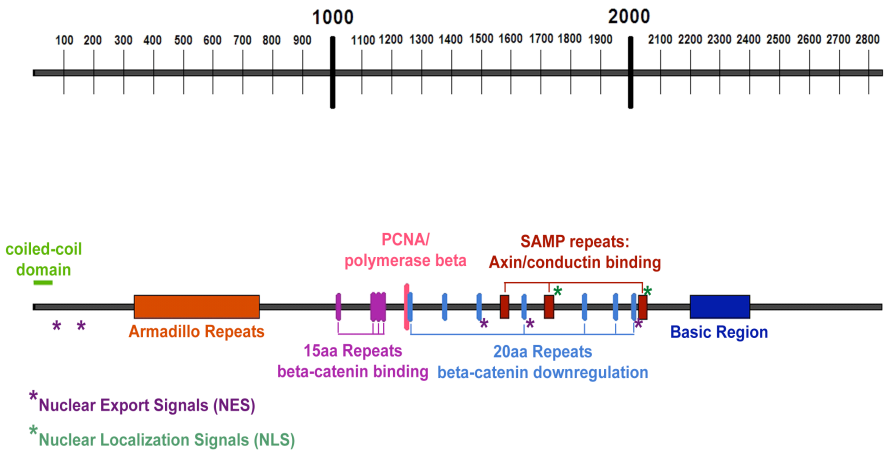

Figure 1.3
A simplified diagram of the binding domains of the APC protein. APC is represented here as a linear peptide with the amino acid scale above. Asterisks represent the characterized nuclear localization sequences (NLS) and nuclear export sequences (NES).

KAP3A reveals that these two proteins co-localized in clusters at the tips of membrane protrusions in migrating cells. Truncated forms of APC commonly associated with disease no longer form these clusters, suggesting that a C-terminal region of APC is also important for APC/KAP3A accumulation at the membrane (34).

The middle third of APC interacts with proteins of the canonical Wnt signaling pathway. Several repeats responsible for binding to and down-regulating β-catenin are located in this region along with the SAMP domains which mediate binding to axin, a scaffolding protein of the β-catenin destruction complex (35). This region also contains the two major nuclear localization sequences (NLS) which are required for optimal nuclear import and are regulated through phosphorylation (28, 36). The observation that APC fragments lacking both of these NLSs appear to maintain some nuclear/cytoplasmic shuttling suggests that there may also be a weaker NLS in the N-terminal domain (31). Experiments performed using fragments of APC suggest that the armadillo repeats can contribute to nuclear transport of smaller pieces of APC lacking the central NLSs (31). Finally, within the central region of APC there are three additional sequences predicted to function as NESs (37). However, direct comparison of the export properties of all of the APC NES suggest that the central NESs exhibit only moderate activity relative to the N-terminal NESs and probably have a minimal role in nuclear shuttling (31).

The C-terminal third of APC is typically lost in the truncation mutants associated with disease. This region is thought to mediate interaction with a variety

of protein binding partners. There is a 200 amino acid stretch composed primarily of positively charged residues which shares some biochemical similarities with the MT binding protein tau; this region has been shown to interact with tubulin and promote microtubule polymerization (38). Also in the C-terminal region of APC is a motif that binds to the PDZ domain of the human homologue of the *Drosophila* discs large protein (hDLG) and to the protein tyrosine phosphatase PTP-BL (39, 40). Both of these proteins are involved in the maintenance of cell polarity, migration, and control of cellular proliferation. A fragment of APC containing the final 155 amino acids has been shown to interact with the human homologue of *Drosophila seven in absentia* (Siah). Siah is a p53 inducible mediator of cell cycle arrest, tumor suppression and apoptosis which down-regulates β-catenin in an APC dependent manner. Furthermore, Siah induced β-catenin degradation is not dependent on Gsk-3β or axin and therefore does not involve the traditional β-catenin destruction complex (41). The C-terminal 170 amino acids have also been found to bind to the microtubule interacting protein End Binding protein-1 (EB1). In wild type ES cells EB1 decorates the mitotic spindle and localizes to the kinetochores; however, cells with APC truncation mutations showed a loss of EB1 accumulation at the kinetochores and an increase in chromosomal instability (42). This suggests that APC interaction with EB1 may be necessary for proper chromosome segregation during mitosis.

APC functions

APC can be seen in a variety of subcellular locations and is able to shuttle in and out of the nucleus. APC has been observed dispersed in the cytoplasm as well as localized near the ends of microtubules and along the leading edge of migrating cells (43). APC has also been observed in the nucleus, usually in a discrete punctate pattern and appears to transiently localize to the nucleolus (44). The plethora of reported binding partners and cellular localizations suggests that APC has a number of roles within the cell. APC has been hypothesized to participate in the regulation of protein phosphorylation and downregulation (45), cytoskeletal rearrangement (46), chromosome segregation (42), DNA repair (47), differentiation (48), transcription (49, 50) and apoptosis (51, 52).

APC in Wnt Signaling

Currently the best characterized role for APC is its function in the canonical Wnt signaling pathway (Figure1.4). The Wnt pathway was originally described as the Wingless pathway in *Drosophila*, but has been shown to be highly conserved in flies, frogs and mammals (reviewed in 53). Wnt signaling plays a key role in development and tissue homeostasis and is found to be compromised in many cancers. Extracellular Wnt binds to and activates membrane receptors which in turn mediate phosphorylation of downstream signaling molecules. Wnt signaling leads to decreased phosphorylation of the oncogene β-catenin. Unphosphorylated β-catenin can accumulate in the cytoplasm, translocate to the nucleus and bind to transcription factors of the T-cell factor/lymphoid-enhancer factor (Tcf/Lef) family to activate

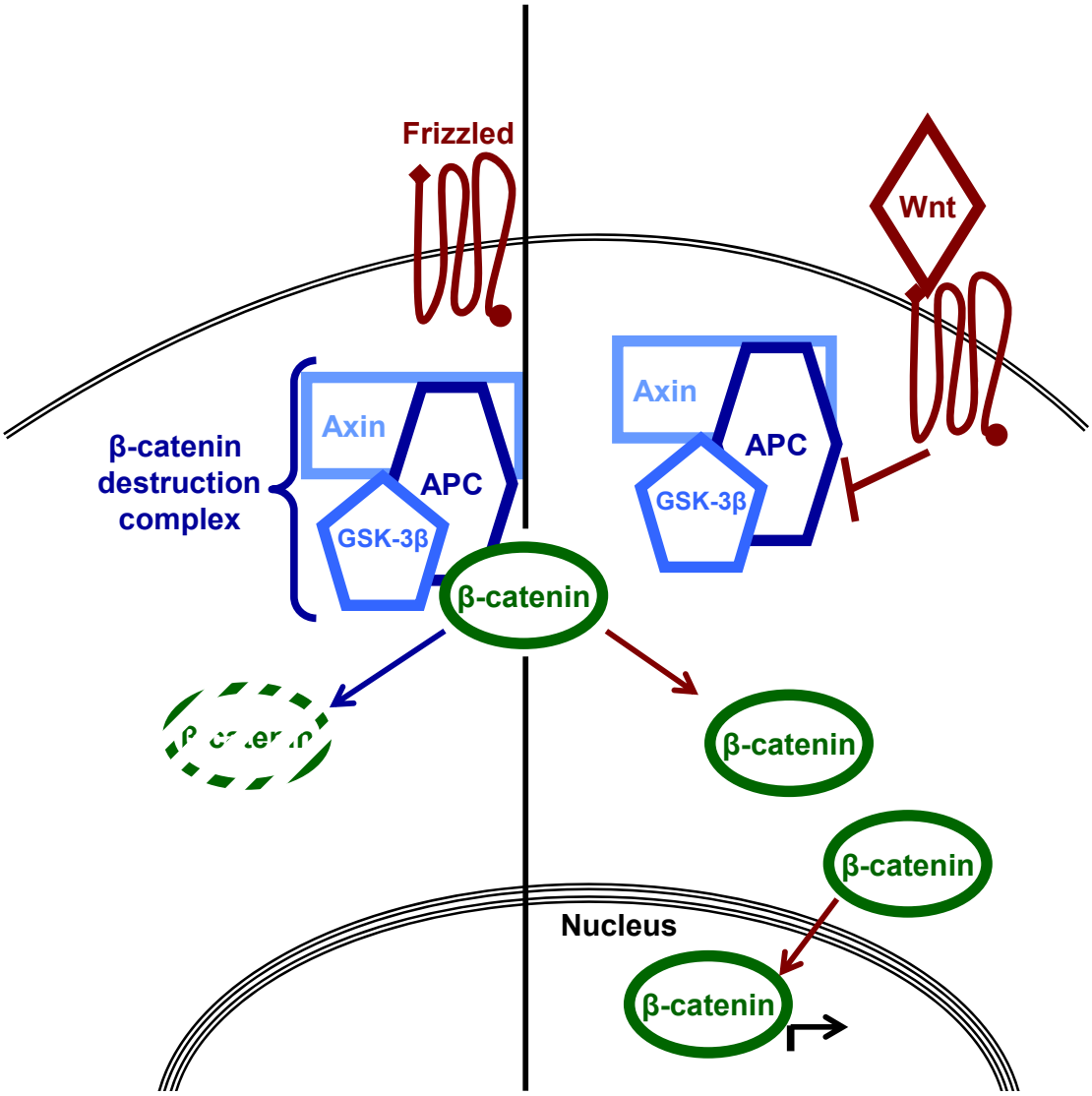

Figure 1.4
A simplified diagram of the canonical Wnt signalling pathway showing the role of APC in the β-catenin destruction complex. On the left APC, Axin and Glycogen Synthase Kinase-3β associate to form the core of the β-catenin destruction complex. This complex binds to and phosphorylates β-catenin protein in the cytoplasm. Once phosphorylated, β-catenin is ubiquitinated which marks it for proteolysis. On the right, a soluble Wnt factor interacts with its receptor complex (Frizzled) on the cell surface. This signaling event leads to an inhibition of the destruction complex allowing for increased cytoplasmic levels of β-catenin. This increase in β-catenin levels leads to the translocation of β-catenin into the nucleus where it acts as a transcription co-activator and leads to increased expression of Wnt targets, many of which are associated with promoting cellular proliferation.

transcription of specific target genes. These genes, including c-Myc, cyclin D1 and axin 2, are predominantly associated with progression of the cell cycle. Thus, in general terms, the presence of a Wnt signal leads to cellular proliferation. In the absence of a Wnt signal the β-catenin destruction complex containing axin, glycogen synthase kinase 3β (Gsk3β) and APC, phosphorylates excess β-catenin in the cytoplasm, targeting it for destruction and therefore down-regulating its activity as a transcription factor. This assures that in the absence of a Wnt signal, there is no aberrant cellular proliferation (reviewed in 54).

APC contains three SAMP repeats that bind to axin, a scaffolding protein of the β-catenin destruction complex. There are also three 15 amino acid repeats that facilitate binding of APC to β-catenin and seven 20 amino acid repeats that appear to be required for the down-regulation of β-catenin. It is interesting that in cancer tissue, APC is often truncated so that one or two of these 20 amino acid repeats are maintained (55). This APC truncation results in a destruction complex that is deficient in its ability to down-regulate β-catenin, but still retains some residual activity, suggesting that the complete loss of β-catenin regulation is less advantageous to growth than a decrease in the regulation of the β-catenin levels (55). Without proper down-regulation of β-catenin, the cell will respond as if it has received a signal to proliferate even in the absence of an actual Wnt ligand.

In addition to its role regulating β-catenin levels in the cytoplasm, it has been suggested that the function of APC in the control of β-catenin's transcriptional activity extends to the nucleus. This hypothesis is supported by the finding that APC

and β-catenin can co-immunoprecipitate from the nuclear fraction of cells (56). A further indication that APC may be interacting with β-catenin in the nucleus comes from an experiment in which APC's nuclear export signals were mutated, trapping a majority of the cell's APC inside the nucleus. With APC trapped in the nucleus, it is no longer available to participate in the cytoplasmic destruction complex and levels of β-catenin increase in both the nuclear and cytoplasmic compartments. In cells that have truncated APC, an increase in the level of nuclear β-catenin coincides with an increase in β-catenin transcription activity. However, with both β-catenin and full-length APC located predominantly in the nucleus, β-catenin transcriptional activity is low, suggesting APC can sequester β-catenin from TCF/LEF-1 (56). There is also evidence that APC is recruited to the enhancer region of Wnt target genes and may participate in the dissociation of β-catenin and other Wnt enhancer proteins and co-activators from their targets at the termination of a Wnt signal (49). APC's role as a direct repressor of Wnt/β-catenin signaling at the DNA is further supported by findings that phosphorylation of APC at the first two 20 amino acid repeats enhances the interaction between APC and β-catenin by 300-500 fold and that this phosphorylated fragment of APC can effectively disrupt Tcf binding to β-catenin *in vitro* (57).

A role for APC beyond Wnt signaling.

Because uncontrolled proliferation is a classic early marker of cancer development, regulation of cellular proliferation through β-catenin stability is

considered by some, to be the primary tumor suppressor function of APC (58). This is supported by the observation that adenomas with no mutations in *APC* commonly have activating mutations in β-catenin which make β-catenin resistant to phosphorylation. However, the idea that APC may have a more complex responsibility in cellular homeostasis is supported by a number of observations. First, APC shuttles in and out of the nucleus and interacts with a variety of nuclear proteins including DNA polymerase-β, Flap endonuclease-1 (Fen-1), PCNA and topoisomerase IIα (47, 59, 60). All of these APC partners are involved in DNA maintenance rather than β-catenin regulation. Second, the Wnt signaling pathway offers a variety of other proteins, the mutation of which would disrupt β-catenin stability. Yet, statistically, it is much more prevalent for both alleles of *APC* to be inactivated than for a single oncogenic mutation to occur at any other step in the pathway including in β-catenin itself (21). Some studies even suggest that activating mutations in β-catenin, in addition to being much rarer in cancers, may result in a less aggressive lesion than those that show mutations in *APC* (61). Taken together, these observations support a multifunctional role for APC in tumor suppression.

APC and DNA repair.

One of the first suggestions that there might be a link between APC and DNA repair was published in 1982, nearly 10 years before the *APC* gene was identified in the early 1990s (17-19). Investigators working with cultured skin fibroblast lines derived from patients with Gardner's Syndrome noticed that the cells taken from

patients with colorectal polyps were more sensitive to both ultraviolet (UV) irradiation and X-rays than cells taken from healthy Non-Gardner donors (62). It is now known that Gardner's Syndrome is a form of Familial Adenomatous Polyposis (FAP) caused by an inherited mutation in *APC*. While polyps typically arise only after the loss of the second allele of *APC*, it is interesting to note that the cultured FAP fibroblasts, expected to maintain one WT *APC* allele, were defective in their ability to respond to DNA damage. Similar work using whole animals suggests that mice heterozygous for APC truncation are more sensitive to gamma irradiation than their wild type counterparts (63).

Other intriguing links between APC and DNA maintenance have since been revealed. When cultured HCT116 human cancer cells were treated with a variety of DNA damaging agents, the levels of APC mRNA and protein increased up to 12 fold (64). This up-regulation of APC was shown to require p53 and could be mimicked by over-expression of wild type p53, suggesting that APC is a downstream target of p53 and expression is up-regulated in response to DNA damage. Further supporting this theory was the identification of two p53 binding sites in the *APC* promoter sequence, which promoted the expression of a reporter construct in response to DNA alkylation damage. However, the mutation of these sites did not completely eliminate reporter construct activation in response to DNA damage, suggesting that the *APC* promoter contains additional uncharacterized sequences that are also responsive to DNA damage (65).

Another interesting piece of evidence, when considering a role for APC in DNA repair, comes from the study of mice mutant for both APC and the DNA repair protein Fen-1. The $APC^{1638N/+}$ mutation interferes with the expression of the APC mutant allele resulting in a null mutation. Heterozygous mice, therefore express only half of the normal level of APC (normal expression from the WT allele and only ~ 2% expression from the mutant allele). $APC^{1638N/+}$ mice display a mild intestinal polyposis phenotype, developing, on average, three tumors per mouse (66). The Fen-1 mutation is also a null mutation, with embryonic lethality in homozygous mice. Mice heterozygous for Fen-1, however, are viable and fertile, with a lifespan indistinguishable from their wild type littermates and little to no intestinal phenotype. When the $APC^{1638N+/-}$ mice were crossed with the Fen-$1^{+/-}$ mice, the resulting double-mutant offspring displayed a shortened lifespan, increased tumor incidence and a more aggressive polyposis phenotype. Polyps in the double-mutant mice were 10 times more likely to progress to malignancy than polyps from mice carrying only a mutation in *APC*. Furthermore, while none of the polyps from the $APC^{1638N/+}$ mice showed microsatellite instability (MSI), all of the polyps from the $APC^{1638N/+}$Fen-$1^{+/-}$ double-mutant mice displayed extensive MSI (67) . The observation that the double-mutant mice exhibited a phenotype that was more severe than the phenotype observed in mice with either of the mutations individually suggests that APC and Fen-1 both contribute to the same end goal, presumably DNA maintenance, but that they do so in parallel pathways.

Numerous parallel pathways exist to maintain DNA integrity. Different types of DNA damage are resolved through different mechanisms (reviewed in 68). For example, there is a subset of DNA repair proteins responsible for fixing mismatched base pairs in newly synthesized DNA, while other types of damage such as bulky DNA adducts or pyrimidine dimers, more typically resulting from exposure to UV irradiation, are predominantly fixed using the nucleotide excision repair (NER) pathway. Replacement of DNA bases that have been oxidized, reduced, alkylated, methlylated or deaminated is usually carried out by the base excision repair (BER) pathway, and repair of double-stranded DNA breaks can be accomplished through either the homologous recombination (HR) or non-homologous end joining (NHEJ) pathways (68). The Fen-1 protein discussed above, is associated with the process of BER (69) suggesting that APC does not aide in BER, but rather, plays a role in maintaining DNA stability by participating in one or several of the other pathways. APC is implicated in both the NER pathway and in the repair of DNA double-strand breaks by the previously described data in which human cell lines and mice deficient in APC show increased sensitivity to gamma irradiation and UV light (62, 63).

APC may also be involved in the sensing or repair of mismatched base-pairs, a hypothesis that is supported by studies of double-mutant $APC^{1638N/+}Exo\text{-}1^{+/-}$ mice. Exonuclease-1 (Exo-1) is a 5'-3' DNA exonuclease in the same family as Fen-1 (70). Though similar in sequence (70), these two proteins operate in different repair pathways. Fen-1 participates in BER while Exo-1 is associated with mismatch repair. Unlike the $APC^{1638N/+}Fen\text{-}1^{+/-}$ mutants, the double-mutant $APC^{1638N/+}Exo\text{-}1^{+/-}$ mice

show no significant increase in tumor incidence, no increase in the rate of tumor advancement and no MSI in any of the polyps tested (71). Because the combined phenotype is the result of the additive effects of the mutations to the individual tumor suppressors, we hypothesize that APC's role in DNA maintenance also includes a function in mismatch repair.

Further complicating the search for APC's role in the maintenance of the genome is that, contrary to what is expected of a proven tumor suppressor protein, APC appears to actively hinder DNA repair by inhibiting the BER pathway. Cells with wild type APC are more sensitive to DNA methylating agents than cells in which APC has been mutated or knocked down by siRNA (59). Cells deficient in APC were also more efficient in repairing a BER-dependent reporter construct, showing a quicker and more complete repair of the damage than cells with wild type APC (47). Further analysis of this phenotype demonstrated a direct interaction between the APC protein and several components of the BER repair pathway including DNA polymerase-β, Fen-1 and PCNA (47, 59). With its suspected role in a number of DNA repair pathways, it might be hypothesized that APC inhibits BER in favor of one of the other repair pathways. However, this does not explain why p53 up-regulates APC expression in response to DNA damaging agents that cause DNA adducts, a type of damage traditionally thought to be repaired by the BER pathway. Another prevalent theory is that APC blocks repair of DNA to induce apoptosis in cells with extensive DNA damage, a function that would be in agreement with the tumor suppressor identity of APC. Colony survival studies suggest that APC assists

in the survival of cells after exposure to other types of DNA damage (62), implying that induction of apoptosis is specific to the BER pathway.

Though the exact nature of APC's role in DNA maintenance is still unclear, the evidence that there is a function for APC in DNA repair is beginning to accumulate. Even with the limited work that has been done in this field, there appears to be a link between APC and members of every major DNA repair pathway.

APC in Animal Models

While some aspects of APC are more easily investigated in cultured cells, other aspects of APC's role in development and tissue homeostasis can only be effectively explored *in situ*. Originally research on intestinal cancer was conducted in rodent models that were induced to develop neoplasms by exposure to carcinogens; however, nearly all of the current animal studies in this area are of mouse models that carry germline mutations in the *APC* gene (72). Below is a summary of some of the more common mouse models used to study APC function in suppression of intestinal carcinogenesis (Table 1.2 and Figure 1.5).

The Min mouse: a beginning

The first APC mutant mouse model to be developed was the Multiple Intestinal Neoplasia or APC Min mouse which resulted from an ethylnitrosourea (Enu) mutagenesis screen (73). The APC Min mice now represent one of the most widely used mouse model systems in the study of APC and intestinal cancer research

Table 1.2 A summary of the phenotypes of common APC mouse models

APC Mutation	Truncation	Average Polyp Number*	Lifespan*	Homozygous Lethal	Extra Intestinal Manifestations
Min** (73)	aa 850	100	<120 days	Yes	No
1638N (83)	aa 1638 2% expression	3	365 days	Yes	Desmoid tumors, Cutaneous cysts
1638T (84)	aa 1638	0	Normal	No	Cutaneous cysts and Postnatal mortality in -/-
Δ1309 (87)	aa 1308	60	120 days	Yes	None reported
Δ716 (89)	aa 716	254	>112 days	Yes	None reported
Δ14 or 580S/D (90)	aa 580	100	120 days	Yes	none reported
Δ474 (92)	aa 474	122	185 days	Yes	Mammary tumors
NeoR (96)	10% expression of full length	<1	Not reported, pressumably normal	Yes	None reported

* Heterozgous phenotype

** on the C57BL/J6 background

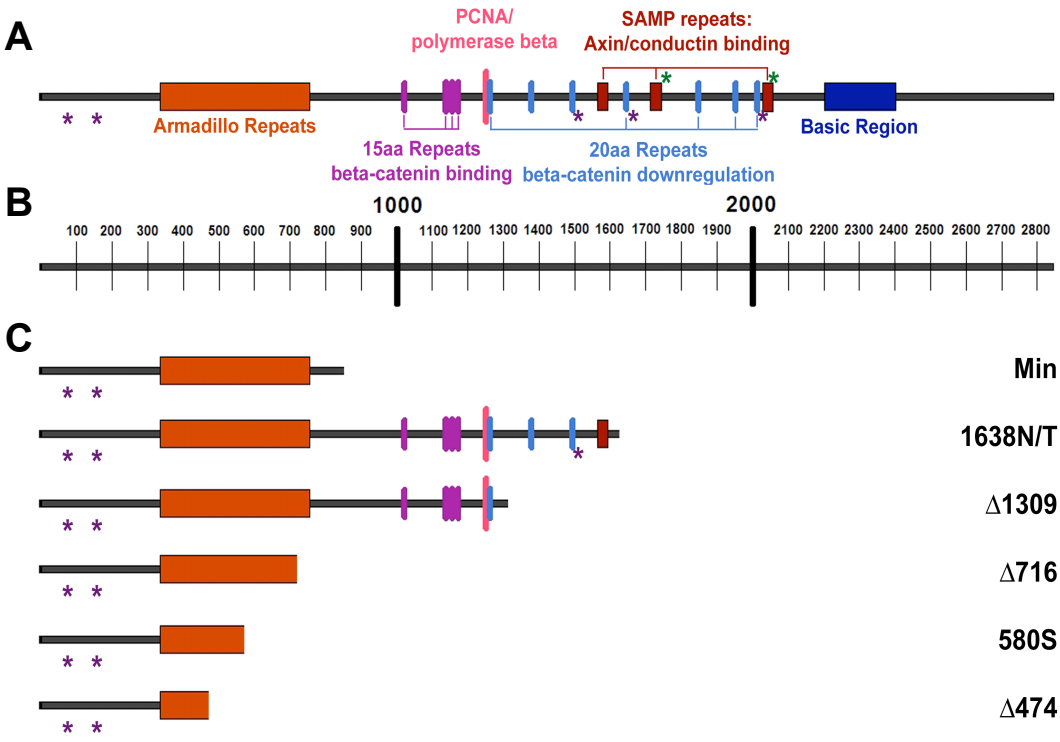

Figure 1.5
A diagram of the APC motifs found in several of the common mouse models for truncated APC. (A) Full length APC with labeled motifs. Asterisks denote NLS and NES locations (green=NLS; purple=NES). (B) Amino acid scale. (C) APC truncations found in the indicated mouse models.

with over 435 published references to date (Pubmed search: APC Min mouse). Min mice develop adenomatous polyps in the intestine with moderate dysplasia, mild nuclear atypia and frequent mitotic figures. The similarity of the Min mouse phenotype to the human disease FAP led to the identification of a germline mutation in Min mice that interrupted the murine *Apc* gene. The mouse *Apc* gene is 86% identical to the human gene at the nucleotide level with the protein 90% identical to the human APC making it a very suitable model in which to study human APC loss (74). The Min mutation is a transversion of nucleotide 2594 from a T to an A which converts a leucine (TTG) to a stop codon (TAG), truncating the protein at amino acid 850 (74). The truncated Min APC protein maintains the armadillo region which is thought to bind to the actin regulator as well as the N-terminal nuclear export sequences. Absent from the Min APC protein are the regions of APC that bind to β-catenin and aid in its down-regulation as well as the SAMP motifs which bind to axin. The Min mutation eliminates both of the central nuclear localization sites as well as the basic domain that is thought to interact with microtubules. Truncated Min APC also lacks a variety of sites thought to interact with various protein binding partners, including DNA polymerase-β, the kinetochore protein EB1 and hDLG.

The polyposis phenotype of the heterozygous Min mice further confirms that APC serves as a tumor suppressor and functions, at least in part, to maintain homeostasis in adult tissue. The Min mouse model also provides strong evidence for a role for APC during development. The Min mutation causes embryonic lethality when homozygous. Embryos with an $APC^{Min/Min}$ genotype are able to implant, but

begin showing obvious abnormalities around embryonic day 6.5 and die due to an apparent failure in the maintenance and development of the early egg cylinder (75).

Following the detection of the *Apc* Min mutation, the mutant mice were crossed with C57BL/J6 mice to obtain a congenic strain. The average lifespan for a C57BL/6J $APC^{Min/+}$ mouse is less than 120 days at which point death usually occurs due to anemia caused by rectal bleeding (73). The Min mutation has also been introduced into other mouse strains and the severity of the Min phenotype can vary greatly depending on the genetic background of the mouse strain being used. While a typical heterozygous Min mouse will develop approximately 100 tumors, the number of polyps developed per mouse can vary significantly, ranging from less than one per mouse to over 200 depending on the specific genetic background (76, 77).

Since the Min mutation can give rise to phenotypes that differ in severity depending on the genetic background, this model is an excellent tool to search for genes that have positive and negative effects on polyp development. The first gene to be isolated from such a genetic search was named Modifier of Min 1, or Mom-1 (76). Some mouse lines including CAST, BALB, DWR, DBA, MA and AKR were observed to be more resistant to Min tumors than other lines such as the B6, 129 and BTBR mouse lines (76, 78, 79). These "sensitive" lines were all revealed to carry a frame shift mutation in the type II secretory phospholipase A2 (Pla2s) gene, suggesting that tumor sensitivity stems in part from either the production of the truncated protein or the loss of the full length WT protein. Pla2s is one of several enzymes involved in generating arachidonic acid which is a rate limiting substrate in

the generation of prostaglandins (80). While the Mom-1 mutation explains some of the variability, it is only able to account for about 50% of the genetic variation that is observed, which suggests the presence of additional modifier proteins (76). The second modifier locus,Mom-2, was shown to have an even greater effect on polyp number and size. Mom-2 was mapped to the mouse chromosome 18 and can reduce polyp number by 88-95%. Though the mechanism of tumor resistance is currently unclear, the effects of Mom-1 and Mom-2 together are greater than the effects of either alone, suggesting that they work in different pathways (81).

The APC Min mouse has proven to be an excellent tool in the study of intestinal tumorigenesis; however, this model is still an imperfect system. The phenotype of the Min mouse does not directly parallel human colorectal cancer. As with many mouse models, the Min mouse develops polyps predominantly in the small intestine rather than in the colon where polyps most commonly occur if there are germline or somatic *APC* mutations in humans (23). Tumors induced by a Min mutation do not follow the same steps in progression as human tumors; for example, Min mouse tumors do not develop mutations in K-ras which is commonly mutated in the development of human colon cancers (15, 72). Also, because of the short lifespan of Min mice, few of the polyps have time to invade and metastasize, making it difficult to study these processes in the APC Min mouse model. Since the somewhat serendipitous development of the APC Min mouse, several targeted APC mouse models have been developed allowing a more in-depth look at APC's function in

tissue homeostasis and tumor progression as well as intestinal carcinogenesis in general.

More mouse models: The ever shrinking APC molecule

Molecular biology techniques allowing a mutation to be targeted to a specific location on a specific gene and the ability to create a mouse line from mutant embryonic stem cells have allowed the creation of a myriad of mouse models with very precise APC genotypes (reviewed in 82). Many APC mutants have been created that code for APC protein products truncated at a variety of specific locations (Table 1.2). This allows for inquiry into the regions of APC that are critical for different cellular functions. As techniques have advanced, there has been an increase in the number of inducible and hypomorphic *APC* mutations as well. All of these APC mouse models have added to our understanding of APC function in development, homeostasis, and tumor suppression.

APC^{1638N} and APC^{1638T}

Using a targeting vector for mouse embryonic stem cells, a neomycin phosphotransferase expression cassette was inserted into exon 15 of the *APC* gene at nucleotide 4913. The resulting frame shift truncated the APC protein at amino acid 1638 (83). The 182kD truncated APC protein lacks the domains thought to interact with DLG, EB1 and PTP-BL and Siah. APC aa1-1638 contains only three of the seven β-catenin down regulating repeats and only one axin binding or "SAMP" motif

(84). However, little to no truncated APC could be detected when lysate from the mutant cells was analyzed by western immunoblot. It was hypothesized that the lack of expression of the truncated protein was due to the Neo^r cassette which had been inserted in the opposite direction as the *APC* gene. Originally this was thought to be a null mutation and so was named APC^{1638N}. Later, it was shown that the mutation created a hypomorphic allele which expressed the truncated APC protein at only 2% of the endogenous level. (48).

The mice heterozygous for the 1638N APC mutation showed polyploid hyperplastic lesions in the colon by 10 weeks, and colonic and small intestinal polyps by 20 weeks (66). Malignant adenocarcinomas developed in the duodenum and jejunum, and mice began to die at 32 weeks of age. The average lifespan of a heterozygous APC^{1638N} mouse is just over 1 year and on average they develop only about three tumors per mouse (66). Because the phenotype of this mouse model is less severe than many of the APC Min mutant mice, they live long enough for their tumors to progress into carcinomas making it possible to study of tumor advancement in this model. However, such studies have shown that while the WT copy of *APC* is lost in nearly all of the adenomas, there were no mutations found in K-ras, H-ras or N-ras, nor were there any detectable abnormalities in the p53 gene (85), all of which are common mutations in human colon carcinogenesis (15). Nonetheless, this APC^{1638N} mouse model does show other similarities to human *APC* loss. For example, in addition to the intestinal polyps APC^{1638N} mice manifest extra-intestinal lesions similar to those common to FAP patients (25, 86).

Extra-intestinal lesions observed in the APC 1638N mouse model included cutaneous cysts which began developing when the mice were between 1 and 3 months old, and desmoid tumors that developed when APC^{1638N} mice are between 1.5 and 2 months of age (86). Interestingly, these extra-intestinal lesions were not commonly observed in $APC^{Min/+}$ mice. This difference could reflect expression of APC Min protein at WT levels, whereas mice containing the *Apc* 1638N mutation produce very little APC protein from the mutant allele. Perhaps this suggests that outside of the intestine, the expression level of the N-terminal region of APC is more important than the presence of the full length protein. As with the APC^{Min} mice, the APC^{1638N} mutation results in embryonic lethality when homozygous (83), suggestive of an important role for APC in early development.

To further study the 1638 amino acid truncation product of *APC*, a second mutant mouse was created using the same techniques, but the antibiotic resistance cassette was inserted in the same direction as the reading frame of the *Apc* gene (84). This mutation, named 1638T, expressed the truncated protein at the same level as WT protein, confirming that the reverse orientation of the Neo^r cassette was the cause of the reduced expression of truncated APC seen in the 1638N mutants. Mice heterozygous for APC 1638T were indistinguishable from their WT littermates. Unlike the previously described mouse lines, mice homozygous for the 1638T mutation were viable. Surprisingly even $Apc^{1638T/1638T}$ homozygous mice are not prone to intestinal polyposis, suggesting that the regions of APC important for continued tissue homeostasis are N-terminal to amino acid 1638. The $Apc^{1638T/1638T}$

mouse does, however, have some developmental defects. Homozygous $APC^{1638T/1638T}$ mice are growth retarded and develop cutaneous cysts which appear to be associated with the pilosebacious unit. There is a higher rate of postnatal mortality which increases as the mice are crossed with the more sensitive C57BL/J6 mice (84).

$APC^{\Delta 1309}$

APC truncation at amino acid 1309 is the most common mutation found in humans with Familial Adenomatous Polyposis. Furthermore, truncation at this site is associated with a relatively severe form of the disease (24). It therefore was logical to create a mouse model that expresses a mutant form of APC truncated at amino acid 1309. The $APC^{\Delta 1309}$ mouse was developed by the Itoh lab in Japan and was created by introducing a nonsense mutation at codon 1309 of the *Apc* gene (87). The $APC^{\Delta 1390}$ mouse has an average lifespan of 120 days, nearly identical to the $APC^{Min/+}$ mouse, but only develops ~60 polyps along the entire gastrointestinal tract. The polyps are located primarily in the upper region of the small intestine which differs from Min mice which mainly develop polyps in the lower region of the small intestine, suggesting that this mutation has a somewhat different mechanism for polyp initiation. (88).

$APC^{\Delta 716}$

$APC^{\Delta 716}$ mice were created with an insertion in *Apc* nucleotide 2150 which results in truncation of the APC protein at amino acid 716 (89). The $APC^{\Delta 716}$ mouse

expresses a shorter version of APC than the Min mouse which is truncated at amino acid 850. Heterozygous APC $^{\Delta 716/+}$ mice have a severe intestinal polyposis phenotype, developing polyps within 5 weeks of birth. The polyps develop primarily in the small intestine and by 16 weeks of age there was an average of 254 polyps per mouse, over twice the average number of polyps that develop in the original Min mouse (73, 89). If APC functioned as a tumor suppressor entirely through its ability to down-regulate a Wnt signal by aiding in the destruction of cytoplasmic β-catenin, one would expect these two APC truncations to result in a similar phenotype. While the truncation in the Min mouse already removes all of the known β-catenin binding and down-regulation domains, the loss of the additional 134 amino acids in the APC $^{\Delta 716}$ mouse still increases the severity of the polyposis phenotype. Similar to the Min mice, all of the polyps tested had lost the WT copy of APC, suggesting again that one WT *Apc* allele is enough to prevent polyp formation at the tissue level. APC $^{\Delta 716/\Delta 716}$ mice die prior to day 8 of gestation (89).

APC$^{\Delta 14}$ (APC ^{580S})

Unlike in many of the previously described APC mutant mouse models, the Δ14 mutation was not a truncation due to the insertion of a drug resistance cassette. In this mouse Lox P sites were introduced into introns 13 and 14 so that the entire region of exon 14 was flanked with Lox P sites, or "floxed" (90). When exposed to Cre DNA recombinase, DNA undergoes a rearrangement that removes the floxed sequence. This deletion of exon 14 caused a frame shift resulting in truncation of the

APC protein at amino acid 580. This truncation removed all of the domains involved in β-catenin binding and down regulation as well as some of the armadillo repeats which stretch from approximately amino acid 435 to amino acid 766 (30). These mice have a severe polyposis phenotype and begin dying at 4 months of age, with similar average lifespans as the Min mouse (90). Interestingly, while these mice also develop similar numbers of polyps as the Min mice, the distribution of their polyps differs. In the $APC^{\Delta 14/+}$ mice there are comparatively more polyps in the colon and fewer in the small intestine when compared to the $APC^{Min/+}$ mice grown under the same conditions. This phenotype more closely resembles the human symptoms associated with mutation of *APC*. However, a control group of $APC^{\Delta 14/+}$ mice raised under specific pathogen-free (SPF) conditions did not show the same shift in polyp distribution. Their phenotype more closely resembled the APC Min mouse distribution of polyps with the vast majority in the small intestine and very few in the colon (90). This suggests that the differences in the polyp distribution between humans and mouse models has a genetic component and is also influenced by the intestinal environment. As in other mouse models, $APC^{\Delta 14/\Delta 14}$ mice die during embryogenesis (91).

$APC^{\Delta 474}$

In humans, germline mutations in *APC* 5' of nucleotide 1578 usually give rise to a milder form of the disease known as Attenuated Familial Adenomatous Polyposis (AFAP). AFAP is associated with fewer polyps and a later age of onset compared to

FAP (25, 50). A mouse model of AFAP was developed by inserting a targeting construct that would result in truncation of APC at amino acid 474. The $APC^{\Delta 474/+}$ mutant mice began developing intestinal tumors at around 8 weeks of age and averaged 122 tumors per mouse similar to mice with an $APC^{Min/+}$ mutation. However, the average lifespan of the $APC^{\Delta 474/+}$ mutant mice was nearly double that of the APC Min mouse. The mice lived approximately 6 months before they died of anemia. In addition to the intestinal lesions 18% of the $APC^{\Delta 474/+}$ mice also developed mammary tumors that usually arose between 3-5 five months of age. No $APC^{\Delta 474/\Delta 474}$ mice were born, suggesting that, like most other APC truncations, homozygous APC truncation at amino acid 474 results in embryonic lethality (92).

Homozygous loss: Learning about APC in embryonic stem cells

Severe defects in APC result in embryonic lethality in the absence of wild type (WT) APC. Therefore, it can be difficult to study the complete loss of WT APC *in situ* because death results before differentiated tissue can develop. However, undifferentiated tissue, specifically embryonic stem cells carrying *Apc* mutations can be studied. Much can be learned about the role of APC in β-catenin regulation, differentiation and proliferation in these tissue precursor cells. Embryonic stem cells will grow into tumors called teratomas when injected into syngenic (immune compatible) mice (93). Because these ES teratoma cells differentiate in a manner that closely parallels the normal behavior of ES cell in an embryo, teratomas provide

valuable insights into the processes required for the development and maintenance of more differentiated tissues (94).

One common method for examining the effect of *APC* mutation on β-catenin transcription activity is a luciferase assay using the TOPFLASH and FOPFLASH reporter constructs (50). TOPFLASH contains three copies of the consensus Tcf binding motif, and the negative control, FOPFLASH, contains three copies of a mutant motif. Both motifs are upstream of a minimal c-Fos promoter driving luciferase expression. In cells transfected with TOPFLASH, luciferase expression is correlated with the ability of β-catenin to interact with Tcf at the promoter binding site and initiate transcription (50). The TOPFLASH assay was used to examine the level to which the mutant *APC* alleles can regulate β-catenin's ability to act as a transcription factor *in vivo* (84). Embryonic stem cells homozygous for the APC 1638T mutation show β-catenin activities similar to WT cells. The phenotype observed in mice homozygous for the APC 1638T mutation is therefore unlikely the result of unregulated β-catenin. A lack of β-catenin up-regulation in cells that carry the APC 1638T mutations also correlates to the absence of a polyposis phenotype in the $APC^{1638T/1638T}$ mice. These observations also suggest that the removal of APC's carboxy-terminus does little to affect APC's ability to regulate β-catenin. Stem cells with an $APC^{1638T/1638N}$ genotype have β-catenin activity levels slightly over twice the WT levels, while cells homozygous for the APC 1638N mutation showed a 30-fold increase in β-catenin transcriptional activity compared to WT cells. The much more dramatic TOPFLASH activation in cells that are homozygous for the APC 1638N

mutation suggests that there is a dose response effect to APC's regulation of β-catenin. It appears that the less APC available in the cell, the less β-catenin is regulated (84).

To examine the importance of axin binding to APC, another *APC* mutation was designed. A targeting construct was created to interrupt the *APC* gene and produce a truncation protein that ended at amino acid 1572. Compared to the APC 1638T mice, the APC 1572T mice lack the 3' 197 base pairs of APC sequence, thus eliminating the last SAMP motif that is present in the 1638T mutants. The $APC^{1638N/1572T}$ double mutant cells had β-catenin activity levels over four times that of WT cells and twice that of $APC^{1638T/1638N}$ cells. However, the $APC^{1638N/1572T}$ cells still expressed significantly less luciferase than the $APC^{1638N/1638N}$ cells. These findings suggests that while the loss of the last SAMP motif significantly decreased APC's ability to regulate β-catenin activity, it does not completely eliminate it (84).

To look at APC's role in differentiation WT and APC-mutant stem cells were injected into syngenic mice to induce teratoma formation (84). $APC^{1638N/1638N}$ cells showed severe defects in teratoma formation when compared to WT stem cells. Teratomas made using $APC^{1638N/1638N}$ showed an absence of neural ectoderm markers which represent 50-75% of the WT teratomas. Other missing cell types include bone, cartilage and ciliated epithelial cells. Gut-like tissues such as smooth muscle, secretory epithelia and non-ciliated epithelia, as well as keratinized, epithelia showed normal or enhanced differentiation. Teratomas formed using $APC^{1638T/1638T}$ stem cells were indistinguishable from WT teratomas. This later result suggests that much of

the phenotype observed in the 1638N cells is due to the reduced level of APC not the truncation of the protein (48). Interestingly the 1638T truncation protein lacks the known nuclear localization sites at amino acids 1773 and 2054, however APC is still found in the nuclear compartment of cells homozygous for the mutation (84). This indicates that there are additional regions that contribute to the nuclear import of APC. These may include other endogenous sites that contribute to APC's import or indicate that APC is able to interact with other nuclear proteins that can facilitate its entry into the nucleus in the absence of APC's endogenous NLSs.

Inducible Apc *mutations: The next generation of mouse models*

The existing mouse models that carry *Apc* mutations almost always display embryonic lethality in the absence of wild type APC, most likely due to a role for APC in development. Recently, due to advances in the technology for making knock-out mice, APC mutations can be induced in adult mice. This allows the observation of homozygous *Apc* loss in the fully developed mouse intestine. One such mouse model is the $APC^{\Delta 14}$ mouse, also referred to as APC^{580D} mice (for mice containing the full length un-recombined gene) or APC^{580S} mice (for the mice that have the recombined and therefore mutant gene resulting in a truncated APC protein) (95). Because the targeting vector used to create these mice utilized Lox P sites inserted around exon 14 of the genomic APC sequence, the mutation can be induced at any time using Cre recombinase. When exposed to Cre, the DNA will recombine, removing the exon that is "floxed", causing a frame shift that truncates APC at amino

acid 580. In the absence of Cre the un-recombined gene will express normal protein. Mutant mice that are homozygous for the un-recombined gene are called $APC^{580D/580D}$ mice and are normal (95). They are not prone to intestinal polyps nor do the animals show any obvious phenotype. However, the $APC^{580D/580D}$ mice display a 30% decrease in APC RNA as detected by northern blot in intestinal tissue (95). The $APC^{580D/580D}$ mice were then crossed with an inducible Cre transgenic mouse (10). When exposed to β-napthoflavone, Cre expression was induced specifically in the intestine under the control of the Cyp1A promoter (10). The APC truncation was induced when the mice were 8-10 wks of age and the $Cre^{+}APC^{fl/fl}$ mice are visibly sick within 5 days, while the $Cre^{+}APC^{+/+}$ mice showed no symptoms of illness. Mice homozygous for the induced APC truncation in the intestine developed a crypt-villus architecture that was noticeably altered so that a discrete crypt was no longer identifiable and all of the recombined tissue had a "crypt-like" appearance (10). This crypt-like phenotype included cells that were more densely packed and therefore clearly distinguishable from normal tissue when stained with hematoxylin and eosin. There was a loss of histological markers for differentiated cells and an increased zone of proliferation that stretched up the entire crypt-like region instead of being confined to the lower mid-region of the crypt. While staining did not show an overall increase in β-catenin, there was an increase in dephosphorylated β-catenin which was relocalized from the cytoplasm to the nucleus by the third day after induction of Cre expression. Microarray analysis also showed a significant change in gene expression between the induced and uninduced tissue (10). These data strongly indicate that the

function of APC is not only important for development and tumor suppression, but the maintenance of the gut as well.

Altering expression levels: How much APC is enough?

By studying the phenotypes associated with mutations in the *Apc* gene, it has become apparent that the degree to which APC is truncated plays a role in determining the severity of the phenotype. However, truncating the APC protein is not the only way to induce polyp formation. Mouse models that affect only the level at which wild type APC is expressed can also have dramatic cellular affects. In the APC^{NeoR} mouse, a PGK-neo cassette was inserted into intron 13 of *Apc* through homologous recombination. In these mice, the cassette is spliced out during RNA processing and only full-length mRNA was detected in the mutants (96). However, the expression of APC protein from the mutant allele was attenuated. Western immunoblot of cell lysate revealed that APC was expressed at only 60% of the WT level in cells heterozygous for this mutation, and in homozygous cells APC was expressed at only 20% of the WT level (96). It was hypothesized that this attenuation was likely due to the disruption of an enhancer element. Mice heterozygous for this mutation were viable and showed a limited polyposis phenotype. At 15 months of age, the tumor incidence was 19% with the mean tumor number of 0.26 ±0.54 (97) . Histologically, the polyps consisted of dysplastic adenomas similar to those seen in other mouse models with mutant *Apc*. Unlike polyps found in other *Apc* mutant mice, the dysplastic cells of the APC^{NeoR} mice only rarely showed an accumulation of

nuclear β-catenin suggesting that nuclear β-catenin localization does not necessarily correlate with adenoma cell proliferation in this model (97). In the ES cells there was a subtle increase in the amount of dephosphorylated and presumably stable β-catenin present. Heterozygous cells had nearly normal levels of β-catenin, while homozygous cells had 2.8 times the WT amount. β-catenin protein level also correlated with the TOPFLASH measurements of β-catenin activity. While heterozygous cells showed β-catenin transcriptional activity nearly identical to WT cells, homozygous ES cells showed an increase in β-catenin activity that measured about 7 times that of WT cells (97). As is commonly seen in APC mouse models, heterozygous animals were born, however homozygous APC^{NeoR} mice were not viable. The observation that APC^{NeoR} mice had a much less dramatic increase in β-catenin activity and yet still displayed embryonic lethality when homozygous may suggest a function for APC in development beyond simply regulating Wnt signaling.

A Mouse Model to Study the Role of APC in the Nucleus

Like the initial cellular studies of APC, the current mouse models focus primarily on the role of APC in the control of β-catenin and cellular proliferation. These mutant mice primarily reproduce various APC truncations associated with human disease and have shown in multiple studies that polyposis can indeed be reproduced in an animal model. However, a comprehensive role of APC as a tumor suppressor still eludes us. The role of APC in the nuclear compartment remains uncertain. While evidence suggests that APC may play a role in the cellular

maintenance of DNA, the methods by which APC may carry-out such a task along with the exact nature of the task itself are enigmatic. Fragments of APC which should lack nuclear import domains can still be observed shuttling into the nucleus; however, whether or not they are capable of carrying out any normal nuclear function is unclear because almost nothing is known about the domains of APC necessary for its nuclear tasks. Perhaps most importantly we still have not established how the nuclear function of APC contributes to its role as a tumor suppressor. Currently this information is impossible to derive from the available mouse model systems and previous studies indicate that cellular phenotypes may not correlate with observations in a whole animal.

In this dissertation we investigate the function of nuclear APC, both in cells and in an animal model. We have generated an original mouse model in which the nuclear localization sequences have been specifically disrupted. The resulting mouse expresses full length mNLS APC at normal levels under its endogenous promoter. APC is only minimally altered so as to preserve the cytoplasmic functions. However, these mice lack the primary nuclear import sequences in APC which direct its interaction with importin-α (98). We are using these APC mNLS mice to further our understanding the role of nuclear APC is whole tissue.

In conjunction with the APC mNLS mice, we will also characterize the role of APC in DNA maintenance. By exposing cultured epithelial cells to ultraviolet light to induce pyrimidine dimers and observing APC during the cellular response to DNA damage we hope to further define the role that APC plays in this process. With these

model systems we will further delineate the function of APC in the nucleus to provide a better understanding of its role as a tumor suppressor.

References

1. Ross, M. H., and Pawlina, W. (2005) *Histology: A text and atlas*, Lippincott Williams & Wilkins, Baltimore, MD
2. Weinberg, R. A. (2007) *The Biology of Cancer*, Garland Science, Taylor & Francis Group, New York
3. Society, A. C. (2007) American Cancer Society. *Cancer Facts & Figures 2007* Atlanta
4. Specian, R. D., and Oliver, M. G. (1991) Functional biology of intestinal goblet cells. *Am J Physiol* 260, C183-193
5. Ouellette, A. J. (1997) Paneth cells and innate immunity in the crypt microenvironment. *Gastroenterology* 113, 1779-1784
6. Dockray, G. J. (2003) Luminal sensing in the gut: an overview. *J Physiol Pharmacol* 54 Suppl 4, 9-17
7. Miller, H., Zhang, J., Kuolee, R., Patel, G. B., and Chen, W. (2007) Intestinal M cells: the fallible sentinels? *World J Gastroenterol* 13, 1477-1486
8. Bach, S. P., Renehan, A. G., and Potten, C. S. (2000) Stem cells: the intestinal stem cell as a paradigm. *Carcinogenesis* 21, 469-476
9. Barker, N., van Es, J. H., Kuipers, J., Kujala, P., van den Born, M., Cozijnsen, M., Haegebarth, A., Korving, J., Begthel, H., Peters, P. J., and Clevers, H. (2007) Identification of stem cells in small intestine and colon by marker gene Lgr5. *Nature* 449, 1003-1007
10. Sansom, O. J., Reed, K. R., Hayes, A. J., Ireland, H., Brinkmann, H., Newton, I. P., Batlle, E., Simon-Assmann, P., Clevers, H., Nathke, I. S., Clarke, A. R., and Winton, D. J. (2004) Loss of Apc in vivo immediately perturbs Wnt signaling, differentiation, and migration. *Genes Dev* 18, 1385-1390
11. Sancho, E., Batlle, E., and Clevers, H. (2004) Signaling pathways in intestinal development and cancer. *Annu Rev Cell Dev Biol* 20, 695-723
12. Hanahan, D., and Weinberg, R. A. (2000) The hallmarks of cancer. *Cell* 100, 57-70
13. Matulic, M., Sopta, M., and Rubelj, I. (2007) Telomere dynamics: the means to an end. *Cell Prolif* 40, 462-474
14. Loeb, L. A. (1991) Mutator phenotype may be required for multistage carcinogenesis. *Cancer Res* 51, 3075-3079
15. Fearon, E. R., and Vogelstein, B. (1990) A genetic model for colorectal tumorigenesis. *Cell* 61, 759-767

16. Midgley, C. A., White, S., Howitt, R., Save, V., Dunlop, M. G., Hall, P. A., Lane, D. P., Wyllie, A. H., and Bubb, V. J. (1997) APC expression in normal human tissues. *J Pathol* 181, 426-433
17. Groden, J., Thliveris, A., Samowitz, W., Carlson, M., Gelbert, L., Albertsen, H., Joslyn, G., Stevens, J., Spirio, L., Robertson, M., and et al. (1991) Identification and characterization of the familial adenomatous polyposis coli gene. *Cell* 66, 589-600
18. Nishisho, I., Nakamura, Y., Miyoshi, Y., Miki, Y., Ando, H., Horii, A., Koyama, K., Utsunomiya, J., Baba, S., and Hedge, P. (1991) Mutations of chromosome 5q21 genes in FAP and colorectal cancer patients. *Science* 253, 665-669
19. Kinzler, K. W., Nilbert, M. C., Su, L. K., Vogelstein, B., Bryan, T. M., Levy, D. B., Smith, K. J., Preisinger, A. C., Hedge, P., McKechnie, D., and et al. (1991) Identification of FAP locus genes from chromosome 5q21. *Science* 253, 661-665
20. Petersen, G. M., Brensinger, J. D., Johnson, K. A., and Giardiello, F. M. (1999) Genetic testing and counseling for hereditary forms of colorectal cancer. *Cancer* 86, 2540-2550
21. Smith, K. J., Johnson, K. A., Bryan, T. M., Hill, D. E., Markowitz, S., Willson, J. K., Paraskeva, C., Petersen, G. M., Hamilton, S. R., Vogelstein, B., and et al. (1993) The APC gene product in normal and tumor cells. *Proc Natl Acad Sci U S A* 90, 2846-2850
22. Powell, S. M., Zilz, N., Beazer-Barclay, Y., Bryan, T. M., Hamilton, S. R., Thibodeau, S. N., Vogelstein, B., and Kinzler, K. W. (1992) APC mutations occur early during colorectal tumorigenesis. *Nature* 359, 235-237
23. Galiatsatos, P., and Foulkes, W. D. (2006) Familial adenomatous polyposis. *Am J Gastroenterol* 101, 385-398
24. Nagase, H., and Nakamura, Y. (1993) Mutations of the APC (adenomatous polyposis coli) gene. *Hum Mutat* 2, 425-434
25. Lal, G., and Gallinger, S. (2000) Familial adenomatous polyposis. *Semin Surg Oncol* 18, 314-323
26. van Es, J. H., Giles, R. H., and Clevers, H. C. (2001) The many faces of the tumor suppressor gene APC. *Exp Cell Res* 264, 126-134
27. Nathke, I. S. (2004) The adenomatous polyposis coli protein: the Achilles heel of the gut epithelium. *Annu Rev Cell Dev Biol* 20, 337-366
28. Neufeld, K. L., Nix, D. A., Bogerd, H., Kang, Y., Beckerle, M. C., Cullen, B. R., and White, R. L. (2000) Adenomatous polyposis coli protein contains two nuclear export signals and shuttles between the nucleus and cytoplasm. *Proc Natl Acad Sci U S A* 97, 12085-12090
29. Henderson, B. R. (2000) Nuclear-cytoplasmic shuttling of APC regulates beta-catenin subcellular localization and turnover. *Nat Cell Biol* 2, 653-660
30. Peifer, M., Berg, S., and Reynolds, A. B. (1994) A repeating amino acid motif shared by proteins with diverse cellular roles. *Cell* 76, 789-791

31. Galea, M. A., Eleftheriou, A., and Henderson, B. R. (2001) ARM domain-dependent nuclear import of adenomatous polyposis coli protein is stimulated by the B56 alpha subunit of protein phosphatase 2A. *J Biol Chem* 276, 45833-45839
32. Kawasaki, Y., Senda, T., Ishidate, T., Koyama, R., Morishita, T., Iwayama, Y., Higuchi, O., and Akiyama, T. (2000) Asef, a link between the tumor suppressor APC and G-protein signaling. *Science* 289, 1194-1197
33. Watanabe, T., Wang, S., Noritake, J., Sato, K., Fukata, M., Takefuji, M., Nakagawa, M., Izumi, N., Akiyama, T., and Kaibuchi, K. (2004) Interaction with IQGAP1 links APC to Rac1, Cdc42, and actin filaments during cell polarization and migration. *Dev Cell* 7, 871-883
34. Jimbo, T., Kawasaki, Y., Koyama, R., Sato, R., Takada, S., Haraguchi, K., and Akiyama, T. (2002) Identification of a link between the tumour suppressor APC and the kinesin superfamily. *Nat Cell Biol* 4, 323-327
35. Behrens, J., Jerchow, B. A., Wurtele, M., Grimm, J., Asbrand, C., Wirtz, R., Kuhl, M., Wedlich, D., and Birchmeier, W. (1998) Functional interaction of an axin homolog, conductin, with beta-catenin, APC, and GSK3beta. *Science* 280, 596-599
36. Zhang, F., White, R. L., and Neufeld, K. L. (2000) Phosphorylation near nuclear localization signal regulates nuclear import of adenomatous polyposis coli protein. *Proc Natl Acad Sci U S A* 97, 12577-12582
37. Rosin-Arbesfeld, R., Townsley, F., and Bienz, M. (2000) The APC tumour suppressor has a nuclear export function. *Nature* 406, 1009-1012
38. Deka, J., Kuhlmann, J., and Muller, O. (1998) A domain within the tumor suppressor protein APC shows very similar biochemical properties as the microtubule-associated protein tau. *Eur J Biochem* 253, 591-597
39. Matsumine, A., Ogai, A., Senda, T., Okumura, N., Satoh, K., Baeg, G. H., Kawahara, T., Kobayashi, S., Okada, M., Toyoshima, K., and Akiyama, T. (1996) Binding of APC to the human homolog of the Drosophila discs large tumor suppressor protein. *Science* 272, 1020-1023
40. Erdmann, K. S., Kuhlmann, J., Lessmann, V., Herrmann, L., Eulenburg, V., Muller, O., and Heumann, R. (2000) The Adenomatous Polyposis Coli-protein (APC) interacts with the protein tyrosine phosphatase PTP-BL via an alternatively spliced PDZ domain. *Oncogene* 19, 3894-3901
41. Liu, J., Stevens, J., Rote, C. A., Yost, H. J., Hu, Y., Neufeld, K. L., White, R. L., and Matsunami, N. (2001) Siah-1 mediates a novel beta-catenin degradation pathway linking p53 to the adenomatous polyposis coli protein. *Mol Cell* 7, 927-936
42. Fodde, R., Kuipers, J., Rosenberg, C., Smits, R., Kielman, M., Gaspar, C., van Es, J. H., Breukel, C., Wiegant, J., Giles, R. H., and Clevers, H. (2001) Mutations in the APC tumour suppressor gene cause chromosomal instability. *Nat Cell Biol* 3, 433-438

43. Nathke, I. S., Adams, C. L., Polakis, P., Sellin, J. H., and Nelson, W. J. (1996) The adenomatous polyposis coli tumor suppressor protein localizes to plasma membrane sites involved in active cell migration. *J Cell Biol* 134, 165-179
44. Neufeld, K. L., and White, R. L. (1997) Nuclear and cytoplasmic localizations of the adenomatous polyposis coli protein. *Proc Natl Acad Sci U S A* 94, 3034-3039
45. Yang, J., Zhang, W., Evans, P. M., Chen, X., He, X., and Liu, C. (2006) Adenomatous polyposis coli (APC) differentially regulates beta-catenin phosphorylation and ubiquitination in colon cancer cells. *J Biol Chem* 281, 17751-17757
46. Nathke, I. (2006) Cytoskeleton out of the cupboard: colon cancer and cytoskeletal changes induced by loss of APC. *Nat Rev Cancer* 6, 967-974
47. Jaiswal, A. S., Balusu, R., Armas, M. L., Kundu, C. N., and Narayan, S. (2006) Mechanism of Adenomatous Polyposis Coli (APC)-Mediated Blockage of Long-Patch Base Excision Repair. *Biochemistry* 45, 15903-15914
48. Kielman, M. F., Rindapaa, M., Gaspar, C., van Poppel, N., Breukel, C., van Leeuwen, S., Taketo, M. M., Roberts, S., Smits, R., and Fodde, R. (2002) Apc modulates embryonic stem-cell differentiation by controlling the dosage of beta-catenin signaling. *Nat Genet* 32, 594-605
49. Sierra, J., Yoshida, T., Joazeiro, C. A., and Jones, K. A. (2006) The APC tumor suppressor counteracts beta-catenin activation and H3K4 methylation at Wnt target genes. *Genes Dev* 20, 586-600
50. Korinek, V., Barker, N., Morin, P. J., van Wichen, D., de Weger, R., Kinzler, K. W., Vogelstein, B., and Clevers, H. (1997) Constitutive Transcriptional Activation by a beta -Catenin-Tcf Complex in APC-/- Colon Carcinoma. *Science* 275, 1784-1787
51. Qian, J., Steigerwald, K., Combs, K. A., Barton, M. C., and Groden, J. (2007) Caspase cleavage of the APC tumor suppressor and release of an amino-terminal domain is required for the transcription-independent function of APC in apoptosis. *Oncogene*
52. Chen, T., Yang, I., Irby, R., Shain, K. H., Wang, H. G., Quackenbush, J., Coppola, D., Cheng, J. Q., and Yeatman, T. J. (2003) Regulation of caspase expression and apoptosis by adenomatous polyposis coli. *Cancer Res* 63, 4368-4374
53. Dierick, H., and Bejsovec, A. (1999) Cellular mechanisms of wingless/Wnt signal transduction. *Curr Top Dev Biol* 43, 153-190
54. Kolligs, F. T., Bommer, G., and Goke, B. (2002) Wnt/beta-catenin/tcf signaling: a critical pathway in gastrointestinal tumorigenesis. *Digestion* 66, 131-144
55. Albuquerque, C., Breukel, C., van der Luijt, R., Fidalgo, P., Lage, P., Slors, F. J., Leitao, C. N., Fodde, R., and Smits, R. (2002) The 'just-right' signaling model: APC somatic mutations are selected based on a specific level of activation of the beta-catenin signaling cascade. *Hum Mol Genet* 11, 1549-1560

56. Neufeld, K. L., Zhang, F., Cullen, B. R., and White, R. L. (2000) APC-mediated downregulation of beta-catenin activity involves nuclear sequestration and nuclear export. *EMBO Rep* 1, 519-523
57. Xing, Y., Clements, W. K., Le Trong, I., Hinds, T. R., Stenkamp, R., Kimelman, D., and Xu, W. (2004) Crystal structure of a beta-catenin/APC complex reveals a critical role for APC phosphorylation in APC function. *Mol Cell* 15, 523-533
58. Taketo, M. M. (2006) Wnt signaling and gastrointestinal tumorigenesis in mouse models. *Oncogene* 25, 7522-7530
59. Narayan, S., Jaiswal, A. S., and Balusu, R. (2005) Tumor suppressor APC blocks DNA polymerase beta-dependent strand displacement synthesis during long patch but not short patch base excision repair and increases sensitivity to methylmethane sulfonate. *J Biol Chem* 280, 6942-6949
60. Wang, Y., Moore, D., Azuma, Y., and Neufeld, K. L. (Manuscript submitted) Tumor Suppressor APC interacts with Topoisomerase IIα PCNA: Implications for G2/M Transition.
61. Samowitz, W. S., Powers, M. D., Spirio, L. N., Nollet, F., van Roy, F., and Slattery, M. L. (1999) Beta-catenin mutations are more frequent in small colorectal adenomas than in larger adenomas and invasive carcinomas. *Cancer Res* 59, 1442-1444
62. Kinsella, T. J., Little, J. B., Nove, J., Weichselbaum, R. R., Li, F. P., Meyer, R. J., Marchetto, D. J., and Patterson, W. B. (1982) Heterogeneous response to X-ray and ultraviolet light irradiations of cultured skin fibroblasts in two families with Gardner's Syndrome. *J Natl Cancer Inst* 68, 697-701
63. Luongo, C., and Dove, W. F. (1996) Somatic genetic events linked to the Apc locus in intestinal adenomas of the Min mouse. *Genes Chromosomes Cancer* 17, 194-198
64. Narayan, S., and Jaiswal, A. S. (1997) Activation of adenomatous polyposis coli (APC) gene expression by the DNA-alkylating agent N-methyl-N'-nitro-N-nitrosoguanidine requires p53. *J Biol Chem* 272, 30619-30622
65. Jaiswal, A. S., and Narayan, S. (2001) p53-dependent transcriptional regulation of the APC promoter in colon cancer cells treated with DNA alkylating agents. *J Biol Chem* 276, 18193-18199
66. Yang, K., Edelmann, W., Fan, K., Lau, K., Kolli, V. R., Fodde, R., Khan, P. M., Kucherlapati, R., and Lipkin, M. (1997) A mouse model of human familial adenomatous polyposis. *J Exp Zool* 277, 245-254
67. Kucherlapati, M., Yang, K., Kuraguchi, M., Zhao, J., Lia, M., Heyer, J., Kane, M. F., Fan, K., Russell, R., Brown, A. M., Kneitz, B., Edelmann, W., Kolodner, R. D., Lipkin, M., and Kucherlapati, R. (2002) Haploinsufficiency of Flap endonuclease (Fen1) leads to rapid tumor progression. *Proc Natl Acad Sci U S A* 99, 9924-9929
68. Sancar, A., Lindsey-Boltz, L. A., Unsal-Kacmaz, K., and Linn, S. (2004) Molecular mechanisms of mammalian DNA repair and the DNA damage checkpoints. *Annu Rev Biochem* 73, 39-85

69. Kim, K., Biade, S., and Matsumoto, Y. (1998) Involvement of flap endonuclease 1 in base excision DNA repair. *J Biol Chem* 273, 8842-8848
70. Tishkoff, D. X., Boerger, A. L., Bertrand, P., Filosi, N., Gaida, G. M., Kane, M. F., and Kolodner, R. D. (1997) Identification and characterization of Saccharomyces cerevisiae EXO1, a gene encoding an exonuclease that interacts with MSH2. *Proc Natl Acad Sci U S A* 94, 7487-7492
71. Kucherlapati, M., Nguyen, A., Kuraguchi, M., Yang, K., Fan, K., Bronson, R., Wei, K., Lipkin, M., Edelmann, W., and Kucherlapati, R. (2007) Tumor progression in Apc(1638N) mice with Exo1 and Fen1 deficiencies. *Oncogene* 26, 6297-6306
72. Corpet, D. E., and Pierre, F. (2003) Point: From animal models to prevention of colon cancer. Systematic review of chemoprevention in min mice and choice of the model system. *Cancer Epidemiol Biomarkers Prev* 12, 391-400
73. Moser, A. R., Pitot, H. C., and Dove, W. F. (1990) A dominant mutation that predisposes to multiple intestinal neoplasia in the mouse. *Science* 247, 322-324
74. Su, L. K., Kinzler, K. W., Vogelstein, B., Preisinger, A. C., Moser, A. R., Luongo, C., Gould, K. A., and Dove, W. F. (1992) Multiple intestinal neoplasia caused by a mutation in the murine homolog of the APC gene. *Science* 256, 668-670
75. Moser, A. R., Shoemaker, A. R., Connelly, C. S., Clipson, L., Gould, K. A., Luongo, C., Dove, W. F., Siggers, P. H., and Gardner, R. L. (1995) Homozygosity for the Min allele of Apc results in disruption of mouse development prior to gastrulation. *Dev Dyn* 203, 422-433
76. Dietrich, W. F., Lander, E. S., Smith, J. S., Moser, A. R., Gould, K. A., Luongo, C., Borenstein, N., and Dove, W. (1993) Genetic identification of Mom-1, a major modifier locus affecting Min-induced intestinal neoplasia in the mouse. *Cell* 75, 631-639
77. Haines, J., Johnson, V., Pack, K., Suraweera, N., Slijepcevic, P., Cabuy, E., Coster, M., Ilyas, M., Wilding, J., Sieber, O., Bodmer, W., Tomlinson, I., and Silver, A. (2005) Genetic basis of variation in adenoma multiplicity in ApcMin/+ Mom1S mice. *Proc Natl Acad Sci U S A* 102, 2868-2873
78. Moser, A. R., Dove, W. F., Roth, K. A., and Gordon, J. I. (1992) The Min (multiple intestinal neoplasia) mutation: its effect on gut epithelial cell differentiation and interaction with a modifier system. *J Cell Biol* 116, 1517-1526
79. Bilger, A., Shoemaker, A. R., Gould, K. A., and Dove, W. F. (1996) Manipulation of the mouse germline in the study of Min-induced neoplasia. *Semin Cancer Biol* 7, 249-260
80. MacPhee, M., Chepenik, K. P., Liddell, R. A., Nelson, K. K., Siracusa, L. D., and Buchberg, A. M. (1995) The secretory phospholipase A2 gene is a candidate for the Mom1 locus, a major modifier of ApcMin-induced intestinal neoplasia. *Cell* 81, 957-966

81. Silverman, K. A., Koratkar, R., Siracusa, L. D., and Buchberg, A. M. (2002) Identification of the modifier of Min 2 (Mom2) locus, a new mutation that influences Apc-induced intestinal neoplasia. *Genome Res* 12, 88-97
82. Babinet, C., and Cohen-Tannoudji, M. (2001) Genome engineering via homologous recombination in mouse embryonic stem (ES) cells: an amazingly versatile tool for the study of mammalian biology. *An Acad Bras Cienc* 73, 365-383
83. Fodde, R., Edelmann, W., Yang, K., van Leeuwen, C., Carlson, C., Renault, B., Breukel, C., Alt, E., Lipkin, M., Khan, P. M., and et al. (1994) A targeted chain-termination mutation in the mouse Apc gene results in multiple intestinal tumors. *Proc Natl Acad Sci U S A* 91, 8969-8973
84. Smits, R., Kielman, M. F., Breukel, C., Zurcher, C., Neufeld, K., Jagmohan-Changur, S., Hofland, N., van Dijk, J., White, R., Edelmann, W., Kucherlapati, R., Khan, P. M., and Fodde, R. (1999) Apc1638T: a mouse model delineating critical domains of the adenomatous polyposis coli protein involved in tumorigenesis and development. *Genes Dev* 13, 1309-1321
85. Smits, R., Kartheuser, A., Jagmohan-Changur, S., Leblanc, V., Breukel, C., de Vries, A., van Kranen, H., van Krieken, J. H., Williamson, S., Edelmann, W., Kucherlapati, R., KhanPm, and Fodde, R. (1997) Loss of Apc and the entire chromosome 18 but absence of mutations at the Ras and Tp53 genes in intestinal tumors from Apc1638N, a mouse model for Apc-driven carcinogenesis. *Carcinogenesis* 18, 321-327
86. Smits, R., van der Houven van Oordt, W., Luz, A., Zurcher, C., Jagmohan-Changur, S., Breukel, C., Khan, P. M., and Fodde, R. (1998) Apc1638N: a mouse model for familial adenomatous polyposis-associated desmoid tumors and cutaneous cysts. *Gastroenterology* 114, 275-283
87. Itoh, M., Maeno, A., Tari, A., Itoh, S., Kawakami, A., Sawada, M., Ohno, T., and Noda, T. (2000) Genetic Analysis of Modifier Genes which Influence the Tumor Multiplicity in FAP Model Mice. In The 14th International Mouse Genome Confrence
88. Quesada, C. F., Kimata, H., Mori, M., Nishimura, M., Tsuneyoshi, T., and Baba, S. (1998) Piroxicam and acarbose as chemopreventive agents for spontaneous intestinal adenomas in APC gene 1309 knockout mice. *Jpn J Cancer Res* 89, 392-396
89. Oshima, M., Oshima, H., Kitagawa, K., Kobayashi, M., Itakura, C., and Taketo, M. (1995) Loss of Apc heterozygosity and abnormal tissue building in nascent intestinal polyps in mice carrying a truncated Apc gene. *Proc Natl Acad Sci U S A* 92, 4482-4486
90. Colnot, S., Niwa-Kawakita, M., Hamard, G., Godard, C., Le Plenier, S., Houbron, C., Romagnolo, B., Berrebi, D., Giovannini, M., and Perret, C. (2004) Colorectal cancers in a new mouse model of familial adenomatous polyposis: influence of genetic and environmental modifiers. *Lab Invest* 84, 1619-1630

91. Santoro, I. M., and Groden, J. (1997) Alternative splicing of the APC gene and its association with terminal differentiation. *Cancer Res* 57, 488-494
92. Sasai, H., Masaki, M., and Wakitani, K. (2000) Suppression of polypogenesis in a new mouse strain with a truncated Apc(Delta474) by a novel COX-2 inhibitor, JTE-522. *Carcinogenesis* 21, 953-958
93. Stevens, L. C. (1970) The development of transplantable teratocarcinomas from intratesticular grafts of pre- and postimplantation mouse embryos. *Dev Biol* 21, 364-382
94. Martin, G. R. (1980) Teratocarcinomas and mammalian embryogenesis. *Science* 209, 768-776
95. Shibata, H., Toyama, K., Shioya, H., Ito, M., Hirota, M., Hasegawa, S., Matsumoto, H., Takano, H., Akiyama, T., Toyoshima, K., Kanamaru, R., Kanegae, Y., Saito, I., Nakamura, Y., Shiba, K., and Noda, T. (1997) Rapid colorectal adenoma formation initiated by conditional targeting of the Apc gene. *Science* 278, 120-123
96. Ishikawa, T. O., Tamai, Y., Li, Q., Oshima, M., and Taketo, M. M. (2003) Requirement for tumor suppressor Apc in the morphogenesis of anterior and ventral mouse embryo. *Dev Biol* 253, 230-246
97. Li, Q., Ishikawa, T. O., Oshima, M., and Taketo, M. M. (2005) The threshold level of adenomatous polyposis coli protein for mouse intestinal tumorigenesis. *Cancer Res* 65, 8622-8627
98. Schlenstedt, G. (1996) Protein import into the nucleus. *FEBS Lett* 389, 75-79

CHAPTER 2

GENERATION OF THE APC mNLS MOUSE: AN ANIMAL MODEL DEFECTIVE IN NUCLEAR IMPORT OF APC

Abstract

To evaluate how nuclear APC is involved in the homeostasis of the intestinal epithelium, a mouse model with specific inactivating mutations in the nuclear localization signals (NLS) of *Apc* was generated. *In vitro*, these mutations inhibit the nuclear import of APC protein (1). The generation of a mouse model containing these NLS mutations in the endogenously expressed APC protein is described in this chapter.

Introduction

The Innovation of Mouse Transgenics

The ability to generate transgenic mice has revolutionized the use of the mouse as a model organism. The contribution of this technology to advancing scientific discovery has been so significant that the 2007 Nobel Prize in physiology or medicine was awarded to Drs. Capecchi, Evans and Smithies for their work developing the techniques that make murine transgenics possible. These techniques enable an investigator to introduce specific mutations into particular genes of interest and study how those alterations influence growth, development and tissue maintenance in a whole-animal mammalian model system. The process of creating a transgenic mouse involves a number of steps, each of which exploits the innate cellular machinery and properties of mouse embryonic stem cells.

The first mouse embryonic stem (ES) cells to be successfully grown in culture were isolated from the inner cell mass of the early embryo in 1981 (2, 3). These pluripotent cell lines possess a number of unique properties that lend themselves to the creation of transgenic animals. First, ES cells contain the capacity for nearly unlimited self-renewal in culture while maintaining a normal diploid genotype as well as their pluripotency (2, 3). While this alone is enough to make mouse ES cells a valuable tool for tissue culture, their significance is further enhanced by their ability to undergo cellular process of homologous recombination. Homologous recombination is an inherent method by which the cell can repair DNA damage by using the homologous undamaged allele on the sister chromatid (4). Exploitation of

homologous recombination by introducing exogenous DNA with sequence nearly homologous to a gene of interest facilitates the insertion of engineered mutations into the targeted gene (5). Using this method to precisely alter the genome allows investigators to produce ES cells of virtually any genotype. ES cells altered in this way can be induced to undergo differentiation in culture to produce cell types of all three germ layers, allowing further exploration of the effect of the mutation on the cellular processes required in more differentiated tissues (2). Moreover, genetically altered ES cells can be re-introduced into an early embryo where they colonize the tissues of the growing animal (6). These exogenous cells, when injected into the hollow portion of young embryos, incorporate into the inner cell mass where they give rise to all of the cell types of the growing mouse, including the germ line cells (6). In this way mouse lines can be created with specifically engineered genotypes, allowing investigators to collect information about the function of their gene of interest in a whole animal, information that would be impossible to obtain using tissue culture cells alone.

The Process of Creating a Transgenic Mouse

The first step in the creation of a transgenic mouse model is to specifically alter the genotype of mouse embryonic stem cells in culture. This requires the design and creation of a gene replacement vector, a DNA plasmid which is then carried into the nuclear compartment via microinjection or electroporation (5). This plasmid must contain all of the genetic material that needs to be introduced into the cells. This

includes not only the sequences necessary to introduce a specific mutation via homologous recombination, but also the sequences that will allow subsequent selection and screening of the engineered ES cells. Even under optimal conditions, the likelihood that a targeting vector will correctly alter the cellular DNA and give rise to the desired genotype is nearly 1 in 1000 (5). For this reason, selectable markers, usually in the form of drug resistance genes, have become an essential component of DNA constructs used for targeted genetic manipulation. Targeting constructs generally contain both a positive selector, and a negative selector, to select for cells that have incorporated the targeted sequence into the genome, and to select against random insertions, respectively (7).

While the initial elimination of incorrect recombinants using the incorporated selectable markers greatly reduces the number of cell lines that must be screened, it does not eliminate the need to verify that the remaining cells have undergone the desired recombination. The early method of choice for screening the remaining potential cell lines was to use Southern blot analysis to verify that the desired mutation had been accurately introduced into the target gene (5). More recently, however, it has also become common for investigators to use PCR as a method to screen and verify correct cell lines (8-10).

After cell lines that contain the appropriate mutation in their genome have been identified, those cell lines are further assessed to identify which of them are the most suitable for creating a mouse model. At this stage, the ES cells have grown in culture, endured either microinjection or electroporation and have grown in selective

media (8). These factors increase the probability that the cells have acquired additional genetic alterations, so an initial characterization of the cell lines is recommended before continuing on to the next steps in the process (8).

It is very important that the cells injected into the blastocysts are euploid, so the candidate transgenic cell lines must be karyotyped to assure that they have maintained the correct number of chromosomes. The possibility of random mutation in addition to the targeted mutation is another concern (11). For this reason it is desirable to have multiple cell lines with the correct gene mutation, which allows the growth and phenotype of these duplicate lines to be compared to each other. While it is possible that some of the cell lines may have additional mutations to the genome, it is unlikely that more than one cell line will have acquired the same random mutation. Though the phenotype of the transgenic cells might differ from the parental wild type (WT) ES cells, any altered characteristics not shared by the majority of the transgenic lines are likely due to random genetic alterations. Cell lines displaying a dramatically different phenotype should not be used to make chimeric mice (11). It is possible that random alterations may be subtle enough so as to present no noticeable effect at the level of the ES cells and must be eliminated at a later stage. For this reason, once chimeric mice are generated multiple generations of breeding to mice from an inbred WT line ensures that the resulting mouse line is congenic, differing from WT only at the selected locus (12).

The cell line(s) that qualify for further investigation can be utilized in a number of ways. The transgenic ES cells can be further evaluated in culture

employing the ability of ES cells to self-renew indefinitely as well as their potential to become a variety of more differentiated cell types. In some cases, the transgenic cells, which are heterozygous for the desired mutation, are used in a second round of selection to produce cell lines that are homozygous for the targeted mutation. However, the main goal in creating ES cells is usually the production of a mouse line. For this procedure, early embryos are isolated from a pregnant female approximately 3 days after mating. At this phase, the embryo consists of a ball of cells called the blastocyst. Within the ball is a hollow cavity known as the blastocoel and the inner cell mass made up of pluripotent embryonic stem cells (8). Cells of the transgenic line that are microinjected into the blastocoel will incorporate into the inner cell mass (6). These chimeric embryos are then implanted into a pseudopregnant female where they will continue to develop into chimeric mice. The tissues of these chimeras, including the gonads, are made up of a mixture of both the endogenous stem cells of the original blastocyst and the transgenic stem cells introduced by microinjection(6).

Most ES cell lines used for genetic manipulation are derived from male embryos and therefore carry an X and a Y chromosome (11). When these male cells are injected into an early embryo several outcomes may arise depending on the sex of the embryo and the number of transgenic cells that successfully incorporate into the inner cells mass. When male transgenic cells are injected into a male embryo, the cells combine to form a male mouse (11). The sperm cells of that mouse can be derived from either the transgenic cells or the endogenous cells of the embryo; accordingly the progeny will be a mixture of mice that are transgenic and mice that

carry only WT genomic sequence. When male transgenic cells are injected into a female embryo, the sex of the resulting mouse will be dependent on the level of incorporation of the transgenic cells. If the male transgenic cells and female endogenous cells make up approximately equal portions of the resulting chimeric embryo, the mouse will display characteristics of both sexes and will likely be infertile. If there are more of the endogenous female cells present, the mouse will display female sex characteristics only. She may be fertile but will only rarely give rise to any transgenic progeny because the female stem cells, not the male transgenic cells, will give rise to the majority of the reproductive organs and germline cells of the female mouse. However, if the embryo is female but the male transgenic cells contribute to more of the inner cell mass, the resulting mouse will be physiologically male and if fertile, will give rise to only transgenic progeny. In this case the endogenous female stem cells will be unable to give rise to any portion of the male reproductive organs and germline cells, therefore all of the sperm will be derived from the targeted ES cells.

Progeny of the chimeric mice must be screened for the presence of the targeted mutation and mated with an inbred wild type mouse strain of choice. This series of backcrosses is required because there is enough variation between mouse strains that it is seldom possible to distinguish more subtle effects of a targeted mutation from background differences between mice (12). To be sure that the phenotype being observed is a consequence of the targeted mutation with no contributions from other genes, it is essential that the mutant and WT mice differ

genetically at only the locus being targeted. Mouse strains that have been bred with an inbred strain for multiple generations until they differ only in a selected differential chromosomal segment are called *congenic* strains. Statistically, by the 5th generation of crosses the developing congenic line will be identical to the inbred line across 94% of the genome. By the 10th generation that identity will have increased to 99.8% of the genome at which point the mouse strain can be considered congenic (12). This process not only eliminates the natural variations that exist between outbred mice, it also eliminates any genetic variation that may have been introduced during the electroporation and subsequent selection of the initial ES cell line used to create the mouse model.

Materials and Methods

Creating the Gene Replacement Vector

The homologous sequences of DNA used for this construct were obtained from a lambda phage library of genomic DNA isolated from mouse 129 ES cells (generously provided by Kirk Thomas and Mario Cappechi, University of Utah). This library was screened for fragments of *Apc* containing the primary *Apc* nuclear localization sites (NLSs). Following identification of a correct plaque by hybridization to a radioactive probe, 14kb of mouse genomic DNA (*Apc* exons 14, 15 and surrounding introns) were cloned from the phage and inserted into a pBluescript KSII+ vector (Stratagene). An EcoRI fragment containing both NLSs was subcloned into a pUC19 vector where mutations that both inactivated the NLSs and introduced

novel restriction sites were inserted by PCR mutagenesis. A second pUC19 vector was modified to destroy its EcoRI restriction site and introduce Nhe I and Not I sites. An 11,537 bp region of *Apc* (NheI/NotI) was then subcloned into this modified vector. The EcoRI fragment of *Apc* containing the mutant NLSs was then introduced into this vector in place of the WT NLSs. A neomycin resistance (Neo^r) gene driven by the promoter for RNA polymerase II and linked to a gene encoding Cre-recombinase driven by the testes-specific murine angiotensin-converting enzyme (tACE) promoter (13) made up the tACE-Cre-Neo^r cassette. This cassette which was also flanked by two LoxP sites was introduced into the pUC19 vector containing the mNLS *Apc* gene fragment between restriction sites for KpnI and AflII in the non-coding region 3' of exon 15. The HSV thymidine kinase gene driven by the PGK promoter was inserted upstream of the APC homology sequences in the pUC19 vector to create the 19,947 bp targeting vector (Figure 2.1).

Electroporation into Embryonic Stem Cells

Once completed, the targeting construct was linearized in a large scale digestion with Not I restriction endonuclease, to cleave the DNA at a unique site 3' of the region homologous to *Apc*. Digestion was followed by two phenol/chloroform extractions before the linear gene replacement vector was electroporated into R1 mouse embryonic stem cells (14) at the Transgenic and Gene-Targeting Institutional Facility at The University of Kansas Medical Center. Cells were selected for growth in 300μg/mL G418 (Cellgro) and 2μM ganciclovir (Roche). Following 8-10 days of

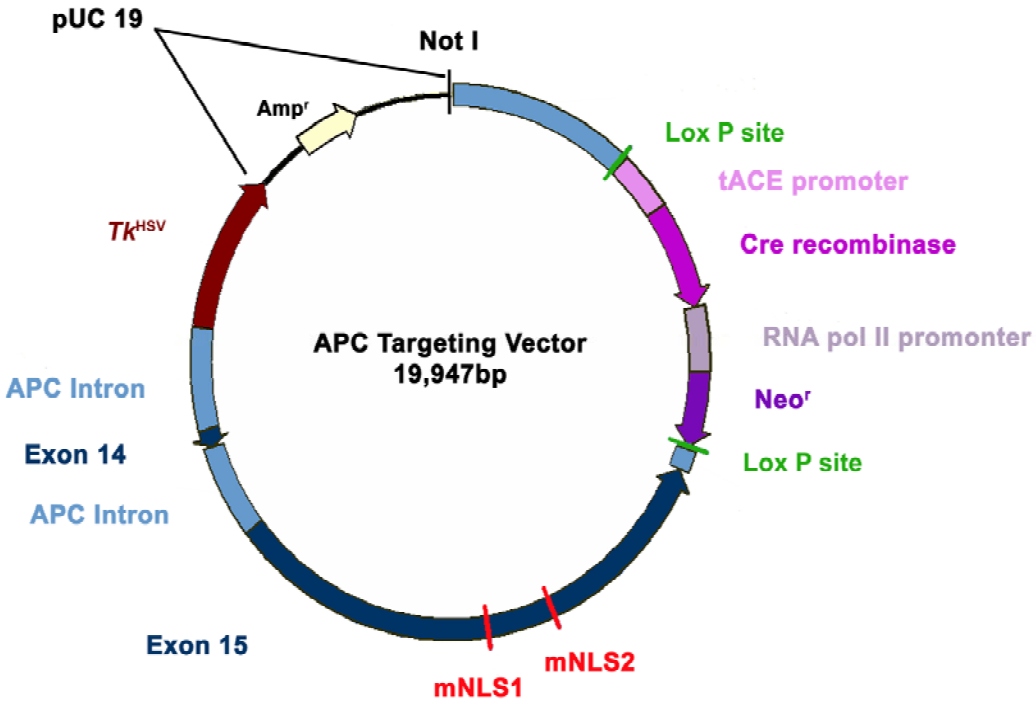

Figure 2.1
A diagram of the targeting vector with the components labeled by color and the mNLS sites indicated in red.

culture in selective medium colonies were picked and expanded into two separate wells. DNA was isolated from one well for genotypic analysis and the cells in the remaining well were frozen in 96 well plates while the DNA was analyzed.

Maintaining Stem Cells in Culture

Wild type and electroporated R1 mouse embryonic stem cells were received from the KU Medical Center and grown in ES media [81% High Glucose DMEM (Gibco), 15% Fetal Bovine Serum (ES cell certified from Hyclone), 1mM sodium pyruvate (Gibco), 0.1mM Non-essential amino acids (Gibco), 100ng/ml of ESGRO (Chemicon), 2mM L-glutamine (Gibco), 0.01mM 2-mercaptoethanol (Fisher)] in a 37°C water jacketed incubator with 7% CO_2. Cells were split ~1:9 every 2 to 3 days as needed and plated directly on a mitomycin C-treated mouse fibroblast feeder layer.

Screening ES cell lines

PCR was used to identify the correct recombinants. Identification of ES cell lines containing mutations in APC NLSs was accomplished using a two step PCR screen and the following primer sets. Step 1: to the WT NLS1 (5'-CTA AGA AAA AGA AGC CTA CTT CAC), to the WT NLS2 (5'-GGC CTT TTC TTT TTT GGC ATG GC), to the mNLS1 (5'-GCA GCC GCG GCA CCT ACT) and to the mNLS2 (5'-TTG AAG GCC TTT TTG CGG CC) (Figure 2.2). Step 2: to a portion of the LoxP/tACE promoter region of the tACE, Cre, Neo cassette (5'-CCT GGCC CCA

TGG AGA TCC AT) and to a region of genomic APC 3' of the targeting construct (5'-CAT ACC ACC CAC CAT CCC TA) (Figure 2.3).

Verifying the ES cell lines

Cell lines that were determined to be correct homologous recombinants were further evaluated based on karyotype, growth rate and β-catenin transcriptional activity (See chapter 3 for a more detailed discussion of the analysis of the APC NLS mutation in cultured cells). Prior to generation of chimeric mice, candidate cell lines were screened for the correct incorporation of the 5' side of the targeting construct using PCR. The primers to the mNLS2 and WT NLS2 previously described were used in conjunction with the following primer to a region of genomic DNA beyond the 5' end of the targeting construct: (5'-AAA TTG AAC TCA GGA CCT TCT C) (Figure 2.4)

Generation of Chimeric Mice

The first mutant stem cell line that was chosen based on criteria further described in Chapter 4. For the generation of chimeric mice APC mNLS cells of the chosen line were injected into C57BL/6J blastocysts at the Gene-Targeting and Transgenic Facility at the University of Virginia. Chimeric mice were bred to C57BL/6J females. Black progeny were culled and progeny with agouti coloring were genotyped using tail DNA (15) and PCR to screen for the presence of the mutant nuclear localization sites. Verification of the loss of the selection cassette in

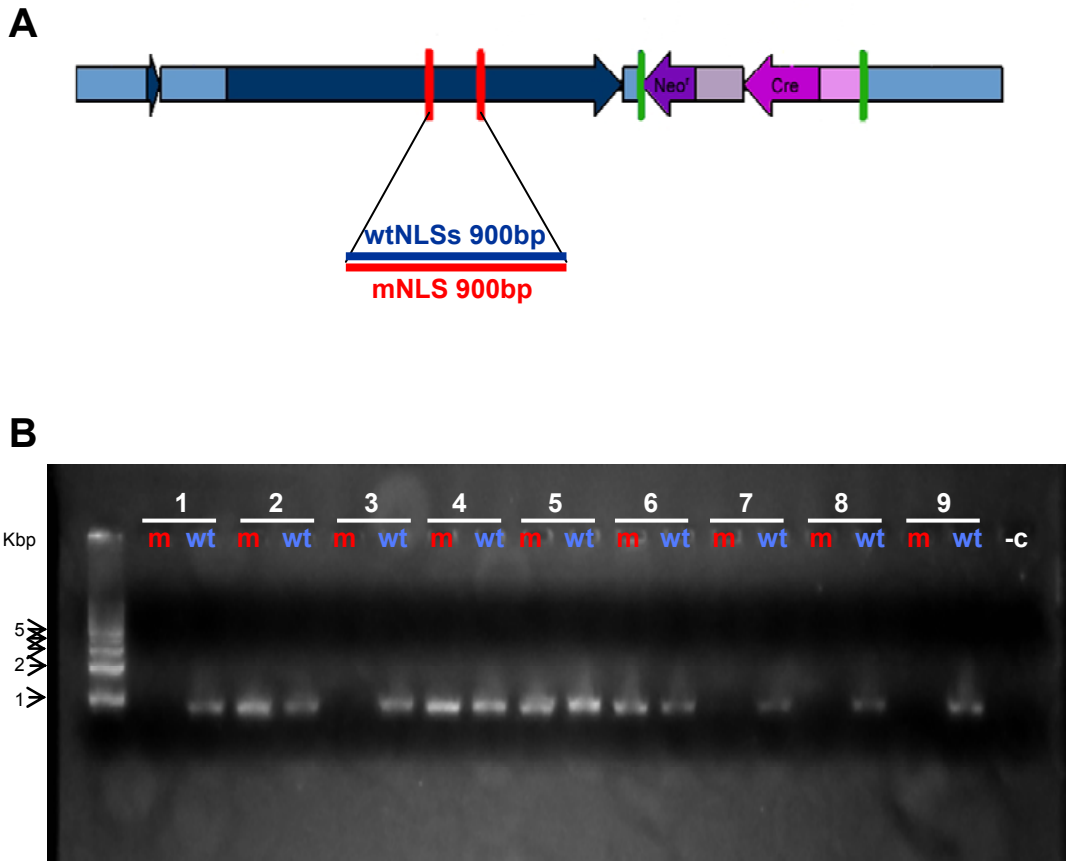

Figure 2.2

Step 1 in the PCR screen for recombinant cell lines. (A) A diagram of the targeting construct colored as in previous figure. Locations of the primers to the mutant and WT NLSs are indicated along with the expected sizes of the amplification products. (B) A representative 0.7% agarose gel. DNA products were visualized using ethidium bromide. DNA extracted from 9 different cell lines was screened. DNA from cell lines 2, 4, 5, 6 and 7 gave amplification products from both primer sets and so these lines were further screened. DNA from cell lines 1, 3,7, 8 and 9 could only be amplified when primers specific to the wild type NLS were used. These cell lines were assumed to lack one or both of the mutant NLSs and were discarded.

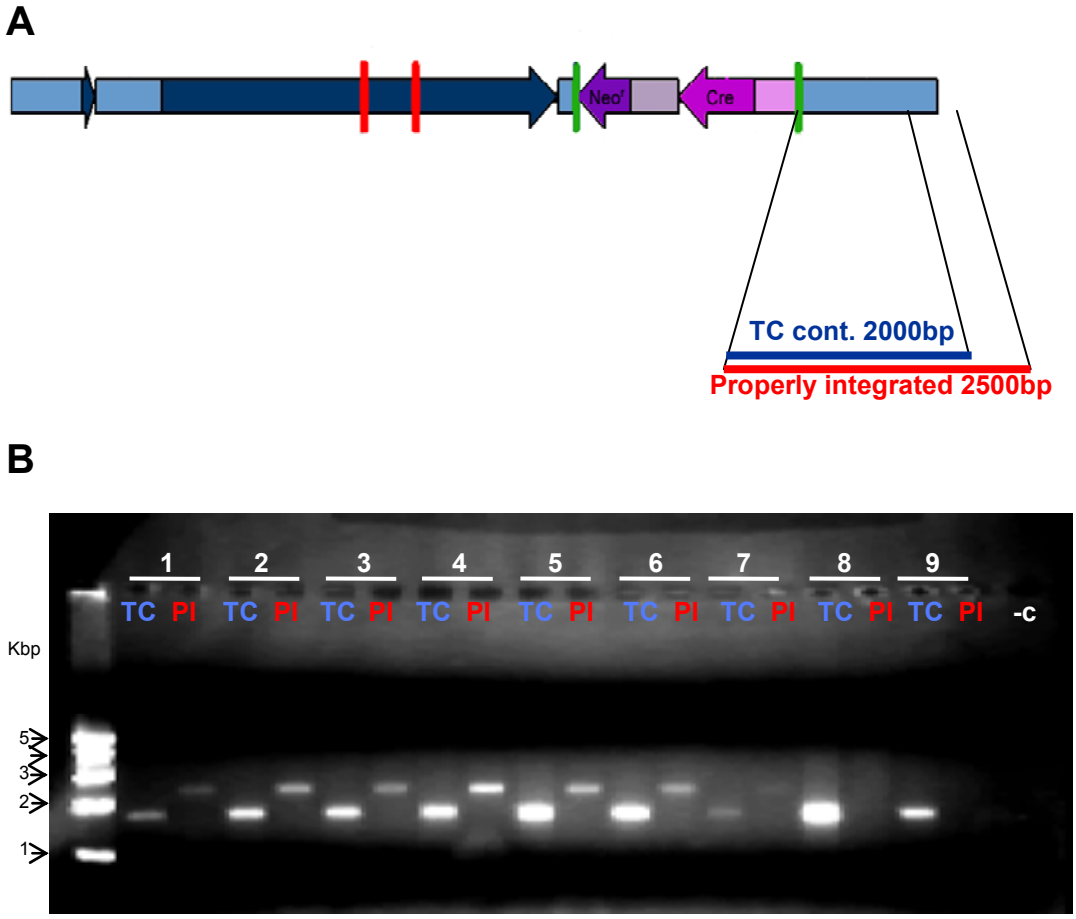

Figure 2.3
Step 2 in the PCR screen for correct recombinant cell lines. (A) A diagram of the targeting construct colored as in Figure 2.1. Locations of the primers are indicated along with the expected sizes of the amplification products. (B) A 0.7% agarose gel of the PCR reactions from all seven of the correct cell lines as well as two of the incorrect cell lines. DNA products are visualized using ethidium bromide. DNA was extracted from 9 different cell lines. Cell lines 1-7 gave amplification products of the appropriate size from the primer extending into the genomic DNA sequence (PI). Cell lines 8 and 9 were only able to amplify product when primers specific to sequence contained within the targeting construct, suggesting that the construct is present but is not integrated into the *Apc* locus. These cell lines were discarded.

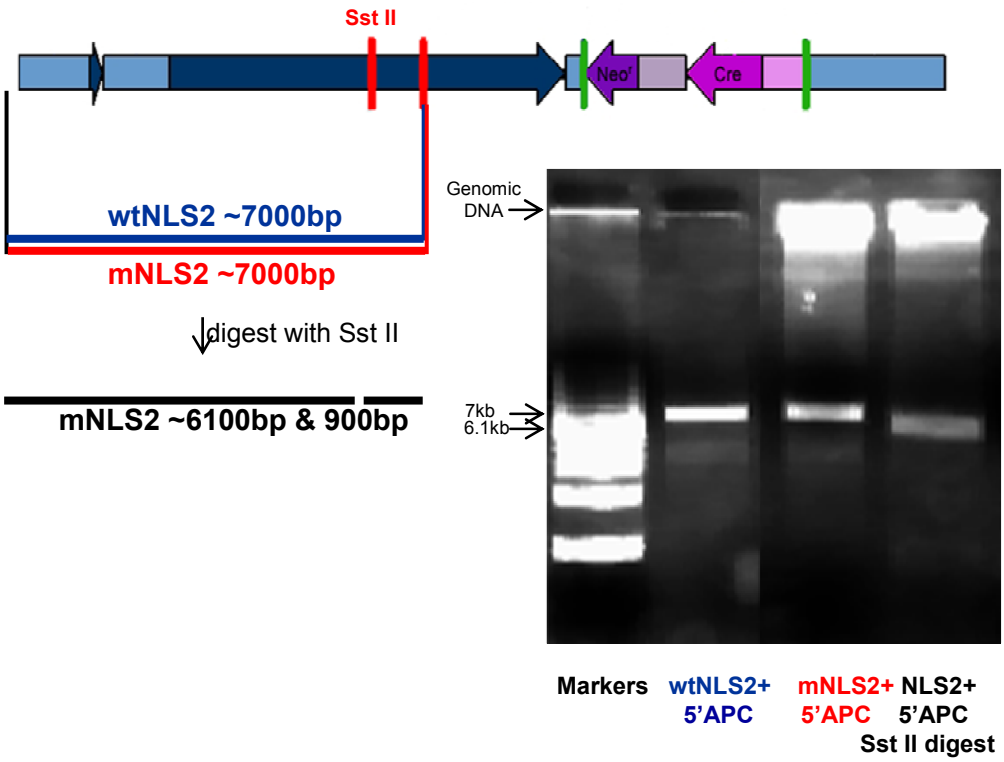

Figure 2.4
The PCR strategy to verify that the 5' end of the targeting construct had correctly incorporated into the APC gene. A diagram of the targeting construct colored as in Figure 1.1 shows the location of the primer sets used. A primer specific to the wtNLS2 and a primer specific to the mNLS2 were used in conjunction with a common primer specific to a region of the APC gene outside of the targeting construct. The WT and mutant primer sets amplified a large region of DNA spanning a 7000bp piece of the WT genome or the 5' end of the targeting construct respectively. Genomic DNA was isolated from mutant and WT ES cells. The PCR products are shown resolved on an 0.7% agarose gel and visualized with ethidium bromide. PCR products from the mutant and WT primers amplified a product of the correct size and the far right lane shows the mutant product after digestion with Sst II to verify the presence of mNLS1 within the PCR product.

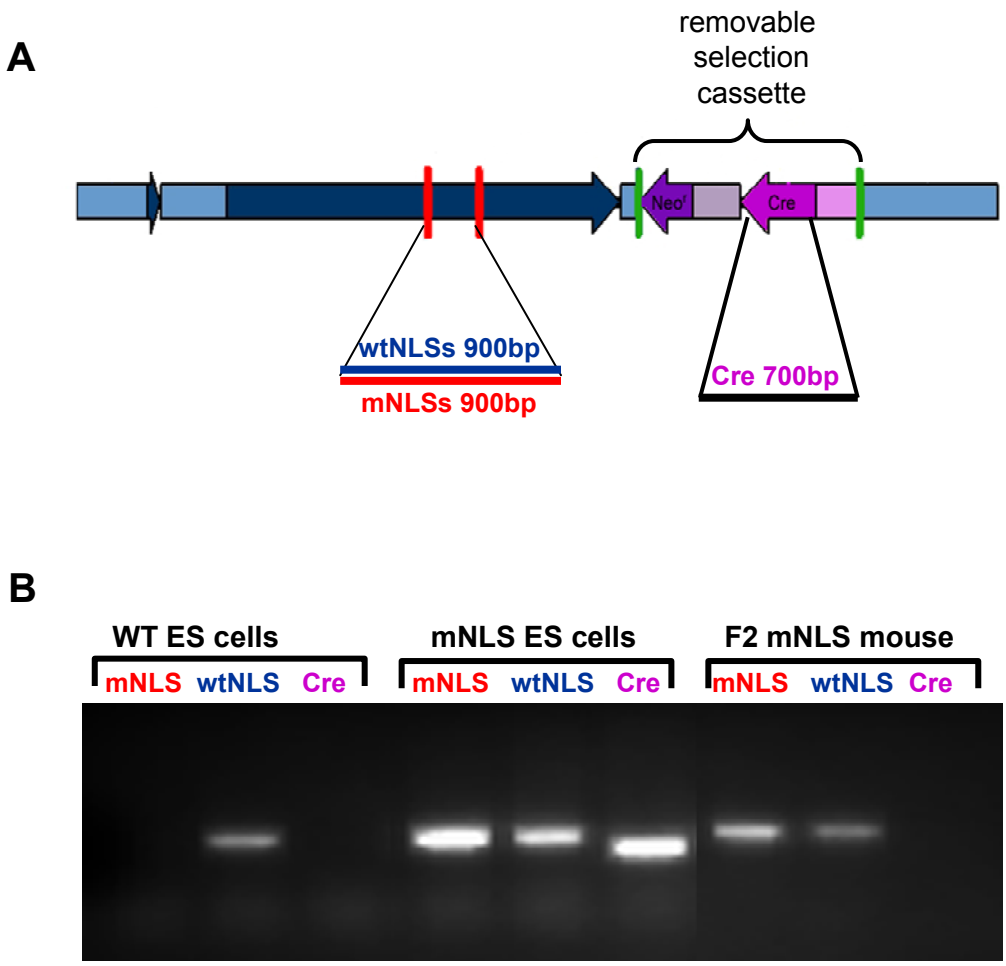

Figure 2.5
The PCR strategy to verify the excision of the selection cassette in the mNLS progeny. (A) A diagram of the targeting construct colored as in Figure 2.1. Location of the PCR primers sets are indicated along with the expected sizes of the PCR products. (B) A representative 0.7% agarose gel stained with ethidium bromide showing PCR products from each of the primer set for DNA isolated from WT R1 stem cells, APC mNLS stem cells, or tail DNA from a heterozygous mNLS mouse (generation F2).

the APC mNLS progeny was conducted using PCR and the following primers: Forward primer, 5'-TCG GCC ATT GAA CAA GAT GGA-3' and Reverse primer, 5'-ATT CGC CGC CAA GCT CTT CA-3' (Figure 2.5).

Mouse Husbandry

Mice were maintained in the University of Kansas Animal Care Unit according to animal use statement number 137-01. The chimeric progenitor mice as well as offspring that carry the mutant copy of *Apc* were crossed with C57BL/6J mice from Jackson Labs to create a congenic line.

Results

Introduction of the mNLS Apc *to ES cells*

A gene targeting vector was generated to introduce specific point mutations into both primary nuclear localization signals of APC in ES cells (Figure 2.1). The targeted mutations alter a total of six amino acids, four in NLS1 and two in NLS2 (Figure 2.6A).

These mutations exchange the basic lysine and arginine residues for neutral alanine residues and thus destroy their ability to interact with importin-α and target full length APC to the nucleus (1). These mutations do not affect the SAMP binding domains as the ability of APC mNLS to interact with axin/conductin is unaffected (unpublished observations of Neufeld and White). These point mutations also introduce two novel

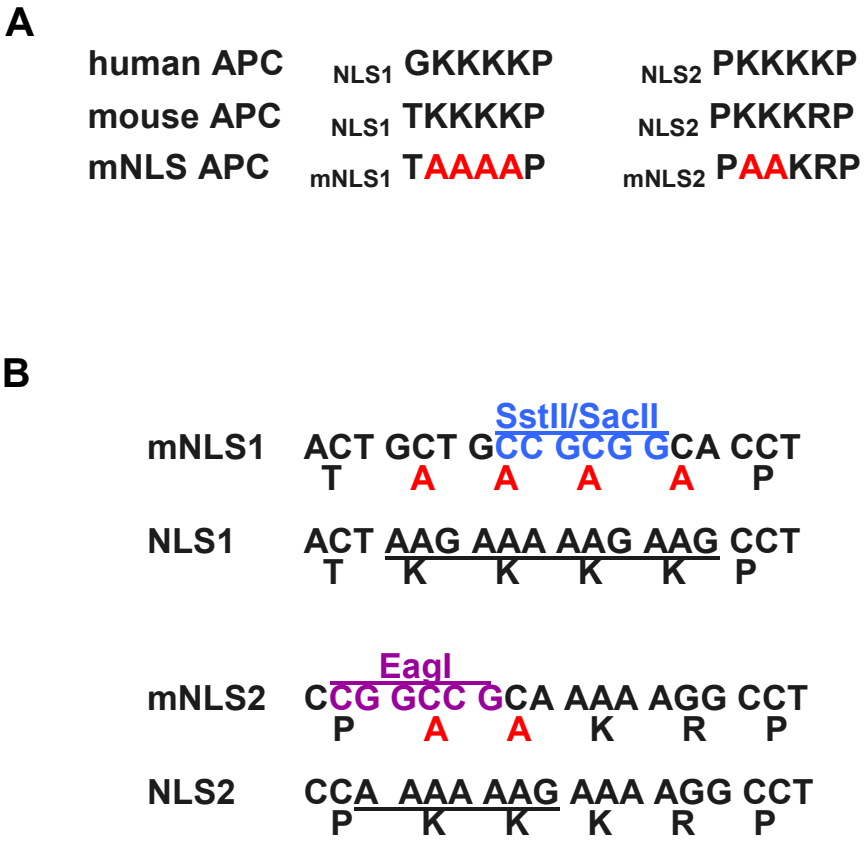

Figure 2.6
The APC mutations knocked-in to the endogenous *Apc*. (A)The amino acid sequences of the NLSs in the human and mouse APC proteins as well as the mutant NLSs used in the targeting construct. The amino acid changes made in the targeting vector are indicated in red. (B) The nucleotide sequences of the genomic mouse APC NLSs 1 and 2 and the nucleotide changes implemented to inactivate the nuclear localization signal and introduce novel restriction sites. Restriction sites are indicated in blue and purple. The amino acids are labeled below each line of nucleotides with altered amino acids in red. Underlined nucleotides in the genomic sequence represent the base pairs that were mutated in the targeting construct.

restriction sites into the genomic sequence, inserting Sac II and EagI sites into NLS1 and NLS2 respectively (Figure 2.6B).

The targeting vector contains an 11.5 kb genomic Nhe I/ Not I fragment encompassing exons 14 and 15 of *Apc* as well as the surrounding introns. The decision to use at least 10kb of homologous sequence was based on work by Thomas and Capecchi showing that the gene-target efficiency relative to the frequency of random integration was based on the extent of the homology between the exogenous and endogenous genomic sequences (5). With greater than 10kb of homologous DNA in the targeting vector, the ratio of correct recombinants should be greater than 1 in 1000 (5).

To facilitate selection of recombined cell lines with G418, a Neo^r gene under the control of the constitutive promoter responsible for the expression of RNA polymerase II was also incorporated into the targeting construct. Others have shown that integration of a strong promoter into *Apc* gene sequence can adversely affect the expression level of APC *in vivo* (10, 16, 17). Therefore, to be certain that the only effects on APC function were the result of the mutations being introduced, the Neo^r gene was removed before evaluation of the phenotype in a whole animal. To accomplish this, a germ-line-induced self-excision cassette was employed (13). A floxed Cre recombinase/Neo^r cassette was inserted into the non-coding homologous sequence 3' of the last *Apc* intron. In mice the tACE promoter initiates transcription of Cre-recombinase during spermatogenesis, which induces Cre-mediated self-

excision of the selectable marker in the germ line of the transgenic animals leaving only one 34bp minimal LoxP element in the last *Apc* intron.

Further screening was required to distinguish homologous recombinants from cells that have taken up the Neo^r cassette through random integration of the plasmid. This negative selection against random events was accomplished by inserting the thymidine kinase gene from the herpes simplex virus at one end of the targeting construct. (18). Unlike homologous recombination, non-homologous insertion incorporates the ends of a linearized DNA plasmid (19). When this occurs the tk^{HSV} gene is also incorporated into the genome (18). Expression of tk^{HSV} results in a cell that is sensitive to ganciclovir. Unlike the endogenous form of thymidine kinase, TK^{HSV} is able to triphosphorylate various nucleoside analogues such as ganciclovir. Ganciclovir triphosphate is incorporated into the DNA strand being synthesized, halting chain elongation and ultimately resulting in cell death (18, 20).

Screening ES cells for targeted recombination

In total, 161 G418-resistant, ganciclovir insensitive ES cell clones were received from the Transgenic and Gene-Targeting Institutional Facility at the University of Kansas Medical Center (Table 2.1A and B). While the initial screening with selective media greatly enhances the ratio of correct recombinants, it only selects for cells that have incorporated the Neo^r cassette without incorporating the tk^{HSV} gene. This selection does not distinguish between correct recombinants and cells that have recombined so that they contain just the Neo^r gene along with only one or neither of the mNLSs. It

Table 2.1A The PCR screening results for the cell lines from the first round of targeting

Cell line	KOmed name	mNLSs+	Cre
KN1	PK1 I A1	No	
KN2	PK1 I A2	Yes	Yes
KN3	PK1 I A3	Yes	No
KN4	PK1 I A4	Yes	No
KN5	PK1 I A5	No	
KN6	PK1 I A6	No	
KN7	PK1 I A7	No	
KN8	PK1 I A8	Yes	No
KN9	PK1 II A1	No	
KN10	PK1 II A2	Yes	No
KN11	PK1 II A3	Yes	No
JC1	PK1 I C4	No	
JC2	PK1 I C3	No	
JC3	PK1 I C2	Yes	No
JC4	PK1 I C1	Yes	No
JC5	PK1 II C3	Yes	No
JC6	PK1 II C2	No	
JC7	PK1 II C1	Yes	No
JC8	PK1 I D4	No	
JC9	PK1 II B1	No	
JC10	PK1 II B2	Yes	No
JC11	PK1 II B3	Yes	No
JC12	PK1 II D1	No	
JC13	PK1 II D3	Yes	No
JC14	PK1 I D1	No	
JC15	PK1 I D2	No	
JC16	PK1 I D3	No	
JC17	PK1 A12	No	
JC18	PK1 I B1	Yes	No
JC19	PK1 I B2	No	
JC20	PK1 I B3	Yes	No
JC21	PK1 I B4	Yes	No
JC22	PK1 I B5	Yes	No
JC23	PK1 B7	Yes	No
JC24	PK1 B11	Yes	No
JC25	PK1 A9	Yes	No
JC26	PK1 A10	Yes	No
JC27	PK1 A11	No	

Cell lines highlighted in grey failed the first round of screening were not screened in the second round. They amplified a WT band but not a Mutant band. Cell lines in white failed the second round of screening. They did not amplify a correct Cre band. Cell lines highlighted in yellow passed both rounds of screening and were characterized further (see Chapter 4 for details).

Table 2.1B The PCR screening results for the cell lines from the second round of targeting

Cell line	KUmed name	mNLSs+	Cre
ES1	PK2I C11	Yes	Yes
ES2	PK2II A5	No	
ES3	PK2II B1	Yes	No
ES4	PK2I E4	No	
ES5	PK2I C1	Yes	No
ES6	PK2I E1	Yes	No
ES7	PK2I D6	No	
ES8	PK2I A5	Yes	No
ES9	PK2III B2	No	
ES10	PK2III B7	Yes	No
ES11	PK2II D2	Yes	No
ES12	PK2II A2	Yes	No
ES13	PK2II D6	No	
ES14	PK2III C6	Yes	No
ES15	PK2I G2	Yes	No
ES16	PK2II A4	Yes	No
ES17	PK2II C2	Yes	Yes
ES18	PK2III C4	Yes	No
ES19	PK2I C2	Yes	No
ES20	PK2I E2	No	
ES21	PK2I G4	Yes	No
ES22	PK2I C4	No	
ES23	PK2I A4	Yes	No
ES24	PK2II B4	Yes	No
ES25	PK2I D4	Yes	Yes
ES26	PK2III A6	No	
ES27	PK2I A2	No	
ES28	PK2II A3	Yes	No
ES29	PK2I D2	No	
ES30	PK2I F3	Yes	No
ES31	PK2II A1	Yes	No
ES32	PK2II D7	Yes	No
ES33	PK2III A3	No	
ES34	PK2III B1	No	
ES35	PK2I F4	Yes	No
ES36	PK2II B5	Yes	No
ES37	PK2II B2	No	
ES38	PK2I H2	Yes	No
ES39	PK2I F1	Yes	No
ES40	PK2II C5	Yes	No
ES41	PK2II B6	Yes	No
ES42	PK2I D3	Yes	No
ES43	PK2II C6	Yes	No
ES44	PK2II D1	Yes	No
ES45	PK2II B8	Yes	No
ES46	PK2I C12	No	
ES47	PK2II D5	No	
ES48	PK2II D4	No	
ES49	PK2I B4	No	
ES50	PK2III A4	Yes	No
ES51	PK2I A12	No	
ES52	PK2I H6	No	
ES53	PK2III A5	Yes	No
ES54	PK2I A9	No	
ES55	PK2I A11	Yes	No
ES56	PK2III D2	No	
ES57	PK2I C3	Yes	No
ES58	PK2I D7	Yes	No
ES59	PK2II B12	No	
ES60	PK2I F2	No	
ES61	PK2I G3	Yes	No
ES62	PK2III A1	No	
ES63	PK2I G5	No	
ES64	PK2I D5	Yes	No
ES65	PK2III C7	Yes	No

Cell line	KUmed name	mNLSs+	Cre
ES66	PK2II B1	No	
ES67	PK2II D3	No	
ES68	PK2III D7	No	
ES69	PK2III C5	Yes	No
ES70	PK2I B10	Yes	No
ES71	PK2I E5	Yes	No
ES72	PK2III D5	Yes	No
ES73	PK2I A7	Yes	No
ES74	PK2I D1	Yes	No
ES75	PK2I D9	Yes	No
ES76	PK2I E3	Yes	No
ES77	PK2I E6	Yes	No
ES78	PK2II C1	Yes	No
ES79	PK2III B4	Yes	No
ES80	PK2I B2	Yes	No
ES81	PK2III B5	Yes	No
ES82	PK2III B5	Yes	No
ES83	PK2I B3	Yes	No
ES84	PK2III B6	Yes	No
ES85	PK2II C4	Yes	No
ES86	PK2I B7	No	
ES87	PK2I G6	Yes	No
ES88	PK2I A8	Yes	No
ES89	PK2III C2	Yes	No
ES90	PK2I D11	Yes	No
ES91	PK2I D10	Yes	No
ES92	PK2I C10	No	
ES93	PK2III C3	Yes	No
ES94	PK2I F5	Yes	No
ES95	PK2I A10	Yes	Yes
ES96	PK2I A6	Yes	No
ES97	PK2I B1	No	
ES98	PK2II B3	Yes	No
ES99	PK2II C8	Yes	No
ES100	PK2III C1	Yes	No
ES101	PK2III B3	Yes	No
ES102	PK2I D8	No	
ES103	PK2I A3	Yes	No
ES104	PK2I B8	Yes	No
ES105	PK2III D1	Yes	Yes
ES106	PK2II A6	Yes	No
ES107	PK2I B9	No	
ES108	PK2II A7	Yes	No
ES109	PK2I A1	Yes	No
ES110	PK2I F6	No	
ES111	PK2I B6	Yes	No
ES112	PK2I C5	Yes	No
ES113	PK2I D11	No	
ES114	PK2III A7	Yes	No
ES115	PK2I H5	No	
ES116	PK2I C9	No	
ES117	PK2I C6	Yes	No
ES118	PK2I H4	Yes	No
ES119	PK2I C7	No	
ES120	PK2I B11	No	
ES121	PK2I H3	Yes	Yes
ES122	PK2I C8	Yes	No
ES123	PK2II A8	Yes	Yes
ES124	PK2III D6	No	
ES125	PK2I B5	No	
ES126	PK2II C7	No	
ES127	PK2I G1	Yes	No
ES128	PK2III D3	Yes	No
ES129	PK2II C3	No	
ES130	PK2III D4	Yes	No
ES131	PK2I H1	Yes	No

also allows for the growth of cells that have incorporated the targeting vector randomly but have lost *tk*^{HSV} expression through other means. To identify which of the remaining cell lines were correct recombinants, the clones were screened using PCR.

Identification of ES cell lines containing mutations to the endogenous NLSs was accomplished using a two step PCR based screen. In the first step, DNA extracted from the transgenic cell lines was used in two separate PCR reactions. Primers for the first reaction were specific for the wild type APC NLS1 and NLS2 genomic sequences and amplified a product from the wild type APC allele. Primers for the second reaction were specific for the mutant NLS1 and NLS2 sequences from the targeting construct and amplified a product from the inserted mutant sequence (Figure 2.2A). Amplification from the wild type allele was detected for all cell lines verifying that all targeted cells retained at least one WT allele of APC. While it was possible that both alleles of APC homologously recombined with the gene replacement vector in a single ES line, this is an unlikely outcome, and was not observed in this screen. The WT reaction therefore served as a positive control for successful DNA isolation. Candidate cell lines in which one of the APC alleles was successfully targeted would also produce an amplification product in the mutant PCR reaction utilizing the primers specific to the targeted mNLSs. Therefore candidate ES cells in which a band was amplified from both the wild type and the mutant NLS primers were further screened to verify that the mutations had incorporated into the endogenous *Apc* gene (Figure 2.2B).

Because the conditions used for the initial PCR screen would amplify product from the mutant reaction regardless of where the mutations were inserted into the genome, the second step of the PCR screen was carried out to verify that the knock-in mutations had incorporated into the *Apc* locus. This step of the screening process was carried out using a primer homologous to a portion of the LoxP/tACE promoter region of the Cre/Neo selection cassette and primer specific to a region of genomic APC sequence that should be 3' of the targeting construct if it had incorporated into the *Apc* gene. A second reaction used the same LoxP/Cre specific primer along with a second primer homologous to sequence located within the targeting construct (Figure 2.3A). This PCR reaction served as a positive control because all cell lines that passed first step of screening should contain the targeting construct. It was observed, however, that incorrect incorporation of the gene replacement vector did not always preserve the ends of the construct. A number of the cell lines gave no PCR product for either reaction. Amplification a 2.5 Kbp region of DNA encompassing the 3' side of the targeting construct and a region of the adjacent endogenous genomic sequence indicated the targeting construct inserted accurately into the *Apc* gene (Figure 2.3B). The cell lines that failed either step of the screen were discarded and the remaining cell lines were thawed and expanded by the Transgenic and Gene-Targeting Institutional Facility at The University of Kansas Medical Center. The results of both phases of the screen are summarized in Tables 2.1A and 2.B).

The initial screen, used to identify cell lines that carried both of the mutant NLS sequences, revealed that 107 of the ES clones (>66%) incorporated both mNLS in addition to the Neo^r cassette somewhere in the genome. These candidates were then further screened for cell lines in which the targeting construct had incorporated correctly into the endogenous *Apc* gene. Eight of the ES cell clones (~5%) gave amplification products indicative of correct placement of the targeting construct in the context of the genome. Of these 8 cell lines, 7 cell lines survived the freeze/thaw process to be expanded and further evaluated (Table 2.2). Three of these cell lines showed growth patterns and/or β-catenin transcriptional activity that were divergent from the majority. These 3 cell lines were eliminated from consideration for further study. The 4 remaining cell lines were extensively karyotyped. The chromosomes of 40 to 50 individual cells were counted for each cell line, revealing that two of the cell lines had abnormal karyotypes in over 25% of the cells screened. These were also eliminated from consideration for further study. Finally, a PCR reaction that amplified over 6500bp of DNA extending from mNLS2 past the 5' end of the targeting construct revealed an amplification product identical in size to the product produced when the same reaction was performed using a primer to the wtNLS2 (Figure 2.4). This confirmed that there was no major loss or addition of DNA during recombination and that the 5' region of the targeting construct had integrated properly. When the products from this PCR reaction were incubated with Sac II restriction endonuclease, the mutant, but not the WT product showed cleavage of the DNA strand, verifying that the mNLS1 was also present in the amplified region

Table 2.2 Screening the targeted ES cell lines.

Stage of screening	Number of cell lines	% of total cell lines
Survived on selective media	161	100%
Contained both mNLSs (Step 1 PCR)	107	66%
Targeting construct correctly integrated (Step 2 PCR)	8	4.90%
Survived freeze/thaw	7	4.30%

(Figure 2.4 and data not shown). The first cell line to complete this final confirmation step (ES121-PK2I-H3 from Table 2.1B) was sent to the Gene Targeting and Transgenic Facility at the University of Virginia where the targeted $APC^{+/mNLS}$ ES cells were injected into C57BL/6J blastocysts to generate chimeric mice. A second ES cell line (KN2-PK1 I A2 from Table 2.1A) was sent for chimeric mouse generation at a later date.

Generation of the mNLS mouse line

Eleven chimeric mice, 4 females and 7 males, were received from the Gene-Targeting and Transgenic Facility at the University of Virginia. All chimeric mice showed substantial agouti coat coloring indicating that there was significant contribution from the transgenic stem cells (agouti color) to the otherwise black-haired animals. The chimeras were crossed with C57BL/6J mice from Jackson Labs (Bar Harbor, Maine). Because the 129/Sv-CP mice from which the R1 transgenic ES cells were originally derived carry a dominant gene for agouti coat color, any F1 offspring carrying transgenic DNA will be agouti while the pups that carry only genes from the original C57BL/6J blastocyst will be black. As expected two of the female mice proved to be infertile were unable to pass the mutation through the germline and the other two produced only black pups. Four of the male chimeras also produced only black pups suggesting low incorporation of the APC mNLS ES cells in the germ line. The remaining three chimeric males produced only agouti offspring. Because the transgenic ES cells were $APC^{+/mNLS}$, only half of the agouti progeny are expected

to carry a mutant copy of APC. All F1 agouti pups were therefore screened for the presence of the mNLS using the PCR primers previously described (Figure 2.2A). Pups that tested positive for the presence of APC mNLS were either crossed with C57BL/6J mice to continue towards a congenic line or were crossed with other heterozygous siblings in an attempt to produce homozygous animals.

Transgenic mice do not carry the Neo^r/Cre selection cassette

In the APC1638N mouse model, a Neo^r selection gene was inserted in exon 15 of the *Apc* gene (21). This insertion resulted in a dramatic decrease in the expression of the mutant protein (22). Because the Neo^r gene was oriented so in the reverse orientation compared to the *Apc* gene, it was hypothesized that the strong promoter driving the Neo^r expression interfered with the expression of the *Apc* gene product (22). A second mouse model, in which the Hyg^r gene was oriented the same direction as the *Apc gene*, showed normal expression levels from the mutant allele (17, 22). In the APC Neo^R and APC Neo^F mouse models a Neo^r gene was inserted into the non-coding sequence of intron 13 and resulted in a similar repression of APC expression. In these mice the mutant allele expressed APC at only 10-20% of the WT level. Furthermore, this repression occurred when the selection cassette was inserted into the gene in either the forward (Neo^F) or the reverse (Neo^R) orientation (10, 16). Although the selection cassette used to create the APC mNLS mutant stem cells was not inserted into a coding region of APC as it was in the APC 1638N mouse model, it is in the reverse orientation compared to the *Apc* gene. Knowing that the selection

cassette has the potential to adversely affect APC expression, the linear targeting vector was designed so that the Neo^r gene and promoter could be removed from the genome once selection of the correct ES cell lines was complete.

The removal of the Neo^r gene and promoter is accomplished through the insertion of Lox P elements around the selection cassette (Figure 2.1). In the presence of the DNA recombinase Cre there is a directed self-induced deletion of the sequence between these two Lox P elements (13). The result is a single Lox P sequence 34 bp in length which remains in the genome, and the removal of the entire selection cassette. To facilitate the removal of the selection cassette in the mouse model, the Cre gene, under the control of a testes-specific promoter, was included in the selection cassette which was flanked by the Lox P sites. In the chimeric males the cassette will be maintained in the somatic cells, but recombination occurs in the ES-cell-derived sperm (13). Therefore all of the APC mNLS progeny from the chimeric mice will carry the recombined gene without the Neo^r/Cre expression cassette.

The absence of the Neo^r/Cre selection cassette was verified by PCR analysis of genomic DNA isolated from several of the heterozygous mNLS mice in the F1 and F2 generations. Genomic DNA isolated from WT and knock-in mNLS ES cell lines was used as negative and positive controls, respectively. Parallel PCR reactions using primers specific to the wtNLS and mNLS sites were preformed to verify that the mouse being screened carried the APC mNLS mutation and that an absence of PCR product was not due to poor DNA quality. As expected, primers specific to the WT APC NLSs amplified a product of the correct size from all DNA samples. DNA

isolated from the knock-in ES cells and the F2 APC mNLS$^{+/-}$ mouse also produced a strong PCR product in the presence of primers specific to the APC mNLSs. Primers within the Neo^{r}/Cre selection cassette amplified product from knock-in ES cell genomic DNA, but this amplification product was absent in a similar reaction using genomic DNA isolated from the mNLS mouse (Figure 2.5). PCR amplification using primers specific for the selection cassette was never achieved with any of the APC mNLS progeny, confirming that the Neo^{R}/Cre cassette was correctly excised in the mouse model.

Mice homozygous for APC mNLS are viable

The homozygous mutant animals of many APC mouse models display early embryonic lethality. However, the APC-mNLS mutation results in a comparatively subtle alteration to the APC protein. The role of nuclear APC in development is generally unknown; therefore, it was of particular interest to see if this mutation would result in prenatal mortality. When mice heterozygous for the APC mNLS mutation were bred together, homozygous mice were obtained at a frequency expected based on Mendelian genetics (Table 2.3). Mice up to generation F5 show no noticeable growth retardation or difference in the lifespan of the homozygous mice when compared to their WT littermates. Furthermore, homozygous mice are fertile and give birth to litters of typical size. The regular growth of homozygous animals suggests that the normal nuclear localization of APC is not essential during development.

Table 2.3
The progeny of the APC mNLS chimeric mice. The table covers the F1-F5 litters. The ***APC mNLS$^{+/-}$ x APC mNLS$^{+/-}$*** portion of the table summarizes the sex and genotypes of the litters born to APC mNLS heterozygous mice bred to APC mNLS heterozygous siblings to produce litters containing all three APC NLS genotypes. The ***APC mNLS$^{+/-}$ x APC wt*** portion of the table summarizes the litters born to APC mNLS heterozygous mice crossed with C57BL/J6 wild type mice.

	APC mNLS+/- x APC mNLS+/-				APC mNLS+/- x APC wt			
	APC +/+	APC +/-	APC -/-	Total	APC +/+	APC +/-	Total	Total
Male	20	27	23	70	31	32	63	133
Female	15	21	17	53	38	35	73	126
Total	35	48	40	123	64	72	136	259
Expected	31	61	31	123	68	68	136	
χ^2 value	5.9				0.471			
p value	0.0524				0.4927			

Discussion

Adenomatous polyposis coli is a large multifunctional protein that serves as a tumor suppressor both in humans and in animal models. Typical disease-associated forms of APC are truncations lacking the C-terminal region of the protein. Truncation of APC at different sites results in varying phenotypes, supporting a model in which APC maintains tissue integrity and suppresses tumor formation through numerous cellular pathways. While a role for APC in canonical Wnt signaling has been established, other cellular functions for APC, including its role in the nuclear compartment, have only begun to be explored.

Part of the difficulty in establishing a better, more comprehensive picture of APC's multiple cellular roles, is finding a suitable model system. While studies concerning various individual domains of APC have been conducted in cultured cells, fully understanding APC's role in tissue maintenance ultimately requires a more complex model. The mouse has been the primary model organism associated with the study of APC to date. The mouse contains an intestinal epithelium that is similar in structure to human intestine, allowing the study of APC in development, maintenance and prevention of tumorigenesis in this tissue. It has been shown in numerous mouse models that the human disease FAP, caused by the heterozygous truncation of APC, can be recapitulated in this model system.

Unfortunately, the current APC mouse models primarily truncate the APC protein or inhibit expression of the endogenous gene product. While this effectively results in a tumorigenesis phenotype, this type of modification does not allow detailed

analysis of the various functional domains of APC or how they sustain homeostasis within the intestinal epithelium. Ideally, to separate and define the individual responsibilities of the APC protein, domains required for specific pathways must be inhibited without eliminating domains required in other cellular activities.

Using established techniques we have successfully knocked in an APC mutation in mouse embryonic stem cells that targets the nuclear localization sequences of the endogenous *Apc* gene. These cell lines were used to generate chimeric mice, three of which produced progeny heterozygous for the APC mNLS genotype. The creation of a mouse model with specific point mutations in the *Apc* gene is unique to this field. The specific loss of nuclear shuttling mediated by the endogenous NLSs allows us to better define the tasks that APC performs in the nuclear compartment without inhibiting its cytoplasmic responsibilities. The role of APC in the nucleus is currently poorly understood. With this mouse model we intend to further delineate the nuclear function of APC and determine how that function contributes to the overall tumor suppressor function of the protein.

References

1. Zhang, F., White, R. L., and Neufeld, K. L. (2000) Phosphorylation near nuclear localization signal regulates nuclear import of adenomatous polyposis coli protein. *Proc Natl Acad Sci U S A* 97, 12577-12582
2. Martin, G. R. (1981) Isolation of a pluripotent cell line from early mouse embryos cultured in medium conditioned by teratocarcinoma stem cells. *Proc Natl Acad Sci U S A* 78, 7634-7638
3. Evans, M. J., and Kaufman, M. H. (1981) Establishment in culture of pluripotential cells from mouse embryos. *Nature* 292, 154-156
4. Haber, J. E. (1999) DNA recombination: the replication connection. *Trends Biochem Sci* 24, 271-275

5. Thomas, K. R., and Capecchi, M. R. (1987) Site-directed mutagenesis by gene targeting in mouse embryo-derived stem cells. *Cell* 51, 503-512
6. Mintz, B., and Illmensee, K. (1975) Normal genetically mosaic mice produced from malignant teratocarcinoma cells. *Proc Natl Acad Sci U S A* 72, 3585-3589
7. Weinberg, R. A. (2007) *The Biology of Cancer*, Garland Science, Taylor & Francis Group, New York
8. Nagy, A., Gertsenstein, M., Vintersten, K., and Behringer, R. (2003) *Manipulating the Mouse Embryo: a laboratory manual*, Cold Spring Harbor Laboratory Press, Cold Spring Harbor
9. Kucherlapati, M., Yang, K., Kuraguchi, M., Zhao, J., Lia, M., Heyer, J., Kane, M. F., Fan, K., Russell, R., Brown, A. M., Kneitz, B., Edelmann, W., Kolodner, R. D., Lipkin, M., and Kucherlapati, R. (2002) Haploinsufficiency of Flap endonuclease (Fen1) leads to rapid tumor progression. *Proc Natl Acad Sci U S A* 99, 9924-9929
10. Ishikawa, T. O., Tamai, Y., Li, Q., Oshima, M., and Taketo, M. M. (2003) Requirement for tumor suppressor Apc in the morphogenesis of anterior and ventral mouse embryo. *Dev Biol* 253, 230-246
11. Papaioannou, V. E., and Behringer, R. R. (2005) *Mouse Phenotypes: A handbook of mutation analysis*, Cold Spring Harbor Laboratory Press, New York
12. Silver, L. M. (1995) *Mouse Genetics: Concepts and Applications*, Oxford University Press
13. Bunting, M., Bernstein, K. E., Greer, J. M., Capecchi, M. R., and Thomas, K. R. (1999) Targeting genes for self-excision in the germ line. *Genes Dev* 13, 1524-1528
14. Nagy, A., Rossant, J., Nagy, R., Abramow-Newerly, W., and Roder, J. C. (1993) Derivation of completely cell culture-derived mice from early-passage embryonic stem cells. *Proc Natl Acad Sci U S A* 90, 8424-8428
15. Laboratory, T. J. Induced Mutant Resources: Tail DNA for PCR (No Organic Solvents). In Vol. 2005, http://www.jax.org/imr/tail_nonorg.html
16. Li, Q., Ishikawa, T. O., Oshima, M., and Taketo, M. M. (2005) The threshold level of adenomatous polyposis coli protein for mouse intestinal tumorigenesis. *Cancer Res* 65, 8622-8627
17. Smits, R., Kielman, M. F., Breukel, C., Zurcher, C., Neufeld, K., Jagmohan-Changur, S., Hofland, N., van Dijk, J., White, R., Edelmann, W., Kucherlapati, R., Khan, P. M., and Fodde, R. (1999) Apc1638T: a mouse model delineating critical domains of the adenomatous polyposis coli protein involved in tumorigenesis and development. *Genes Dev* 13, 1309-1321
18. Mansour, S. L., Thomas, K. R., and Capecchi, M. R. (1988) Disruption of the proto-oncogene int-2 in mouse embryo-derived stem cells: a general strategy for targeting mutations to non-selectable genes. *Nature* 336, 348-352

19. Roth, D. B., Porter, T. N., and Wilson, J. H. (1985) Mechanisms of nonhomologous recombination in mammalian cells. *Mol Cell Biol* 5, 2599-2607
20. Cheng, Y. C., Dutschman, G., Fox, J. J., Watanabe, K. A., and Machida, H. (1981) Differential activity of potential antiviral nucleoside analogs on herpes simplex virus-induced and human cellular thymidine kinases. *Antimicrob Agents Chemother* 20, 420-423
21. Fodde, R., Edelmann, W., Yang, K., van Leeuwen, C., Carlson, C., Renault, B., Breukel, C., Alt, E., Lipkin, M., Khan, P. M., and et al. (1994) A targeted chain-termination mutation in the mouse Apc gene results in multiple intestinal tumors. *Proc Natl Acad Sci U S A* 91, 8969-8973
22. Kielman, M. F., Rindapaa, M., Gaspar, C., van Poppel, N., Breukel, C., van Leeuwen, S., Taketo, M. M., Roberts, S., Smits, R., and Fodde, R. (2002) Apc modulates embryonic stem-cell differentiation by controlling the dosage of beta-catenin signaling. *Nat Genet* 32, 594-605

CHAPTER 3

INITIAL CHARACTERIZATION OF THE APC mNLS MOUSE MODEL

Abstract

We have generated a mouse line that carries specific point mutations in the NLSs of the endogenous *Apc* gene. To fully characterize the phenotype of these mice requires the production of a congenic line. This chapter describes the ongoing process of generating the congenic APC mNLS line, as well as the preliminary characterization of the APC mNLS phenotype in the non-congenic mice. An analysis of APC localization in the small intestinal epithelium showed little to no difference in the subcellular targeting of APC in the APC mNLS mutant mice. A slight defect in the nuclear targeting is visible in the colonic epithelium, however. There is also preliminary evidence of a role for APC in the regulation of intestinal lymphoid tissue that is altered by mutation of the APC NLSs.

Introduction

The need for inbred, genetically homogenous lines of mice was recognized in the early 1900s. Clarence Little began production of the first inbred mouse line in 1909, and he and his associates are responsible for the development of some of the most well known mouse lines in use today including the CBA, BALB/c and C57BL/6 mouse lines (1). There are now thousands of inbred and standardized mouse lines available. The Jackson Laboratory distributes over 3,500 inbred strains of laboratory mice (2). The current availability of standardized strains is one of the advantages of working in a mouse model system. The introduction of inbred mice allowed research conducted in any laboratory to be compared with research conducted using mice of the same background strain in any other laboratory, even if the work was conducted halfway around the world or decades earlier. Working with inbred strains of mice also eliminates the variability in development and physiology that is associated with outbred mice, allowing the more subtle effects of a targeted mutation to be revealed (1).

If a single new mutation occurs within a strain of mice that is already inbred, then the mutant and wild type animals are said to be coisogenic (identical across the entire genome with the exception of the mutant locus). For a variety of reasons the mouse strain in which the mutation was initially created may differ from the mouse strain in which the mutation will be studied. For example, targeting a specific mutation into the mouse genome begins with the mutation of ES cells in culture (3,

4). Most ES cell lines have been derived from the 129/SvJ mouse strain (5). To study the new mutation in a different mouse strain therefore requires the creation of a congenic strain. This is accomplished by breeding mice that carry the targeted mutation with mice from an inbred strain until it is essentially isogenic except at a selected differential chromosomal segment and therefore it approximates a coisogenic strain to the greatest extent possible (1). To be considered congenic a mouse line must be identical to the inbred line across 99.8% of the genome; mathematically, this occurs after being bred with mice of the inbred line for 10 generations (6). Once congenic, the mice that carry the targeted mutation can be directly compared to the WT mice of the parental line. If mice homozygous for the desired mutation are viable and fertile, the mutation can be maintained by breeding homozygous mice, which eliminates the labor intensive step of tagging and genotyping every litter. Furthermore, once congenic, the mice can be bred with other congenic mouse models of the same strain to generate animals that carry multiple targeted mutations(1). This allows the interaction of two or three mutant proteins to be examined in a live animal. Because it is most efficient if these matings occur with other mice that are congenic and are the same strain, it important to consider which background lines will allow the best evaluation of the targeted mutation when choosing to generate a congenic mouse line.

Developing a congenic line is a time consuming process. With a 19-21 day gestation period and 5-7 weeks to reach sexual maturity, the generation time for a mouse is effectively 10 weeks. This process, from the birth of the chimeric mice to

the birth of the first litter of congenic mice ten generations later, requires roughly two years. For this reason, it is not uncommon to begin a preliminary analysis of the phenotype of the mutant animals in the earlier generations (6-8). While the earlier generations would be too dissimilar from the inbred WT line for more subtle effects of the mutation to be reliably detected, some phenotypes might be observable at this stage. However, even obvious phenotypes must be pursued carefully. The process of making a congenic line also serves to eliminate any additional mutations induced during the process of creating the mutant ES cells (5). Because these untargeted mutations may not be entirely eradicated in the earlier generations of mice, it is difficult to be certain that a given phenotype is the result of the targeted mutation until that phenotype is observed in the fully congenic line. Because any non-targeted mutations would be expected to appear at a similar frequency in the WT and mutant animals, littermates of the mutant animals, rather than the inbred WT mice, were used as the controls when conducting experiments using non-congenic animals.

The APC mNLS mouse line is currently at generation F6 towards becoming a fully congenic line with the C57BL/6J background. In the interim we have begun analyzing the F1-F5 generations of mice. The APC NLS mutations were designed to block the nuclear import of APC without affecting other functions or the expression of endogenous APC. It was therefore important to verify that full length APC was expressed at the correct level in intestinal tissue and to evaluate the localization of the mutant APC protein. Another area of focus for preliminary characterization was the oncogene β-catenin. Because one of the established functions of APC involves the

regulation of β-catenin levels, the level and localization of the β-catenin protein in the intestinal epithelium was of particular interest (9). Finally, to further characterize the tumor suppressor function of nuclear APC, proliferation of the intestinal epithelium, average lifespan of the mice and the gross intestinal histology were examined in the early pre-congenic generations.

Materials and Methods

Mouse Husbandry

Mice were maintained in the University of Kansas Animal Care Unit according to animal use statement number 137-01. The chimeric progenitor mice as well as offspring that carry the mutant copy of *Apc* were bred with C57BL/6J mice from Jackson Labs (Bar Harbor, Maine) to generate a congenic line. Detailed records including the date of birth, lineage, coat color, sex, genotype and date of sacrifice were maintained for each pup. For the survival curve the male and female mice were housed with same sex siblings rather than individually, which resulted in a fairly even mixture of APC $mNLS^{+/+}$, APC $mNLS^{+/-}$ and APC $mNLS^{-/-}$ mice in each cage. All mice received the same food, water and bedding and were housed at the same temperature. As soon as dead mice were discovered, they were removed and recorded. Necropsies were performed when possible.

Necropsy to preserve tissue from dead mice

When histological analysis of mouse organs other than the intestine was required, necropsies were performed following a protocol provided by Dr. David Pinson from the Veterinary Lab Resources Department of the University of Kansas Medical Center. Following death or sacrifice, the mouse was placed in dorsal recumbence and soaked in 70% ethanol. The abdomen was opened along the ventral midline and organs including the tongue, trachea, esophagus, heart, lungs, liver, spleen, kidneys, reproductive organs and brain were placed in10% buffered formalin. Any apparent abnormalities were recorded and the organs were sent by courier to the Veterinary Lab Resources Department of the University of Kansas Medical Center for complete histological analysis by Dr. Pinson.

Tagging and DNA isolation for genotyping

Mouse pups were tagged after weaning. Each mouse was injected with an implantable electronic transponder (Bio Medic Data Systems Inc.) using a prepackaged implant device. The transponders were inserted into the subcutaneous space above the hips and shoulders. Transponders transmit a unique 10 digit mouse ID number to a radio scanner (Bio Medic Data Systems Inc.) which was used to identify the mice. Following insertion of the transponder, approximately 2mm of tissue was removed from the tip of the tail for DNA isolation as previously described (10). Briefly, the tail tissue was placed directly into labeled ependorf tubes containing 200µl of 1X PCR Buffer with Nonionic Detergents (PBND) [50mM KCL, 10mM Tris-HCl pH 8.3, 2.5mM $MgCl_2$-$6H_2O$, 0.1 mg/ml gelatin, 0.45% v/v Nonidet

P40, 0.45 v/v Tween 20 made up in H_2O]. 1X PCR Buffer was autoclaved, aliquoted and stored at -20°C. A fresh aliquot was thawed for each round of DNA isolation. Proteinase K (5µL of a 20mg/mL stock) was added to each tube containing a section of tail tissue and tubes were incubated at 55°C with occasional vortexing until the tail tissue dissolved (~2 hours). Samples were heated to 95°C for 10 minutes to deactivate the Proteinase K. Between 3µL and 6µL of each sample was used in two PCR amplification reactions to determine the genotype of each mouse.

Determining the* Apc *NLS genotype of mice

The *Apc* genotype of the mouse pups was determined using tail DNA and PCR to screen for the presence of the WT and mutant nuclear localization sites. The following primer set was used to screen for the WT allele of APC: NLS1-forward (5'-CTA AGA AAA AGA AGC CTA CTT CAC) and NLS2-reverse (5'-GGC CTT TTC TTT TTT GGC ATG GC). In a separate reaction the following primer set was used to screen for the presence of the mutant allele of APC: mNLS1-forward (5'-GCA GCC GCG GCA CCT ACT) and mNLS2-reverse (5'-TTG AAG GCC TTT TTG CGG CC). PCR reactions utilized Taq or GoTaq polymerase (Promega) in the supplied buffer and 1.5mM $MgCl_2$ and were carried out as follows: hot start at 95°C for 15 minutes followed by 30 cycles of 94°C for 1 minute, 58°C for 1 minute, 72°C for 2 minutes. After the last cycle, tubes were incubated for 7 minutes at 72°C before samples were held at 4°C.

Western blot analysis of APC and β-catenin in intestinal tissue

Isolation of intestinal epithelial cells was performed with modifications to a previous protocol (11). At the time of sacrifice, the mouse small and large intestines were removed, opened lengthwise and rinsed with cold PBS. Tissue was incubated in 0.04% sodium hypochlorite for 15 minutes on ice and again rinsed in cold PBS. The colon and small intestine were placed into individual 15mL conical tubes containing EDTA/DTT solution (3mM EDTA and 0.5mM DTT in PBS). Tubes were incubated on ice for 15 minutes, after which the EDTA/DTT was poured off and replaced with cold PBS. Tubes were shaken forcefully for about 10 seconds to release the epithelial cells from the underlying tissue. The intestinal tissue was removed and placed in a fresh 15mL conical tube of EDTA/DTT solution and the process was repeated two additional times. The released epithelial cells were collected by centrifugation at 700xg for 5 minutes at room temperature. Pellets of the colonic epithelia resulting from all three rounds of extraction were combined into one sample. Because the surface area of the small intestine is significantly greater, there was no need to combine the epithelial tissue from the replicate extractions. The small intestinal epithelial cells from the second round of extraction were used in the experiments described here. Cells pellets were lysed in Reporter Lysis Buffer (Promega) and briefly sonicated. Samples were boiled in 3X Loading Dye [6% w/v Sodium Dodecyl Sulfate, 30% Glycerol, 150mM Tris pH 6.8, ~0.2mg/mL Bromophenol Blue in water] before proteins were resolved using SDS-PAGE and transferred to nitrocellulose membranes. Immunoblotting was performed using standard protocols. Membranes

were probed with the following primary antibodies diluted as indicated in 5% nonfat dry milk: rabbit anti-APC M2 (1:3000, generated by the Neufeld and Azuma labs), rabbit anti-β-catenin (1:1000, Sigma), mouse anti-α-tubulin (1:50, Developmental Studies Hybridoma Bank). The following secondary antibodies were diluted as indicated in 5% non-fat dry milk: HRP goat anti-mouse (Zymed) 1:10,000 and HRP goat anti-rabbit (Bio-Rad) 1:10,000. Blots were developed using Western Lightning Chemiluminescence Reagent Plus (PerkinElmer) or SuperSignal West Femto Maximum Sensitivity Substrate (Pierce) and a Kodak Image Station 1000. Band analysis was conducted using Kodak ID Image Analysis Software.

Confocal evaluation of the intestinal epithelia

Mouse intestines were prepared for cryosectioning and immunostaining based on methods previously described (12). At the time of sacrifice, mouse small and large intestines were removed, filled with PLP fixative [1% paraformaldahyde 0.01M *m*-sodium periodate, 0.075 M lysine, 0.037 M Na-phosphate (13)] and open lengthwise. The colon, and proximal, middle and distal regions of the small intestine were individually rolled as described (14) to form multiple "Swiss Rolls". The sections of rolled colon and small intestine were incubated in fixative on ice for 1 hour then cryo-preserved in 2.5M sucrose at 4°C overnight. Rolled tissue sections were then frozen in OTC tissue freezing media (VWR) under the cryostat heat sink at -20°C. Sections were sliced immediately or stored at -80°C. Tissue was sliced into 7μm thick sections using a Leica CM1900 cryotome and mounted onto glass slides for

immunohistochemistry. Slides were air dried for approximately 1 minute and stored in room temperature PBS for no more than 15 minutes. Tissue slices were permeabilized in CSK buffer (50mM NaCl, 300mM sucrose, 10mM Pipes pH 6.8, 3mM $MgCl_2$, 0.5% Triton X-100) for 10 minutes then blocked for 2 hours (1% BSA, 5% goat serum, 50mM NH_4Cl) at room temperature. After block, slides are washed 3 times for 20 minutes in wash buffer (0.2% BSA in TBS) and incubated in primary antibody overnight at 4°C. Slides were washed 3 times for 40 minutes at room temperature and incubated in secondary antibody for 2 hours in the dark. To visualize the DNA, slides were co-stained with DAPI for the last 5 minutes of the incubation with secondary antibody. Antibodies for immunohistochemistry of frozen sections included the following: mouse anti-β-catenin (1:1000, Transduction Laboratories), anti-APC-M2 rabbit polyclonal antibody made against amino acid 1000-1326 and affinity purified (1:3000), rat anti-Ki67 (1:300, Dako) goat anti-mouse IgG Alexa 488 (1:1000, Molecular Probes), goat anti-rat IgG Alexa 488 (1:1000, Molecular Probes), goat anti-rabbit IgG Alexa 568 (1:1000, Molecular Probes). Finally, slides were washed 3 times for 40 minutes in wash buffer, coverslips were mounted using ProLong AntiFade (Invitrogen) and the edges were sealed with nail polish. Images were collected at 400X, 600X or 1000X magnification using an Olympus 3I spinning disc confocal TIRF inverted microscope and analyzed using *SlideBook* software. Analysis of proliferation in the colon was conducted using 15-25 separate crypt images for each genotype. Measurements of crypt length were made

using *SlideBook* software. The p-values were calculated using *Prism GraphPad* software.

Analysis of the gross histology of the intestine

The gross and cellular histology of the intestinal tissue were examined in the F1-F3 generations of APC mNLS mice. At the time of sacrifice, the mouse ID number from the implanted transponder was recorded and the small intestine and colon were removed. Thread was used to tie off the proximal and distal ends of each organ and a 25 gauge syringe was used to fill the entire length of both the small intestine and the colon with 10% buffered formalin. The intestinal tissue was allowed to fix for 30 minutes before being opened longitudinally. A dissecting microscope was used to examine the intestinal luminal surface for irregularities. Regions of tissue with abnormalities were recorded, removed from the surrounding tissue, stored in 10% buffered formalin and sent by courier to The Veterinary Lab Resources department at the University of Kansas Medical Center for histological analysis. The mouse ID numbers were later used to correlate the number of lesions in each mouse with the age and genotype of the animal.

Analysis of the organs and cells of the immune system

At the time of sacrifice the thymus, spleen, inguinal lymph nodes (located near the groin), peyers patches (small intestinal lymph nodes) and bone marrow cells (from the femur) were harvested with the assistance of the lab of Dr. Steven Benedict

(Molecular Biosciences, KU). Analysis of the splenocytes was conducted as described previously (15). Thymocyte analysis was conducted using the same protocol with the omission of the step to lyse red blood cells.

Results

Generation of a congenic APC mNLS mouse

When choosing a background strain in which to study the APC NLS mutations it was important to select a strain that would allow direct comparison between the APC mNLS mouse model and other existing APC mouse models. Another consideration was that the knock-in APC NLS mutations only change six amino acids in the entire APC protein and therefore might result in a subtle phenotype. Such a phenotype would make it difficult to characterize mice that carry the APC mNLS mutations. To more fully evaluate the phenotype, it may be necessary to characterize the APC mNLS mutation in combination with mutations in other proposed nuclear binding partners. Evaluation of the APC mNLS phenotype in the presence of specific mutations in other genes of interest would require that the APC mNLS mice be bred with other mouse models. Therefore the background strain chosen for the APC NLS mutations should also facilitate intercrossing of the APC mNLS mice with other mouse lines that carry mutations of interest.

The C57BL/6J line was selected for our study of the targeted APC NLS mutations. This line is one of the most common background strains for the evaluation of targeted mutations (6). Most of the other APC mouse models generated to date are

also maintained in C57BL/6J mice (7, 8, 16-21) as are the Fen-1 and Exo-1 mouse models (22, 23), which carry mutations in genes important for DNA repair (Table 3.1). C57BL/6J mice are also more prone to intestinal polyposis upon loss of full length APC than many other mouse strains (24), making them especially useful for the study of the tumor suppressor function of APC.

APC mNLS chimeric males were crossed with C57BL/6J females. The F1 generation was initially evaluated for coat color. The APC mNLS$^{+/-}$ ES cells were generated by electroporating the gene replacement vector into cells of the WT R1 ES cell line (4). The R1 ES cells were derived from inbred 129/SvJ mice which carry a dominant gene for agouti coat color (6). The blastocysts that were injected with the R1 APC mNLS$^{+/-}$ ES cells to generate chimeras were taken from a C57BL/6J mouse, a line which carries genes that result in black coat coloring (6). Therefore, agouti (brown) F1 offspring represented germline transmission of the APC mNLS ES cells while back offspring carried only genetic material from the C57BL/6J blastocyst. Black F1 pups were culled and brown F1 pups were further evaluated. Because the APC mNLS$^{+/-}$ ES cells where heterozygous for the APC NLS mutations, brown coat color indicated that the pups had received one *Apc* allele from the knock-in ES cells, but did not indicate if they had received the mutant or the WT allele. At the time of weaning all brown pups were tagged and genotyped to determine which ones carried the targeted APC NLS mutations. F1 mice that were heterozygous for the APC NLS mutations where bred with C57BL/6J mice to produce the F2 generation. The process of tagging the pups in each litter, screening them for the APC mutation, and

Table 3.1
A list of the common APC mutant mice as well as other mouse models of interest and the background strain of the WT mice they were bred to for the purpose of generating a congenic line

Mouse line	Genetic Background*	Description of mutation
APC Min	C57BL/6J; AKR	APC truncation at aa850 (18)
APC 1638N	C57BL/6JIco	APC null allele (2% expression of the truncated allele) (19)
APC 1638T	C57BL/6JIco	APC truncation at aa1638 (8)
APC 1309	C57BL/6J	APC truncation at aa1309 (16)
APC 716	C57BL/6	APC truncation at aa716 (20)
APC 580S/D	C57BL/6	APC inducible truncation at aa580 (7)
APC 474	C57BL/6J	APC truncation at aa474 (17)
APC NeoR	C57BL/6N	APC hypomorphic allele-reduced experssion of FL protein (21)
Fen-1	C57BL/6	Null allele of DNA repair protein Fen-1 (22)
Exo-1	C57BL/6	Null allele of DNA repair protein Exo-1 (23)

*For many of the mouse lines above the strain name (C57BL/6) is followed by a laboratory code (J, N, etc). Laboratory codes are added to the strain names due to the potential of genetic drift when mouse colonies are maintained independently (1). The above laboratory codes signify the following mouse colonies: J-Jackson Laboratories; N-National Institute of Health; Ico-a retired laboratory code for IFFA-Credo. The absence of a laboratory code denotes that the origin of the inbred strain was not indicated in the initial description of the mutant line.

then breeding the heterozygous APC mNLS mice to WT C57BL/6J mice was continued for each generation with the goal of establishing a congenic line.

After the F1 generation, coat color could no longer be used as an indication of genotype. As expected, breeding the APC mNLS$^{+/-}$ mice to C57BL/6J mice resulted in a gradual loss of the agouti phenotype. For the most part, an increasing ratio of black to brown mice was observed in litters with each subsequent generation (Table 3.2). At generation F5, APC mNLS mice should be identical to the WT C57BL/6J mice across 95% of their genome and all pups were black.

The following analysis of the APC mNLS phenotype was conducted in pups that were the product of mating F4 or F5 heterozygous mice to their heterozygous siblings to achieve litters of mixed genotypes. For other analyses the generation of the mice used is indicated. In all cases the WT control mice are the APC mNLS$^{+/+}$ littermates of the APC mNLS heterozygous and homozygous mutant animals.

Full length APC is expressed at normal levels in the intestine of APC mNLS$^{-/-}$ mice

The observation that endogenous APC could be seen in the nucleus of cultured cells led to the characterization of two classic monopartite NLSs in the central region of the APC protein (25, 26). Furthermore, mutation of these NLSs led to the nuclear exclusion of exogenously expressed APC in cultured cells (25). By generating a mouse line that carries these mutations in the endogenous *Apc* gene we intend to better define the function of nuclear APC in intestinal tissue. Prior to fully analyzing the phenotype in the APC mNLS mice it was important to establish that the

Table 3.2
A summary of the percentage of black pups and brown pups born in each generation. Litters from black heterozygous mice bred to black WT mice contain only black pups, litters from brown heterozygous mice crossed to black WT mice contain both brown and black pups. Therefore the number of brown pups in each of the first three generations decreases. While the total number of brown pups in the F3 generation was fewer than in the F2 and F1 generations, the heterozygous mice in this generation were brown resulting in the increase in the percentage of brown pups in the F4 generation. Black heterozygous F4 pups were bred to WT C57BL/6J animals and the resulting F5 generation was an all black litter

Generation	Total mice	% Brown	% Black
F1	47	100%	0%
F2	40	32%	67%
F3	24	29%	71%
F4	13	62%	38%
F5	7	0%	100%

mutation was having the expected effect on the levels and localization of APC. The *Apc* NLS mutations were designed to block nuclear import of APC through the classical importin-α nuclear import pathway without affecting the overall level of protein expression from the *Apc* gene. Western blot analysis of protein from the intestinal epithelium revealed that full length APC was expressed in the APC $NLS^{-/-}$ animals. Furthermore, there was no discernable difference in the level of APC expression when comparing the homozygous mutant animals with their APC mNLS WT littermates (Figure 3.1).

Analysis of APC localization in mouse intestine

The pattern of APC localization in the small intestine has been challenging to observe. Paraffin embedding has been the preferred method for analysis of protein localization in the delicate crypt-villus structures of the small intestinal epithelium (27). However, it is suspected that the processing required to paraffin embed tissue can result in the permanent loss of APC epitopes, making paraffin embedding a poor choice for tissue in which APC will be examined (Anderson and White, personal communication). Previous analysis of APC staining has been performed in frozen tissue slices (12) and microdisected crypts (26); however, the latter is more suited to the colonic crypts than to the villi of the small intestine. Analysis of APC expression and localization in the entire crypt-villus structure from the small intestine has rarely been reported in the literature. Several factors, in addition to the difficulties of staining APC in tissue, are likely contributing to the rarity of a complete examination

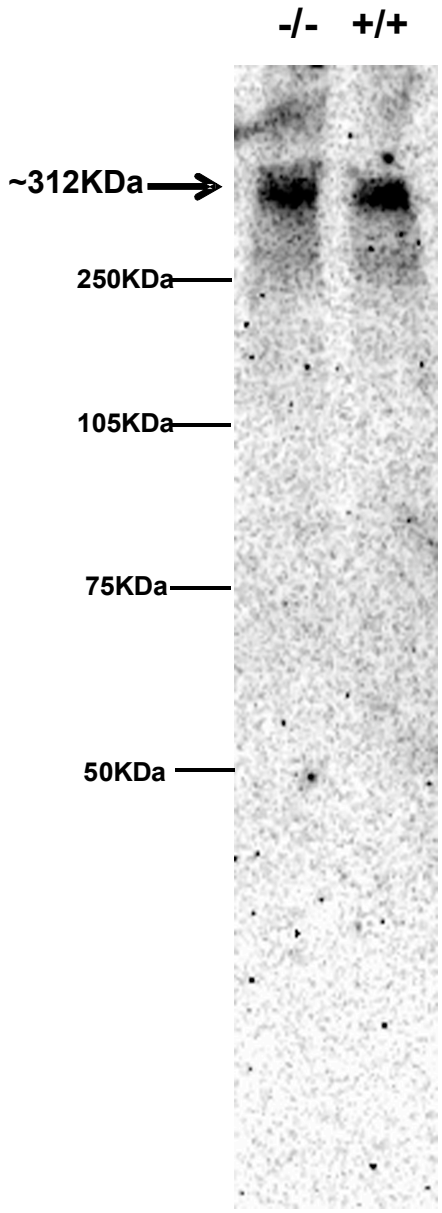

Figure 3.1
Western immunoblot of lysate from mouse intestinal tissue probed with anti-APC M2 antibody. Full length APC in intestinal epithelia of the APC mNLS$^{-/-}$ mouse is detected at approximately the same level as in the APC mNLS$^{+/+}$.

of intestinal APC. The process of removing and fixing the small intestinal epithelium without shearing the tall slender villi from the mucosal surface is not trivial. Neither is the preparation of tissue slices that allow the visualization of an entire crypt-villus structure within a single 7μm tissue slice. Furthermore, capturing images of entire villi generally requires the use of an objective with a large field of view due to the size of these structures, while analysis of the subcellular localization of APC requires an objective with a higher magnification and numerical aperture. In the following analysis of APC and β-catenin in the mouse intestinal epithelium, a two day tissue processing procedure allowed cryo-preservation of the colonic crypt structures as well as the fragile crypt-villus structures of the small intestine. The intestinal sections were rolled during fixation and freezing so that each slice contained several concentric layers of tissue, maximizing the potential to capture an entire crypt-base to villus-tip image with the minimum number of tissue slices. Finally, the use of *SlideBook* software facilitated the creation of montage images. A montage of a single crypt-base to villus-tip region of the epithelium generally contained 30-60 individual confocal images captured at 600x magnification to render a nearly seamless high-resolution illustration of the subcellular protein localization pattern across an entire crypt-villus structure. Using these techniques we have characterized the localization of APC and β-catenin in the small and large intestinal epithelia of APC mNLS mutant and WT animals.

APC localization in the small intestine

A previous report described APC localized to the lateral junctions in the cells that form the base of mouse small intestine crypts (12), a pattern consistent with APC localization observed in human colon crypts (26). Reports also describe a gradient of APC with the highest expression levels in the villus tips and the lowest level of APC at the base of the crypts (12, 28). In the villi, the localization of APC has also been reported to be more cytoplasmic with less pronounced staining at the plasma membrane (12).

Our analysis of APC expression has also revealed a subtle APC gradient in APC mNLS$^{+/+}$ mice (Figure 3.2). APC in the cells at the base of the crypts displayed a slightly lower intensity of APC staining with more of the APC signal localized to the plasma membrane (Figure 3.2 and 3.5). In agreement with previous reports, an increased staining intensity of APC was observed in the villi (Figure 3.2). The most intense APC staining in the villus cells was observed basal to the nuclei, a staining pattern that was not observed in the cells of the crypt. Furthermore APC localization was less nuclear in the cells of the villi, displaying a predominantly cytoplasmic distribution (Figure 3.2 and 3.7). When stained in conjunction with β-catenin, APC in cells of the villus was observed beyond the apical edge of the β-catenin at the plasma membrane, suggesting that APC localizes to the microvilli extensions of the intestinal enterocytes.

The same overall pattern of APC expression was also observed in mice that carry the APC NLS mutations. Both heterozygous and homozygous APC mNLS mice displayed the same relative levels of APC with a pattern of localization

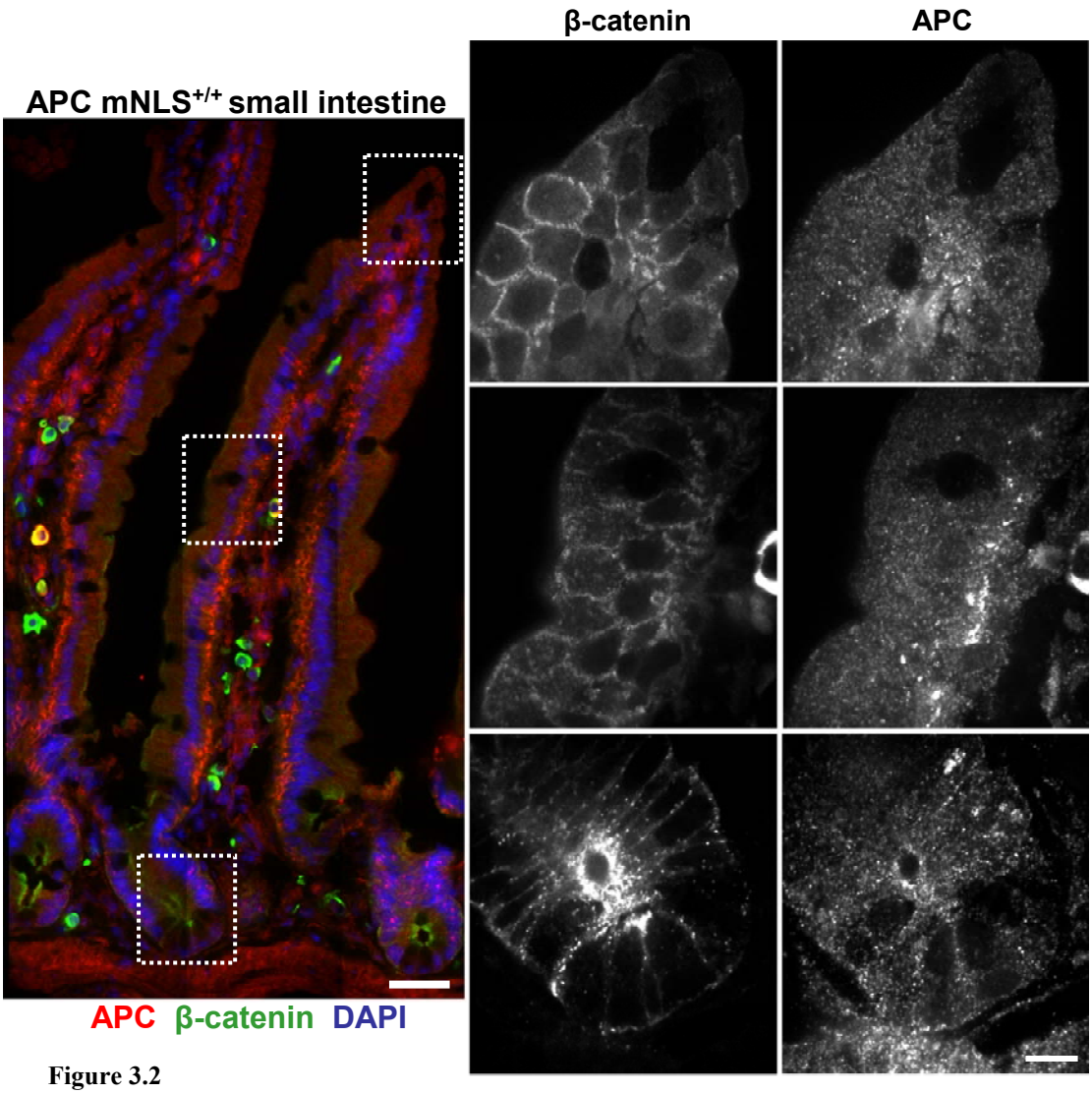

Figure 3.2
APC and β-catenin localization in the small intestine of a APC mNLS$^{+/+}$ mouse. The colored image on the left is a montage generated from multiple confocal images taken at 600X magnification and shows the entire crypt-villus structure. The black and white images on the right show APC or β-catenin localization in the regions of the crypt indicated by the white boxes. The confocal images on the right are taken at 1000x magnification and may be on a slightly different focal plane compared to the montage on the left. (The images of DAPI, used to indicate the location of the nucleus are epifluorescent images not confocal). Scale bar on montage = 30μm. Scale bar for 1000X confocal images= 3μm.

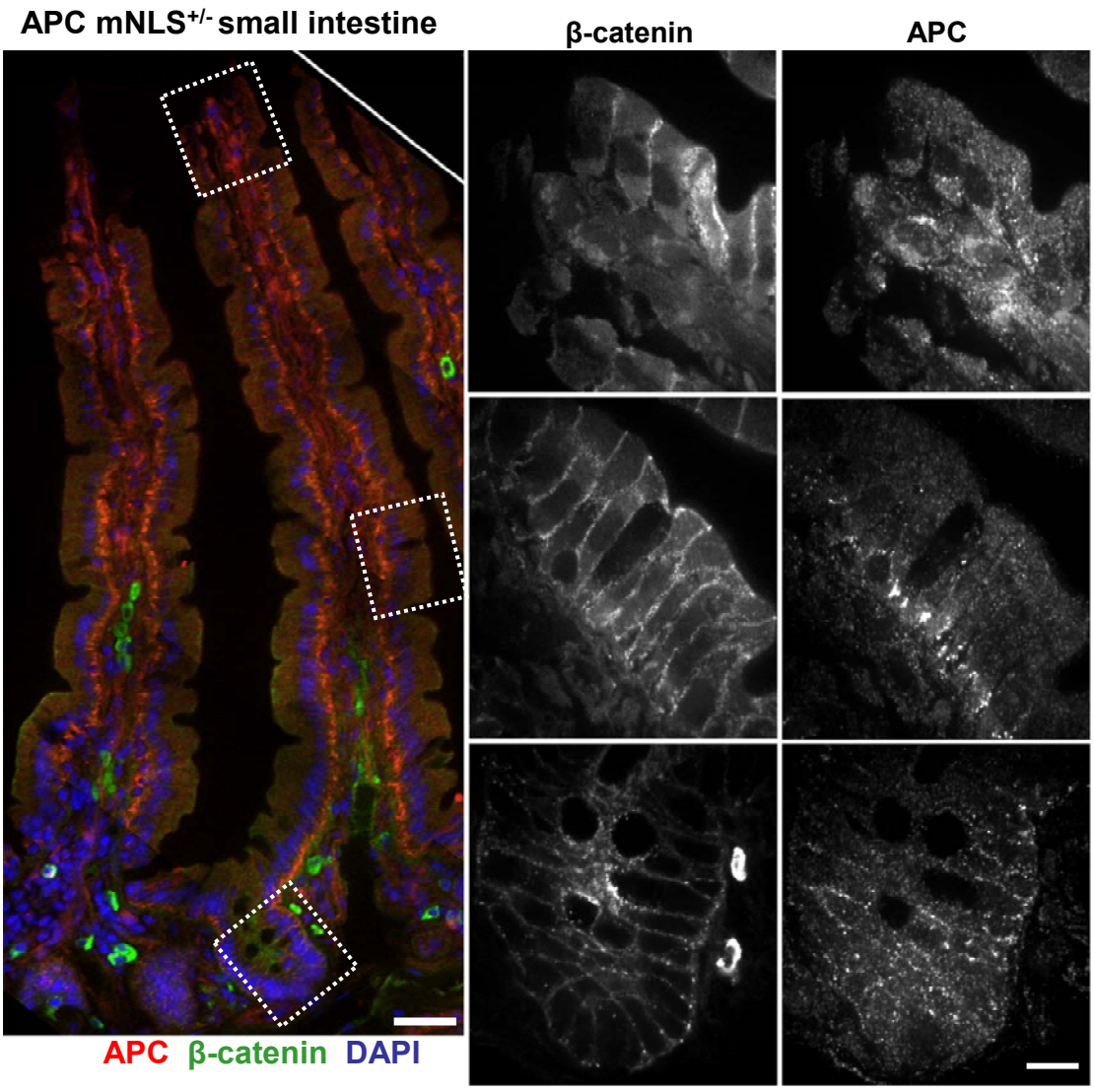

Figure 3.3
APC and β-catenin localization in the small intestine of a APC mNLS$^{+/-}$ mouse. The colored image on the left is a montage generated from multiple confocal images taken at 600X magnification and shows the entire crypt-villus structure. The black and white images on the right show APC or β-catenin localization in the regions of the crypt indicated by the white boxes. The images on the right are confocal images taken at 1000X magnification and may be on a slightly different focal plane compared to the montage on the left. (The images of DAPI, used to indicate the location of the nucleus are epifluorescent images not confocal). Scale bar on montage = 30μm. Scale bar for 1000X confocal images = 3μm.

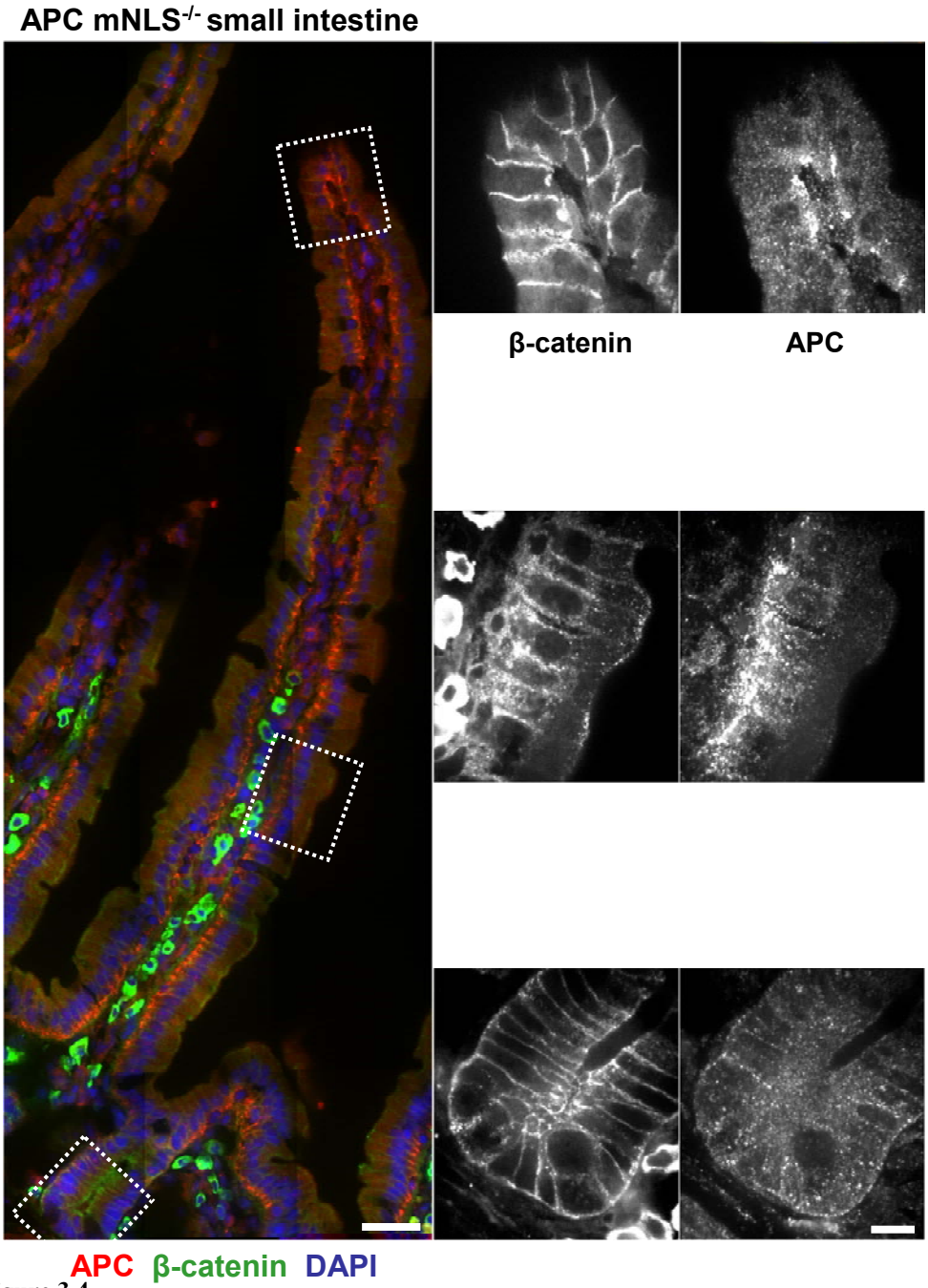

Figure 3.4

APC and β-catenin localization in the small intestine of a APC mNLS$^{-/-}$ mouse. The colored image on the left is a montage generated from multiple confocal images taken at 600X magnification and shows the entire crypt-villus structure. The black and white images on the right show APC or β-catenin localization in the regions of the crypt indicated by the white boxes. The confocal images on the right are taken at 1000X magnification and may be on a slightly different focal plane compared to the montage on the left. (The images of DAPI, used to indicate the location of the nucleus are epifluorescent images not confocal). Scale bar on montage = 30μm. Scale bar for 1000X confocal images = 3μm.

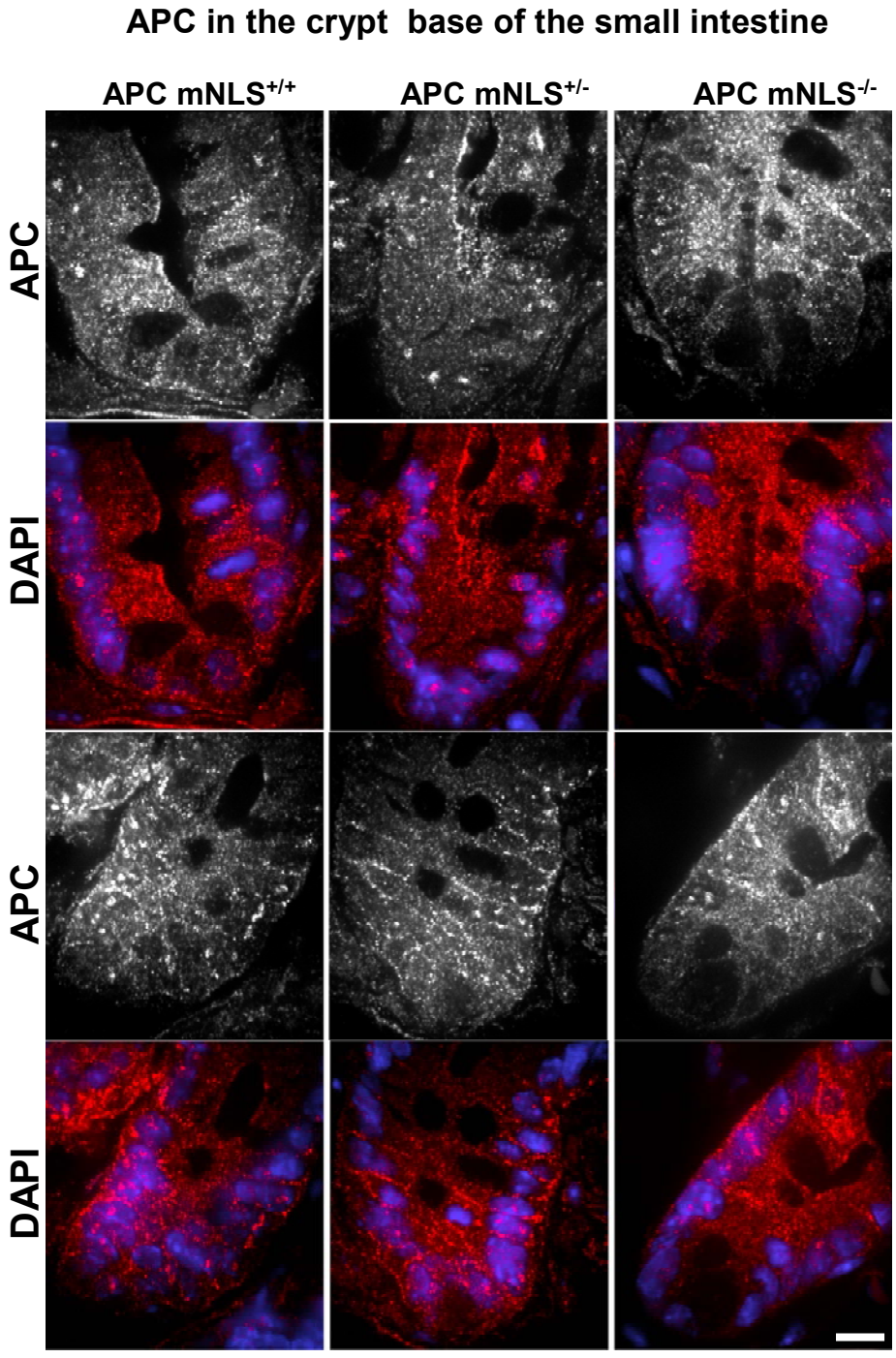

Figure 3.5
APC localization in the base of the crypt from the small intestine in APC mNLS$^{+/+}$, APC mNLS$^{+/-}$, and APC mNLS$^{-/-}$ mice. Images compare APC localization in the base of two separate crypts for each genotype. Confocal images taken at 1000X magnification. Scale bar = 3.0μm

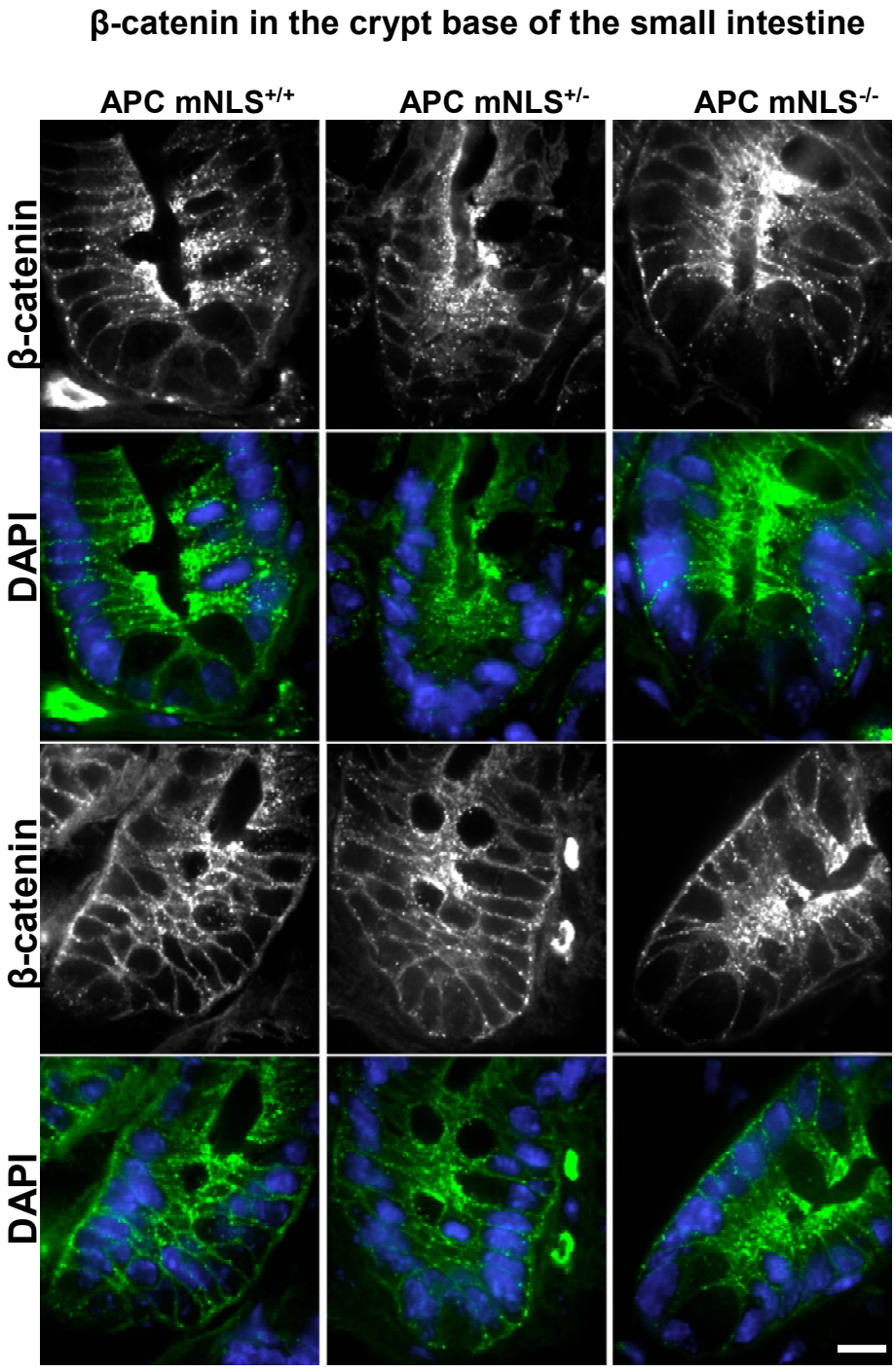

Figure 3.6
β-catenin localization in the base of the crypt from the small intestine in APC mNLS$^{+/+}$, APC mNLS$^{+/-}$, and APC mNLS$^{-/-}$ mice. Images compare β-catenin localization in the base of two separate crypts for each genotype. Confocal images taken at 1000X magnification. Scale bar = 3.0μm

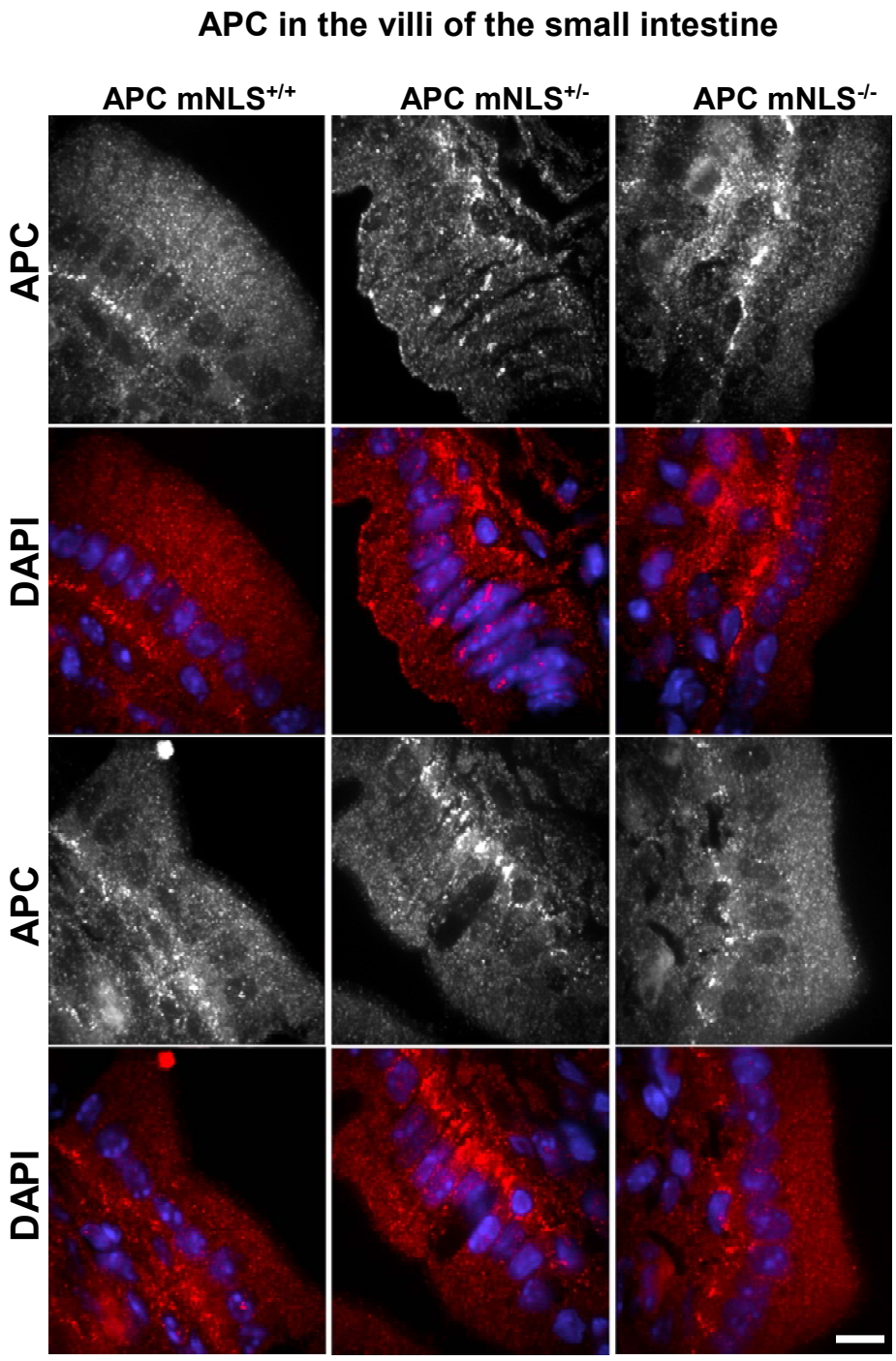

Figure 3.7
APC localization in the villi from the small intestine in APC mNLS$^{+/+}$, APC mNLS$^{+/-}$, and APC mNLS$^{-/-}$ mice. Images compare APC localization in cells approximatly halfway up two separate villi for each genotype. Confocal images taken at 1000X magnification. Scale bar = 3.0μm

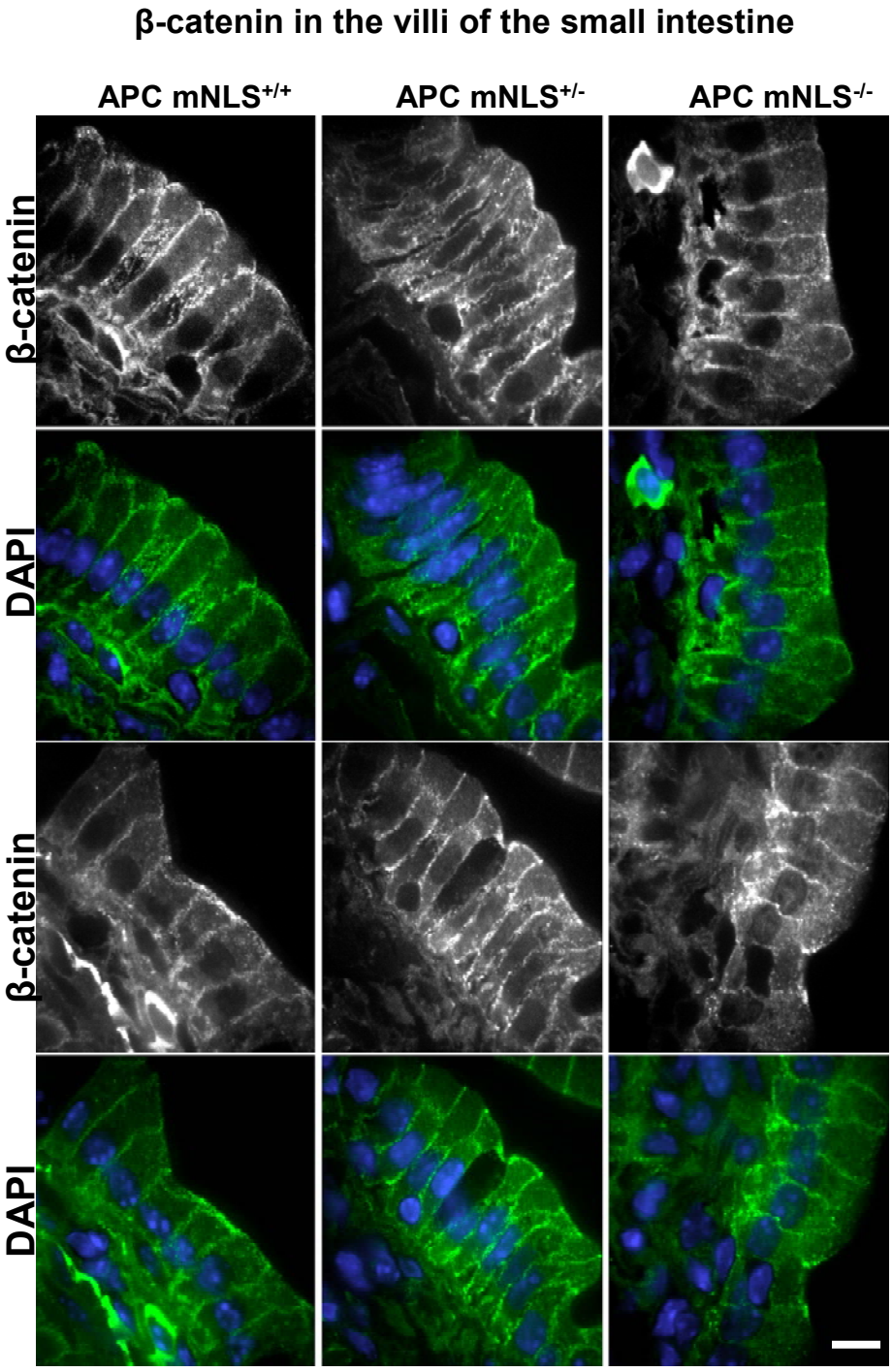

Figure 3.8
β-catenin localization in the villi from the small intestine in APC mNLS$^{+/+}$, APC mNLS$^{+/-}$, and APC mNLS$^{-/-}$ mice. Images compare β-catenin localization in cells approximatly halfway up two separate villi for each genotype. Confocal images taken at 1000X magnification. Scale bar = 3.0μm

comparable to the WT animals (Figure 3.3 and 3.4). APC localization in small intestine of the mutant APC mNLS mice did not appear to be less nuclear than APC in the WT mNLS mice. Even the more intense APC nuclear foci, occasionally observed in the WT crypt cells, were present in the mutant APC mNLS animals (Figure 3.5).

Nuclear localization of APC in mice mutant for the characterized NLSs suggests that there are additional methods by which APC can gain entry into the nucleus. It has been suggested that supplementary sequences with weaker nuclear import ability can be found in the N-terminal region of the APC protein (29). This suspected N-terminal nuclear import site has been proposed to account for the observation that truncated forms of APC, lacking the characterized NLSs, appear to enter the nucleus in human polyp tissue and cancer cell lines (30, 31). There is also the possibility that APC is no longer controlling its own nuclear import, but is interacting with other nuclear proteins that can facilitate import and/or retention of APC in the nucleus. A third explanation for the presence of mutant APC in the nucleus comes from recent evidence that APC may possess an alternate method of nuclear ingress not dependent on the classical importin-α mediated pathway (see Chapter 5). It has been established that cellular stress leads to a blockage of conventional nuclear import by inhibiting the nuclear to cytoplasmic recycling of the importin-α protein (32). Heat shock proteins as well as heat shock cognate proteins, however, continue to localize to the nucleus, despite this import block, through an as yet undetermined method (33, 34). The recent observation that APC is able to

localize to the nuclear compartment in cells following exposure to ultraviolet light supports the idea that APC can also enter the nucleus by this alternative mechanism (See Chapter 5 for further analysis of APC localization following UV exposure). Because the characterized APC NLSs facilitate nuclear import by interacting with importin-α, mutation at these sites would not be expected to prevent nuclear import through a mechanism that is not reliant on the importin-α nuclear import pathway. The APC mNLS mouse model therefore has the potential to be tool to investigate alternative nuclear import mechanisms.

Analysis of APC localization in mouse colon

In normal human colonic epithelium the APC protein has been observed in the nuclear compartment as well as localized to the lateral cell junctions of the epithelial cells (30). A similar staining pattern was observed in the colons of APC $mNLS^{+/+}$ mice. APC was predominantly localized to the membrane of the epithelial cells at the base of the crypt with a more diffuse cytoplasmic staining evident in the cells at the luminal surface (Figures 3.9, 3.12 and 3.14). The overall staining pattern for APC was similar in the mutant and WT APC mNLS mice (Figures 3.10, 3.11, 3.12 and 3.14). Foci of higher APC intensity similar to those observed in the small intestine could occasionally be seen in the cells at the base of the colon crypts as well (Figures 3.9, 3.11 and 3.12). There was no detectable difference in the APC localization at the base of the crypts. However, analysis of the more differentiated cells at the tops of the crypts revealed a reduced intensity of APC staining in the

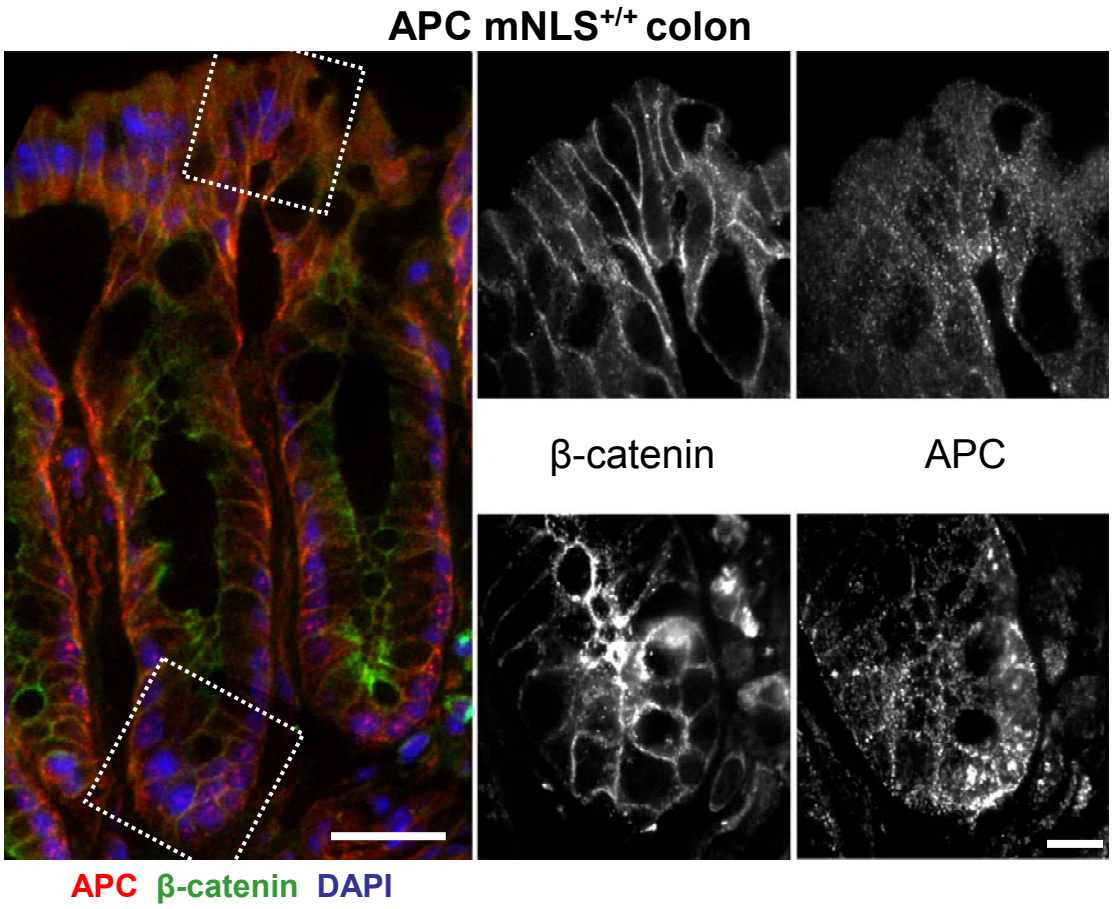

Figure 3.9
APC and β-catenin localization in the colon of a APC mNLS$^{+/+}$ mouse. The colored image on the left is a montage generated from multiple confocal images taken at 600X magnification and shows the entire crypt structure. The black and white images on the right show APC or β-catenin localization in the regions of the crypt indicated by the white boxes. The confocal images on the right were taken at 1000X magnification and may be on a slightly different focal plane compared to the montage on the left. The images of DAPI, used to indicate the location of the nucleus are epifluorescent images not confocal. Scale bar for the montage = 30μm. Scale bar for 1000X confocal images = 3μm.

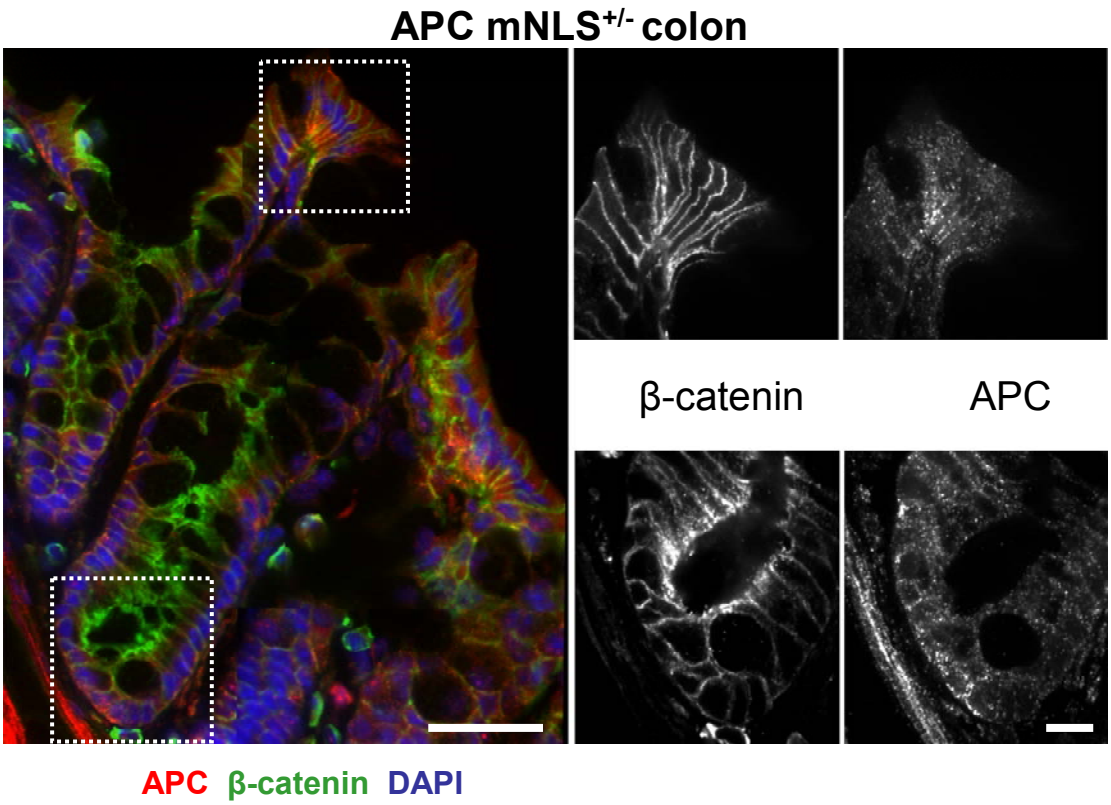

Figure 3.10
APC and β-catenin localization in the colon of a APC mNLS$^{+/-}$ mouse. The colored image on the left is a montage generated from multiple confocal images taken at 600X magnification and shows the entire crypt structure. The black and white images on the right show APC or β-catenin localization in the regions of the crypt indicated by the white boxes. The confocal on the right were taken at 1000X magnification and may be on a slightly different focal plane compared to the montage on the left. The images of DAPI, used to indicate the location of the nucleus are epifluorescent images not confocal. On the montage scale bar = 30μm. Scale bar for 1000X confocal images = 3.0μm.

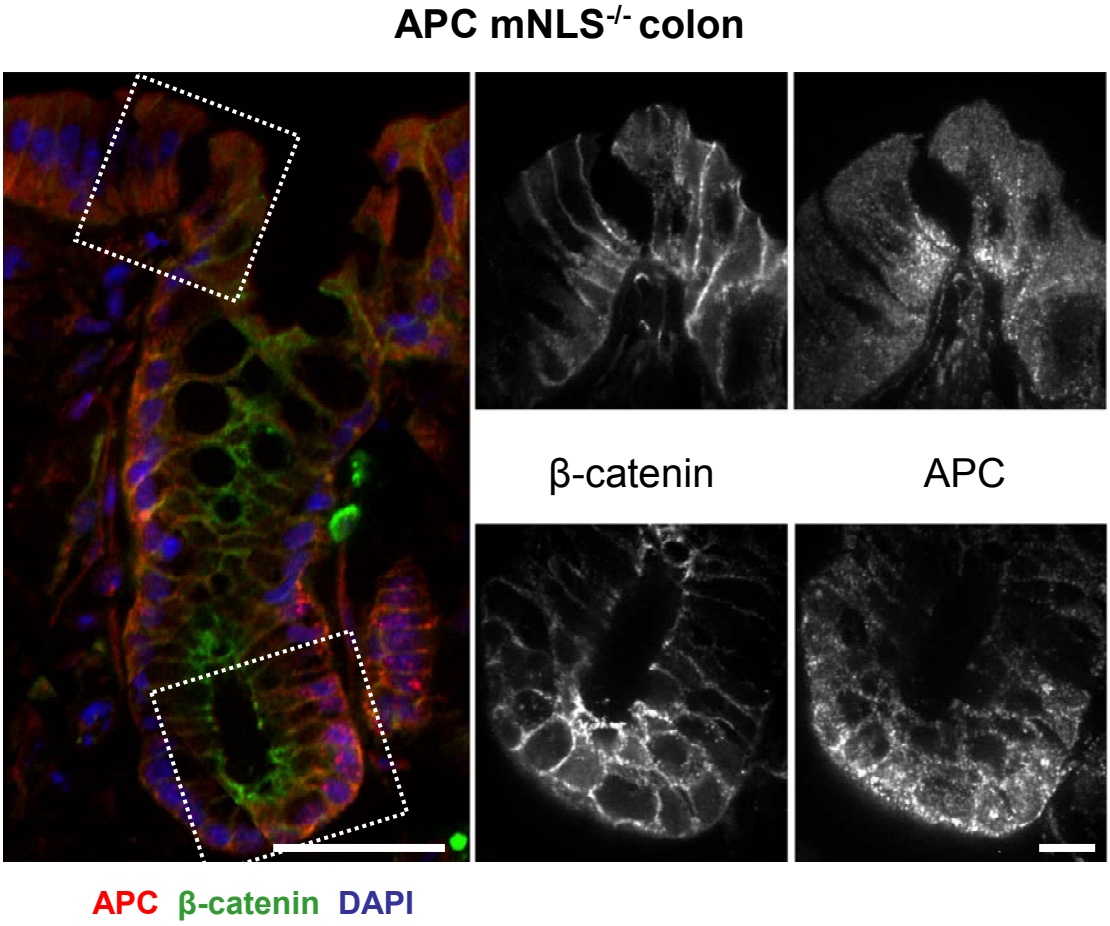

Figure 3.11
APC and β-catenin localization in the colon of a APC mNLS$^{-/-}$ mouse. The colored image on the left is a montage generated from multiple confocal images taken at 600x magnification and shows the entire crypt structure. The black and white images on the right show APC or β-catenin localization in the regions of the crypt indicated by the white boxes. The confocal images on the right were taken at 1000X magnification and may be on a slightly different focal plane compared to the montage on the left. The images of DAPI, used to indicate the location of the nucleus are epifluorescent images not confocal. The scale bar for the montage = 30 μm. Scale bar for the 1000X confocal images = 3.0μm.

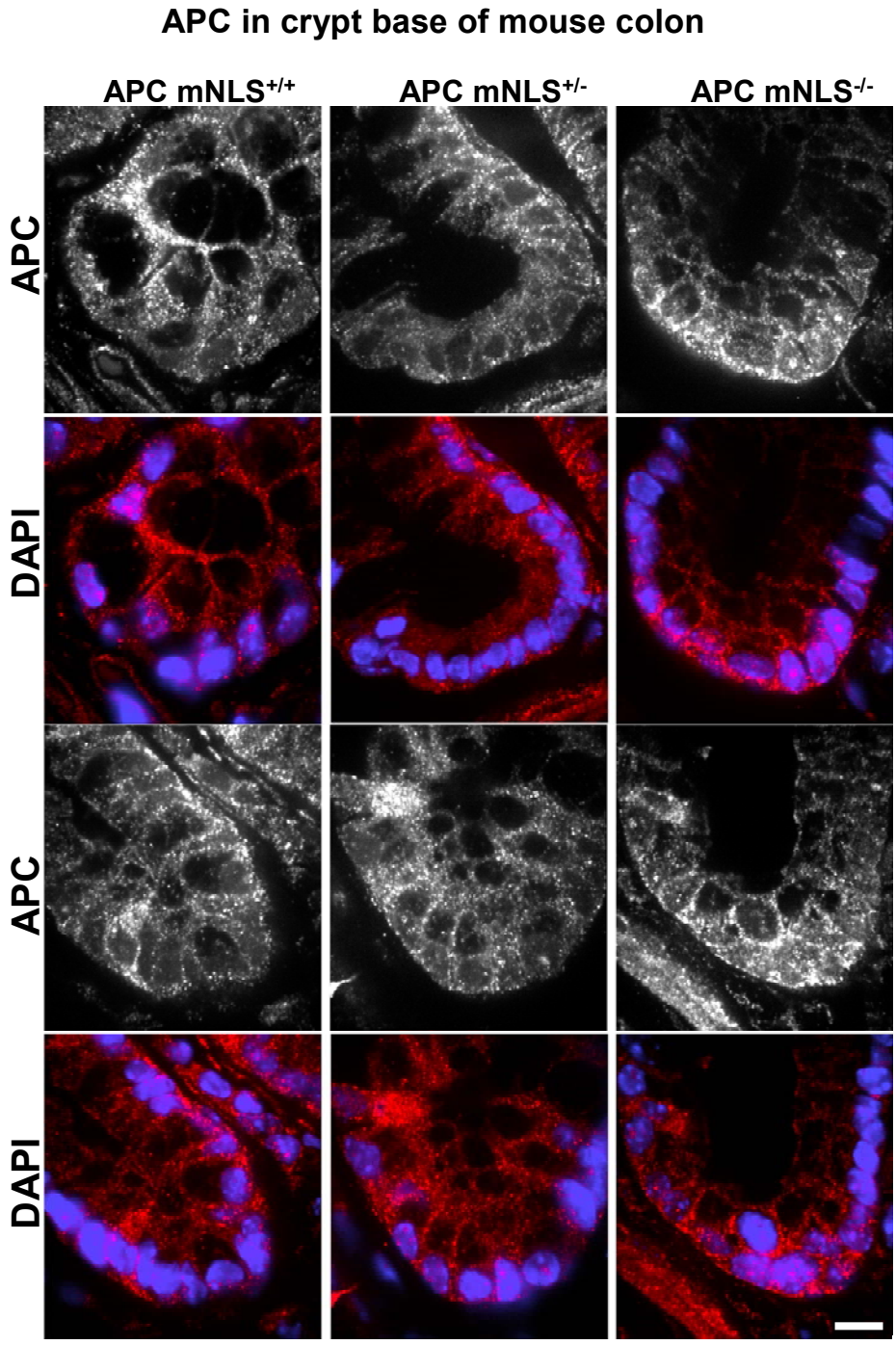

Figure 3.12
APC localization at the crypt base from the colon in APC mNLS$^{+/+}$, APC mNLS$^{+/-}$, and APC mNLS$^{-/-}$ mice. Images compare APC localization in cells at the base of two separate crypts for each genotype. Confocal images taken at 1000X magnification. Scale bar = 3.0μm

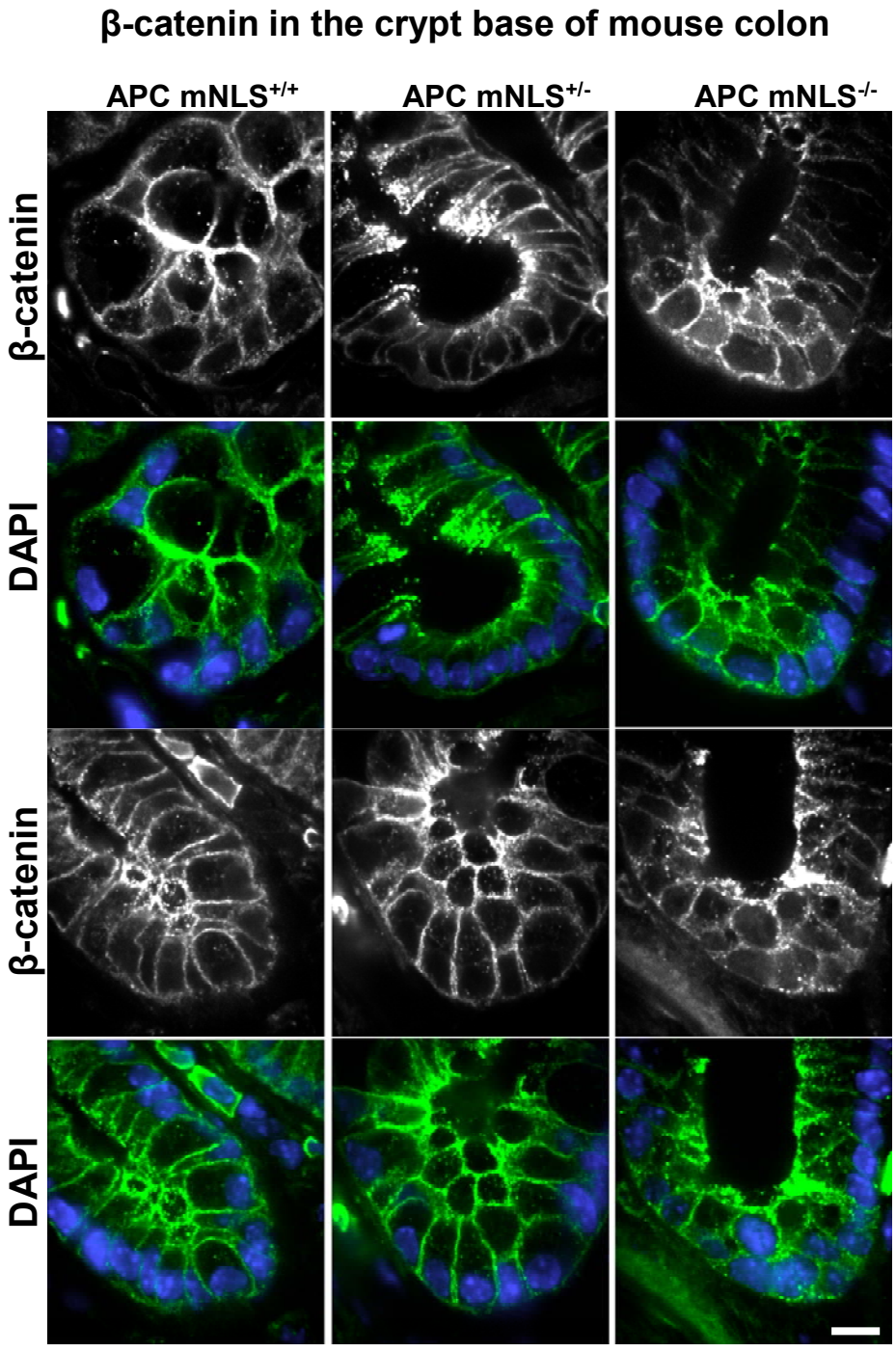

Figure 3.13
β-catenin localization at the crypt base from the colon in APC mNLS$^{+/+}$, APC mNLS$^{+/-}$, and APC mNLS$^{-/-}$ mice. Images compare β-catenin localization in cells at the base of two separate crypts for each genotype. Confocal images taken at 1000X magnification. Scale bar = 3.0μm

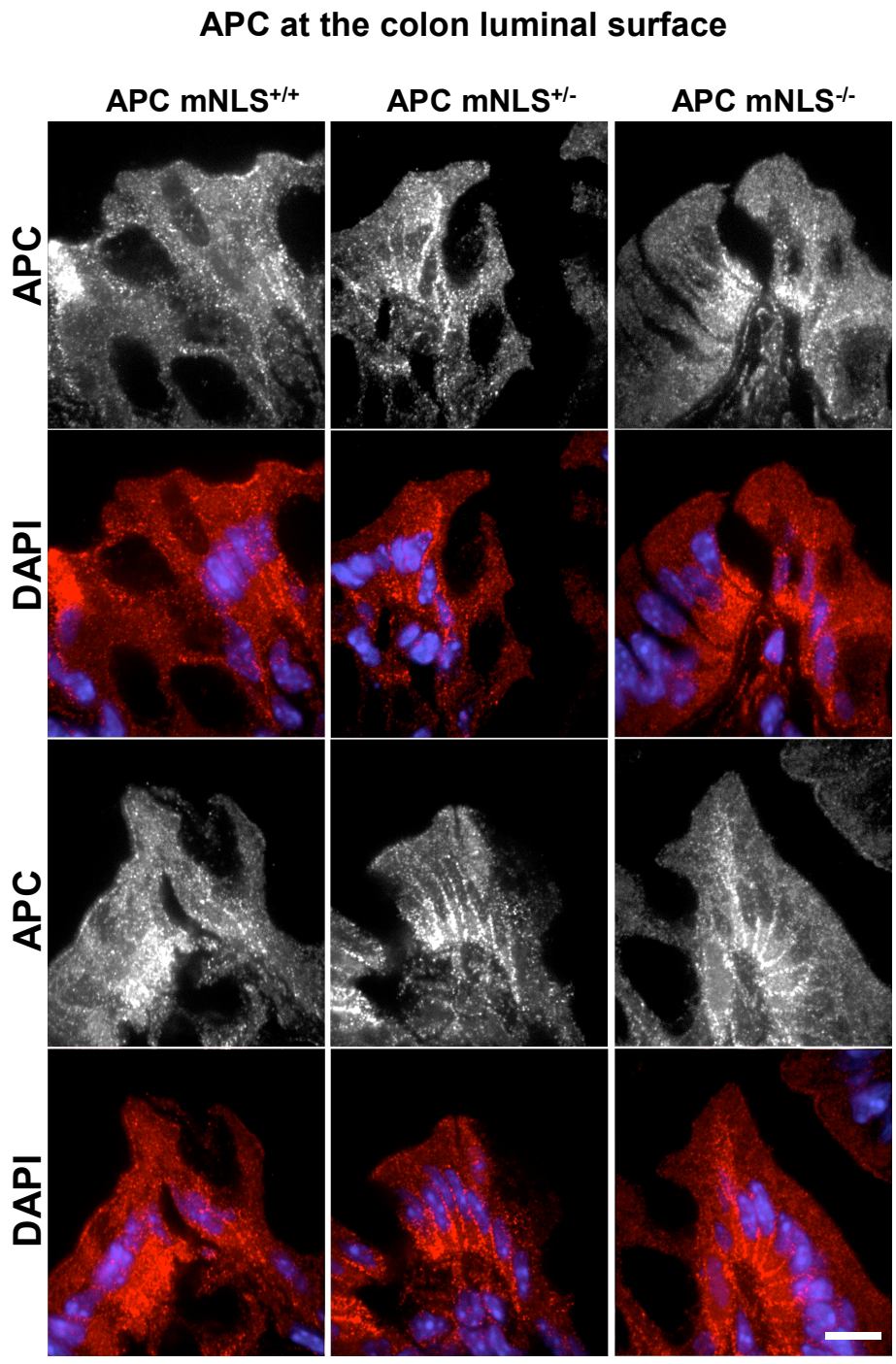

Figure 3.14
APC localization at the luminal surface from the colon in APC mNLS$^{+/+}$, APC mNLS$^{+/-}$, and APC mNLS$^{-/-}$ mice. Images compare APC localization in cells at the top of two separate crypts for each genotype. Confocal images taken at 1000X magnification. Scale bar = 3.0μm

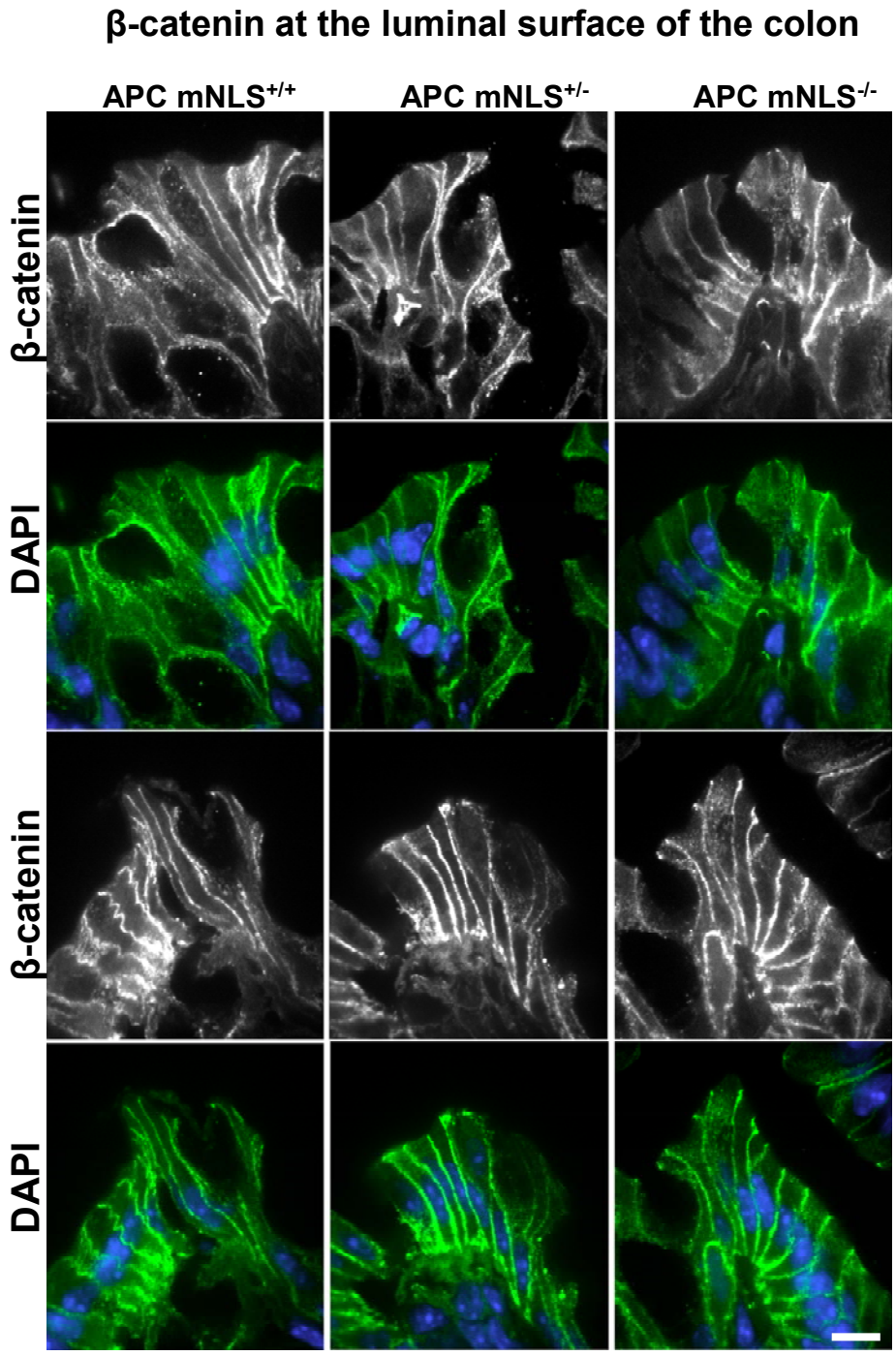

Figure 3.15
β-catenin localization at the luminal surface from the colon in APC mNLS$^{+/+}$, APC mNLS$^{+/-}$, and APC mNLS$^{-/-}$ mice. Images compare β-catenin localization in cells at the top of two separate crypts for each genotype. Confocal images taken at 1000X magnification. Scale bar = 3.0μm

nuclear compartment of the APC mNLS$^{+/-}$ and APC mNLS$^{-/-}$ animals (Figure 3.14). The APC mNLS heterozygous and homozygous mice both displayed a region of decreased APC staining that corresponds to the location of the nucleus. There was no such distinction between the nuclear and cytoplasmic compartments in the WT APC mNLS animals which displayed a more diffuse APC localization pattern in the cells at the luminal surface (Figure 3.14). While a decreased intensity of the nuclear staining existed in regions of the colon, APC protein never appeared to be completely excluded from the nuclear compartment, even in homozygous animals in which both APC alleles were mutant for the known NLSs. The continued presence of APC in the nuclear compartment of the colonic epithelial cells again supports the existence of alternate processes by which APC may gain nuclear entry.

β-catenin levels and localization are altered in the APC mNLS mice.

To further characterize the intestinal epithelium of the APC mNLS mice, western blot analysis was used to evaluate the level of β-catenin in intestinal tissue. APC interacts with β-catenin in the cytoplasm and promotes β-catenin degradation (35). APC also interacts with β-catenin in the nuclear compartment and inhibits β-catenin's transcriptional activity (36). These observations led to the hypothesis that APC may facilitate the export of β-catenin from the nucleus to the cytoplasm. In APC mNLS$^{+/-}$ and APC mNLS$^{-/-}$ mice, we observed that APC was not entirely excluded from the nucleus, and yet β-catenin levels in the intestinal epithelial cells were altered. When compared to their APC NLS WT littermates, APC mNLS$^{-/-}$ mice

expressed more β-catenin in the epithelial cells of their small intestines. Mice heterozygous for the APC NLS mutations expressed an intermediate amount of β-catenin, less than the homozygous mice, but more than the WT mice (Figure 3.16). A similar trend, albeit more subtle, was also observed in the colonic epithelium, with β-catenin levels in heterozygous and homozygous mutant animals greater than the levels in the WT mice (Figure 3.16).

Confocal microscopy of the small intestinal epithelia revealed a gradient of β-catenin staining that was the inverse of the APC expression gradient. β-catenin was expressed at the highest levels in cells at the base of the crypts. Expression levels appeared to decrease as cells migrated upward along the villi towards the tip (Figures 3.2-4). At the base of the crypts, β-catenin was localized almost entirely to the plasma membrane; however, as the overall fluorescent intensity representing β-catenin decreased, it also appeared more evenly distributed through the cytoplasm (Figures 3.6 and 3.8). We observed very little nuclear β-catenin in any cell along the crypt-villus axis (Figures 3.6 and 3.8). There was almost no difference in the localization pattern of β-catenin when APC mNLS mutant and WT animals were compared (Figures 3.2-4, 3.6 and 3.8). The overall level of β-catenin expression, however, did seem to be higher in the intestines of the mutant animals, with the most intense β-catenin staining observed in the APC mNLS homozygous mutant mice (Figures 3.2-4).

The APC NLS mutations do not affect APC's ability to interact with axin to form the β-catenin destruction complex (unpublished observations of Neufeld and

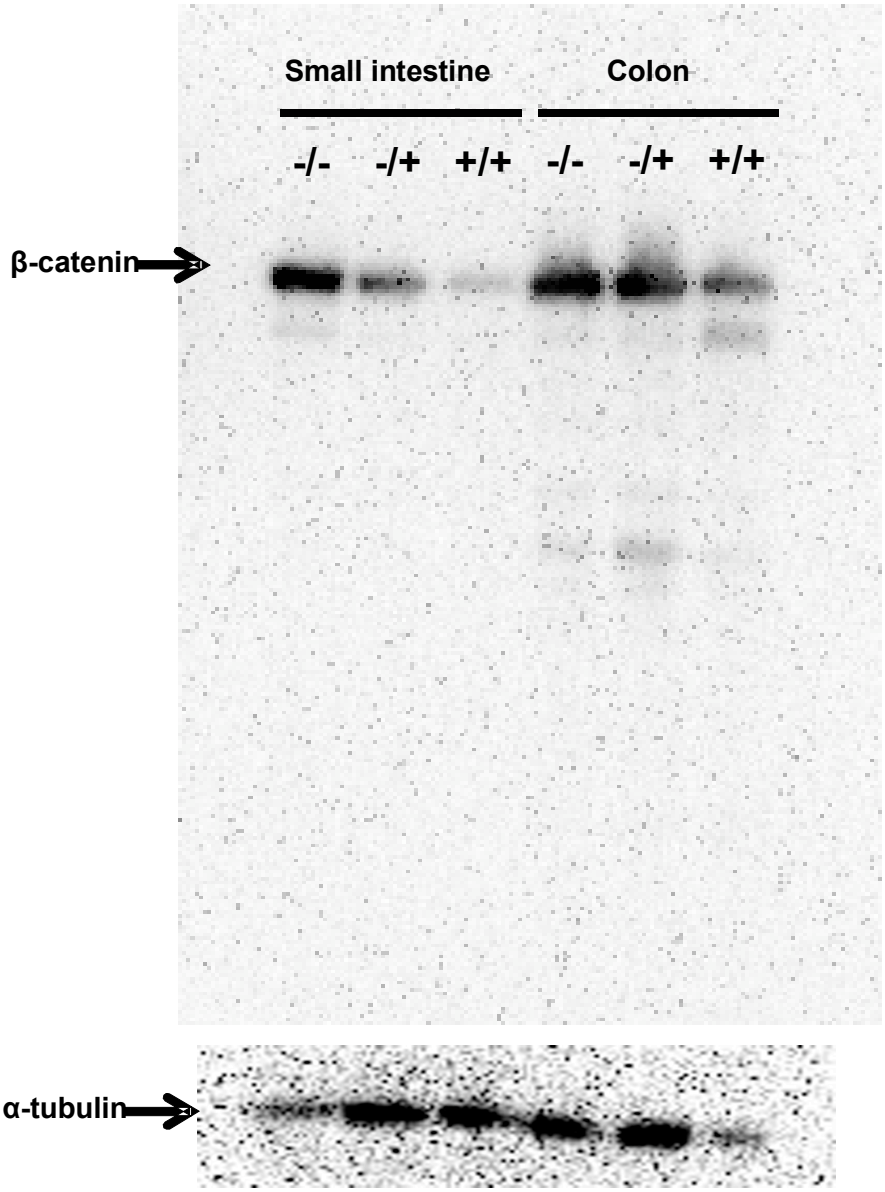

Figure 3.16
Immunoblot of protein from mouse intestinal epithelia of the APC mNLS $^{-/-}$, APC mNLS$^{+/-}$ and APC mNLS$^{+/+}$ mice. Blot is probed with rabbit anti-β-catenin antibody. Colon and small intestinal epithelia were processed separately. Below, an identical blot was probed for α-tubulin to control for loading differences.

White). Therefore, this increase in β-catenin level in the mutant animals supports a role for nuclear APC in regulation of β-catenin. The observation that this regulation is dependent on the NLSs supports the hypothesis that APC regulates the nuclear shuttling of β-catenin.

Colons from APC mNLS$^{+/-}$ mice display a decreased proliferative zone.

Most of the target genes for which β-catenin serves as a co-activator are associated with cell cycle progression (9). An increase in the cellular level of β-catenin would be expected to correlate with an increase in β-catenin's activity as a transcription factor. If the defective nuclear import of APC results in an increase in the transcriptional activity of β-catenin, we would expect to see an elevated level of proliferation in the mutant tissue. To evaluate proliferation levels in the mouse epithelial tissue, we used an anti-Ki67 antibody to detect cycling cells. Ki-67 was originally defined as a monoclonal antibody that reacted to nuclei from Hodgkin's lymphoma cells (37). Little about the cellular function of the Ki-67 antigen is known other than its expression pattern (38). Ki-67 can be detected in the nucleus of actively cycling cells but not quiescent cells (39). This specificity for dividing cells has made Ki-67 a widely used proliferation marker (38).

For our analysis, frozen sections of colon tissue from APC mNLS$^{+/+}$, APC mNLS$^{+/-}$ and APC mNLS$^{-/-}$ mice were evaluated. In the colon, new cells arise from division of the adult stem cells residing at the base of the crypt (40). Asymmetric division of crypt stem cells generally gives rise to one stem and one transiently

amplifying daughter cell which will continue to divide as it migrates up the crypt toward the luminal surface. After several rounds of division, the progeny of the transiently amplifying cells become quiescent and differentiate (41). Therefore, there is a proliferative zone at the base of the crypt and a non-proliferative zone of differentiated cell types at the luminal surface. Aberrant proliferation in the upper portion of the crypt is usually associated with neoplastic transformation (41). Previous analysis of proliferation in the colon revealed actively cycling cells in the lower third of the crypt only (41).

For our analysis, the number of Ki-67 positive cells per crypt was recorded along with the length of the proliferative zone compared to the total length of the crypt as measured using the *SlideBook* software. To determine the length of the proliferative zone a measurement was made from a nucleus at the base of the crypt to highest cell positive for Ki-67 staining. Because the total crypt length progressively changes from the proximal to distal end of the colon, the length of the proliferative zone was divided by the total length of the crypt as measured from a nucleus at the base of the crypt to a nucleus at the luminal surface.

Between 15 and 25 crypts were examined for each genotype and the results are summarized in Table 3.3. The total number of proliferative cells was slightly increased in the tissue from mutant mice when compared to WT littermates. Tissue from the APC mNLS$^{+/+}$ mice displayed an average of 2.8 Ki-67 positive cells per crypt slice while tissue from the APC mNLS$^{+/-}$ and APC mNLS$^{-/-}$ mice displayed on average 3.4 and 3.6 Ki-67 positive cells per crypt, respectively. These very subtle

Table 3.3
Proliferation in the colon of APC mNLS mice

Measurements	APC mNLS+/+	APC mNLS+/-	APC mNLS-/-
Average height of crypt (μm)	166.1	163.7	142.5
Average height of top dividing cells	56.8	37.6	50
Proliferative zone (% of total crypt)	35%	23%	33%
Average number of dividing cells/crypt	2.8	3.4	3.6
Number of crypts measured	21	26	17

differences in the numbers of dividing cells were not considered significantly different from WT using an unpaired t-test (p-values of 0.14 and 0.06 respectively).

There was very little difference in the size of the proliferative zone in homozygous mutant APC mNLS mice and their WT littermates. Both APC mNLS$^{+/+}$ and APC mNLS$^{-/-}$ mice were observed to have a Ki-67 positive cells only in the bottom third of the crypt (35% and 33% respectively). In contrast, the heterozygous mice displayed a reduced proliferative zone. On average, the Ki-67 positive cells were restricted to the bottom 23% of the crypt (Figure 3.17). This difference was significant when analyzed using the unpaired t-test ($p=0.0042$) suggesting that heterozygous APC mNLS mice may have a more severe proliferation defect than the homozygous APC mNLSs mice.

Analysis of gross intestinal phenotype in older APC mNLS mice.

The initial characterization of the intestinal epithelium of the F5 APC mNLS mice established a subtle phenotype at the cellular level. To determine how this cellular phenotype might affect tumor suppression, the gross intestinal phenotype of the oldest available APC mNLS mice was examined. APC mNLS WT and heterozygous mutant mice of the F1 and F2 generations were sacrificed at 40 to 70 weeks of age. At the time of sacrifice the small intestine and colon were removed, fixed and examined for the presence of abnormal tissue. Any regions of irregularity were recorded along with the ID number of the mouse which would later be correlated with the sex, age and genotype of the animal. Pending a more complete

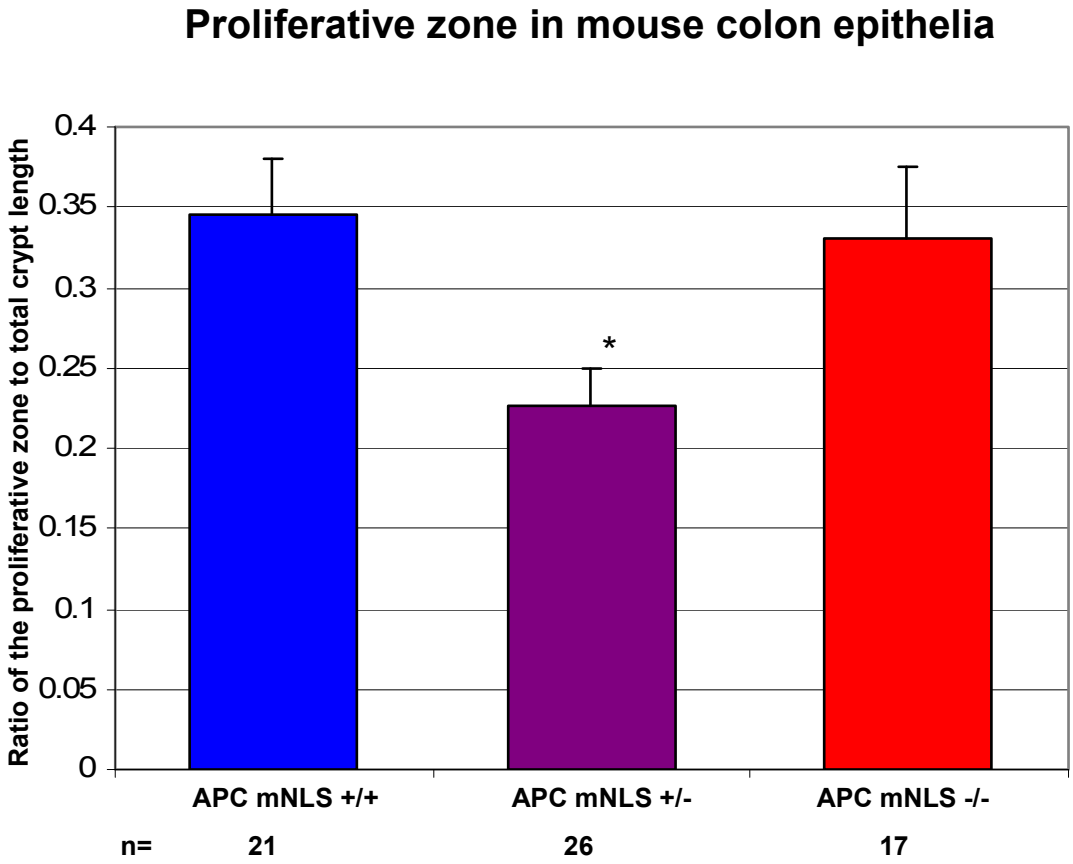

Figure 3.17
Images of colonic crypts stained for Ki-67 proliferation marker were captured on an Olympus 3I spinning disc TIRF inverted microscope and analyzed using *Slidebook* software. The length of the proliferative zone was determined by measuring the distance between the base of the crypt and the most luminal Ki-67 positive nucleus. Total crypt length was measured from a nucleus in the base of the crypt to a nucleus at the intestinal lumen. *p= 0.0042

analysis, these regions of abnormal tissue were termed "intestinal lesions". Generally it was found that the number of lesions per mouse increased as the mice aged. This trend of increased numbers of lesions in the older mice was observed for both the APC mNLS WT and heterozygous mutant mice (Figure 3.18). We did not have a large cohort of older APC mNLS$^{-/-}$ mice for this analysis.

While the overall trend of lesions appearing as a function of time was similar in the heterozygous mutant and WT APC mNLS mice, there was a noticeable difference in the number of lesions per mouse in these two populations. APC mNLS$^{+/-}$ mice developed lesions earlier and at higher numbers than their WT littermates. While the WT mice displayed no lesions in animals less than 60 weeks of age, lesions were found in the heterozygous animals as early as 42 weeks (Figure 3.18). Furthermore, over half of the APC mNLS WT mice were found to have no lesions. Less than one third of the WT mice had one or two lesions and less than 10% of the WT mice displayed more than two intestinal lesions (Figure 3.19). The opposite trend was observed in the APC mNLS$^{+/-}$ mice. Only 25% of the heterozygous APC mNLS mice were lesion-free, while nearly half of the heterozygous animals displayed more than 2 intestinal lesions per mouse (Figure 3.19).

The intestinal regions containing abnormal tissue were removed and stored in formalin. A subset of these samples was sent for histological analysis at the Veterinary Lab Resources department at the University of Kansas Medical Center. All of the intestinal lesions examined were determined to be hyperplastic lymphoid

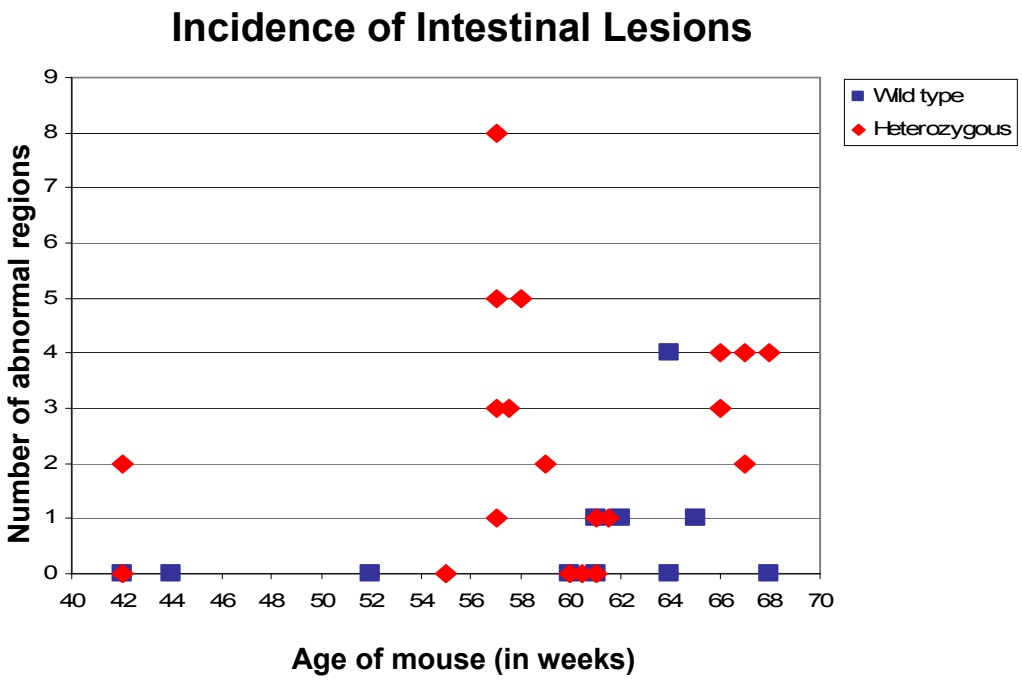

Figure 3.18
Incidence of intestinal lesions per mouse as a function of age in weeks. Generation F1 and F2 heterozygous APC mNLS$^{+/-}$ and APC mNLS$^{-/-}$ mice were sacrificed between 40 and 70 weeks of age. The small intestine and colon were fixed and examined for regions of irregular tissue physiology. The number of irregularities for each mouse was recorded along with the animal's ID number. ID numbers were later used to correlate lesion incidence with the age and genotype of the animal. Each point on the graph above represents one mouse.

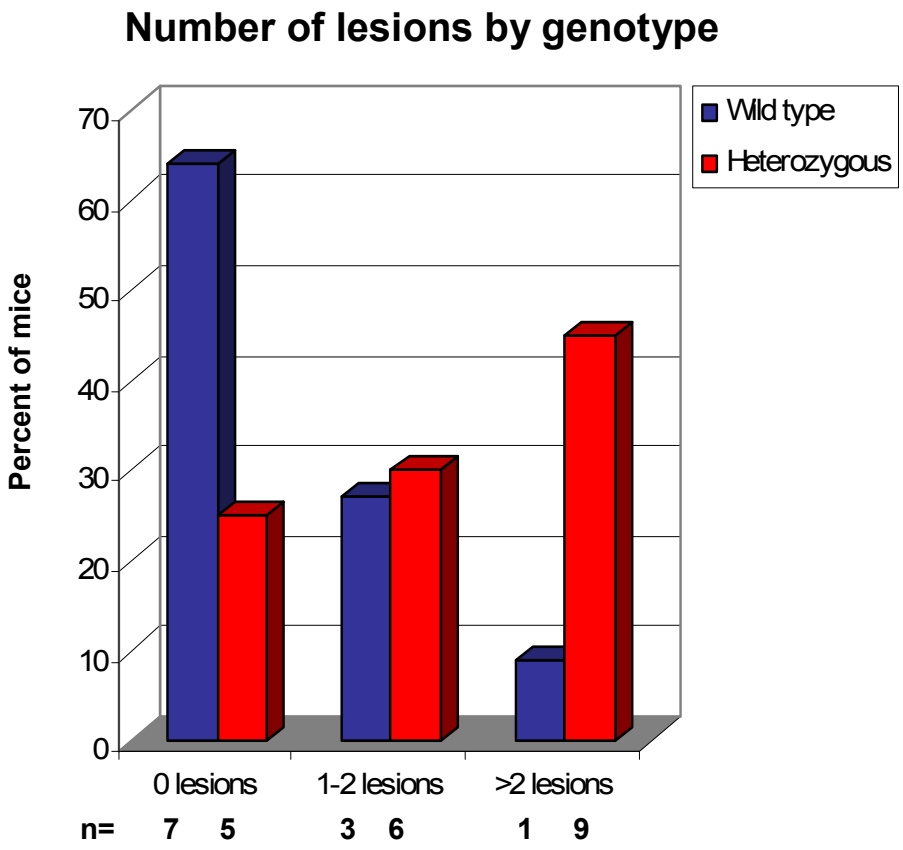

Figure 3.19
The number of intestinal lesions by genotype. APC mNLS$^{+/-}$ mutant animals compared to APC mNLS$^{+/+}$ animals. Mice were assigned to one of three categories based on the total number of lesions that were detected in the intestine. The percent of mice in each category is summarized above. The bars represent the percentage of the total heterozygous (red) or WT (blue) mice in each category. The number of mice in each category is indicated below the graph.

nodules. While the presence of gut-associated lymphoid tissue (GALT) in the intestinal tract is normal, the disparity in the number of macroscopically observable nodules seen in the mutant mice compared to their WT littermates hinted at a potential role for APC in intestinal immune regulation. Tentative links between inflammation and APC mutation have been suggested in previous APC mouse model systems (42-46). Further work in congenic APC mNLS animals that are WT, heterozygous and homozygous mutant for the APC NLSs is necessary to better define this possible role for nuclear APC in the intestinal immune response.

Preliminary analysis of the lymphoid tissue in the mutant and WT APC mNLS mice

There is strong evidence supporting a role for the immune system in the inhibition of cancer (47) and a suggested role for APC in the regulation of the gut associated lymphoid tissue (19-23; and this chapter). Therefore the status of the immune system in the APC mNLS mice was of interest. Previously, our analysis focused on the APC mNLS phenotype as it pertained to intestinal tissue. However, the APC mNLS mutation is not specific to the intestinal tract; all somatic cells of the mutant animals carry the APC NLS mutations. The APC mNLS mouse model, therefore, provides an ideal system for the evaluation of nuclear APC in the development of the various immune organs and cells. The animals used for this preliminary investigation were 13 week old APC mNLS mice, the progeny of two heterozygous F2 APC mNLS mice. At generation F2 the mice should be identical to the C57BL/6J mice across approximately 75% of the genome. Two mice, one APC

mNLS$^{+/+}$ and one APC mNLS$^{-/-}$, were sacrificed for this analysis. Analysis of the splenocytes revealed no significant differences in the white blood cell count, the ratio of T-cells to B-cells, or the ratio of cytotoxic T-cells to helper T-cells in the spleen. There were also no significant differences in the percentage of cells in the various stages of thymocyte development or in the ratios of T-cells to B-cells or cytotoxic T-cells to helper T-cells in the inguinal lymph nodes, peyers patches or bone marrow (personal communication, K. Cool, A. Dotson and S. Benedict). While these data do not support a role for nuclear APC in the development of the immune system, there are several factors to take into account, including the extremely small number of mice analyzed, the young age of the mice analyzed and that these mice are far from congenic. A comprehensive analysis of immune function in the APC mNLS mice would require the use of congenic mice and involve analyzing a larger pool of animals. Another factor to consider is that the appearance of irregular intestinal lymph nodules was associated with a more advanced age in the F1 through F3 generations of mice. Therefore future analysis should examine the state of the immune system in mice that are approaching 52 weeks of age rather than in mice at 13 weeks of age.

Heterozygous and Homozygous APC mNLS mice appear to have a normal lifespan

The normal lifespan of a mouse is between 1.5 and 2.5 years. To assess the average lifespan in the APC mNLS WT, heterozygous and homozygous mutant mice, heterozygous mice of the F1 generation were bred to heterozygous littermates. The

resulting litters contained mice of all three APC mNLS genotypes. These mice are considered outbred and are expected to be only 50% identical to the C57BL/6J. However, because these mice would reach the estimated end of their lifespan at approximately the same time that the first congenic mice would be born, the use of these outbred mice allowed us to evaluate differences in survival nearly two years before this analysis could be accomplished using fully congenic mice. The mice in the survival curve represent the pups from 7 separate litters yielding a total of 70 mice.

At one year the percentage of surviving mice is nearly identical for all three genotypes (Figure 3.20). Because the mice can be expected to begin dying of old age at 1.5 years, the similarity in the number of surviving mice for each of the three genotypes would suggest that the APC mNLS mutations do not affect lifespan. Only seven of the mice assigned to the survival experiment died prior to 1 year. A complete necropsy was performed on one of the dead heterozygous mice. No apparent cause of death was detected. Organs were stored in formalin and subject to histological analysis at the Veterinary Lab Resources Department at the University of Kansas Medical Center. No abnormal physiology was detected in any of the samples sent for analysis. The tendency of the mice to cannibalize dead littermates made cause of death impossible to determine for the other six dead mice.

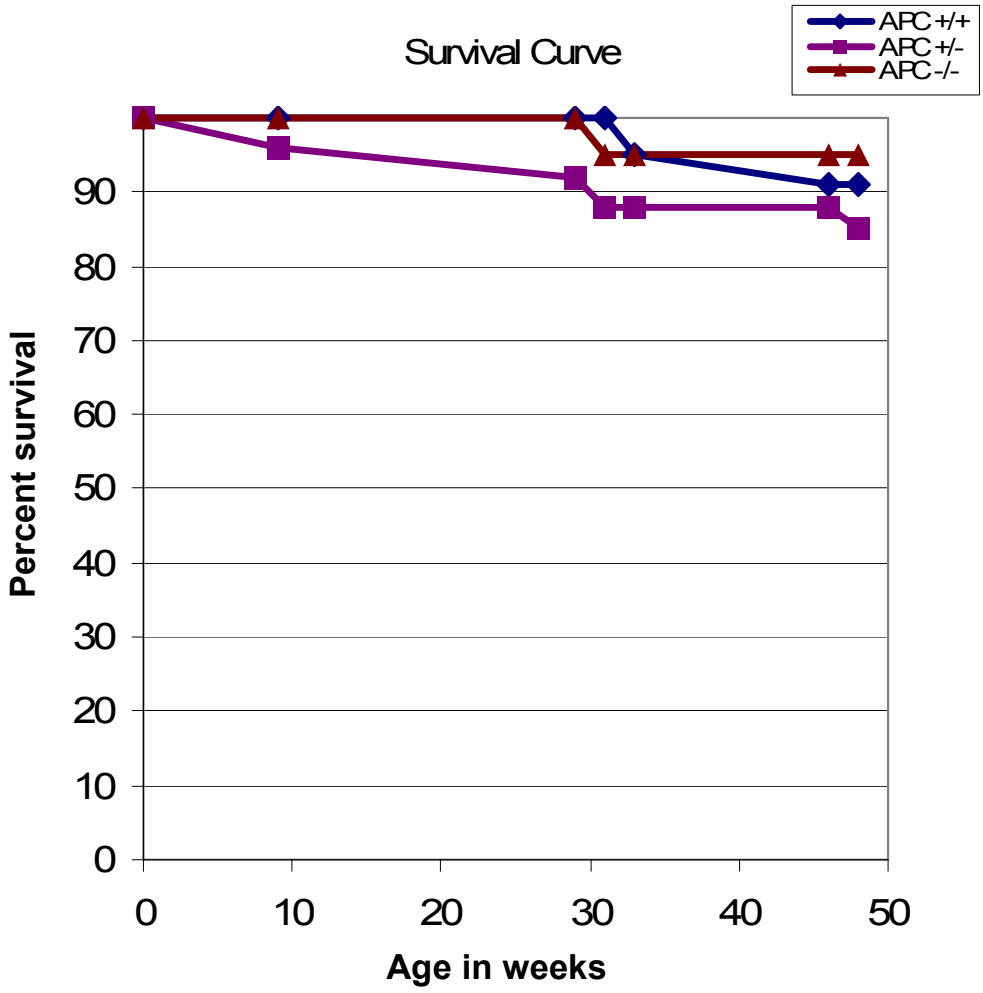

Figure 3.20
A Kaplan-Meyer plot comparing the relative survival rates of APC mNLS$^{+/+}$, APC mNLS$^{+/-}$ and APC mNLS$^{-/-}$ mice. All mice are the result of F1 APC mNLS$^{+/-}$ mice bred to F1 APC mNLS$^{+/+}$ siblings. The curve extends 50 weeks. The oldest litter of mice was born 2/07/07 and the youngest litter was born 4/11/07.

A possible dominant negative effect for the APC mNLS mutation

We saw in the proliferation analysis that heterozygous animals appeared to have a slightly increased number of Ki-67 positive cells and yet displayed a proliferative zone that was reduced in size. This phenotype was not seen in the homozygous mutant animals suggesting that a more severe phenotype may result from heterozygosity for the APC mNLS mutations. There also appears to be a disparity in the number of heterozygous mice born in the APC mNLS mouse colony. In the seven litters of mice that were used for the survival curve, the ratios of APC mNLS$^{+/+}$, APC mNLS$^{+/-}$ and APC mNLS$^{-/-}$ mice varied from the ratios expected based on Mendelian genetics (25:50:25) (Table 3.4). The observed percentages, however, were 33:37:30, indicating that a lower than expected number of heterozygous mice was born. While this disparity was surprising, the chi squared test gave a value of 4.743 correlating with a p-value of 0.0933, which is above the value at which the disparity would be considered statistically significant (a p-value of 0.05 or below is considered statistically significant). To determine if this disparity between the observed and expected distributions would persist, the genotype distribution of the mice in future litters was also analyzed. At generation F5, when all APC mNLS pups resulting from the mating of two heterozygous parents were taken into account, the chi squared test gave a value of 5.9 correlating with a p-value of 0.0524 (Table 2.3). While this value was still above the value considered statistically significant, the discrepancy in the expected and observed distribution of mice was not only still observed but had become more pronounced. Compared to the predicted

Table 3.4 A summary of the genotypes of the mice in the survival curve

	mice born	dead mice
APC mNLS +/+	23	2
APC mNLS +/-	26	4
APC mNLS -/-	21	1
χ^2 value	4.743	2.217
p value	0.0933	0.33

Mendelian ratio, there was still a lower than expected number of heterozygous mice born.

A possible explanation for the lower than expected ratio of heterozygous pups, was that some of the APC mNLS heterozygous mice were dying prior to birth. If the APC mNLS$^{+/-}$ mice die during development, a similar disparity in the distribution of progeny would be expected when the heterozygous APC mNLS mice are bred to WT C57BL/6J mice. Mendelian genetics would predict when a heterozygous mutant mouse is bred to a WT mouse the progeny should be heterozygous mutant or WT with a 50:50 distribution of the two genotypes. Currently there have been 136 pups born as a result of breeding APC mNLS$^{+/-}$ mice to C57BL/6J WT mice. An evaluation of the genotypes in those litters revealed no shortage of heterozygous mice; instead the distribution closely resembled the expected Mendelian values (Table 2.3).

The observation that fewer than expected heterozygous animals were born when both parents carried the APC mNLS mutation, but a normal distribution was observed when one of the parents was a WT mouse suggested that there may be a parental effect. To evaluate the possibility that the genotype of the dam or sire was affecting the genotype distribution of the pups, the litters born to heterozygous females bred to WT males were evaluated separately from the litters born to WT females bred to heterozygous males Table 3.5). Heterozygous pups were born in expected numbers when either the dam or the sire was a WT mouse, regardless of which parent supplied the mutant *Apc* allele.

Table 3.5 A summary of the total mice born to APC mNLS+/- mice bred to WT C57BL/6J mice. The distribution of WT and hetrozygous pups born is analyzed independently for litters in which the mutant APC allele came from the dam versus litters in which the mutant allele was passed down from the sire.

	Heterozygous Sire	Heterozygous Dam	Total
Wild type	38	26	64
Heterozygous	48	24	72
Total	86	50	136
χ^2	1.163	0.080	0.471
p-value	0.2809	0.7773	0.4927

A phenotype suggesting a subtle disadvantage for the heterozygous APC mNLS mice was further supported by the mice in the survival curve. Seven of the 70 mice included in the survival curve died prior to one year. Interestingly, of the 7 mice to die within the first year, 4 of them were heterozygous for the APC mNLS mutation. If mouse deaths were not connected to the APC genotype, it would be expected that the dead mice would be evenly distributed across all three genotypes. Again this discrepancy is not considered significant according a chi squared test (Table 3.4). However, the higher than expected ratio of heterozygous mice to die early in conjunction with the lower than expected ration of heterozygous mice born is grounds for continued close observation of the heterozygous phenotype in the mouse colony.

Discussion

The APC mNLS mice carry knock-in mutations to the endogenous *Apc* gene. These mutations consist of alanine substitutions for the lysine and arginine residues that form the APC NLSs (Figure 2.1). The loss of these highly charged amino acids prevents these sites from binding to importin-α, resulting in an APC protein that is deficient in its ability to be effectively targeted to the nucleus (25). Endogenous APC with knock-in mutations to the NLSs was observed at normal levels in the intestinal epithelium with an overall localization pattern similar to WT APC. Confocal analysis

of the intestinal epithelia of the APC mNLS mutant animals revealed a decrease in the ratio of APC in the nuclear compartment in the colon but no apparent phenotype in the small intestine. APC was never observed to be completely excluded from the nucleus even in the homozygous mutant animals. The continued presence of APC in the nucleus suggests that another method of nuclear import is able to at least partially compensate for the loss of APC's NLSs. It is currently not known if APC is routinely imported through this alternate method, or if the cell is initiating an alternative nuclear import pathway in response to APC levels in the nucleus falling below some critical threshold level. The existence of a compensatory pathway is supported by the observation that the heterozygous mutant mice seem to be subtly disadvantaged. It is conceivable that in a subset of animals with only one mutant APC allele, the nuclear levels of APC are too low to maintain proper tissue integrity, but high enough that no cellular counterbalance action is initiated. The homozygous APC mNLS mice, which would be expected to completely lack nuclear APC, seem to survive as well as the WT animals and perhaps slightly better than their heterozygous littermates. One explanation is that cells that completely lack APC mNLS activity are able to initiate an emergency mechanism to counteract the loss of correct APC nuclear shuttling.

While this sustained nuclear import makes the nuclear function of APC more complicated to analyze in these mice, there is the potential that the APC mNLS mouse line will be a valuable tool for the investigation of alternate nuclear import strategies. It has been observed previously that truncated forms of APC can retain some of their nuclear shuttling ability even after the loss of the NLSs (29). This,

however, is the first reported observation of full length APC protein shuttling into the nucleus without the characterized NLSs.

Further analysis of the intestinal epithelium revealed that β-catenin protein levels were elevated in mice that carried APC mNLS mutations. A potential role for APC in the regulation of the nuclear level of β-catenin has long been supported (36, 48, 49). It is known that the APC NLSs are regulated by phosphorylation (25, 50). It is possible that APC is phosphorylated in response to cell signaling events and that this modification results in APC targeting to the nucleus to down-regulate β-catenin transcriptional activity and facilitate β-catenin export to the cytoplasm for proteolysis (36, 48, 49). The inhibition of the NLSs through mutation would then result in a loss of correct nuclear targeting in response to APC phosphorylation. However, the size of the proliferative compartment in the intestinal epithelium of APC mNLS mutant mice was not what would be expected to accompany transcriptionally active β-catenin. While there appeared to be a slight increase in the total number of Ki-67 positive cells in the mutant APC mNLS compared to their WT littermates, these differences were not significant.

Despite some observed changes in APC localization, β-catenin abundance, and proliferation seen at the cellular level, at the organismic level, APC mNLS mutant mice appear to be phenotypically normal, with a similar lifespan as their wild type siblings and no apparent polyposis phenotype. At the macroscopic level, the only observed difference in the intestine of the heterozygous mutant and WT APC mNLS animals was an increase in the number of lymphoid nodules in the intestines of the

mutant animals. Lymphoid nodules are present in both mutant and WT APC mNLS mice and the incidence of macroscopically observable nodules increases with age for both genotypes. However, the APC mNLS$^{+/-}$ mice appeared more likely to develop nodules at an earlier age and displayed a greater number of total nodules than the APC mNLS$^{+/+}$ mice.

A link between APC function, intestinal polyposis and inflammation has been suggested previously. Both animal studies and epidemiological evidence in human FAP patients suggest that non-steroidal anti-inflammatory drugs (NSAIDs) are able to inhibit polyp development and progression in the intestine (51). Previous APC mouse models have also reported a phenotype in both the local and systemic immune system of the mutant mice. In general APC mutations seem to cause a decrease in immune function (42, 45) and a stimulation of intestinal immune activity leads to an inhibition of polyp formation in APC mutant mice (43, 46). While there is no apparent polyposis phenotype in the APC mNLS mice, there does appear to be an age dependent stimulation of the gut associated lymphoid tissue. If a local immune response can be stimulated by a C-terminal domain of APC in the cytoplasm it would explain the observations that truncated APC results in a decreased immune response. In that same scenario, a stimulation of the intestinal immune system would be expected in the APC mNLS mice in which full length APC is retained in the cytoplasm due to defective nuclear shuttling. Further studies of the immune system in older APC mNLS mice are needed to establish a more definitive relationship between APC status and immune function.

Another hypothesis explaining why there is no apparent polyposis phenotype in the APC mNLS mice is that nuclear APC may not be essential for tumor suppression under normal physiological conditions. This does not preclude the possibility that nuclear APC may play a role in other processes such as the protection against DNA damage or DNA repair. Should APC participate in the cellular DNA damage response, a phenotype would only become apparent if the mice were to encounter stresses that are improbable given the highly controlled environment in which they are maintained. It is also possible that one or several of APC's multiple nuclear binding partners may be assisting in nuclear import. This assisted shuttling in conjunction with the suspected weaker nuclear import sites may result in enough APC being shuttled into the nucleus to maintain at least the appearance of normalcy in a controlled environment. We have received approval to conduct an animal study in which the APC mNLS mice will be treated with reagents that will induce genotoxic stress in the intestinal epithelium. However, an analysis of this magnitude can not be properly performed without a fully congenic APC mNLS mouse colony.

To date, the generation of a congenic APC mNLS mouse line in the C57BL/6J genetic background is ongoing, with the first congenic mice expected to be born within by early 2009. The establishment of a colony of congenic APC mNLS C57BL/6J mice will allow for a more complete evaluation of the APC mNLS phenotype. The fully congenic mice will allow direct comparison of the APC mNLS phenotype with the WT C57BL/6J animals as well as other existing APC mouse models currently on the C57BL/6 background. In addition, the congenic APC mNLS

mice will be bred with other mouse models that carry mutations in proteins of interest. We currently have a colony of APC Min mice which we intend to breed with APC mNLS congenic animals. We are also expecting delivery of mice that carry a Fen-1 mutation. The Fen-1 mice carry a knock-out mutation in an allele of the Flap endonuclease-1 (*Fen-1*) gene, a component required for the base excision pathway of DNA repair. An analysis of the phenotype in the congenic APC mNLS mice as well as $APC^{Min/mNLS}$ mice and Fen-$1^{-/-}$ APC $mNLS^{-/-}$ double mutant animals will further our understanding of the role for nuclear APC in tissue maintenance and tumor suppression. Preliminary data collected in the non-congenic APC mNLS animals over the past year has suggested a role for nuclear targeted APC in the regulation of cellular levels of the oncogene β-catenin. Furthermore, our initial analysis has also hinted at a possible function for nuclear APC in the intestinal immune response. These and other avenues of investigation will be further pursued using the congenic APC mNLS mouse colony.

Acknowledgements

I would like to thank Preston Alltizer for assistance preparing and imaging the intestinal tissue and William McGuinness for assistance evaluating intestinal lesions in the APC mNLS mice. A special thanks to Abby Dotson and Kelli Cool for the analysis of the lymphoid tissue from APC $mNLS^{+/+}$ and APC $mNLS^{-/-}$ mice.

References

1. Silver, L. M. (1995) *Mouse Genetics: Concepts and Applications*, Oxford University Press
2. Laboratories, J. (2008) JAX Mice & Services. In
3. Thomas, K. R., and Capecchi, M. R. (1987) Site-directed mutagenesis by gene targeting in mouse embryo-derived stem cells. *Cell* 51, 503-512
4. Nagy, A., Rossant, J., Nagy, R., Abramow-Newerly, W., and Roder, J. C. (1993) Derivation of completely cell culture-derived mice from early-passage embryonic stem cells. *Proc Natl Acad Sci U S A* 90, 8424-8428
5. Nagy, A., Gertsenstein, M., Vintersten, K., and Behringer, R. (2003) *Manipulating the Mouse Embryo: a laboratory manual*, Cold Spring Harbor Laboratory Press, Cold Spring Harbor
6. Papaioannou, V. E., and Behringer, R. R. (2005) *Mouse Phenotypes: A handbook of mutation analysis*, Cold Spring Harbor Laboratory Press, New York
7. Colnot, S., Niwa-Kawakita, M., Hamard, G., Godard, C., Le Plenier, S., Houbron, C., Romagnolo, B., Berrebi, D., Giovannini, M., and Perret, C. (2004) Colorectal cancers in a new mouse model of familial adenomatous polyposis: influence of genetic and environmental modifiers. *Lab Invest* 84, 1619-1630
8. Smits, R., Kielman, M. F., Breukel, C., Zurcher, C., Neufeld, K., Jagmohan-Changur, S., Hofland, N., van Dijk, J., White, R., Edelmann, W., Kucherlapati, R., Khan, P. M., and Fodde, R. (1999) Apc1638T: a mouse model delineating critical domains of the adenomatous polyposis coli protein involved in tumorigenesis and development. *Genes Dev* 13, 1309-1321
9. Kolligs, F. T., Bommer, G., and Goke, B. (2002) Wnt/beta-catenin/tcf signaling: a critical pathway in gastrointestinal tumorigenesis. *Digestion* 66, 131-144
10. Laboratory, T. J. Induced Mutant Resources: Tail DNA for PCR (No Organic Solvents). In Vol. 2005, http://www.jax.org/imr/tail_nonorg.html
11. Whitehead, R. H., Demmler, K., Rockman, S. P., and Watson, N. K. (1999) Clonogenic growth of epithelial cells from normal colonic mucosa from both mice and humans. *Gastroenterology* 117, 858-865
12. Nathke, I. S., Adams, C. L., Polakis, P., Sellin, J. H., and Nelson, W. J. (1996) The adenomatous polyposis coli tumor suppressor protein localizes to plasma membrane sites involved in active cell migration. *J Cell Biol* 134, 165-179
13. McLean, I. W., and Nakane, P. K. (1974) Periodate-lysine-paraformaldehyde fixative. A new fixation for immunoelectron microscopy. *J Histochem Cytochem* 22, 1077-1083
14. Magnus, H. A. (1937) Observations on the presence of intestinal epithelium in the gastric mucosa. *The Journal of Pathology and Bacteriology* 44, 389-398

15. Mitchell, K. M., Dotson, A. L., Cool, K. M., Chakrabarty, A., Benedict, S. H., and LeVine, S. M. (2007) Deferiprone, an orally deliverable iron chelator, ameliorates experimental autoimmune encephalomyelitis. *Mult Scler* 13, 1118-1126
16. Itoh, M., Maeno, A., Tari, A., Itoh, S., Kawakami, A., Sawada, M., Ohno, T., and Noda, T. (2000) Genetic Analysis of Modifier Genes which Influence the Tumor Multiplicity in FAP Model Mice. In The 14th International Mouse Genome Confrence
17. Sasai, H., Masaki, M., and Wakitani, K. (2000) Suppression of polypogenesis in a new mouse strain with a truncated Apc(Delta474) by a novel COX-2 inhibitor, JTE-522. *Carcinogenesis* 21, 953-958
18. Moser, A. R., Pitot, H. C., and Dove, W. F. (1990) A dominant mutation that predisposes to multiple intestinal neoplasia in the mouse. *Science* 247, 322-324
19. Fodde, R., Edelmann, W., Yang, K., van Leeuwen, C., Carlson, C., Renault, B., Breukel, C., Alt, E., Lipkin, M., Khan, P. M., and et al. (1994) A targeted chain-termination mutation in the mouse Apc gene results in multiple intestinal tumors. *Proc Natl Acad Sci U S A* 91, 8969-8973
20. Oshima, M., Oshima, H., Kitagawa, K., Kobayashi, M., Itakura, C., and Taketo, M. (1995) Loss of Apc heterozygosity and abnormal tissue building in nascent intestinal polyps in mice carrying a truncated Apc gene. *Proc Natl Acad Sci U S A* 92, 4482-4486
21. Ishikawa, T. O., Tamai, Y., Li, Q., Oshima, M., and Taketo, M. M. (2003) Requirement for tumor suppressor Apc in the morphogenesis of anterior and ventral mouse embryo. *Dev Biol* 253, 230-246
22. Kucherlapati, M., Yang, K., Kuraguchi, M., Zhao, J., Lia, M., Heyer, J., Kane, M. F., Fan, K., Russell, R., Brown, A. M., Kneitz, B., Edelmann, W., Kolodner, R. D., Lipkin, M., and Kucherlapati, R. (2002) Haploinsufficiency of Flap endonuclease (Fen1) leads to rapid tumor progression. *Proc Natl Acad Sci U S A* 99, 9924-9929
23. Wei, K., Clark, A. B., Wong, E., Kane, M. F., Mazur, D. J., Parris, T., Kolas, N. K., Russell, R., Hou, H., Jr., Kneitz, B., Yang, G., Kunkel, T. A., Kolodner, R. D., Cohen, P. E., and Edelmann, W. (2003) Inactivation of Exonuclease 1 in mice results in DNA mismatch repair defects, increased cancer susceptibility, and male and female sterility. *Genes Dev* 17, 603-614
24. Dietrich, W. F., Lander, E. S., Smith, J. S., Moser, A. R., Gould, K. A., Luongo, C., Borenstein, N., and Dove, W. (1993) Genetic identification of Mom-1, a major modifier locus affecting Min-induced intestinal neoplasia in the mouse. *Cell* 75, 631-639
25. Zhang, F., White, R. L., and Neufeld, K. L. (2000) Phosphorylation near nuclear localization signal regulates nuclear import of adenomatous polyposis coli protein. *Proc Natl Acad Sci U S A* 97, 12577-12582

26. Neufeld, K. L., and White, R. L. (1997) Nuclear and cytoplasmic localizations of the adenomatous polyposis coli protein. *Proc Natl Acad Sci U S A* 94, 3034-3039
27. Ross, M. H., and Pawlina, W. (2005) *Histology: A text and atlas*, Lippincott Williams & Wilkins, Baltimore, MD
28. Aust, D. E., Terdiman, J. P., Willenbucher, R. F., Chew, K., Ferrell, L., Florendo, C., Molinaro-Clark, A., Baretton, G. B., Lohrs, U., and Waldman, F. M. (2001) Altered distribution of beta-catenin, and its binding proteins E-cadherin and APC, in ulcerative colitis-related colorectal cancers. *Mod Pathol* 14, 29-39
29. Galea, M. A., Eleftheriou, A., and Henderson, B. R. (2001) ARM domain-dependent nuclear import of adenomatous polyposis coli protein is stimulated by the B56 alpha subunit of protein phosphatase 2A. *J Biol Chem* 276, 45833-45839
30. Anderson, C. B., Neufeld, K. L., and White, R. L. (2002) Subcellular distribution of Wnt pathway proteins in normal and neoplastic colon. *Proc Natl Acad Sci U S A* 99, 8683-8688
31. Fagman, H., Larsson, F., Arvidsson, Y., Meuller, J., Nordling, M., Martinsson, T., Helmbrecht, K., Brabant, G., and Nilsson, M. (2003) Nuclear accumulation of full-length and truncated adenomatous polyposis coli protein in tumor cells depends on proliferation. *Oncogene* 22, 6013-6022
32. Miyamoto, Y., Saiwaki, T., Yamashita, J., Yasuda, Y., Kotera, I., Shibata, S., Shigeta, M., Hiraoka, Y., Haraguchi, T., and Yoneda, Y. (2004) Cellular stresses induce the nuclear accumulation of importin alpha and cause a conventional nuclear import block. *J Cell Biol* 165, 617-623
33. Tsukahara, F., and Maru, Y. (2004) Identification of novel nuclear export and nuclear localization-related signals in human heat shock cognate protein 70. *J Biol Chem* 279, 8867-8872
34. Chu, A., Matusiewicz, N., and Stochaj, U. (2001) Heat-induced nuclear accumulation of hsc70s is regulated by phosphorylation and inhibited in confluent cells. *Faseb J* 15, 1478-1480
35. Behrens, J., Jerchow, B. A., Wurtele, M., Grimm, J., Asbrand, C., Wirtz, R., Kuhl, M., Wedlich, D., and Birchmeier, W. (1998) Functional interaction of an axin homolog, conductin, with beta-catenin, APC, and GSK3beta. *Science* 280, 596-599
36. Neufeld, K. L., Zhang, F., Cullen, B. R., and White, R. L. (2000) APC-mediated downregulation of beta-catenin activity involves nuclear sequestration and nuclear export. *EMBO Rep* 1, 519-523
37. Gerdes, J., Schwab, U., Lemke, H., and Stein, H. (1983) Production of a mouse monoclonal antibody reactive with a human nuclear antigen associated with cell proliferation. *Int J Cancer* 31, 13-20
38. Scholzen, T., and Gerdes, J. (2000) The Ki-67 protein: from the known and the unknown. *J Cell Physiol* 182, 311-322

39. Gerdes, J., Lemke, H., Baisch, H., Wacker, H. H., Schwab, U., and Stein, H. (1984) Cell cycle analysis of a cell proliferation-associated human nuclear antigen defined by the monoclonal antibody Ki-67. *J Immunol* 133, 1710-1715
40. Barker, N., van Es, J. H., Kuipers, J., Kujala, P., van den Born, M., Cozijnsen, M., Haegebarth, A., Korving, J., Begthel, H., Peters, P. J., and Clevers, H. (2007) Identification of stem cells in small intestine and colon by marker gene Lgr5. *Nature* 449, 1003-1007
41. Sancho, E., Batlle, E., and Clevers, H. (2004) Signaling pathways in intestinal development and cancer. *Annu Rev Cell Dev Biol* 20, 695-723
42. Coletta, P. L., Muller, A. M., Jones, E. A., Muhl, B., Holwell, S., Clarke, D., Meade, J. L., Cook, G. P., Hawcroft, G., Ponchel, F., Lam, W. K., MacLennan, K. A., Hull, M. A., Bonifer, C., and Markham, A. F. (2004) Lymphodepletion in the ApcMin/+ mouse model of intestinal tumorigenesis. *Blood* 103, 1050-1058
43. Pierre, F., Perrin, P., Champ, M., Bornet, F., Meflah, K., and Menanteau, J. (1997) Short-chain fructo-oligosaccharides reduce the occurrence of colon tumors and develop gut-associated lymphoid tissue in Min mice. *Cancer Res* 57, 225-228
44. Pierre, F., Perrin, P., Bassonga, E., Bornet, F., Meflah, K., and Menanteau, J. (1999) T cell status influences colon tumor occurrence in min mice fed short chain fructo-oligosaccharides as a diet supplement. *Carcinogenesis* 20, 1953-1956
45. Fox, J. G., Dangler, C. A., Whary, M. T., Edelman, W., Kucherlapati, R., and Wang, T. C. (1997) Mice carrying a truncated Apc gene have diminished gastric epithelial proliferation, gastric inflammation, and humoral immunity in response to Helicobacter felis infection. *Cancer Res* 57, 3972-3978
46. Churchill, M., Chadburn, A., Bilinski, R. T., and Bertagnolli, M. M. (2000) Inhibition of intestinal tumors by curcumin is associated with changes in the intestinal immune cell profile. *J Surg Res* 89, 169-175
47. Weinberg, R. A. (2007) *The Biology of Cancer*, Garland Science, Taylor & Francis Group, New York
48. Henderson, B. R. (2000) Nuclear-cytoplasmic shuttling of APC regulates beta-catenin subcellular localization and turnover. *Nat Cell Biol* 2, 653-660
49. Rosin-Arbesfeld, R., Townsley, F., and Bienz, M. (2000) The APC tumour suppressor has a nuclear export function. *Nature* 406, 1009-1012
50. Zhang, F., White, R. L., and Neufeld, K. L. (2001) Cell density and phosphorylation control the subcellular localization of adenomatous polyposis coli protein. *Mol Cell Biol* 21, 8143-8156
51. Berkel, H., Holcombe, R. F., Middlebrooks, M., and Kannan, K. (1996) Nonsteroidal antiinflammatory drugs and colorectal cancer. *Epidemiol Rev* 18, 205-217

CHAPTER 4

THE APC mNLS MUTATION IN CULTURED CELLS

Abstract

Characterization of the mNLS mutation in mouse intestinal epithelium will provide the most complete view of nuclear APC's role in tissue maintenance and tumor suppression. However, a significant amount of data can also be collected in cultured cells that carry the APC mNLS mutations. An evaluation of the APC mNLS ES cells supplied information that was required prior to generating the APC mNLS mouse line. Further analysis of cells in culture was conducted to supplement the preliminary evaluation of the mouse model. This chapter describes the work done in cultured cell lines that carry the targeted APC mNLS mutation.

Introduction

In 1907, Ross Harrison used cells dissected from a frog embryo and grown in a hanging drop of frog lymphatic fluid to observe the out-growth of nerve fibers (1). While bacteria and molds had been grown using similar methods, the ground-breaking idea that cells from a complex multi-cellular organism could be removed from where they grew *in vivo* (in life) and kept alive *in vitro* (in glass) began a new field of science known as tissue culture (reviewed in 2). It took another 50 years of developing and refining techniques before the use of cells grown in culture became widespread. Now nearly every aspect of biology has been impacted by this technology. The ability to grow cells in culture opened up new avenues for the study of viruses and the development of vaccines (2). The production of monoclonal antibodies is reliant on the ability grow and manipulate mouse B cells in culture (3). Cancer research has used tumor cells grown in culture to establish much of our current understanding of the disease (4). Even the current animal models used to study cancer and other diseases are generated using transgenic technologies which are possible because embryonic stem cells can be maintained in culture(5-8).

While cells grown in culture are unable to provide the same types of data that can be collected from whole animals and tissues, there are a number of advantages to working with cultured cells (9). Cells grown in culture exist in a controlled environment with limited variables. The cellular response to chemicals, pH, irradiation, temperature and a variety of other factors can be conducted in a highly

controlled manner. Cells grown in a dish are more available for examination, be it through direct observation, protein extraction or immunohistochemical analysis, and require less preparative processing than cells that are part of a more complex tissue. Maintaining cells in culture is far cheaper as well as more time and labor efficient than maintaining animals. Unlike animal work, which requires extensive paperwork and approval, work in cell culture can be conducted as the experiments are formulated leading to a more direct examination of the question at hand. For these reasons cell culture work often precedes and lays the foundation for work in animal models.

The creation of the APC mNLS mouse model began with the manipulation of mouse Embryonic Stem (ES) cells in culture. ES cells are derived from 3.5 day old mouse embryos, and can self-renew indefinitely in culture without loosing their potential to differentiate into normal tissues of a variety of lineages (10). This unlimited ability to self-renew is a significant advantage of working with ES cell lines. Cells derived from other tissue types undergo a limited number of cell divisions before they become senescent and stop dividing (11). Because most cell lines possess a limited mitotic potential, the long term use of other primary cells in culture requires that they be immortalized (4). Immortalization of primary cell lines generally requires the same mutations commonly associated with cancer cells (12). Cells lines derived from cancerous tumors generally grow very well in culture. The first widely used cultured human cells, the HeLa cell line, was derived from a malignant tumor (2). Previous to the culture of ES cells, cell culture primarily used genetically normal cell lines with a limited life span, or immortalized cell lines that

were genetically abnormal. Much of cancer research has utilized cancer derived cell lines and immortalized primary cell lines (4). However, these cell lines are not genetically or biochemically "normal" cells, a factor that must be considered when evaluating experimental results. ES cells are unique in that they retain an unlimited potential for self-renewal that is maintained through proper handling and media supplements rather than genetic alteration.

ES cell lines may have the potential to be grown perpetually without the need for genetic mutation; however, this does not mean that they can be maintained forever without genetic alterations occurring. If ES cells are cultured inappropriately, they progressively acquire genetic lesions (10). The extensive manipulation and selection required to create a knock-in ES cell line increases the likelihood that some of the cell lines will have accumulated genetic alterations in addition to the knock-in mutation (10). Therefore, an initial characterization of the seven APC mNLS candidate cell lines was necessary prior to generating a mouse model. Obtaining multiple separate cell lines was ideal because it allowed a straightforward identification of outliers. Only one cell line was needed to generate each mouse model with a total of two APC mNLS mouse models to be established. Therefore five of the seven cell lines were discarded following the preliminary characterization. In addition to identifying which cell lines were to be used for the generation of the mouse model, the initial characterization of the APC mNLS ES cell lines represents the first data collected from cells that carry mNLS mutations in the endogenous *Apc* gene.

Materials and Methods

Maintaining ES cells

Wild type R1 mouse ES cells were originally received from Dr Andras Nagy, Dr Reka Nagy, Dr Janet Rossant and Dr Wanda Abramow-Newerly (13). R1 mouse embryonic stem cells with the mNLS knock-in mutations were generated as described in chapter 2. Wild type and APC mNLS R1 mouse embryonic stem cells were grown in ES media [81% High Glucose DMEM (Gibco) supplemented with 15% Fetal Bovine Serum (ES cell certified from Hyclone), 1mM sodium pyruvate (Gibco), 0.1mM Non-essential amino acids (Gibco), 100ng/ml of ESGRO (Chemicon), 2mM L-glutamine (Gibco), 0.01mM 2-mercaptoethanol (Fisher)] in a 37°C water jacketed incubator with 7% CO_2. Cells were split ~1:9 every 2 to 3 days as needed and plated directly onto a mitomycin C-treated mouse embryonic fibroblast (MEF) cells or STO cell feeder layer. STO cells are derived from **S**IM mice and are a **t**hioguanine- and **o**uabain-resistant sub-line of mouse fibroblast.

Preparing MEF and STO feeder layer cells

Vials of immortalized STO cells were obtained from the KU Medical Center. Neomycin resistant MEF cells were purchased from Chemicon. All feeder cell lines were grown in High Glucose DMEM (Gibco) supplemented with 10% Fetal Bovine Serum (Hyclone). Prior to use as a feeder layer, cells were expanded and growth arrested with 10μg/mL mitomycin C (Sigma) as previously described (10). Vials of

growth arrested cells were stored in liquid nitrogen and thawed as needed. A feeder layer of STO cells was plated at least 12 hours prior to the addition of ES cells to allow the feeder layer to establish a uniform monolayer on which the ES cells could be cultured.

Karyotype analysis of ES cells

To obtain slides with chromosome spreads, WT and APC mNLS ES cells were incubated for 5 hours in ES growth media supplemented with 40ng/mL demecolcine (Fisher) to arrest the cells in metaphase. Cells were then rinsed with PBS, dispersed with trypsin and pelleted by centrifugation. The cell pellets were resuspended in 1mL of hypotonic buffer (40mM KCl and 25mM sodium citrate in water) and incubated for 20 minutes at 37°C to swell the cells. After 20 minutes, 3mLs of fixative [75% methanol, 25% acidic acid] was added directly to cells in hypotonic buffer while vortexing. Cells were pelleted by centrifugation at 1000xg, resuspended in 1mL fresh fixative while vortexing and incubated on ice for 10 minutes. Cells were pelleted by centrifugation at 8000xg for 2 minutes and resuspended in 0.5mLs fresh fixative. Using a pasture pipette, cells in fixative were dropped onto clean glass slides from a height of 5-7 feet. Slides were briefly passed over a flame to dry, incubated in 0.1μg/mL DAPI for 10 minutes to label the DNA and incubated in TBS for 5 minutes to wash away excess DAPI. Coverslips were mounted with Prolong Anti-Fade (Invitrogen). DAPI-labeled chromosomes were examined using a Zeiss Axiovert 135 inverted fluorescent microscope. Images were

collected at 1000X magnification using an Olympus MC100spot camera and analyzed using *Magnafire* software (Olympus).

Immunohistochemistry

Immunostaining was performed essentially as previously described (14) using the following antibodies: Mouse anti-β-catenin (1:1000, Transduction Laboratories), mouse anti-APC (Ali-12-28 1:100, Abcam), anti-APC-M2 rabbit polyclonal antibody made against amino acid 1000-1326 and affinity purified (1:3000), mouse anti-BrdU (1:1000, Becton Dickinson) goat anti-mouse IgG Alexa 488 (1:1000, Molecular Probes), goat anti-rabbit IgG Alexa 568 (1:1000, Molecular Probes). DNA was labeled with DAPI (0.1μg/mL). Briefly, wild type, heterozygous and homozygous mutant MEF cells and wild type and heterozygous mutant ES cell lines were seeded onto glass 22x22mm coverslips (Fisher) and allowed to adhere for at least 24 hours. Coverslips used in ES experiments were coated with Poly-L-Lysine (Sigma) prior use to enhance adhesion. Cells on coverslips were removed from media, rinsed twice with PBS and fixed for 30 min on ice in 4% paraformaldehyde containing 0.1% Triton X-100. Prior to incubation with primary antibody, coverslips were rinsed twice for 5 minutes in PBS, permeabilized with 0.2% Triton X-100 in TBS and rinsed 3 times for 5 minutes in TBS before being inverted over drops of primary antibody for 90 minutes. After incubation with primary antibody, coverslips were rinsed 3 times for 5 minutes in TBS, inverted for 30 minutes over drops of secondary antibody and 5 minutes over DAPI (0.1μg/mL) before being washed three times for 5 minutes

in TBS. Stained coverslips were mounted onto glass slides with Prolong Anti-Fade (Invitrogen) and viewed on a Zeiss META 510 upright confocal microscope with a 60X water objective or an Olympus 3I spinning disc confocal TIRF inverted microscope and analyzed using *SlideBook* software.

Measuring β-catenin activity with Topflash/Fopflash assay

Wild type and APC mNLS ES cells were plated into 12-well culture dishes and transfected when approximately 70% confluent. Cells were co-transfected with 1μg of TOPFLASH or FOPFLASH vector (15) and 50ng of a β-galactosidase vector using 5μL Fugene HD (Roche) per transfection and incubated according to manufacturer's protocol. Luciferase activities were determined after 48 hours using the Luciferase Assay System (Promega) in an LMAX II plate reader (Molecular Devices) using 96-well white polystyrene plates (Corning Incorporated). All luciferase values were normalized for transfection efficiency based on the β-galactosidase activity as determined using Galacto-Light Plus assay kit (Tropix). Each transfection was performed in triplicate.

Generation of Homozygous ES cells

Several attempts were made to isolate ES cell lines homozygous for the APC mNLS mutations according to previously described methods (16). ES cells from the MES-4 cell line were reselected on 4.0mg/mL G418 (Sigma or Gibco). For these experiments ES cells were grown on gelatin coated wells or growth-arrested Neo^r

primary mouse embryonic fibroblasts (PMEF-NL from Chemicon) and G418 media was changed daily. After 8 days of G418 selection, the surviving ES colonies were picked as described (10) and transferred to individual wells of duplicate 96-well plates over gelatin or growth-arrested PMEF-NL cells. ES Cells were grown in high LIF media [51% High Glucose DMEM (Gibco) supplemented with 30% Fetal Bovine Serum (ES cell certified from Hyclone), 1mM sodium pyruvate (Gibco), 0.1mM Non-essential amino acids (Gibco), 1600ng/ml of ESGRO (Chemicon), 2mM L-glutamine (Gibco), 0.01mM 2-mercaptoethanol (Fisher)]. Media was supplemented with 4mg/mL G418 for an additional 4 days at which point the cells were cultured without selection to encourage growth. DNA was isolated from cells in one of the 96-well plates as described (17) and screened using PCR to determine the APC genotype (as described for the original ES cell lines in Chapter 2).

Isolation of Mouse Embryonic Fibroblasts

Mouse Embryonic Fibroblasts (MEFs) were isolated essentially as described (10). Embryos were obtained by crossing an F2 APC $mNLS^{+/-}$ female with an APC $mNLS^{+/-}$ male sibling to produce APC $mNLS^{-/-}$, APC $mNLS^{-/+}$ and APC $mNLS^{+/+}$ embryos. Fifteen days after mating the pregnant female was sacrificed by CO_2 asphyxiation, briefly ethanol flamed to sterilize the exterior surfaces and the uterus was removed using aseptic technique. Embryos were processed individually in a laminar flow hood to maintain pure genotypes in each of the MEF cell lines. After removal of internal organs, limbs and head, the remaining embryonic tissues were

minced and placed into sterile tubes containing 5mM autoclaved glass beads and treated 3x 30 minutes with 1x trypsin while shaking at 37°C. DMEM supplemented with 10% FBS and 1% Penicillin-Streptomycin (Gibco) was used to wash cells and seed them onto 75cm^2 cell culture flasks. The media was changed daily until the cells were completely confluent. Cells were split 1:6 and again allowed to grow until confluent. At this time cells from five 75cm^2 flasks for each cell line were cryo-preserved for later use as *Passage 1 MEF cells*. The sixth flask of each cell line was split 1:5 and cells were again allowed to reach confluence before being cryo-preserved as *Passage 2 MEF cells*.

Maintaining MEF cells

MEF cell lines were stored in cryovials in liquid nitrogen until needed. After thawing, cells were maintained in growth media [High Glucose DMEM (Gibco) supplemented with 15% FBS (Hyclone) and 1% Penicillin-Streptomycin (Gibco)]. Cells were kept in a 37°C water jacketed incubator with 7% CO_2 and split as necessary. Once thawed, cells were maintained in culture for a maximum of two weeks. All experiments are conducted on cells within the first 3-6 passages.

Growth Curve analysis in MEF cells

MEF cells were thawed and grown for 1-2 passages in culture. Following trypsinization, media containing FBS was added to neutralize the trypsin and cells were pelleted by centrifugation at 700xg for 5 minutes. Cell pellets were resuspended

in fresh media and one tenth of the cells from each cell line were removed and quantified using a cell counter (Beckman Coulter). The remaining cells were diluted as needed to achieve similar starting concentrations for all cell lines and plated into 6-well or 24-well plates. At the indicated time intervals all cells in a single well were trypsinized, pelleted and resuspended in isotonic dilution buffer (Beckman Coulter) and counted. At the first time interval, the media was removed from all wells and replaced with fresh media to remove any non-attached cells.

UV irradiation of MEF cells

MEF cells were plated into 2-well chamber slides and allowed to adhere. Regular media was removed after ~24 hours and replaced with media supplemented with 30μM BrdU (Sigma) for an additional 20 hours. Prior to UV irradiation, media was removed and cells were rinsed once with 37°C sterile PBS. A thin layer of PBS was left over cells to prevent drying. Cells were placed into an Ultraviolet Crosslinker (UVP) and irradiated for 83 seconds at an intensity of 120mJ/sec resulting in a total exposure of ~10J/m^2. The non-irradiated control cells were processed identically except that the chamber slides were covered with aluminum foil during UV exposure. Following UV irradiation the PBS was removed and replaced with fresh media. Cells were placed back into the incubator for 1 hr to begin the process of DNA repair. At the end of an hour cells were fixed and stained as described above.

Results

Growth characteristics of the APC mNLS ES cells resemble those of WT ES cells

PCR screening of the targeted stem cells identified seven ES cell lines as potential candidates for use in generating a mouse model. Four to six frozen vials of each cell line were received from the Transgenic and Gene-Targeting Institutional Facility at The University of Kansas Medical Center (Table 4.1). Prior to evaluation of the individual cell lines, cells from each line were expanded to make additional frozen stocks of the early passage cells. These stocks were thawed and used as needed for the following experiments. The remaining original vials were stored in liquid nitrogen to be used for the generation of a mouse model.

All seven APC mNLS$^{+/-}$ cell lines and wild type ES cells were grown in parallel and relative growth characteristics were observed. Most of the APC mNLS$^{+/-}$ cells were estimated to maintain an average level of growth that was comparable to wild type ES cells; however, there were outliers that did not fit this pattern. Cells from ES line MES-3 consistently grew more rapidly than cells from other lines, needed to be passed more often and became confluent more quickly. In contrast MES-7 cells exhibited a slower rate of growth and were rarely as confluent as the other cell lines when grown for an equal amount of time. The observation that the majority of the APC mNLS$^{+/-}$ ES lines grew at

Table 4.1 Potential knock-in mNLS stem cell lines received from the Transgenic and Gene-Targeting Institutional Facility at The University of Kansas Medical Center

KU med designation	Neufeld lab designation*	number of cells per vial	# of vials
PK1 I-A2	**MES-1**	$2x10^6$	3
		$1x10^6$	2
PK2 I-A10	**MES-2**	$2x10^6$	3
		$1x10^6$	2
PK2 I-D4	**MES-3**	$2x10^6$	4
		$1x10^6$	2
PK2 I-H3	**MES-4**	$2x10^6$	2
		$1x10^6$	3
PK2 II-A8	**MES-5**	$2x10^6$	3
		$1x10^6$	2
PK2 II-C2	**MES-6**	$2x10^6$	1
		$1x10^6$	3
PK2 III-D1	**MES-7**	$2x10^6$	4
		$1x10^6$	2

*Mutant Embryonic Stem (MES) cell lines

approximately the same rate as the wild type ES cells suggested that the APC mNLS mutation did not dramatically alter the proliferation rate of ES cells when heterozygous.

The transcription activity of β-catenin in APC mNLS ES cells resembles WT ES

One of the best characterized functions of APC is its role in the down-regulation of β-catenin. APC is known to participate in the destruction complex that targets β-catenin for proteolysis in the cytoplasm (18). APC has also been shown to inhibit the transcriptional activity of β-catenin in the nucleus (19). β-catenin's function as a transcriptional activator was, therefore, evaluated in APC mNLS$^{+/-}$ ES cell lines.

When β-catenin is translocated to the nucleus, it serves as a co-activator protein and stimulates expression from target genes. The use of the TOPFLASH reporter construct has become a standard method to measure the transcriptional activity of β-catenin in cells bearing *Apc* mutations (15). In previous reports, *Apc* truncation corresponded with TOPFLASH reporter activity in a dose dependent manner (20, 21). To test the hypothesis that the APC mNLS mutation may significantly alter the transcriptional activity of β-catenin in the APC mNLS ES cells, all seven knock-in cell lines and wild type ES cells were transfected with the TOPFLASH/FOPFLASH reporter system (15). As expected, the WT ES cells showed slightly higher luciferase expression from the β-catenin-specific TOPFLASH reporter than from the FOPFLASH control reporter (Figure 4.1). Results were similar

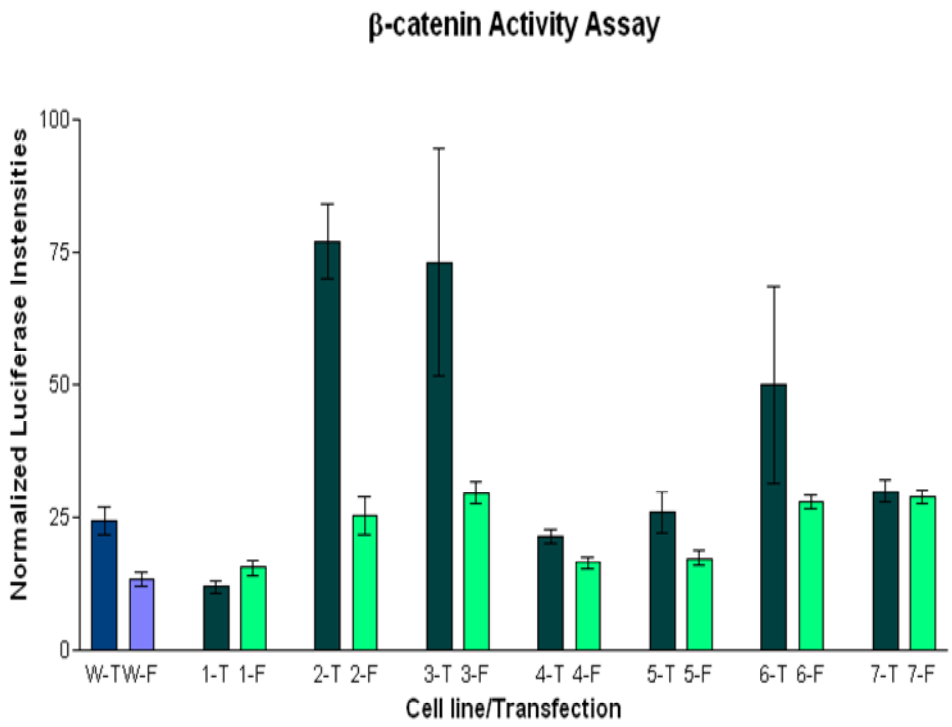

Figure 4.1
β-catenin transcriptional activity as measured by the TOPFLASH assay. WT (blue bars) and APC mNLS$^{+/-}$ (green bars) ES cells were transfected with TOPFLASH (dark bars) or FOPFLASH (pale bars) luciferase expression vectors. Luciferase intensity was normalized to the β-galactosidase transfection control values and expressed as an arbitrary luciferase intensity value.

to relative levels of TOPFLASH and FOPFLASH activity previously reported for WT ES cells. In this preliminary assessment, APC mNLS$^{+/-}$ cell lines MES-4, MES-5 and MES-6 showed relative TOPFLASH and FOPFLASH ratios similar to wild type cells. MES-1 and MES-7 cells showed slightly lower TOPFLASH to FOPFLASH ratios while MES-2 and MES-3 cells showed slightly increased levels of TOPFLASH reporter activity relative to the FOPFLASH values (Figure 4.1). Because β-catenin transcriptional activity is associated with cell proliferation, the observation that the MES-3 cell line exhibited relatively high β-catenin transcriptional activity was consistent with the slightly faster rate of proliferation that was previously observed. Similarly, the MES-7 cell line exhibited a comparatively lower level of β-catenin transcriptional activity compared to wild type cells and also seemed to proliferate more slowly. However, MES-1 cells and MES-2 cells also demonstrated TOPFLASH activities that varied slightly from the wild type values, yet they displayed no obvious differences in proliferation. Our observation that the TOPFLASH values for APC mNLS transgenic ES cells did not differ much from the wild type values suggests that the targeted mutation does not significantly affect β-catenin activity, at least in ES cells heterozygous for the mutation.

Karyotype analysis of APC mNLS ES cells

A normal mouse genome contains 40 chromosomes, 19 pairs of somatic chromosomes and the two sex chromosomes. Because cells that exhibit aneuploidy (an abnormal number of chromosomes) have low integration efficiency when injected

into blastocysts, it is very important that cells being used for generation of a mouse model display normal karyotypes. The Gene-Targeting and Transgenic Facility at the University of Virginia requires that cell lines being used for injection into mouse blastocysts display a normal karyotype in at least 75% of the cells. Cells still being considered as potential candidates for use in mouse generation were therefore subject to extensive karyotype evaluation. Slides of chromosome spreads were prepared from the transgenic cell lines and wild type ES cells (Figure 4.2). An initial evaluation was conducted by counting the number of chromosomes in 5 separate spreads for some of the cell lines. This initial count revealed that MES-2 and MES-7 had a higher number of cells with abnormal karyotypes than the wild type controls (Table 4.2). In addition to a poor initial karyotype, cell lines MES-2 and MES-7 had given abnormal TOPFLASH and growth characteristics, respectively. Thus they were eliminated from consideration as potential cell lines to be used in the generation of the mouse model. Cell line MES-3, though not yet considered karyotypically abnormal, was also not analyzed further due to outlying results in both growth rate and TOPFLASH analysis. Cell lines MES-1, MES-4, MES-5 and MES-6 were selected for more extensive analysis of karyotype. Over 44 individual chromosome spreads were counted for each of the four cell lines (Results in Table 4.3). To be considered for blastocyst injections, more than 75% of the cells counted needed to contain 40 chromosomes. Cell lines MES-5 and MES-6 did not pass the karyotype analysis with only 56% and 63.6% of the chromosome spreads containing a normal number of chromosomes. This was primarily due to a single extra chromosome or a

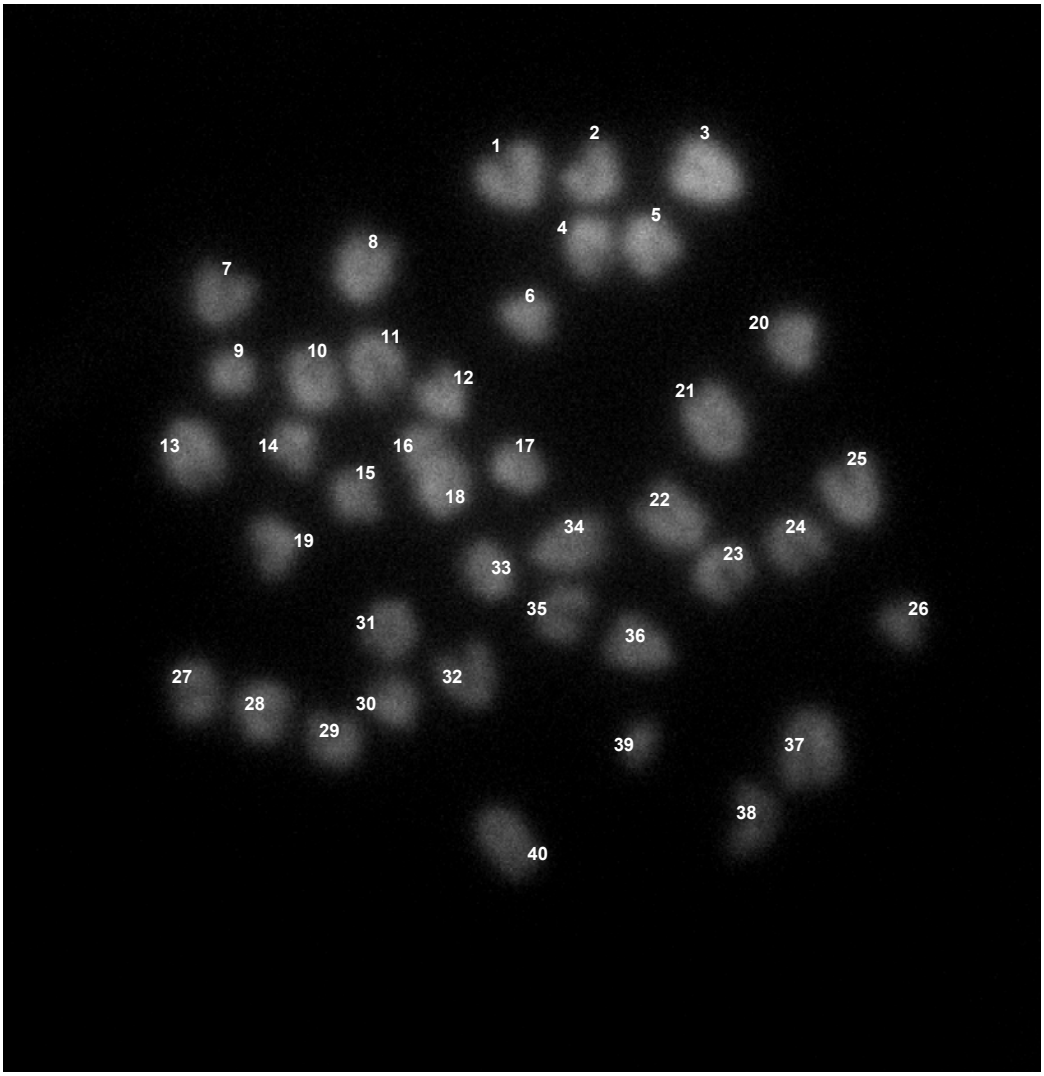

Figure 4.2
An example of a typical chromosome spread prepared using mouse ES cells. The chromosomes above are randomly numbered and display a correct karotype of 40 total chromosomes. DNA is visualized with DAPI. Image was captured on a Zeiss inverted fluorescent scope equipped with an Olympus camera.

Table 4.2
Initial karyotype results of the wild type and APC mNLS knock-in ES cell lines. Five separate chromosome spreads were counted for each of the indicated cells lines. The number of chromosomes in each spread is indicated in the table below. The mouse genome should contain 40 chromosomes. Abnormal karyotypes are indicated in red.

WT	40	40	40	39	40
MES-1	40	39	40	40	40
MES-2	35	39	39	40	41
MES-3	37	40	40	40	40
MES-4	40	40	40	39	40
MES-5	40	40	40	40	40
MES-6	no viable cells for analysis				
MES-7	36	40	39	40	40

Table 4.3
More extensive karyotype analysis of selected APC mNLS knock-in ES cell lines. Cell lines with a stable enough karyotype to be considered for the generation of a mouse model are highlighted in yellow.

Cell line	cells with <40 chromosomes	cells with 40 chromosomes	cells with >40 chromosomes	cells with a normal karyotype/ total cells	% of cells with normal karyotype
MES-1	8	43	3	43/54	79.63%
MES-4	11	36	1	36/48	75%
MES-5	9	28	13	28/50	56%
MES-6	6	28	10	28/44	63.64%

single missing chromosome, however, cell line MES-6 contained 42 chromosomes in 18% of the cell spreads that were scored. Cell lines MES-1 and MES-4 contained 40 chromosomes in 79.6% and 75% of cells respectively. These two cell lines were use to generate chimeric mice (Table 4.4).

Optimizing conditions for ES cell immunofluorescence

Epithelial cells and fibroblast cells will grow directly on glass slides and generally display a flattened morphology that facilitates microscopic imaging. ES cells, however, grow in spherical clusters over a layer of feeder cells, rather than directly on glass, making them non-adherent and difficult to image. In general, most of the ES cells were lost during the processing required for immunofluorescent analysis, resulting in a number of slides containing STO cells and little else. Several techniques were employed to increase cell adherence when it became obvious that ES cells grown on glass slides would not yield enough attached ES cells for imaging.

Initially, a Cytospin 3 cell preparation system (Shandon) was used to pellet suspended ES cells onto glass slides. This did not result in an increase in the number of ES cells retained on the slide after processing. The cell and tissue adhesive Cell-Tak (BD) was added to the chamber slides at 20µL/mL in 0.1M $NaHCO_3$ for 30 minutes to coat the glass prior to being seeded with ES cells. For this method, ES cells were mechanically disrupted from their clusters by pipetting or proteolytically disrupted using trypsin, added to the Cell-Tak coated chamber slides, and allowed to adhere for 15-90 minutes before being rinsed, fixed and stained. This method led to

Table 4.4
A summary of the initial characterization of the of the APC mNLS transgenic ES cell lines. Bolded entries represent ideal results, italicized entries represent results that eliminated the indicated cell line from further consideration for generation of a mouse model

Cell line	Growth rate	TOPFLASH assay	Karyotype
MES-1	**normal**	slightly low	**Normal (79.6%)**
MES-2	**normal**	high	*poor in initial analysis*
MES-3	*fast*	slightly high	ok in initial
MES-4	**normal**	**normal**	**Normal (75%)**
MES-5	**normal**	**normal**	*Abnormal (56 % correct)*
MES-6	**normal**	**normal**	*Abnormal (63.6% correct)*
MES-7	*slow*	slightly low	*poor in initial analysis*

a slightly increased number of retained ES cells following processing for immunofluorescent analysis. The resulting slides generally contained a fairly small number of whole ES cells and a large amount of cellular debris adhered to the Cell-Tak. In an attempt to further increase adherence, highly concentrated Cell-Tak was applied to glass slides and ES cells were plated directly on top of the Cell-Tak, which led to an increase in both the number of ES cells and the amount of debris retained on the slide.

While this method proved to be an effective way of retaining enough ES cells on the slide to image, there was concern that this treatment of the cells would affect the observed staining pattern for some proteins. We typically grow most cell types for 12-24 hours on the glass slide on which they are fixed and stained. The use of Cell-Tak to enhance ES adhesion required that the ES cells be removed from the feeder layer and disrupted from their spherical clusters, either through mechanical disruption or by using trypsin, immediately prior to fixation for staining. It was feared that stressing the cells in this manner would alter the localization pattern of APC. To avoid this stress, ES cells would need to be grown for a more extend time on glass coverslips that had been treated to enhance cell adhesion. ES cells plated on collagen IV coated slides were retained quite well even after extensive washes; however, this method also resulted in a significant increase in the non-specific background signal following antibody incubation. Eventually, it was determined that the most effective method to retain ES cells on the slide while producing the least amount of background signal was to grow the ES cells on coverslips that had been

coated with poly-L-lysine. Poly-L-lysine (Sigma) was applied to glass coverslips according to manufacturer's instructions. The poly-L-lysine coated coverslips were then sterilized under UV light and placed into the wells of a 6-well tissue culture plate. ES cells were seeded into the wells and allowed to attach to the coverslips for at least 12 hours before being processed for imaging. While a significant amount of cell loss during the staining procedure was still observed, sufficient numbers of ES cells were typically retained to allow imaging.

β-catenin localization in the APC mNLS ES cells is unaltered

There is evidence that APC and β-catenin interact in the nucleus and that APC participates in the export of β-catenin from the nuclear compartment (19, 22, 23). It is therefore possible that inhibition of nuclear targeting of APC protein would result in a change in the localization pattern of β-catenin. In most cell lines a majority of the β-catenin is localized to the adherens junctions where β-catenin interacts with E-cadherin (24). When the localization of β-catenin in WT ES cells was analyzed using confocal microscopy, the cells displayed the expected antibody staining pattern. The most intense β-catenin staining was localized to the plasma membrane between cells with only a small signal observed in the cytoplasm and nucleus (Figure 4.3). The β-catenin localization in the APC mNLS ES cells showed no significant variation between cell lines, and the overall staining pattern was indistinguishable from the pattern observed in WT ES cells (Figure 4.3). The absence of a noticeable alteration of the β-catenin staining pattern in the APC mNLS cells was not necessarily

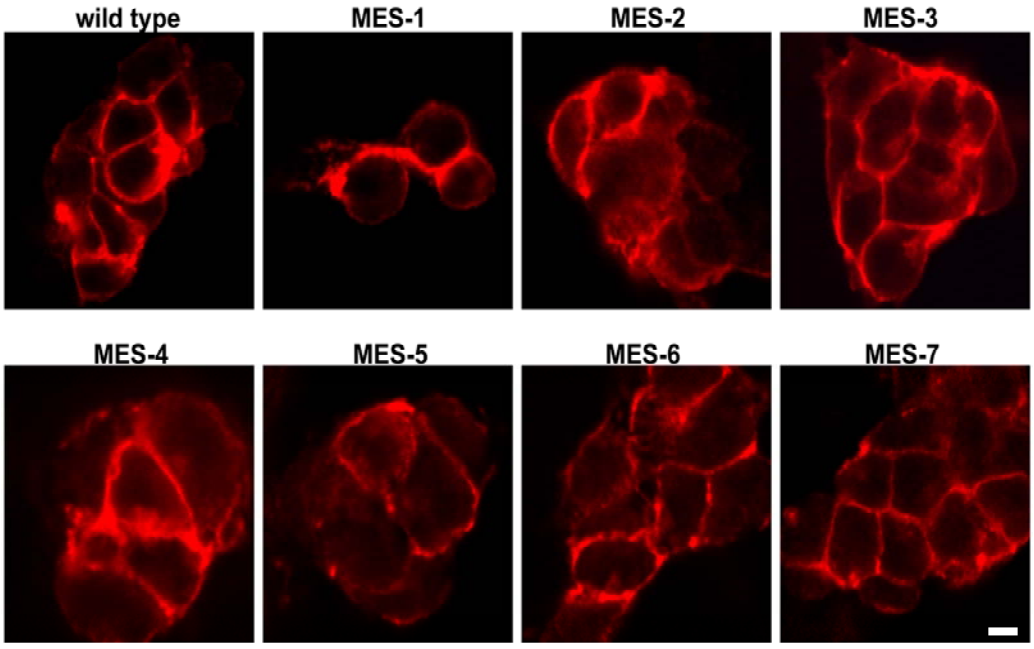

Figure 4.3
β-catenin localization in WT and APC mNLS$^{+/-}$ ES cells. ES cells were grown on poly-L-lysine coated coverslips and visualized using a rabbit anti-β-catenin antibody (Sigma). Images were taken on a Zeiss upright confocal microscope with a 60X water objective. Scale bar = 5μm.

unexpected. These cells are heterozygous for the knock-in APC mNLS mutation; therefore the APC protein expressed from the WT allele is capable of normal nuclear import. That amount of nuclear APC was apparently sufficient for the normal regulation and localization of β-catenin in these cells.

The localization of APC in the APC mNLS candidate cell lines

Unlike β-catenin, for which numerous dependable, high quality antibodies are commercially available, staining for APC in ES cells proved to be much more difficult. While a number of commercially available APC antibodies exist, there is much debate in the field as to the specificity and reliability of many of those antibodies (25, 26) Furthermore, the few commercially available APC antibodies that are considered to be specific for APC have demonstrated a great deal of variability in quality between antibody batches (unpublished observations and personal communications). An analysis of APC localization using multiple APC antibodies in all of the APC mNLS cell lines was attempted; however, the inherent difficulties involved in staining ES cells in conjunction with the generally poor quality and extreme variability in the staining patterns of the various commercially available APC antibodies resulted in an incomplete analysis. In general, very little difference was observed in the APC localization patterns of the mutant ES cells lines. All seven of the mutant cell lines were indistinguishable from each other and the WT ES cells (data not shown).

The absence of a noticeable alteration in the APC staining pattern in the APC mNLS ES cells was unexpected. Even though only one allele of APC carries the mutant NLSs, it was anticipated that there would be some decrease in the level of nuclear APC in the mutant cell lines compared to WT ES cells. It is possible that some threshold level of APC is maintained in the nucleus and that the APC protein from the WT allele was able to compensate for a decreased level of the total APC being targeted to the nucleus.

Attempts to generate homozygous APC mNLS cells

The *Neo*^{r} gene encodes the enzyme neomycin phosphotransferase II which confers cellular resistance to a variety of antibiotics including G418. Cells expressing the WT Neo^r are capable of growth in 5-10mg/mL G418 at which point the concentration of drug in the media begins to cause a general cell toxicity (10). The WT version of the Neo^r gene therefore provides a robust antibiotic resistance but no ability to select for different levels of gene expression in the targeted cells. In 1990 a mutant version of this enzyme was reported with significantly reduced phosphotransferase activity (27). The gene replacement vector used to target the APC mNLS knock-in mutations carried a copy of the mutant *Neo*^{r} gene. As a result, APC mNLS ES cells expressing a singe copy of the mutant *Neo*^{r} gene were be able to grow in the presence of low concentrations of G418 (~0.2mg/mL) but were sensitive to G418 at higher concentrations. Cells containing two copies of the mutant *Neo*^{r} gene, however, can be expected to survive G418 selection at concentrations as high as

4mg/mL, providing a method to differentiate between cells that were heterozygous for the gene replacement vector and cells that were homozygous for the targeted locus.

It has been demonstrated that loss of heterozygosity (LOH) frequently occurs in mouse cells, usually due to a loss/duplication event at the chromosome level (28). It is probable that in a percentage of the APC mNLS cells LOH has already occurred. Selection for cells that can grow on high levels of G418 (at least 2-6x that used in the primary selection to identify the heterozygous ES cells) has been shown to be an efficient method to acquire homozygous mutant cell lines without a second round of targeting (16, 28).

The heterozygous mutant APC mNLS ES cell lines demonstrated a phenotype that was indistinguishable from that of WT ES cells. The localization of APC, the localization pattern and transcriptional activity of β-catenin and the growth rate of the majority of the knock-in cell lines closely resembled the characteristics of the WT ES cells. This lack of detectable phenotype suggested that a heterozygous loss of the APC NLSs had no effect on ES cells. We therefore wished to analyze the phenotype in homozygous cells. To acquire homozygous mutant APC mNLS ES cells, MES-4 cells were subjected to a second round of selection on G418 media.

To determine the optimal concentration of G418 for selection of homozygous cells, MES-4 cells were grown in media containing 0, 0.2, 1.2, 2.0, 3.0 and 4.0 mg/mL G418. Because the STO feeder layers did not express Neo^r and would therefore not survive G418 selection, 6-well tissue culture plates were treated with

0.1% gelatin prior to the addition of the ES cells to facilitate ES cell growth and adherence in the absence of a feeder layer. Selection media was replaced daily to maintain a consistent concentration of the drug on the cells. After six days, the APC mNLS ES cells growing in the presence of 0 and 0.2mg/mL G418 were over-crowded and showed evidence of differentiation. In the wells that contained 1.2, 2.0, 3.0 and 4.0mg/mL G418, a majority of the ES cells had died. Clumps of dead floating cells were removed daily from these wells during the media changes. However, a small number of ES cell colonies appeared firmly adhered and growing in the presence of the higher concentrations of G418, suggesting that some of the ES cells had duplicated the *Neo*^{r} gene. Following 8 days of selection, 17 ES cell colonies were picked from the wells that had been treated with 3.0 and 4.0mg/mL G418. The colonies were treated with trypsin to disperse the cells and re-plated in individual, gelatin coated wells of duplicate 96-well dishes. These cells were grown in 4.0mg/mL G418 for an additional three days. DNA was isolated from the ES cells in one of the 96-well plates and PCR was used to screen for the presence of the mutant and WT *Apc* alleles. All 17 samples were able to amplify product that contained the WT *Apc* allele.

There were several explanations to account for the presence of ES cells retaining the WT *Apc* allele after selection in higher concentrations of G418. Instead of chromosome loss and duplication, the *Neo*^{r} gene may have been duplicated through the process of mitotic recombination, allowing a portion, but not all, of the targeted chromosome to be replicated. This could result in a LOH of the *Neo*^{r} gene

while maintaining heterozygosity for the *Apc* mNLSs. In theory, mitotic recombination should occur rarely and be less likely than chromosome loss and duplication (28). The apparent selection against an LOH event that would result in two copies of the mutant *Apc* allele suggests that nuclear APC plays an important function in ES cells. A second possibility was that the cell lines were not completely homogeneous. While the intent was to pick individual colonies and re-plate them into separate wells, heterozygous cells growing close to homozygous cells could have escaped being killed by the higher G418 concentrations and become contaminants in the homozygous cell lines after drug selection was discontinued. Several of the homozygous-candidate cell lines that produced significantly less PCR product from the WT allele of *Apc* were sub-cultured and grown for several more days in the presence of 4mg/mL G418, however, no pure homozygous cell lines were produced.

A second attempt was made to select for homozygous APC mNLS ES cells. In the initial attempt, ES cells had been plated in gelatin coated wells and allowed to attach prior to beginning G418 treatment. In an attempt to eliminate heterogeneous colonies of cells, MES-4 cells were dispersed with trypsin and pelleted, then the cell pellet was re-suspended directly in media containing 4mg/mL G418. It was thought that immediate treatment with drug while the cells were still dispersed in solution would eliminate non-resistant cell survival by preventing them from growing in close association with the drug-resistant cells. Most of the cells died in suspension and were removed with the first media change. The ES cell colonies that did survive and adhere appeared to grow better than the colonies observed in the previous round of

selection. It was likely that the ES cell colonies were able to grow better without the contact inhibition of dying ES colonies around them. ES cells were sub-cultured once during the initial selection period. This served both to prevent the cells from becoming too confluent during the 8 day selection with G418, and also to provide another round of drug selection on dissociated cells. Following selection, colonies were picked, dispersed with trypsin and plated in individual wells of duplicate 96-well plates. In this round of selection, 179 ES colonies were picked. DNA isolated from the cells in one set of 96-well plates was used to PCR screen for the mutant and WT *Apc* alleles by PCR. Again, WT *Apc mNLSs* were detected in every cell line.

Two of the cell lines that appeared to be potentially mixed populations of cells were sub-cultured and used in a second round of selection. These cells were treated with trypsin and thoroughly pipetted to assure that colonies were completely dissociated into single cells before re-plating into gelatin coated 96-well plates. Approximately 200 wells for each cell line appeared to contain only one colony after several days of growth in selective media. Two distinct colony morphologies were observed, the normal spherical colonies with smooth edges and a flatter colony type with a more irregular edge. Once selection with G418 was discontinued to allow for better cell growth, several of the wells were observed to contain bacterial contamination. Uncontaminated wells were sub-cultured to fresh plates and the ES media was supplemented with 1% penicillin/ streptomycin (Gibco). DNA was isolated from the remaining 72 cell lines and used to screen for the presence of the mutant and WT alleles of *Apc*. Again all cell lines contained WT *Apc*.

While ES cells are capable of growing for short periods of time on gelatin in place of fibroblast feeder layers, the removal of a feeder layer has been known to induce ES cell "crisis". This crisis is associated with a flattened cell morphology and increased differentiation at the colony edges (10). It is possible that homozygous mutation of APC is already a growth disadvantage in ES cells. This disadvantage in combination with the stress of being grown on gelatin coated plates for the extent of the drug selection may have resulted in the extremely inefficient selection for homozygous mNLS *Apc* that was observed. To prevent further negative selection due to ES cell crisis, Primary Mouse Embryonic Fibroblasts that express Neo^r (PMEF-NL) were purchased from Chemicon. These PMEF-NL cells were growth arrested using mitomycin-C so that they might serve as a feeder layer for the ES cells during G418 selection. The selection for homozygous mutant APC mNLS ES cells was repeated using Neo^r feeder cells in place of gelatin during selection with 4.0mg/mL G418. An initial PCR analysis revealed several potential homozygous cell lines, however, bacterial contamination following the discontinued use of G418 resulted in a loss of viable cell lines at the conclusion of the selection process.

Isolating Mouse Embryonic Fibroblast cells from the APC mNLS mouse embryos

An alternative method for the acquisition of homozygous APC mNLS cells was to derive cell lines from the embryos of APC mNLS homozygous mice. ES cells are somewhat complicated to derive, however mouse embryonic fibroblasts (MEFs) can be obtained using relatively straightforward techniques. Unlike ES cells, primary

MEF lines have a limited mitotic potential in culture. At most these cells will survive a few dozen passages before becoming senescent. Therefore all experiments in MEF cells needed to be done in the first few passages, and further experiments required that a new vial of cells be thawed. This limitation to the use of MEF cell lines was balanced by the fact that, unlike ES cells, MEF cells do not require a feeder layer. This eliminated the time and energy involved in maintaining a feeder layer as well as the additional processing required to remove these contaminating cells from PCR and protein analysis of the APC mNLS ES cells. MEF cells are also easier to process for immunohistochemical analysis and imaging because they adhere easily to glass slides and display a flattened morphology.

To obtain embryos for cell derivation, an F2 heterozygous female was bred to an F2 heterozygous male sibling. Mendelian genetics predicts that this cross will result in a mix of APC $mNLS^{+/+}$, $mNLS^{-/+}$ and $mNLS^{-/-}$ embryos. The selection process required for obtaining a homozygous ES cell line has the potential to result in additional mutations in the genome, however, sibling embryos should provide the APC mNLS heterozygous and homozygous cells with the same genetic background as the cells derived from APC mNLS WT embryos. At generation F2 the mice are estimated to be 75% C57BL/6J and 25% R1. While the F2 mice are not considered congenic, they are genetically less outbred than the targeted ES cells and therefore represent an excellent model system in which to study the cellular effect of the APC mNLS mutations.

Ten 13-14 day old embryos were isolated and processed separately to preserve uncontaminated cell lines from each embryo. All three APC mNLS genotypes were represented in these embryos. All ten embryos gave rise to MEF cell lines which were aliquoted and cryo-preserved in the early passages for use in future research.

APC and β-catenin localization in MEF cells

Analysis of β-catenin staining in the APC mNLS$^{+/+}$, APC mNLS$^{+/-}$, and APC mNLS$^{-/-}$ MEF cell lines revealed similar staining patterns in the mutant and WT cell lines (Figure 4.4). APC staining however, showed an increasing ratio of cytoplasmic to nuclear APC in the heterozygous and homozygous mutant cells (Figure 4.4). Unlike previous observations in cells expressing exogenous APC mNLS protein, endogenous APC was never completely excluded from the nuclear compartment, even in the homozygous mutant cells. The exact method by which nuclear entry is achieved in the APC mNLS homozygous mutant cells is not understood; however, we speculate that the concentration of APC in the cytoplasm just surrounding the nucleus in the mutant cell lines indicates that that some cellular stress is occurring to maintain the detectable levels of nuclear APC.

APC mNLS mutant and WT cells grow at the same rate

Primary MEF cells have a finite life span. When the APC mNLS MEFs were first derived they grew very quickly in culture. After several passages the growth rate decreased, then halted completely. MEF cells were dividing rapidly during initial

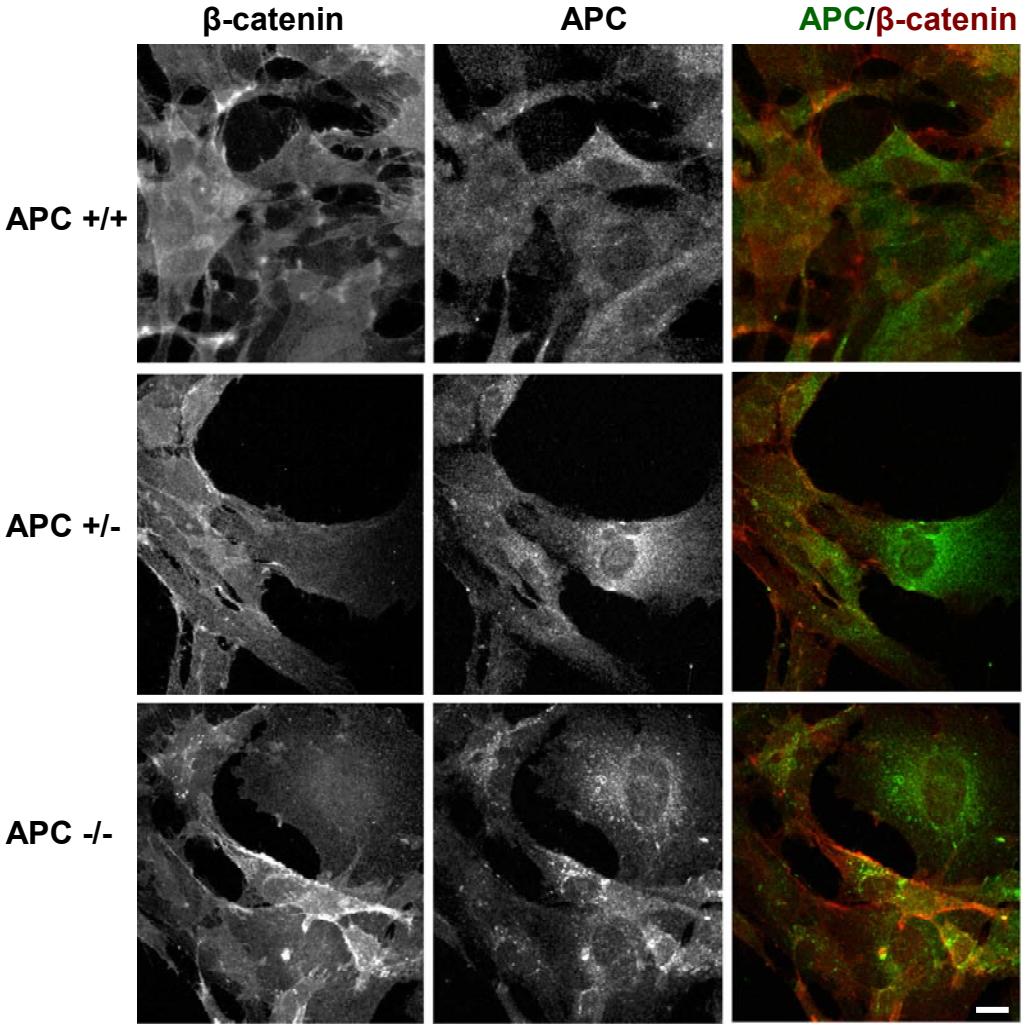

Figure 4.4
The co-localization of APC and β-catenin in MEF cell lines that are APC mNLS$^{+/+}$, APC mNLS$^{+/-}$ or APC mNLS $^{-/-}$ using mouse anti-APC Ali-12-28 and rabbit anti-β-catenin. Images were taken on a Zeiss upright confocal microscope with a 60X water objective. Scale bar = 6μm.

passages just prior to cryopreservation. Upon being thawed and re-plated, the MEF lines of all APC mNLS genotypes exhibited a shorter than expected proliferative phase before entering senescence. While MEF cells are generally expected to continue dividing for 15-30 passages in culture (11), the APC mNLS mutant and WT MEF lines were generally able to survive at most 10 passages before becoming senescent. When the growth rate was evaluated in cells at passages 3-6, little growth was apparent (Figure 4.5). This basic profile was similar for cells at various concentrations and the homozygous mutant or the homozygous WT APC mNLS ES cell lines gave comparable results.

DNA damage causes the nuclear translocation of APC in APC mNLS$^{+/+}$ and APC mNLS$^{-/-}$ MEFs

The nuclear functions of APC are not currently well understood. In the mutant APC mNLS MEF lines, APC is not excluded from the nucleus in the homozygous cells. Nevertheless, nuclear targeting appears to be somewhat deficient. It was hypothesized that supplementary pathways might exist for APC to be transported into the nucleus or retained in the nucleus after the nuclear envelope reforms following mitosis. It is possible that because cells were grown in optimal conditions, the low level of APC that was able to enter the nucleus by alternative means was sufficient for normal growth. The APC mNLS mutant cells show no abnormal localization of β-catenin when compared with cells derived from their APC mNLS WT siblings. To observe how cells react to the loss of targeted APC under

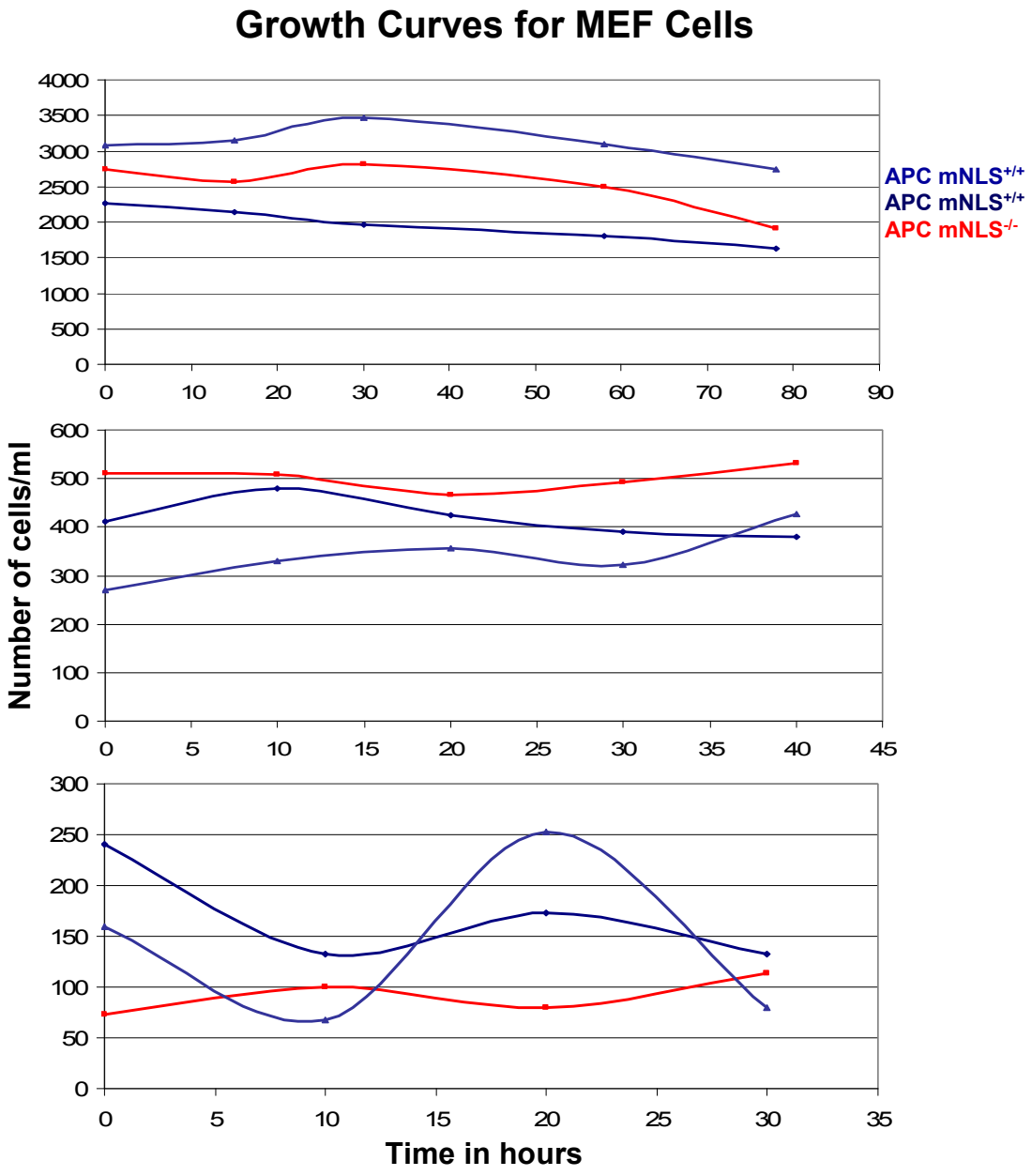

Figure 4.5
The growth pattern of MEF cells. Time in hours is indicated on the x-axis and the concentration of cells per mL of media is indicated on the y-axis. APC mNLS$^{-/-}$ cell line #8 is represented by the red lines. APC mNLS$^{+/+}$ cell lines #7 and #9 are represented by the blue lines

more stressful conditions, APC localization was analyzed in cells that had experienced DNA damage by UV light treatment.

Exposure to UV light induces pyrimidine dimers (reviewed in 29). These dimers are recognized by DNA damage-sensing proteins and removed through the Nucleotide Excision Repair (NER) pathway of DNA repair. NER involves the removal of the dimerized bases along with the surrounding nucleotides, leaving a region of single stranded DNA approximately 30 bp in length (29). A protocol devised by Rubbi and Milner (30) was used to detect these single stranded transients generated during NER. Cells were grown in bromodeoxyuridine (BrdU) prior to UV light exposure, allowing the BrdU to incorporate into the newly synthesized DNA strand in place of thymidine. Normal antibody detection of BrdU requires that cells be treated with a weak HCl acid solution to denature the DNA prior to antibody incubation because the double stranded nature of DNA prevents the BrdU antibody from finding its epitope. However, in UV exposed cells that are not treated with HCl, BrdU antibodies will localize specifically to the single stranded DNA intermediates of NER. Previous reports have shown that one hour after UV irradiation, BrdU was found in multiple repair foci in cells that had been exposed to 10-40 J/m^2 of UV light (30).

When mutant and WT MEF cells were grown in BrdU-supplemented media and exposed to 10 J/m^2 of UV light, BrdU antibody staining was consistent with NER occurring in the nucleus (Figure 4.6). Cells that had not been exposed to UV light displayed only a dim background staining with BrdU but no specific nuclear staining

(Figure 4.6). When APC localization was analyzed in the UV and non UV irradiated MEFs several of the UV irradiate cells displayed predominantly nuclear APC (Figure 4.6). APC localized to the nucleus to differing degrees in different cells on the same slide, however both APC mNLS mutant and WT MEFs displayed a dramatically nuclear localization of APC in at least some of the UV irradiated cells (Figures 4.6 and 4.7).

The dramatic relocalization of the APC mNLS mutant protein was unexpected. Others have shown that importin-α is sequestered in the nucleus following many types of cellular stresses, and is therefore unavailable in the cytoplasm to facilitate nuclear import (31). The reduction of cytoplasmic importin-α causes classic nuclear import to be blocked following UV irradiation of cells in culture (31). Therefore, the observed nuclear localization of APC likely takes place though an entirely different pathway not dependent on importin-α. Other proteins, such as heat shock protein 70 (hsp70) and its cognate (hsc70) have been observed to localize to the nucleus during the time frame in which nuclear import is blocked (32). Though the mechanism by which importin-α independent nuclear import occurs is not currently known (33), our evidence strongly suggests that APC is also capable of nuclear import through this mechanism. A novel method for APC import is a possible explanation for the continued presence of APC in the nucleus of homozygous mutant APC mNLS cells in culture and in animals.

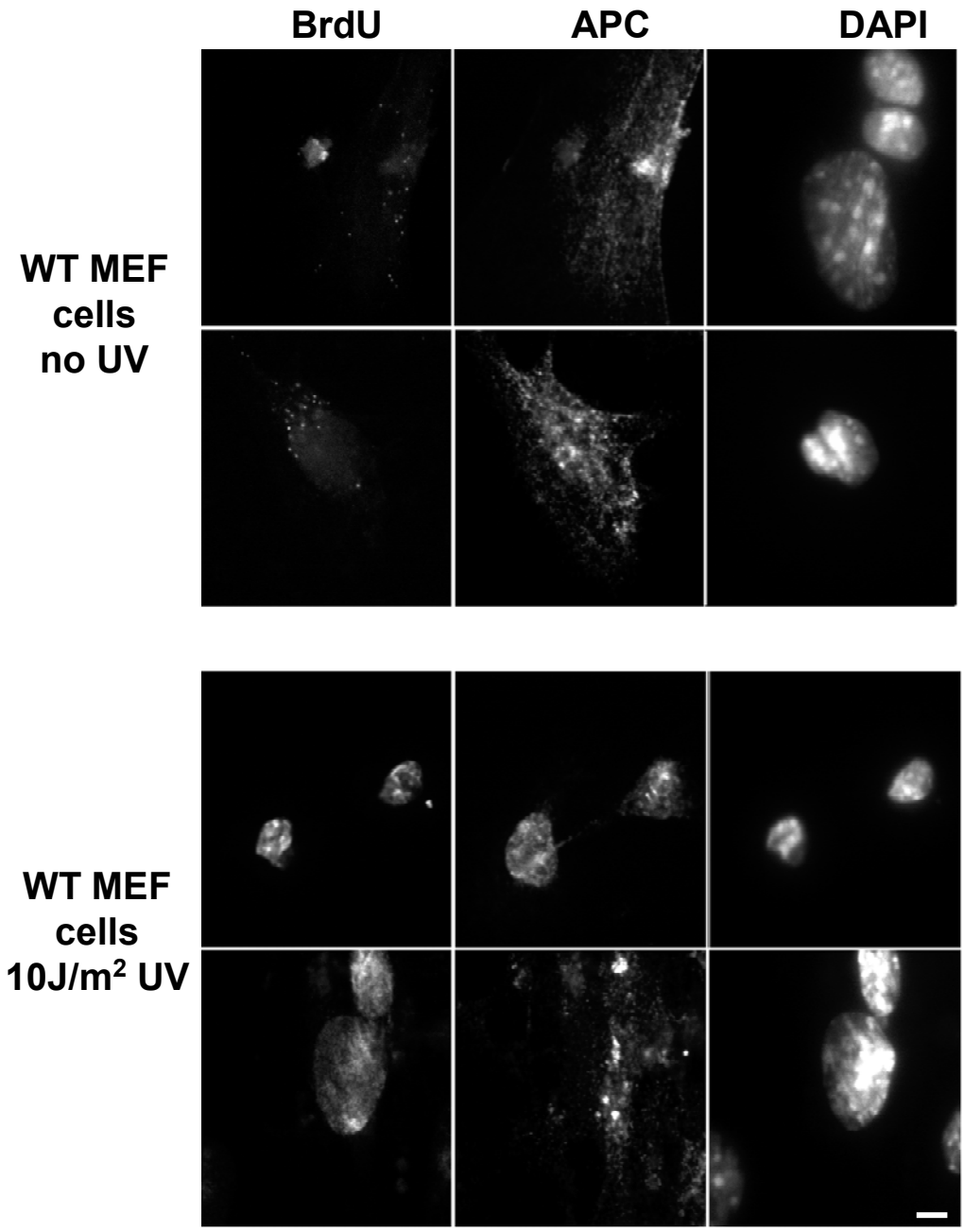

Figure 4.6
APC distribution in APC mNLS$^{+/+}$ MEF cells with and without UV treatment. DNA repair is visualized using BrdU to stain single-stranded DNA intermediates of the NER pathway. Rabbit anti-APC M2 was used to stain for APC. Cells were exposed to 10J/m^2 of UV light and allowed to recover for 1 hour before being fixed and stained. Images were captured on an Olympus 3I spinning disc confocal TIRF inverted microscope and analyzed using *Slidebook* software. Scale bar = 3μm

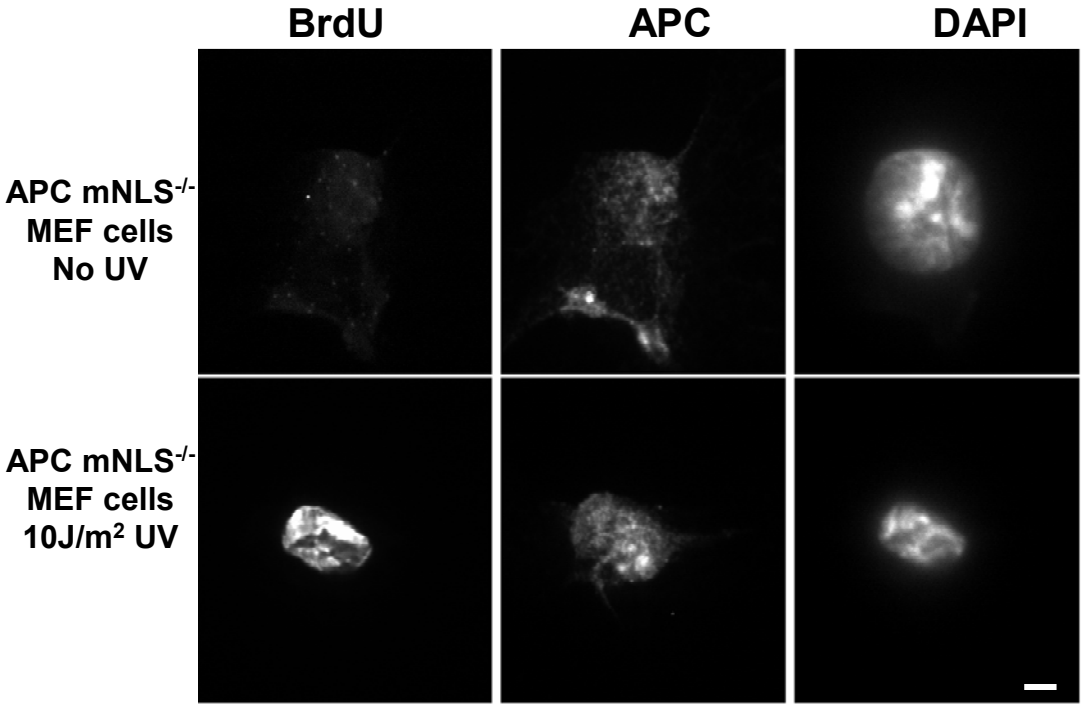

Figure 4.7
APC distribution in APC mNLS$^{-/-}$ MEF cells with and without UV treatment. DNA repair is visualized using BrdU to stain single-stranded DNA intermediates of the NER pathway. Rabbit anti-APC M2 was used to stain for APC. Cells were exposed to 10J/m^2 of UV light and allowed to recover for 1 hour before being fixed and stained. Images were captured on an Olympus 3I spinning disc confocal TIRF inverted microscope and analyzed using *Slidebook* software. Scale bar = 3μm

Discussion

Results from a preliminary evaluation of the APC mNLS heterozygous ES cell lines were used to select the cell lines used to generate our APC mNLS mouse model. Early observations of growth rate revealed that cell lines MES-3 and MES-7 represented the outliers, showing growth characteristics that were not shared by the other APC mNLS cell lines. Cell line MES-3 consistently grew more rapidly than the other transgenic cell lines suggesting that this phenotype resulted from an unwanted genetic alteration rather than from a targeted mutation of *Apc*. Cell line MES-3 also appeared to diverge slightly from the majority of the transgenic cell lines with respect to β-catenin transcriptional activity. The ratio of TOPFLASH to FOPFLASH reporter activity in MES-3 cells suggests that the MES-3 cell line had an increased expression of the Wnt/β-catenin target genes. While this discrepancy in the TOPFLASH to FOPFLASH ratio was slight, when viewed in conjunction with the previously observed increase in growth rate, it cast doubt about the integrity of the MES-3 genome. It is conceivable that that the insertion of the targeting construct in this cell line may have altered the *Apc* gene beyond the intended mutations to the NLSs or that one or more of the other components of the Wnt signaling pathway was affected during the process of electroporation and selection. While these results alone are not definitive evidence of such an alteration, they were sufficient to remove the MES-3 cell line from consideration for further study. Similarly, the cell line MES-7 was eliminated from consideration for exhibiting characteristics that varied from the mean in the opposing direction. The MES-7 cell line displayed a low TOPFLASH to

FOPFLASH ratio that correlated with a slower rate of growth when compared to the other APC mNLS transgenic cell lines. The MES-2 cell line was observed to proliferate at an expected rate, yet demonstrated the most divergent TOPFLASH to FOPFLASH ratio. An initial inspection of the chromosome number suggested that many MES-2 cells displayed abnormal karyotypes, and thus the MES-2 line was considered a poor choice to use in the generation of a mouse model. After the elimination of cell lines MES-2, MES-3 and MES-7, a more extensive karyotype analysis was performed with the remaining cell lines. Two of these cell lines, MES-1 and MES-4, displayed normal karyotypes in over 75% of cells and were considered for further use. The other two cell lines, MES-5 and MES-6, were determined to have an abnormal number of chromosomes in greater than 25% of the chromosome spreads counted and therefore were not good candidates for generation of a knock-in mouse model.

The cell lines MES-1 and MES-4 were identified as potential candidates for the generation of a mouse model (Table 4.4). Further PCR analysis was used to confirm that the ends of the gene replacement vector had appropriately inserted (see Chapter 2 for details). The MES-4 cell line was used for injection into blastocysts to generate the first set of chimeric mice. The MES-1 cell line was also used to generate a mouse model, but at a later date.

The evaluation of β-catenin localization by immunohistochemistry revealed no significant differences between APC mNLS$^{+/-}$ and WT ES cells or between APC mNLS$^{+/+}$, APC mNLS$^{+/-}$ or APC mNLS$^{-/-}$ MEF cell lines suggesting that altering the

nuclear targeting of APC does not have a large affect on the localization of the β-catenin protein. More surprising was that the APC mNLS$^{+/-}$ ES cell and WT ES cells showed no differences in APC localization. Because the APC mNLS$^{+/-}$ ES cells still express WT APC from the non-targeted allele, at least half of the APC protein in the cells is still capable of nuclear import. The cell may be able to utilize the WT protein to maintain a threshold level of APC in the nuclear compartment while the APC mNLS mutant protein fulfills the cytoplasmic functions. In contrast, analysis of APC localization in the MEF cells revealed a different pattern of staining for the mutant and WT protein. APC mNLS$^{+/+}$ cells show a very diffuse pattern of staining with little difference in the nuclear and cytoplasmic levels of APC. The APC mNLS heterozygous and homozygous cells showed a definite decrease in the ratio of nuclear to cytoplasmic APC. Furthermore, the cytoplasmic APC staining in the mutant cells was observed to be the most intense in the area immediately surrounding the nuclear compartment. However, APC was never completely excluded from the nucleus. Some APC protein was visible in the nuclear compartment in even the homozygous mutant MEFs. This suggests that there are other methods for APC to gain entry into the nucleus.

It has been hypothesized that supplementary NLSs or NLS-like regions exist in the ARM domain of APC which could lead to a low level of APC translocation into the nucleus (34). In addition to APC's own nuclear import abilities, other APC binding partners such as β-catenin, PCNA, topo IIα and DNA polymerase β have the ability to localize to the nucleus (24, 35-37) Furthermore APC has been shown to

interact with microtubules at the kinetochore (38), localizing to the DNA following the breakdown of the nuclear envelope during mitosis (39). It is possible that some APC can be carried into the nucleus, or that APC is retained at the DNA after cell division, through interactions with APC binding partners in the nucleus.

The potential for an alternative nuclear import strategy was revealed by experiments in which APC mNLS MEF cell lines were irradiated with UV light. Following a DNA damaging dose of UV irradiation, APC protein in mutant and WT cells relocalized to the nucleus. This new phenomenon will be further explored in Chapter 5, but the preliminary results suggest that APC is required in the nucleus after certain types of DNA damaging events and that the method by which APC is targeted to the nucleus is not dependent on the characterized NLSs. An alternate means of nuclear import could explain the continued presence of APC in the nucleus of the mutant cell lines. The APC mNLS cell lines and mouse model might prove useful to study this alternate pathway of nuclear localization.

References

1. Harrison, R. (1907) Observations on the Living Developing Nerve Fiber. *Proceedings of the Society for Experimental Biology and Medicine* 4, 140-143
2. Landecker, H. (2007) *Culturing Life: How cells became technologies*, Harvard University Press, Cambridge
3. Kohler, G., and Milstein, C. (1975) Continuous cultures of fused cells secreting antibody of predefined specificity. *Nature* 256, 495-497
4. Weinberg, R. A. (2007) *The Biology of Cancer*, Garland Science, Taylor & Francis Group, New York
5. Martin, G. R. (1981) Isolation of a pluripotent cell line from early mouse embryos cultured in medium conditioned by teratocarcinoma stem cells. *Proc Natl Acad Sci U S A* 78, 7634-7638

6. Evans, M. J., and Kaufman, M. H. (1981) Establishment in culture of pluripotential cells from mouse embryos. *Nature* 292, 154-156
7. Thompson, S., Clarke, A. R., Pow, A. M., Hooper, M. L., and Melton, D. W. (1989) Germ line transmission and expression of a corrected HPRT gene produced by gene targeting in embryonic stem cells. *Cell* 56, 313-321
8. Thomas, K. R., and Capecchi, M. R. (1987) Site-directed mutagenesis by gene targeting in mouse embryo-derived stem cells. *Cell* 51, 503-512
9. Freshney, R. I. (2000) *Culture of Animal Cells: A manual of basic technique*, Wiley-Liss, New York
10. Nagy, A., Gertsenstein, M., Vintersten, K., and Behringer, R. (2003) *Manipulating the Mouse Embryo: a laboratory manual*, Cold Spring Harbor Laboratory Press, Cold Spring Harbor
11. Sherr, C. J., and DePinho, R. A. (2000) Cellular senescence: mitotic clock or culture shock? *Cell* 102, 407-410
12. vom Brocke, J., Schmeiser, H. H., Reinbold, M., and Hollstein, M. (2006) MEF immortalization to investigate the ins and outs of mutagenesis. *Carcinogenesis* 27, 2141-2147
13. Nagy, A., Rossant, J., Nagy, R., Abramow-Newerly, W., and Roder, J. C. (1993) Derivation of completely cell culture-derived mice from early-passage embryonic stem cells. *Proc Natl Acad Sci U S A* 90, 8424-8428
14. Neufeld, K. L., and White, R. L. (1997) Nuclear and cytoplasmic localizations of the adenomatous polyposis coli protein. *Proc Natl Acad Sci U S A* 94, 3034-3039
15. Korinek, V., Barker, N., Morin, P. J., van Wichen, D., de Weger, R., Kinzler, K. W., Vogelstein, B., and Clevers, H. (1997) Constitutive Transcriptional Activation by a beta -Catenin-Tcf Complex in APC-/- Colon Carcinoma. *Science* 275, 1784-1787
16. Mortensen, R. M., Conner, D. A., Chao, S., Geisterfer-Lowrance, A. A., and Seidman, J. G. (1992) Production of homozygous mutant ES cells with a single targeting construct. *Mol Cell Biol* 12, 2391-2395
17. Ramirez-Solis, R., Rivera-Perez, J., Wallace, J. D., Wims, M., Zheng, H., and Bradley, A. (1992) Genomic DNA microextraction: a method to screen numerous samples. *Anal Biochem* 201, 331-335
18. Kolligs, F. T., Bommer, G., and Goke, B. (2002) Wnt/beta-catenin/tcf signaling: a critical pathway in gastrointestinal tumorigenesis. *Digestion* 66, 131-144
19. Neufeld, K. L., Zhang, F., Cullen, B. R., and White, R. L. (2000) APC-mediated downregulation of beta-catenin activity involves nuclear sequestration and nuclear export. *EMBO Rep* 1, 519-523
20. Smits, R., Kielman, M. F., Breukel, C., Zurcher, C., Neufeld, K., Jagmohan-Changur, S., Hofland, N., van Dijk, J., White, R., Edelmann, W., Kucherlapati, R., Khan, P. M., and Fodde, R. (1999) Apc1638T: a mouse model delineating critical domains of the adenomatous polyposis coli protein involved in tumorigenesis and development. *Genes Dev* 13, 1309-1321

21. Ishikawa, T. O., Tamai, Y., Li, Q., Oshima, M., and Taketo, M. M. (2003) Requirement for tumor suppressor Apc in the morphogenesis of anterior and ventral mouse embryo. *Dev Biol* 253, 230-246
22. Rosin-Arbesfeld, R., Townsley, F., and Bienz, M. (2000) The APC tumour suppressor has a nuclear export function. *Nature* 406, 1009-1012
23. Henderson, B. R. (2000) Nuclear-cytoplasmic shuttling of APC regulates beta-catenin subcellular localization and turnover. *Nat Cell Biol* 2, 653-660
24. Henderson, B. R., and Fagotto, F. (2002) The ins and outs of APC and beta-catenin nuclear transport. *EMBO Rep* 3, 834-839
25. Brocardo, M., Nathke, I. S., and Henderson, B. R. (2005) Redefining the subcellular location and transport of APC: new insights using a panel of antibodies. *EMBO Rep* 6, 184-190
26. Davies, M. L., Roberts, G. T., Stuart, N., and Wakeman, J. A. (2007) Analysis of a panel of antibodies to APC reveals consistent activity towards an unidentified protein. *Br J Cancer* 97, 384-390
27. Yenofsky, R. L., Fine, M., and Pellow, J. W. (1990) A mutant neomycin phosphotransferase II gene reduces the resistance of transformants to antibiotic selection pressure. *Proc Natl Acad Sci U S A* 87, 3435-3439
28. Lefebvre, L., Dionne, N., Karaskova, J., Squire, J. A., and Nagy, A. (2001) Selection for transgene homozygosity in embryonic stem cells results in extensive loss of heterozygosity. *Nat Genet* 27, 257-258
29. Sancar, A., Lindsey-Boltz, L. A., Unsal-Kacmaz, K., and Linn, S. (2004) Molecular mechanisms of mammalian DNA repair and the DNA damage checkpoints. *Annu Rev Biochem* 73, 39-85
30. Rubbi, C. P., and Milner, J. (2001) Analysis of nucleotide excision repair by detection of single-stranded DNA transients. *Carcinogenesis* 22, 1789-1796
31. Miyamoto, Y., Saiwaki, T., Yamashita, J., Yasuda, Y., Kotera, I., Shibata, S., Shigeta, M., Hiraoka, Y., Haraguchi, T., and Yoneda, Y. (2004) Cellular stresses induce the nuclear accumulation of importin alpha and cause a conventional nuclear import block. *J Cell Biol* 165, 617-623
32. Chu, A., Matusiewicz, N., and Stochaj, U. (2001) Heat-induced nuclear accumulation of hsc70s is regulated by phosphorylation and inhibited in confluent cells. *Faseb J* 15, 1478-1480
33. Tsukahara, F., and Maru, Y. (2004) Identification of novel nuclear export and nuclear localization-related signals in human heat shock cognate protein 70. *J Biol Chem* 279, 8867-8872
34. Galea, M. A., Eleftheriou, A., and Henderson, B. R. (2001) ARM domain-dependent nuclear import of adenomatous polyposis coli protein is stimulated by the B56 alpha subunit of protein phosphatase 2A. *J Biol Chem* 276, 45833-45839
35. Mirski, S. E., Sparks, K. E., Friedrich, B., Kohler, M., Mo, Y. Y., Beck, W. T., and Cole, S. P. (2007) Topoisomerase II binds importin alpha isoforms and exportin/CRM1 but does not shuttle between the nucleus and cytoplasm in proliferating cells. *Exp Cell Res* 313, 627-637

36. Prelich, G., Tan, C. K., Kostura, M., Mathews, M. B., So, A. G., Downey, K. M., and Stillman, B. (1987) Functional identity of proliferating cell nuclear antigen and a DNA polymerase-delta auxiliary protein. *Nature* 326, 517-520
37. Taladriz, S., Hanke, T., Ramiro, M. J., Garcia-Diaz, M., Garcia De Lacoba, M., Blanco, L., and Larraga, V. (2001) Nuclear DNA polymerase beta from Leishmania infantum. Cloning, molecular analysis and developmental regulation. *Nucleic Acids Res* 29, 3822-3834
38. Honnappa, S., John, C. M., Kostrewa, D., Winkler, F. K., and Steinmetz, M. O. (2005) Structural insights into the EB1-APC interaction. *Embo J* 24, 261-269
39. Fodde, R., Kuipers, J., Rosenberg, C., Smits, R., Kielman, M., Gaspar, C., van Es, J. H., Breukel, C., Wiegant, J., Giles, R. H., and Clevers, H. (2001) Mutations in the APC tumour suppressor gene cause chromosomal instability. *Nat Cell Biol* 3, 433-438

CHAPTER 5

NUCLEAR RELOCALIZATION OF APC IN UV-TREATED CELLS

Abstract

We observed APC to localize predominantly to the nucleus in a subset of the APC mNLS MEF cells that were exposed to UV light. It has been suggested that APC may play a role in DNA repair, though no mechanism for such a role has been elucidated. Due to the limited lifespan of primary MEF cell lines, the HCT116βw human colon cancer cell line was chosen for evaluation of APC in the nucleus following DNA damage. This chapter discusses the characterization of the nuclear accumulation of APC following UV induced DNA damage in HCT116βw cells.

Introduction

Cancer is a disease caused by an accumulation of mutations to cellular DNA (1). Therefore, in the prevention of cancer, the ability to maintain the integrity of the genome is paramount (2). For this reason, mammalian cells have multiple pathways for the detection and repair of damage to their DNA (reviewed in 3). A number of different cellular mechanisms exist to cope with the range of possible types of DNA damage and to delay or arrest the cell cycle to allow repair to proceed before the cell enters mitosis (3).

The cell cycle is made up of several distinct phases (4) (Figure 5.1). Following mitosis, cells enter a growth phase referred to as G_1. Following G_1 the cell enters S-phase during which the DNA is replicated. At the end of S-phase the cell, containing two full copies of the genome, enters a second growth phase referred to as G_2 during which the cell prepares for another round of cell division. The actual process of nuclear division followed by cell division is called M-phase. At the end of M-phase, the two daughter cells re-enter G_1 and the process begins again (reviewed in 4). At several stages during this cycle, mechanisms exist to halt progression and delay the transition to the next phase of the cell cycle. These decisive stages have been termed "cell cycle checkpoints" (5, 6). These checkpoints are activated by replicative stress and in response to the detection of damaged DNA (6). The cellular DNA damage response consists of three steps: 1) recognition of a damaged region of DNA, 2) activation of the mitotic checkpoint machinery to halt progression of the cell

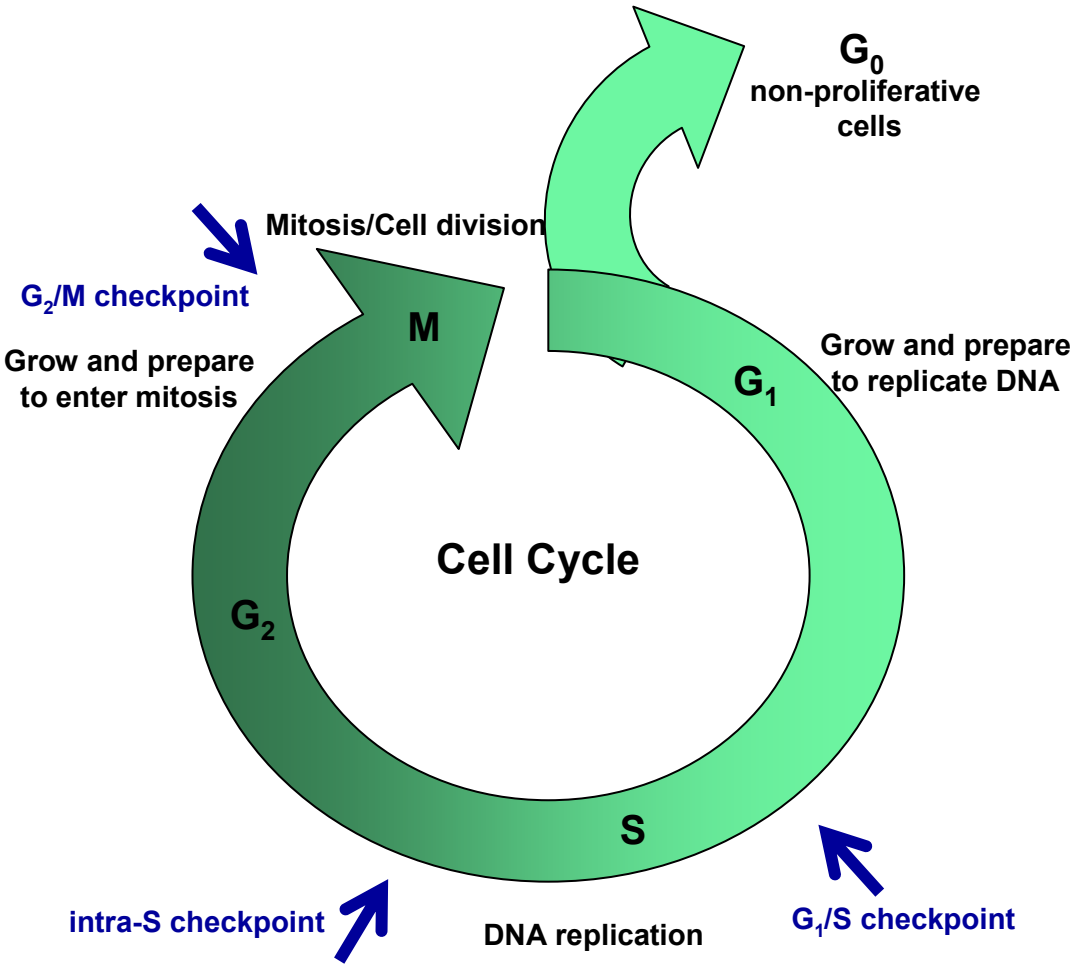

Figure 5.1
A simplified diagram of the phases of the cell cycle. Cell cycle checkpoints that respond to DNA damage are indicated in blue. Adapted from Alberts, B., Bray, D., Lewis, J., Raff, M., Roberts, K., and Watson, J. D. (1994) *Molecular Biology of the Cell*, Garland Publishing Inc., New York

cycle and 3) the resolution of the crisis, either through repair of the damage or initiation of apoptosis (3).

There are multiple and somewhat contradictory reports in the literature of potential roles for APC in the DNA damage response. In cultured human cells and in mouse models, data indicates that mutations to APC result in a reduced ability to cope with UV and ionizing radiation (7, 8). These studies suggest that APC may play a supporting role in the cellular DNA damage response, but do not suggest the step in which APC is involved. These data are not in agreement with reports that cells with mutant APC are less sensitive to DNA methylating agents, and that APC directly interacts with and inhibits the DNA repair proteins polymerase-β and Flap endonuclease 1 (Fen-1) *in vitro* (9, 10). The reports that APC inhibits repair of methylated DNA seem incongruent with reports that APC is up-regulated by p53 in response to DNA damage caused by methylating agents (11, 12). In addition to evidence for a direct interaction between APC and DNA repair proteins, there are also reports that APC may play a role in the DNA damage checkpoint. The activation of the G_2/M checkpoint leading to cell cycle arrest has been reported following the stabilization of endogenous APC (13). Our own lab has recently demonstrated that over-expression of an APC fragment encompassing amino acids 1000-1326 also leads to G_2 arrest (14).

In Chapter 4 we reported that APC was observed to accumulate in the nucleus of primary MEF cells in response to UV irradiation. In this chapter, we further characterize APC localization in UV-irradiated HCT116βw cells. We show that APC

is transiently targeted to the nucleus in response to UV irradiation in a cell cycle dependent manner. Furthermore, optimal nuclear accumulation appears to be dependent on the function of cell cycle checkpoint kinases.

Materials and Methods

Cell culture and synchronization

HCT116βw human epithelial cell lines, originally derived from colon cancer tissue were received from Bert Volgelstein (15) and maintained in growth media [McCoy's 5A Media (Cellgro) supplemented with 10% Fetal Bovine Serum (Hyclone)]. Cells were kept in a 37°C water jacketed incubator with 7% CO_2 and passaged when they reached confluence.

To obtain synchronized cells, HCT116βw cells were plated at approximately 50% confluency. Cell cycle was blocked by the addition of 1μg/mL aphidicolin (Sigma or Calbiochem) to the normal growth media. Following 24 hours in aphidicolin, cells were washed 3 times with fresh McCoy's 5A media and allowed to resume cycling in normal growth media for the desired length of time.

UV irradiation

Prior to UV irradiation, growth media was removed and cells were rinsed with sterile PBS. A thin layer of PBS was maintained to prevent drying. Cells were placed in an Ultraviolet Crosslinker (UVP) and irradiated for 2.8 minutes at an

intensity of 240mJ/sec resulting in a total exposure of ~40J/m^2. The sham-irradiated control cells were processed identically except that cells were covered with aluminum foil during UV exposure. Following UV irradiation, the PBS was removed and replaced with fresh growth media. Cells were incubated at 37°C for the indicated time before being processed.

Inhibition of DNA repair kinases

To inhibit kinases involved in DNA repair, the following inhibitors were added to the normal growth media 30 minutes prior to UV irradiation of the cells. Wortmannin (Calbiochem) was used at a final concentration of 20μM. Chk 2 inhibitor [2-(4-(4-Chlorophenoxy)phenyl)-1H-benzimidole-5-carboxamide (Calbiochem)] was used at 10μM. Chk 1 inhibitor [SB-218078 (Calbiochem)] was used at 5μM. Inhibitors were made up at a 250X concentration in DMSO and added to media 4μL/mL. Control cells were incubated in 4μL/mL DMSO for the same duration.

Immunofluorescence

Immunostaining was performed essentially as previously described (16) using the following antibodies: Mouse anti-APC (Ali-12-28 1:50, Abcam), anti-APC-M2 rabbit polyclonal antibody made against amino acids 1000-1326 and affinity purified (1:3000), mouse anti-β-catenin (1:1000 Transduction Laboratories), rabbit anti-β-catenin (1:1000, Sigma), mouse anti-PCNA (1:500, Zymed) goat anti-mouse IgG

Alexa 488 (1:1000, Molecular Probes), goat anti-rabbit IgG Alexa 568 (1:1000, Molecular Probes). DNA was labeled with DAPI (0.1μg/mL). Briefly, cells were seeded on 22x22mm glass coverslips (Fisher) and allowed to settle overnight. Following the desired treatment, coverslips containing cells were rinsed 2 times with PBS then fixed (4% paraformaldehyde and 0.1% Triton X-100 in PBS) on ice for 30 minutes. Cells were either stained immediately or stored for up to a week in PBS at 4°C. Cells were made permeable by incubation in 0.2% Triton X-100 (in TBS) or -20°C methanol for 5 minutes and rinsed 2 times in TBS prior to incubation with primary antibody. Coverslips were inverted over drops of primary antibody for 90 minutes, rinsed 3 times in TBS, inverted over drops of secondary antibody for 30 minutes, DAPI (0.1μg/mL) for 5 minutes and again washed 3 times for 5 minutes in TBS. Stained coverslips were mounted onto glass microscope slides (Fisher) using ProLong Antifade (Invitrogen) and the edges were sealed with nail polish (Revlon). Images were captured using one of the following: a Zeiss inverted fluorescent microscope equipped with an Olympus camera and analyzed using *Magnafire* software, a Nikon TU2000 microscope equipped with a Letiga EXI camera (Q Imaging) and analyzed using *Phylum Live* software, or an Olympus 3I spinning disc confocal TIRF inverted microscope and analyzed using *SlideBook* software.

Flow Cytometry

Propidium iodide staining of synchronized and unsynchronized HCT116βw cells in solution was performed using a standard protocol (17). Briefly, HCT116βw

cells at 50% confluencey were synchronized by incubation with aphidicolin for 24 hours then washed 3 times with fresh McCoy's 5A media. Cells were allowed to resume cell cycle progression for 0, 2, 4, or 7 hours before being trypsinized, pelleted, and fixed in cold 100% ethanol. Cells were fixed for 30 minutes on ice then washed 2 times for 10 minutes with PBS to rehydrate. Rehydrated cells were then stained with 40μg/ml propidium iodide (Sigma) in PBS for 1 hour. Cells were pelleted and resuspended in 400μL PBS and filtered through a 40μm nylon cell strainer (BD Falcon) to remove cell aggregates. FACS analysis was performed using a Becton Dickinson FACScan and evaluated using *CellQuest* software. At least 10,000 cells were analyzed for each time point.

Immunoprecipitation and western blot analysis

Immunoprecipitation and western blots were performed using standard protocols (18). HCT 116 cells used to prepare lysates were grown in 10cm tissue culture dishes (Falcon) until approximately 50% confluent. Cells were synchronized using aphidicolin to block cell cycle progression and allowed to resume cycling for 4 hours after the removal of the drug. Following UV or sham irradiation, cells were placed in growth media for 40 minutes before being processed. To prepare lysates, cells were placed on ice and washed 2 times with cold PBS. Roughly $2x10^7$ cells were lysed using 1mL of cold Lysis Buffer [50mM Tris pH 7.5. 0.1% NP40, 00mM NaCl, 1mM $MgCl_2$, 5mM EDTA]. Immediately prior to use, Protease Inhibitors [100mM PMSF (Sigma), 1mg/mL Apoprotinin (MP Biomedicals), 1mg/mL

Leupeptin trifluoroacetate (MP Biomedicals), 1mg/mL Pepstatin A (MP Biomedicals) all in 200 proof ethanol] were added to the Lysis Buffer at a concentration of 1:50. A cell scraper was used to mechanically dislodge cells and suspend them in Lysis Buffer. Cell suspensions were moved to 1.5mL ependorf tubes which were placed on an orbital shaker at 4°C for 8 minutes. Cells were sonicated for 10 seconds (tip setting of 1) every 2 minutes for the duration of the 8 minute incubation. Lysates were then centrifuged at 13,000xg for 20 minutes at 4°C to remove any insoluble material. Following centrifugation the supernatant was removed and placed in a fresh tube. The insoluble pellets were resuspended in 3X SDS Loading dye [6% w/v Sodium Dodecyl Sulfate, 30% Glycerol, 150mM Tris pH 6.8, ~0.2mg/mL Bromophenol Blue in water] and heated to 95°C for 10 minutes before storage at -20°C. The protein concentrations of the supernatant fluids were determined using the Bio-Rad Protein Assay reagent according the manufacturer's instructions. The lysates were placed into tubes containing 30µl of Protein A Dynabeads (Invitrogen) conjugated to rabbit anti-APC M2 antibody (generated against APC amino acids 1000-1326 in the Neufeld and Azuma labs) or rabbit IgG control (Sigma). An equal protein concentration was used for each tube and the final volume was adjusted to 0.8mL using fresh Lysis Buffer. Tubes were placed on an orbital shaker at 4°C overnight. The following day the supernatant for each tube was removed and saved as the "unbound fraction". The Dynabeads were washed 2x15 minutes with 0.5mL Lysis Buffer and 1x 15 minutes with PBS-T at 4°C and then protein was eluted from the beads in 80µL of PBS ($1/10^{th}$ the volume of the original lysates) and 40µL of 3X

SDS loading buffer. Loading buffer was also added 1:3 to the unbound fractions for each tube and to the 250μg of total lysate frozen the previous day. All tubes were heated to 95°C for 10 minutes to denature the protein. Samples were resolved using SDS PAGE. Western blots were probed with anti-APC-M2 rabbit polyclonal antibody (1:3000) and rabbit anti-β-catenin (1:1000, Sigma).

Results

APC protein associates with the nucleus after UV irradiation

In the APC mNLS MEF cell lines, APC was observed to dramatically shift from a diffuse nuclear and cytoplasmic localization pattern to a predominantly nuclear localization pattern after exposure to UV light (Figure 4.6 and 4.7). This shift was observed in both the APC mNLS WT MEF lines and the APC mNLS homozygous mutant cell lines. Because the homozygous mutant MEFS lack the characterized NLS domains which interact with importin-α to achieve nuclear import, we hypothesized that this dramatic relocalization of APC was occurring through an alternate mechanism. Furthermore, this shift was not observed in every cell that was exposed to UV light. BrdU staining, used to identify cells with single stranded DNA intermediates of NER, revealed that a majority of the cells irradiated were undergoing DNA repair (data not shown). However, only a subset of these cells exhibited a striking alteration in APC localization (Figure 4.6). This selective APC response

suggested that additional control mechanisms must also play a role in the regulation of APC targeting.

Further analysis of the APC relocalization phenomenon required a large number of cells for experimentation. The MEF lines had the advantage of being a primary cell line lacking mutations typical of cells adapted to growth in culture (19). However, MEF cells entered senescence after a small number of population doublings, making generation of the quantity of cells necessary for analysis extremely difficult. For this reason, HCT116βw cells, an immortalized epithelial cell line originally derived from a human colonic carcinoma (20), were used for the evaluation of this phenotype. HCT116 cells grow very well in culture and have a short doubling time, facilitating the generation of large quantities of cells. Unlike many colon cancer cell lines the HCT116 cells express full length APC (21) and a mutant allele of β-catenin (22). The HCT116 cells also exhibit a normal mitotic check point response (23) and normal p53-mediated growth arrest (24). The HCT116βw cell line that was used in the following experiments has been engineered to eliminate the oncogenic allele of β-catenin, leaving only the WT β-catenin in these cells (15)

The nuclear localization of APC after UV irradiation is cell cycle dependent

We observed that some, but not all UV irradiated MEF cells displayed prominent nuclear localization of APC (Figure 4.6) suggesting that factors regulating the cellular response to DNA damage were differentially directing APC localization. We hypothesized that cell cycle would affect the nature of the DNA damage response

and could therefore be involved in the variation in APC localization that was observed. To test this hypothesis, cells were synchronized by the addition of aphidicolin to the growth media prior to UV irradiation.

Aphidicolin is a drug that specifically inhibits DNA polymerase-α, the primary polymerase responsible for the replication of nuclear DNA (25). Unlike many other inhibitors of DNA synthesis, aphidicolin does not bind directly to DNA, does not interfere with RNA or protein synthesis and has a very low toxicity (25). The addition of aphidicolin to the medium of growing cells causes an immediate inhibition of DNA synthesis that is completely reversible following the removal of the drug (25). Aphidicolin treatment is a well established method for cell synchronization, blocking cell cycle at the beginning of S-phase upon addition and allowing the cell cycle to resume within 15 minutes of removal (17).

Following the removal of aphidicolin, cells were allowed to continue cycling in a synchronized manner for various lengths of time. Examination of APC localization in the synchronized UV-irradiated HCT116βw cells revealed a noticeable homogeneity of response to UV exposure (data not shown). The more uniform APC response of synchronized cells supported our hypothesis that cell cycle stage is an important factor in determining how APC was targeted following DNA damage.

The non-irradiated control cells released from aphidicolin block for 3 or 4 hours were observed to have nearly identical APC localization. These cells exhibited APC at nearly equal nuclear and cytoplasmic proportions. This APC staining was punctate in the cytoplasm and nuclear compartments with slightly increased APC

localized along cellular junctions and at the leading edge of cell extensions, consistent with previous reports (16, 26) (Figure 5.2 B and D). On the other hand, the UV-irradiated cells released from aphidicolin for 4 hours had at strikingly different APC staining pattern from the cells that were released from aphidicolin block for only 3 hours prior to UV irradiation. Approximately 40 minutes after UV irradiation, cells that had been released from aphidicolin block for 4 hours had a vastly decreased level of cytoplasmic APC and an evident increase in the level of APC located within the nuclear compartment (Figure 5.2 C). In cells released for only 3 hours prior to UV irradiation APC appeared to be essentially excluded from the nucleus. While some APC was always visible in the nuclear compartment, a vast majority of the APC in these cells was localized to the cytoplasm surrounding the nuclear compartment (Figure 5.2 A).

UV-induced nuclear accumulation of APC correlates with the G_2/M checkpoint

The most significant change in APC localization appeared to occur in cells that had been released from aphidicolin block for 4 hours. To determine which phase of the cell cycle this time point represented, cells were fixed, permeabilized and incubated in saturating amounts of propidium iodide, which fluoresces when intercalated into double stranded DNA (27). This resulted in fluorescently labeled cells, in which the intensity of the fluorescence emitted was directly proportional to the amount of DNA contained within the cell (27).

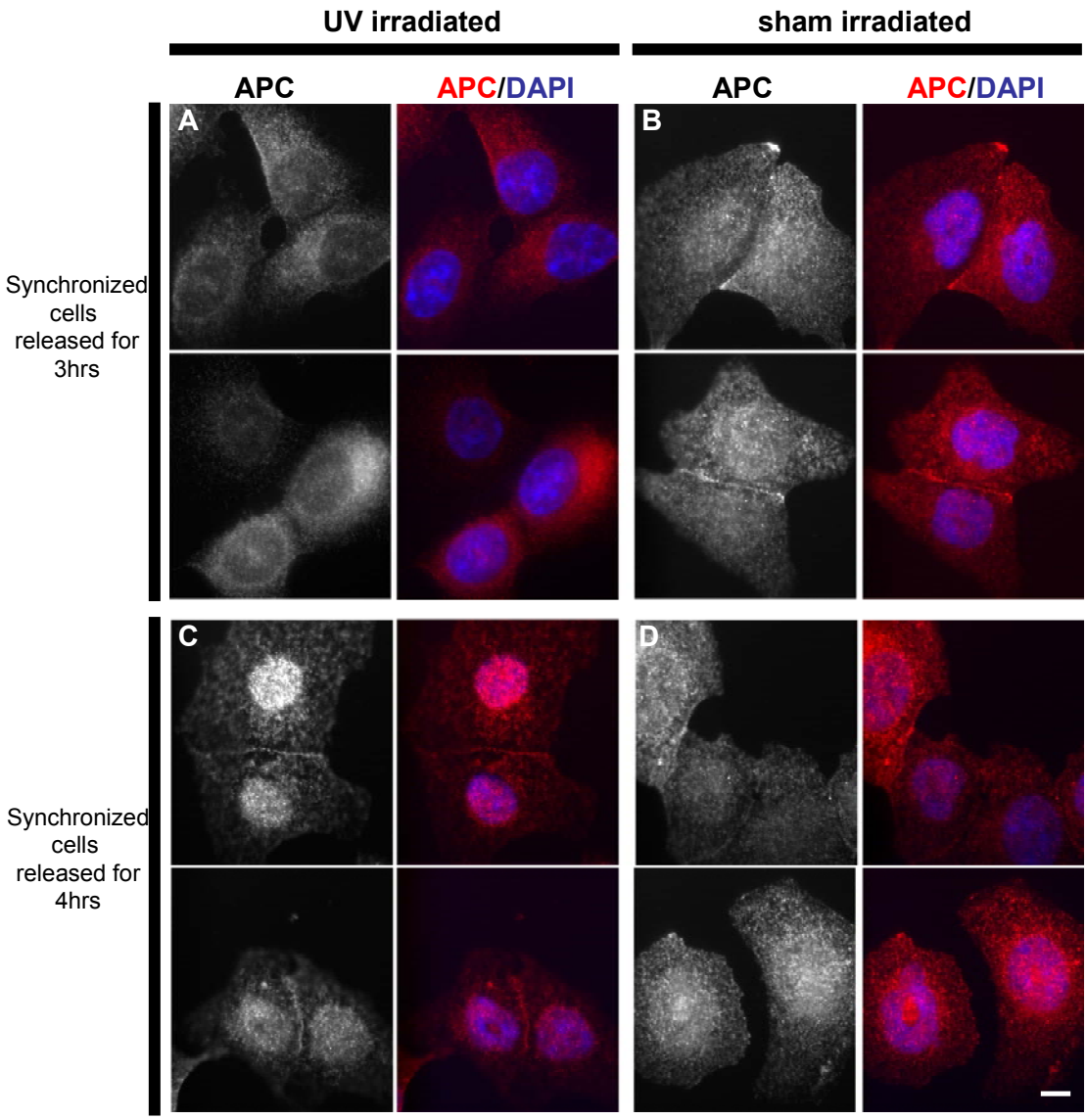

Figure 5.2
APC distribution in cells synchronized by aphidicolin block and released for 3 or 4 hours prior to UV-irradiation or sham-irradiation. Cells were fixed 40 minutes after irradiation and stained with rabbit anti-APC M2 antibody. DNA was visualized with DAPI. Images were taken with a Zeiss inverted fluorescent microscope equipped with an Olympus camera and analyzed using *Magnafire* software. Scale bar = 3μm.

At the time of fixation, cells that were in G_0 and quiescent, or cells in G_1 that had recently undergone division and had not yet re-entered the cell cycle would contain a single copy of the genome (4). G_2 cells and M-phase cells, that had replicated their DNA but had not completed cell division contained two full copies of the genome (4). When stained with propidium iodide, cells in G_2/M fluoresce at twice the intensity of the cells in the G_0/G_1 phases of the cell cycle . Cells in S-phase contain a full copy of the genome as well as a partially replicated portion of the genome. The S-phase cells therefore emit an intermediate amount of fluorescent signal, more intense than the G_0/G_1 cells but less intense than the G_2/M cells. Cells in late S-phase are expected to have fluorescent intensities that approach cells in G_2/M. The intensity of the propidium iodide staining was determined in 10,000 cells for each time point using a flow cytometer. In this device, cells are pulled single-file past a detector which records the intensity of the fluorescent signal being emitted (28). The cell intensities were displayed as histogram plots in which relative propidium iodide intensity was expressed on the x-axis and the number of cells was expressed on the y-axis (Figure 5.3).

The unsynchronized HCT116βw cells displayed a typical cell cycle distribution (Figure 5.3). A little over one third of the cell population resided in a concise peak representing the G_0/G_1 cells. A slightly smaller peak with twice the relative fluorescent intensity represented the G_2/M cells. Between these two peaks were the cells in the various points of S-phase. Because the drug aphidicolin blocks polymerase activity, the cells that had already entered S-phase were halted there.

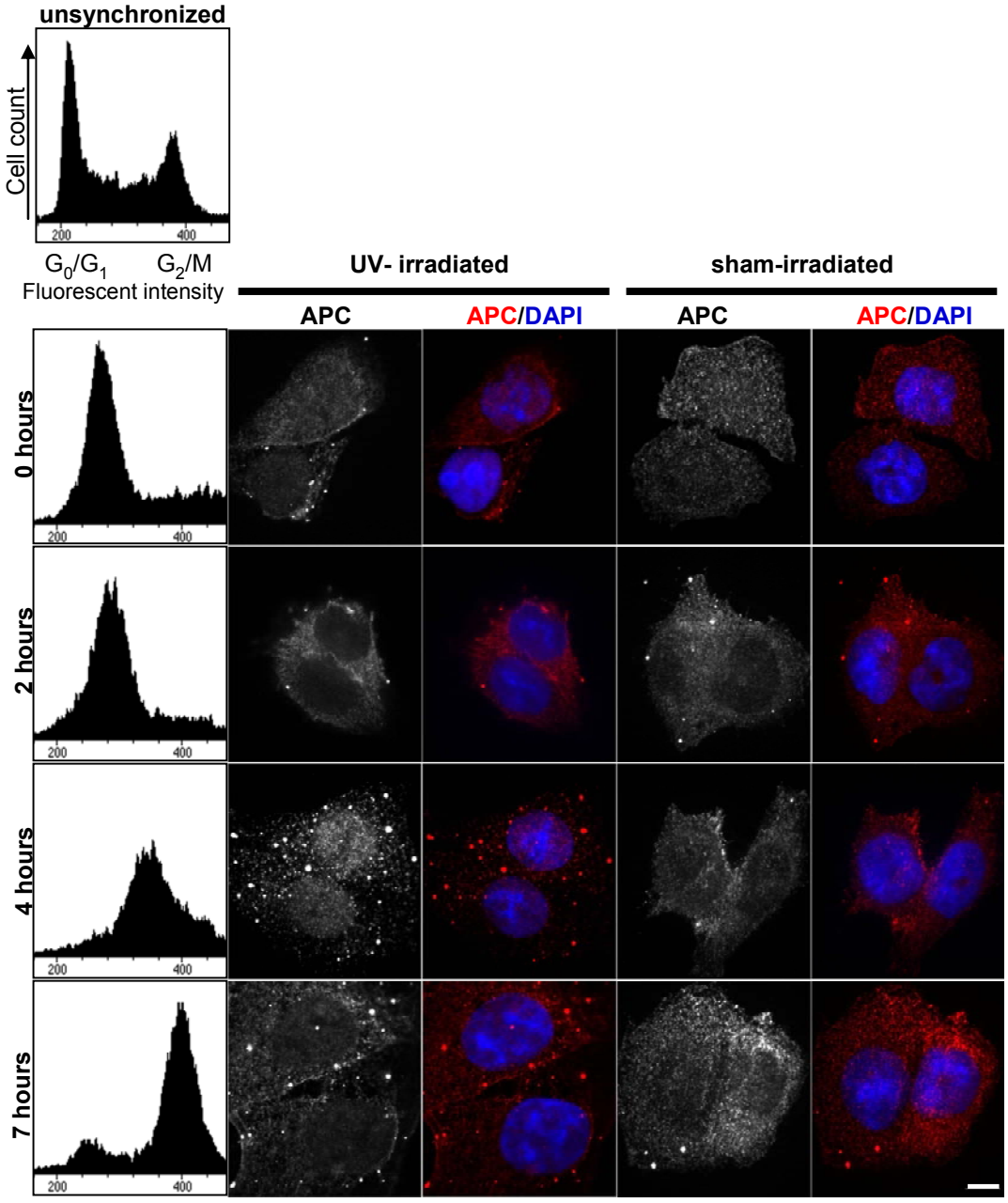

Figure 5.3
Analysis of APC distribution in UV-irradiated and sham-irradiated cells at various points of the cell cycle. Cells were synchronized using aphidicolin block and released for the indicated amount of time before being UV/sham-irradiated or processed for FACs analysis. Cells for images were fixed 40 minutes after irradiation and stained with rabbit anti-APC M2 antibody. DNA was visualized with DAPI. Images were taken with an Olympus 3I spinning disc confocal TIRF inverted microscope and analyzed using *Slidebook* software. Scale bar = 3μm.

Cells that were in the G_0/G_1 or G_2 phases of the cell cycle when aphidicolin was introduced would be expected continue to cycle until they reached the beginning of S-phase. In the cells that were released for 0 hours following aphidicolin block, a small number of cells were observed in mid and late S-phase; however, as expected, most of the cells accumulated in a peak representing the beginning of S-phase (Figure 5.3). Two hours after aphidicolin was removed, cells were observed to be in S-phase and the peak population of cells had shifted to the right signifying that synthesis of DNA had resumed in all cells (Figure 5.3). Four hours after cells were released from aphidicolin block the peak population of cells was again shifted to the right (Figure 5.3). Using the relative intensities observed in asynchronous cells for comparison, these cells appeared to straddle the late S-phase to G_2 and M phases of the cell cycle. In the cells that were released from aphidicolin block for 7 hours the main peak of cells appeared in G_2/M. These cells have two full copies of the genome and were likely committed to undergoing mitosis. Some of the cells were also observed to have completed cell division, as a small peak was visible representing a G_0/G_1 population of cells (Figure 5.3).

APC localization at 0, 2, 4 and 7 hours following release from aphidicolin block confirmed that nuclear accumulation was only observed when cells were UV treated at the 4 hour time point. At all other points in the cell cycle, APC was both nuclear and cytoplasmic or predominantly cytoplasmic following UV irradiation. APC has previously been implicated in control of the G_2/M checkpoint (13, 14). Upregulation of endogenous full length APC by zinc treatment or exogenous

expression of specific APC protein fragments have been shown to induce cell cycle arrest in G_2 (13, 14). Our results are consistent with a proposed role for APC in the G_2/M transition.

Alternate pathway implicated in nuclear import of APC

Classical import through the nuclear pore complex requires a cargo protein that carries an NLS as well as the function of importin-α and importin-β (29). Importin-α binds directly to the NLS(s) of the cargo protein in the cytoplasm and facilitates the interaction with importin-β. Importin-β docks to the nuclear pore complex where an energy-dependent, Ran-dependent translocation moves the importin-α/importin-β/cargo complex from the cytoplasm to the nucleus through the nuclear pore (29). APC contains two characterized monopartite NLSs (Figure 2.5) (30, 31). It was assumed that the nuclear cytoplasmic shuttling of full length WT APC occurred predominantly through the NLS/importin pathway. However, the localization of APC to the nucleus of UV irradiated cells is unlikely to occur through the interaction between the APC NLSs and importin-α for two reasons. First, the redistribution of APC to the nucleus following DNA damage was observed in homozygous mutant APC mNLS MEF cells. In these cells both *Apc* alleles express a mutant APC protein that lacks functional NLSs and therefore should be unable to interact with importin-α. Second, several types of cell stresses including starvation, heat shock, ethanol, oxidative stress and UV irradiation result in inhibition of classical nuclear import (32, 33). It has been demonstrated that UV irradiation

induces the nuclear accumulation of importin-α, which suppresses nuclear import of NLS bearing proteins. Because dramatic nuclear accumulation of APC was observed in cells lacking both APC NLSs and available importin-α, we assume that a novel method of nuclear import mediates nuclear APC relocalization following UV treatment.

Import of APC through this novel pathway is selectively accessible: the cell cycle stage dictates whether APC is translocated into the nucleus by this as yet uncharacterized mechanism for nuclear entry. APC was observed to localize to the nucleus after UV irradiation in cells that were at the end of S or in the G_2-phase of the cell cycle (Figure 5.3). However, cells in other phases of the cell cycle often showed a decreased level of nuclear APC (Figures 5.2 and 5.3). The stress induced block of classical nuclear import was likely the reason for the cytoplasmic accumulation of APC in the majority of the UV irradiated cells. In both APC mNLS$^{-/-}$ MEF cells and intestinal tissue of the APC mNLS$^{-/-}$ mice, when importin-α mediated nuclear entry is inhibited, APC accumulates around the nuclear envelope (Figure 5.4).

APC does not relocate in response to double-strand DNA breaks

Other proteins have demonstrated the ability to enter the nucleus despite a cell-stress-mediated block of nuclear import. Heat shock cognate protein 70 (hsc70) has been shown to localize to the nuclear compartment in response to cellular heat stress (34, 35). However, hsc70 enters the nucleus in response to cellular stress in unsynchronized HeLa cells, suggesting that the reaction is not cell cycle specific (34).

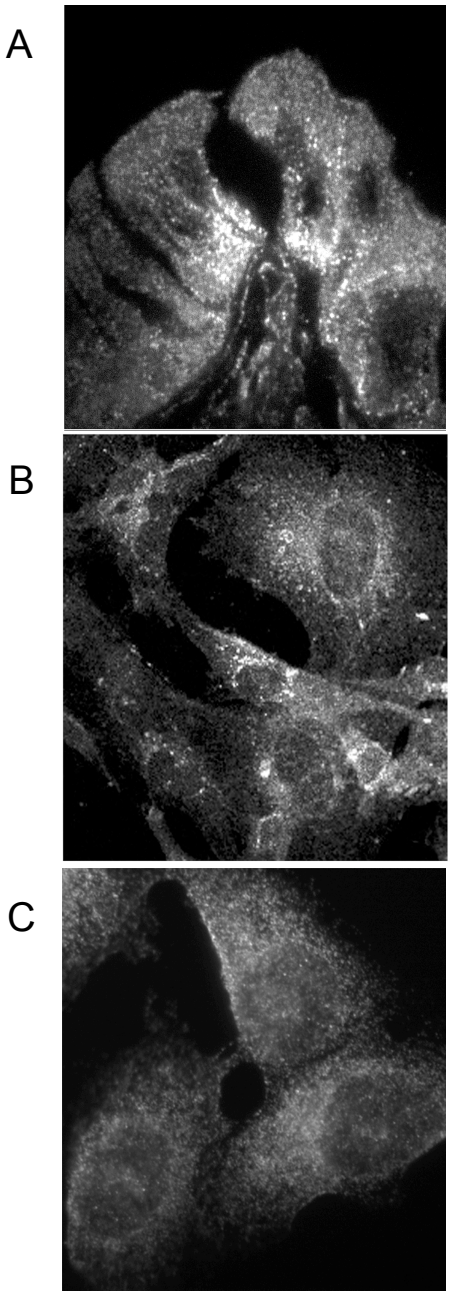

Figure 5.4
A comparison of APC distribution in cells/tissue in which APC NLS/importin-α import is suspected to be blocked. A) Intestinal epithelia from the colon of APC mNLS-/-. B) APC mNLS-/- MEF cells. C) HCT116βw cells UV irradiated 3 hours after release from aphidicolin block

The observation that APC is not translocated to the nucleus during a majority of the cell cycle and dramatically accumulates in the nucleus at the late S and G_2 phases implies that APC may have a specific role in the nucleus at this time. It is possible that APC performs a specific task in the G_2/M DNA damage checkpoint. Alternatively, APC may play a role in the homologous repair of DNA double-strand breaks. Generally double-strand DNA breaks are produced by ionizing radiation while UV irradiation is associated with pyrimidine dimer formation (3). However, during DNA replication, UV-induced DNA lesions can result in stalled replication forks which can lead to double-strand breaks (36). If the nuclear accumulation of APC is a response to a specific type of DNA damage, in this case double-strand breaks, an increased level of UV-induced double strand breaks in late S-phase may create the appearance of cell cycle specificity. To determine if APC accumulation in the nucleus was in response to double strand breaks, unsynchronized HCT116βw cells were exposed to ionizing radiation to induce DNA double-strand breaks in cells of all phases of the cell cycle.

One of the earliest cellular events associated with DNA double-strand breaks is a serine phosphorylation of the histone H2A variant H2AX to create γH2AX. γH2AX accumulates at sites of DNA damage within minutes of exposure to ionizing radiation (37). An antibody to γH2AX was used to verify that double-strand breaks had occurred following exposure to γ-irradiation and to serve as a marker for the location of the repair foci. As expected, there was little visible γH2AX in un-irradiated HCT116 cells (Figure 5.5). In contrast the HCT116 cells that were exposed

to γ-irradiation displayed prominent nuclear staining of γH2AX, which localized to sub-nuclear foci (Figure 5.5). APC localization was examined 20, 40 and 60 minutes after γ-irradiation. In the irradiated cells, APC displayed both a nuclear and cytoplasmic distribution that was indistinguishable from the non-irradiated control cells. Furthermore, the APC staining that was visible in the nucleus did not coincide with the γH2AX marker for double stand break repair foci (Figure 5.5).

While these results do not rule out the possibility that APC plays a role in some aspect of the cellular response to DNA double strand breaks, they support that UV induced double-strand breaks are not the reason for the nuclear targeting of APC. It is therefore more likely that the observed accumulation of APC in the nuclear compartment is specific to a mechanism involved in G_2/M checkpoint of the cell cycle.

APC localization to the nucleus is transient

Importin-α localizes to the nucleus within 30 minutes of UV irradiation (32). If the nuclear accumulation of APC precedes the nuclear accumulation of importin-α, it is possible that the classical nuclear import pathway may still play a role in the nuclear targeting of APC. To evaluate how long APC is targeted to the nucleus, synchronized HCT116βw cells were exposed to UV irradiation and fixed at different time intervals following UV exposure. APC localization in cells that were fixed 20 and 30 minutes after UV irradiation revealed a nuclear and cytoplasmic localization pattern that did not differ significantly from APC in the sham-irradiated control cells

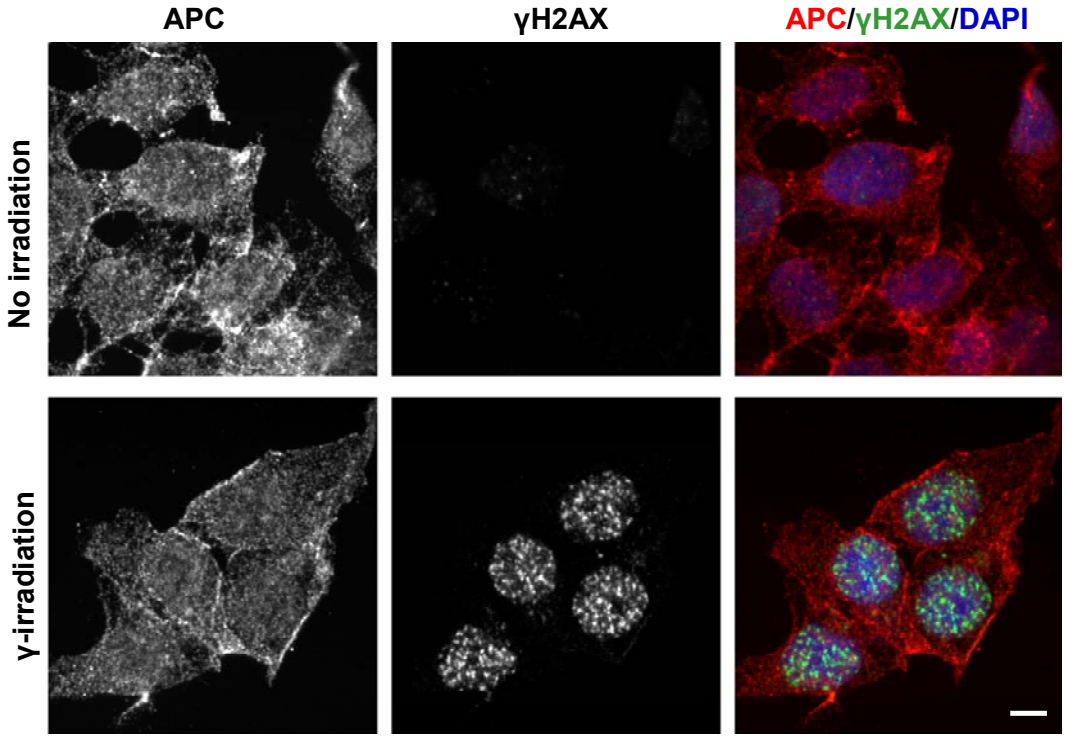

Figure 5.5
APC distribution in HCT116 cells exposed to ionizing-irradiation. Unsynchronized HCT116βw cells were exposed 10Gy of γ-irradiation to induce DNA double-strand breaks. Cells were fixed 40 minutes (above) and 60 minutes (data not shown) after irradiation and stained with rabbit anti-APC M2 and mouse anti-γH2AX (to visualize DNA double-strand breaks) DNA was visualized with DAPI. Images were captured using a Nikon TU2000 microscope equipped with a Letiga EXI camera (Q Imaging) and analyzed using *Phylum Live* software. Scale bar = 3μm.

(Figure 5.6). It was not until 40 minutes after UV irradiation that APC was observed to be targeted to the nucleus. APC was observed to reach a maximal level of nuclear accumulation approximately 40 minutes following exposure to UV (Figure 5.6). One hour after UV irradiation, APC appeared to be redistributed back to the cytoplasm in most cells (Figure 5.6).

APC did not accumulate in the nucleus until 40 minutes after UV irradiation. Importin-α is reported to be completely translocated to the nuclear compartment prior to 40 minutes following cellular stress implying that cytoplasmic importin-α would be unavailable to bind to and facilitate the nuclear targeting of APC (32). The targeting of APC to the nucleus that we observed in cells treated with UV light was also transient. The nuclear accumulation of APC was only clearly seen during a short window of time, between 30 and 50 minutes following exposure to UV irradiation.

APC localization to the nucleus occurs only in sub-confluent cells

In the course of characterizing the accumulation of nuclear APC in cells exposed to UV light, it became clear that the cellular density at the time of UV exposure influenced the response of APC. Cells exhibited far less nuclear accumulation of APC when grown more densely on the coverslips prior to UV irradiation. In completely confluent cultures, there was often no visible nuclear accumulation of APC in any of the cells. Cultures approaching confluency often displayed nuclear targeted APC only at the periphery of the slide where cells were the least dense (Figure 5.7). Initially it was hypothesized that more confluent cultures did

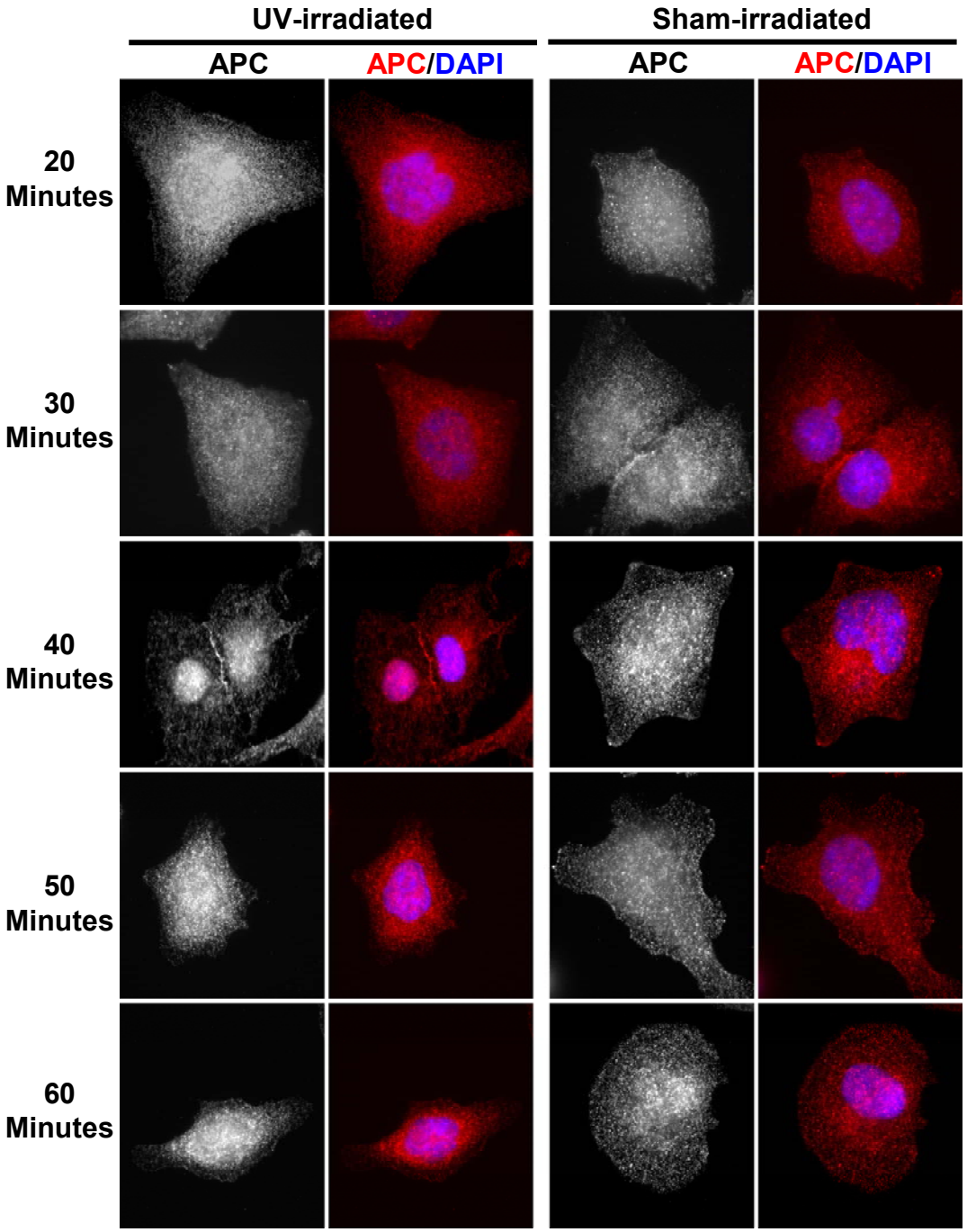

Figure 5.6
Analysis of APC distribution in UV-irradiated and sham-irradiated cells at various points following irradiation. Cells were synchronized using aphidicolin block and released 4 hours before being UV/sham-irradiated. Cells for images were fixed the indicated amount of time following irradiation and stained with rabbit anti-APC M2 antibody. DNA was visualized with DAPI. Images were captured on a Nikon TU2000 microscope equipped with a Letiga EXI camera (Q Imaging) and analyzed using *Phylum Live* software. Scale bar = 3µm.

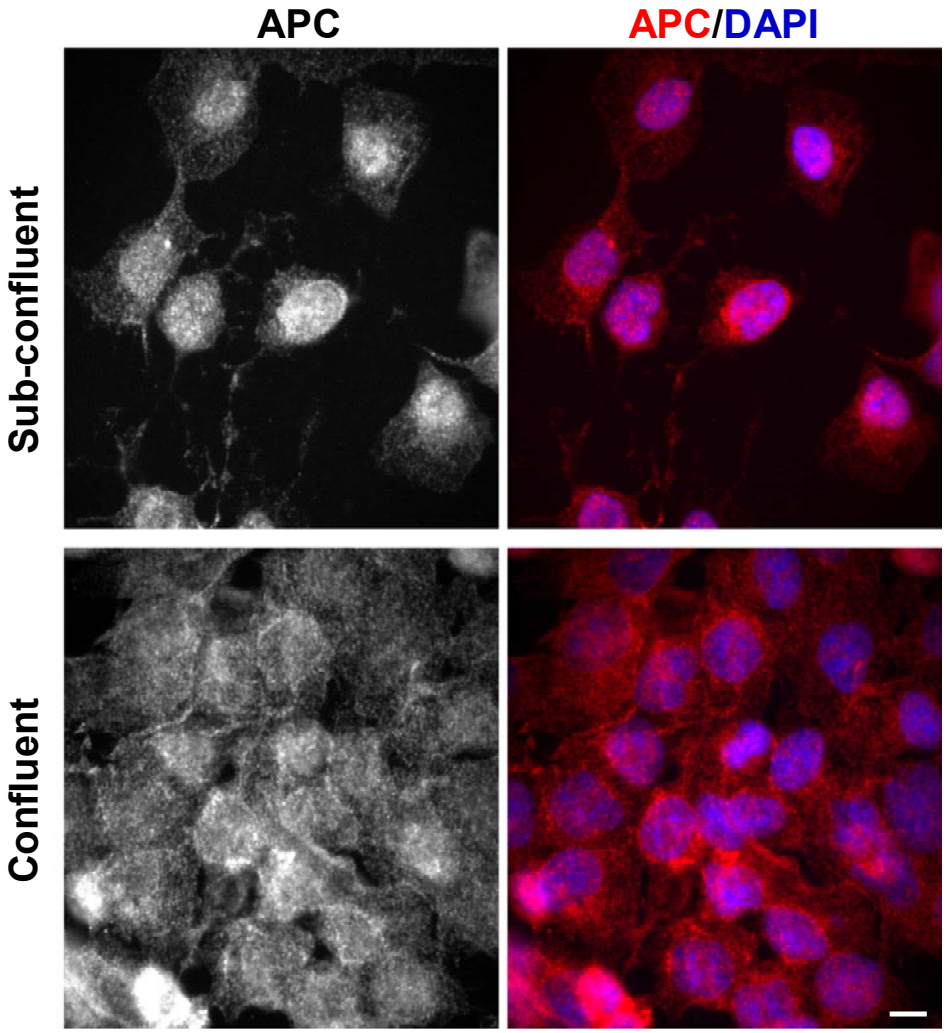

Figure 5.7
APC distribution in confluent and sub-confluent cells. Images of cells from different regions of the same 22x22mm glass coverslip. Cells were synchronized by aphidicolin block and released for 4 hours prior to UV-irradiation. Cells were fixed 40 minutes after irradiation and stained with rabbit anti-APC M2 antibody. DNA was visualized with DAPI. Scale bar = 7μm.

not synchronize as well as sub-confluent cultures or that confluent cells did not resume progress through the cell cycle at the same rate as sub-confluent cells. However it was observed using flow cytometry that aphidicolin treated cells did synchronize, even when cells were confluent (data not shown).

The nuclear localization of APC was previously observed to be affected by cell density (38). However, it was determined that increased cell density altered phosphorylation of the APC NLSs leading to increased nuclear translocation through the importin-α pathway (38). Because it is probable that UV induced nuclear import occurs through an importin-α-independent pathway, this previously described mechanism of cell density controlled nuclear targeting is not necessarily applicable. However, this does not rule out the possibility that similar post-transcriptional modifications to the APC protein also mediate the nuclear accumulation of APC following UV irradiation. The hsc70 protein has been shown to accumulate in the nuclear compartment of HeLa cells following heat shock through an NLS/importin independent mechanism (35). The nuclear targeting of hsp70 was also inhibited in confluent cells (34), further supporting a cell density regulated modification of stress related nuclear import.

APC displays a mobility shift following UV irradiation

In an attempt to better define a function for nuclear targeted APC, APC was immunoprecipitated (IP) from the lysates of cells that had been exposed to UV irradiation. Western blots revealed that nearly all of the APC in the lysates from both

the UV irradiated cells and the non-irradiated control cells immunoprecipitated with beads conjugated to a specific anti-APC antibody while little to no APC could be detected in the protein eluted from the IgG-conjugated control beads (data not shown).

The western blot of APC from non-irradiated control cells produced the expected band at 312 kDa representing full length APC (Figure 5.8). This was not the case for the cells exposed to UV irradiation. APC antibody detected a band from UV irradiated cell lysates that migrated slower than the full length APC from non-irradiated cells. It appeared that APC from the lysate of UV-irradiated cells was immobilized in the well and at the interface between the stacking gel and the resolving gel (Figure 5.8). When proteins were resolved on a 4-12% gradient gel to eliminate the stacking gel interface, two distinct APC bands could be resolved in the UV-irradiated lysate (Figure 5.9). Cell lysates from the UV-irradiated cells were treated with DNase, RNase, shrimp alkaline phosphatase or all three enzymes to determine if the observed APC mobility shift was due to a specific interaction stimulated by UV-induced DNA damage. The mobility shift of APC could not be completely reversed with any of the treatments (Figure 5.9).

To determine if the observed mobility shift occurred specifically in cells that displayed APC accumulation in the nucleus, cell lysates were prepared from cells that were UV or sham-irradiated either 2 or 4 hours after release from aphidicolin. Cells released from aphidicolin block for two hours were predominantly in early S-phase and showed no nuclear accumulation of APC when exposed to UV light (Figure 5.3).

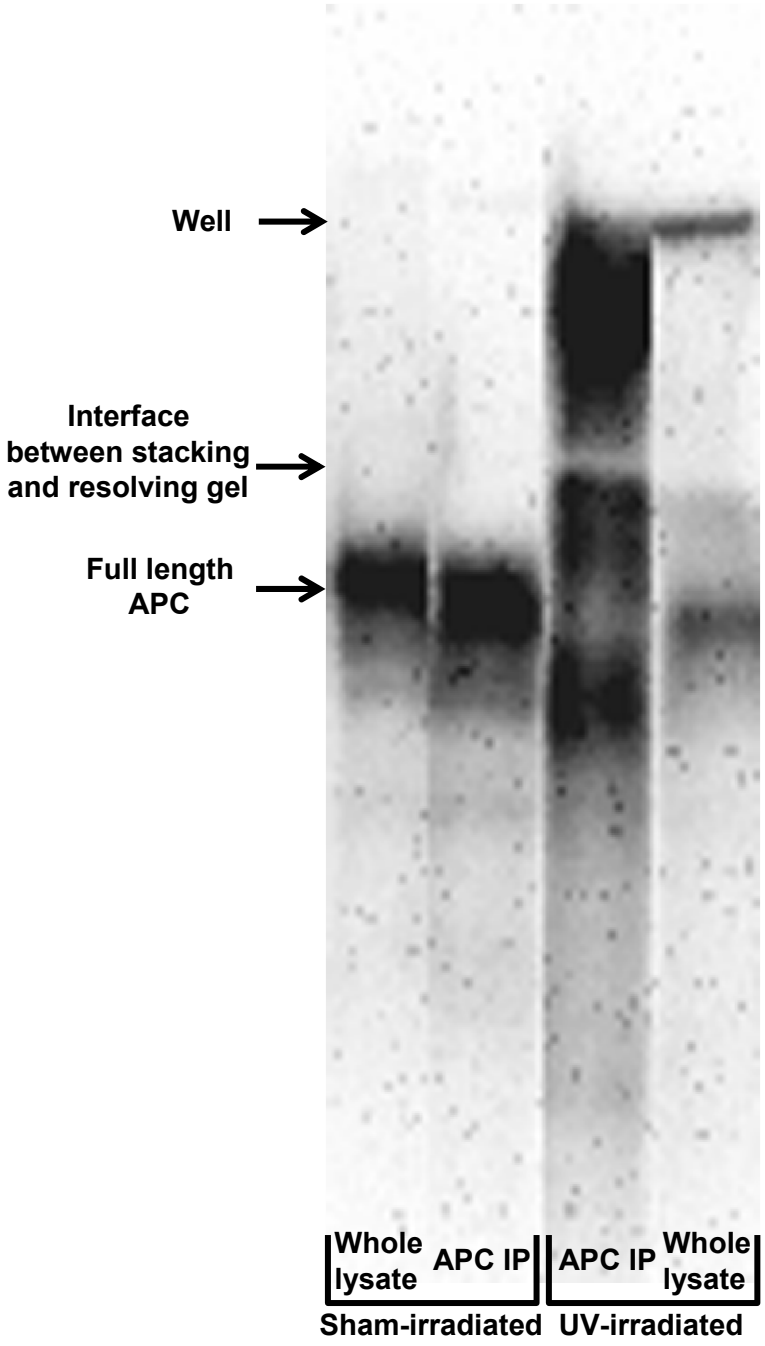

Figure 5.8
Western immunoblot probed with rabbit anti-APC M2 antibody. HCT116βw cells were synchronized using aphidicolin block and released for 4 hours prior to sham or UV-irradiation. Cell lysates were prepared 40 minutes after irradiation. IP was preformed with protein A beads conjugated to APC specific antibody (rabbit anti-APC M2). Proteins were resolved on a 7% polyacrylimide gel with a 3% stacking gel.

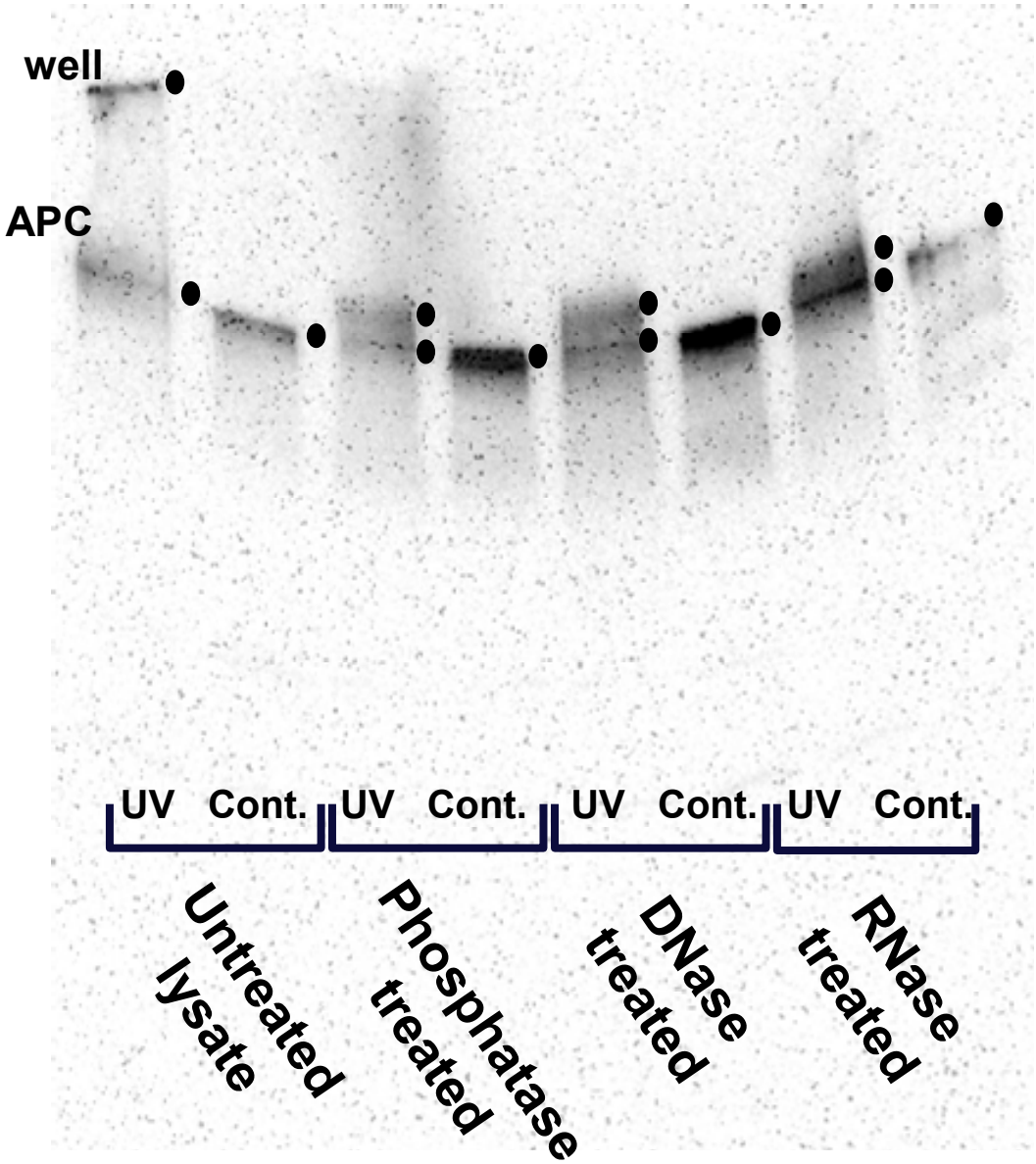

Figure 5.9
Western immunoblot probed with rabbit anti-APC M2 antibody. HCT116βw cells were synchronized using aphidicolin block and released for 4 hours prior to sham or UV-irradiation. Cell lysates were prepared 40 minutes after irradiation and resolved on a 4-12% gradient gel. Lysates were treated with 2μL of shrimp alkaline phosphatase (Roche), DNase (Invotrogen) or a 10mg/mL stock of RNase A in a 25μL volume on ice for 30 minutes.

Western blot analysis of lysates from cells irradiated following a two hour release from aphidicolin block revealed a mobility shift for APC that was identical to the shift observed when cells were irradiated 4 hours after release from aphidicolin block (Figure 5.10). The observation that the mobility shift was not limited to the G_2/M phase of the cell cycle suggests that this APC modification is unrelated to the nuclear targeting of APC. Furthermore, when control cell lysate from the non-irradiated cells was exposed to UV light, the 312 kDa APC band displayed the same mobility shift seen in lysates from UV irradiated cells (Figure 5.10). The observation that APC mobility is shifted in the absence of intact cells and in the absence of intact DNA implies that the observed shift is an artifact of UV irradiation rather than a specific interaction due to the cellular response to DNA damage. It is possible that APC formed a UV-induced crosslink to another cellular molecule upon exposure to UV light. Another possibility is that a UV-crosslink was induced within the polypeptide chain of APC and prevented APC from completely denaturing prior to being loaded on the gel. The mobility shift of APC in response to UV irradiation is previously unreported and currently uncharacterized.

It is important to note that whatever induces the observed APC mobility shift also occurs in the cells in which APC nuclear accumulation is observed. Because the nature of the mobility shift is undefined, the effect on the cellular function of APC is unknown. If amino acid residues were cross-linked within the APC polypeptide chain, there may have been no resulting alteration in the globular structure. This type

of modification could, in theory, have resulted in little to no cellular effect. It is unlikely

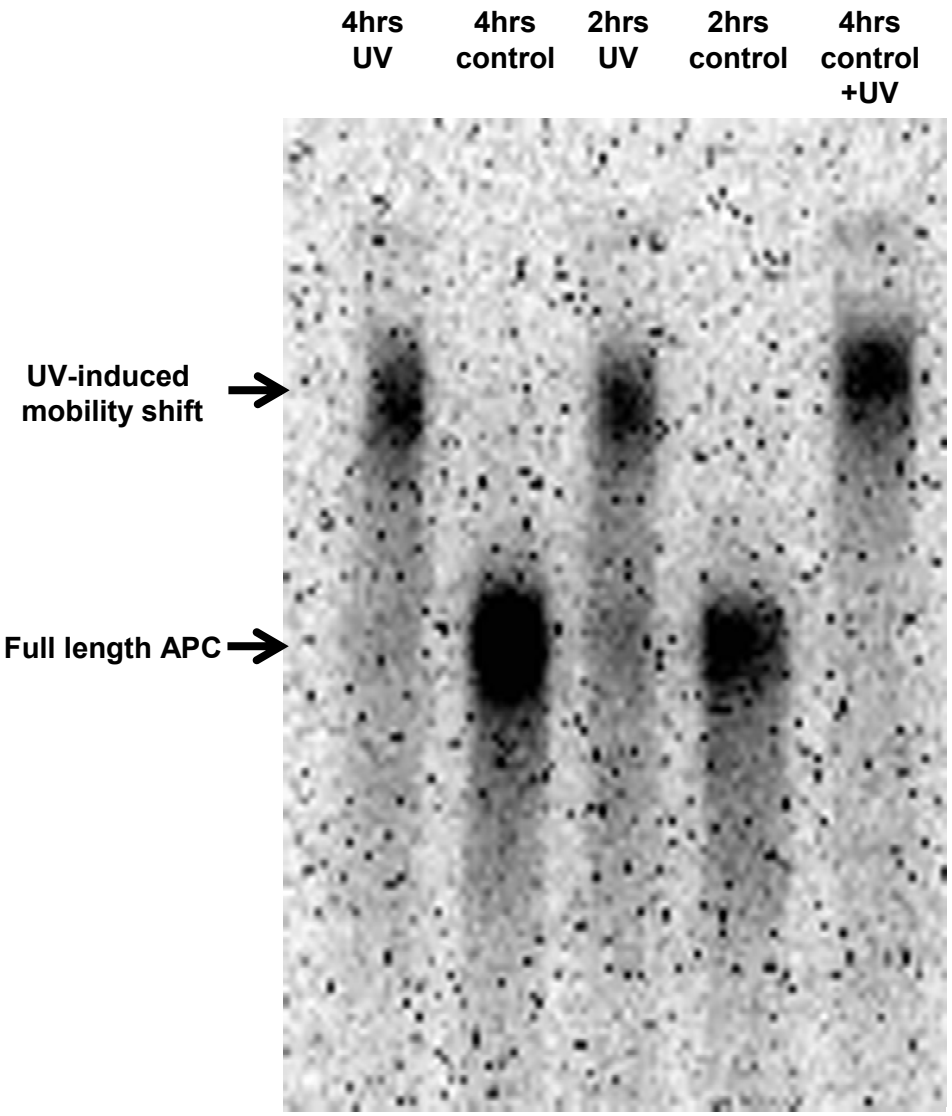

Figure 5.10
Western immunoblot probed with rabbit anti-APC M2 antibody. HCT116βw cells were synchronized using aphidicolin block and released for 4 hours prior to sham or UV-irradiation. Cell lysates were prepared 40 minutes after irradiation and resolved on a 4-12% gradient gel. An immunoblot of cell lysates from synchronized cells released from aphidicolin block for 2 or 4 hours. Probed with rabbit anti-APC M2 antibody. Lysate from cells that were UV irradiated 2 or 4 hours after aphidicolin release demonstrate the APC mobility shift. An aliquot of control lysate from the cells released from aphidicolin block for 4 hours and UV irradiated on a glass slide demonstrates the same APC mobility shift as the APC from cells that were UV irradiated.

that the nuclear accumulation of APC induced by UV irradiation results from this non-specific modification because, unlike the observed nuclear targeting, the change in mobility showed no cell cycle specificity. The APC mobility shift was observed in cells UV irradiated 2 and 4 hours after aphidicolin release while the nuclear accumulation of APC is specific for the 4 hour time point. Because there was no evidence for a connection between the UV induced mobility shift and the UV/cell cycle specific nuclear accumulation of APC, the nature of the mobility shift was not further examined.

APC binding to β-catenin does not appear altered by UV irradiation

In the non-irradiated control cells, β-catenin was consistently observed to co-precipitate with APC (Figure 5.11). β-catenin is a well characterized APC binding partner so this interaction was expected. In all immunoprecipitation experiments, protein was eluted from the antibody conjugated beads in one-tenth of the original lysate volume and equal volumes of the bound and unbound samples were loaded for SDS-PAGE and western blot analysis. Therefore, the protein in the "IP" lanes should be ten times more concentrated than it was in the "unbound" fraction. The intensity of the β-catenin band that co-precipitated with APC was observed to be approximately equal to the intensity of the β-catenin band in the fraction that did not co-precipitate with APC. Taking into account the relative concentrations of these two fractions, we determined that approximately one tenth of the total β-catenin in the cell was interacting with APC. Surprisingly there was no significant difference between

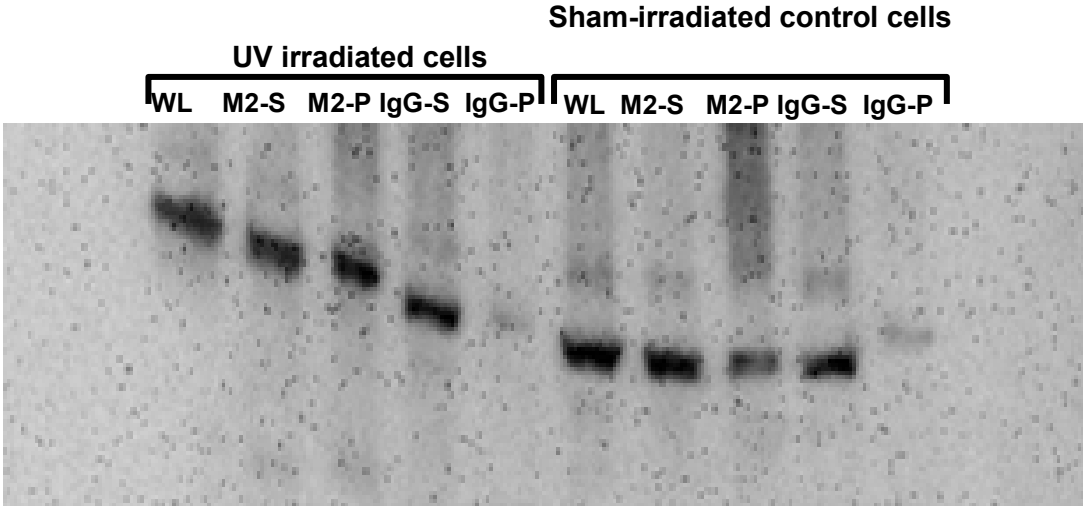

WL = whole lysate
M2-S = unbound supernatant
M2-P = co-precipitated with APC
IgG-S = unbound super from control beads
IgG-P = co-precipitated with IgG control

Figure 5.11
Western immunoblot probed with rabbit anti-β-catenin antibody. HCT116βw cells were synchronized using aphidicolin block and released for 4 hours prior to sham or UV-irradiation. Cell lysates were prepared 40 minutes after irradiation. IP was preformed with protein A beads conjugated to APC specific antibody (rabbit anti-APC M2). Protein was eluted from the beads in 1/10th the volume of the original lysate. Proteins were resolved on a 4-12% gradient gel.

the amount of β-catenin that co-precipitated with APC from UV irradiated cells versus non-irradiated control cells. We had anticipated that a dramatic shift in the localization of APC would result in a similarly dramatic change in the observed protein interactions; however, at least in the case of β-catenin, no such alteration is induced. APC and β-catenin continue to interact at the same level before and after UV irradiation.

The transient localization of APC to the nucleus is mirrored by β-catenin

Co-immunoprecipitation experiments suggested that APC and β-catenin may continue to interact during the nuclear accumulation of APC. To ascertain if β-catenin is also influenced by exposure to UV light, synchronized cells were UV irradiated and co-stained with antibodies to APC and β-catenin. In the non-irradiated control cells, APC and β-catenin did not show substantial co-localization (Figures 5.12). Like APC, β-catenin was also observed in the nuclear and cytoplasmic compartments (Figures 5.12). In UV irradiated cells, however, β-catenin displayed the same nuclear accumulation that was observed for APC (Figures 5.12). Furthermore, β-catenin demonstrated a transient nuclear localization similar to the time course of nuclear accumulation observed for APC (Figure 5.13). However, despite the observation that APC and β-catenin both accumulated in the nucleus, they did not seem to do so as a complex. Western blots did not reveal an increased level of β-catenin co-precipitating with APC in the UV-irradiated cell

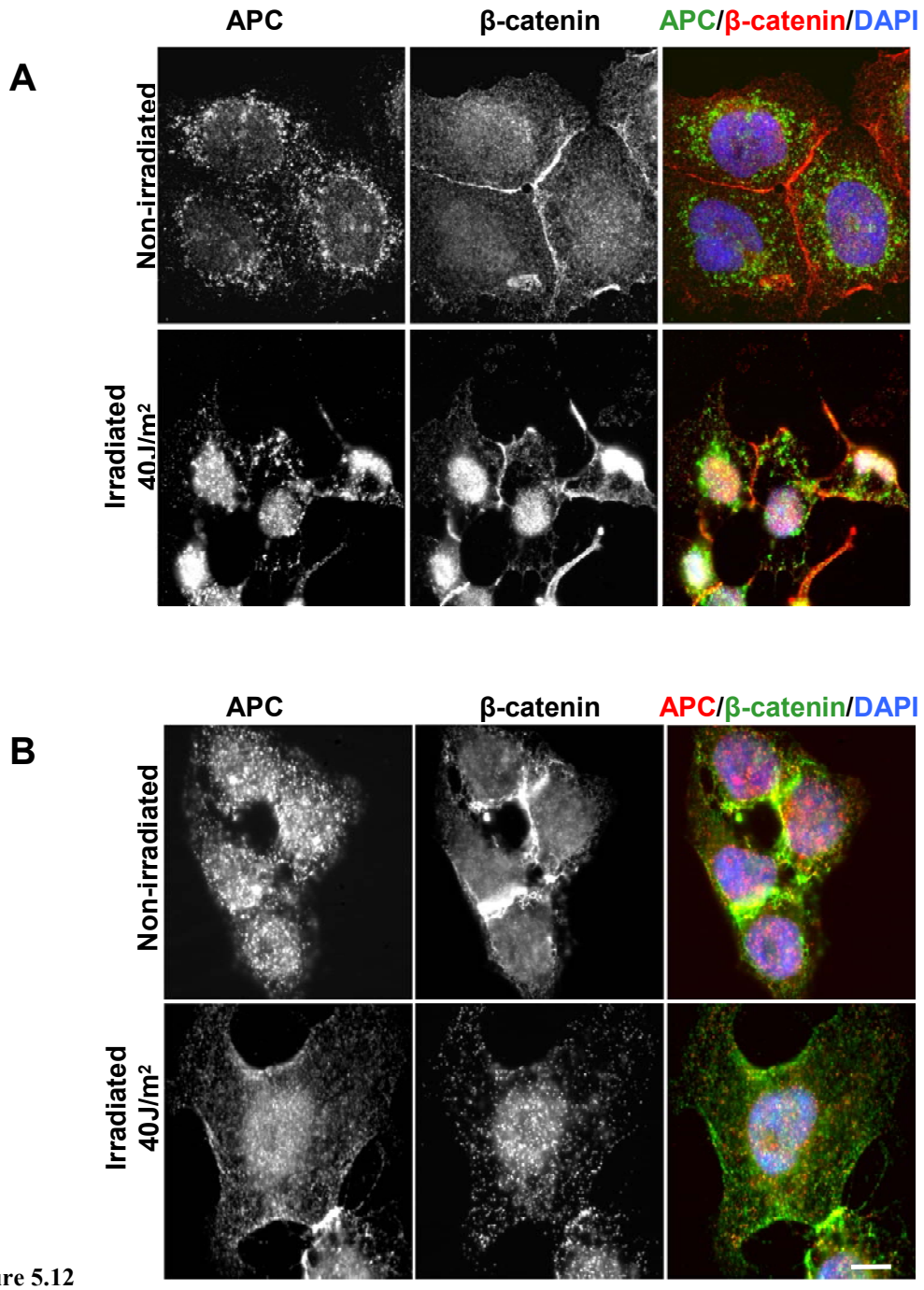

Figure 5.12
The co-localization of APC and β-catenin in irradiated and non-irradiated cells using two sets of antibodies. A) Mouse anti-APC (12-28, Abcam) and rabbit anti-β-cateinin (Sigma). B) Rabbit anti-APC M2 (developed in the Neufeld and Azuma labs) and mouse anti-β-catenin (Transduction Laboratories). Cells were synchronized using aphidicolin block and released for 4 hours before being UV/sham-irradiated. Cells for images were fixed 40 minutes after irradiation and stained. Scale bar = 3μm.

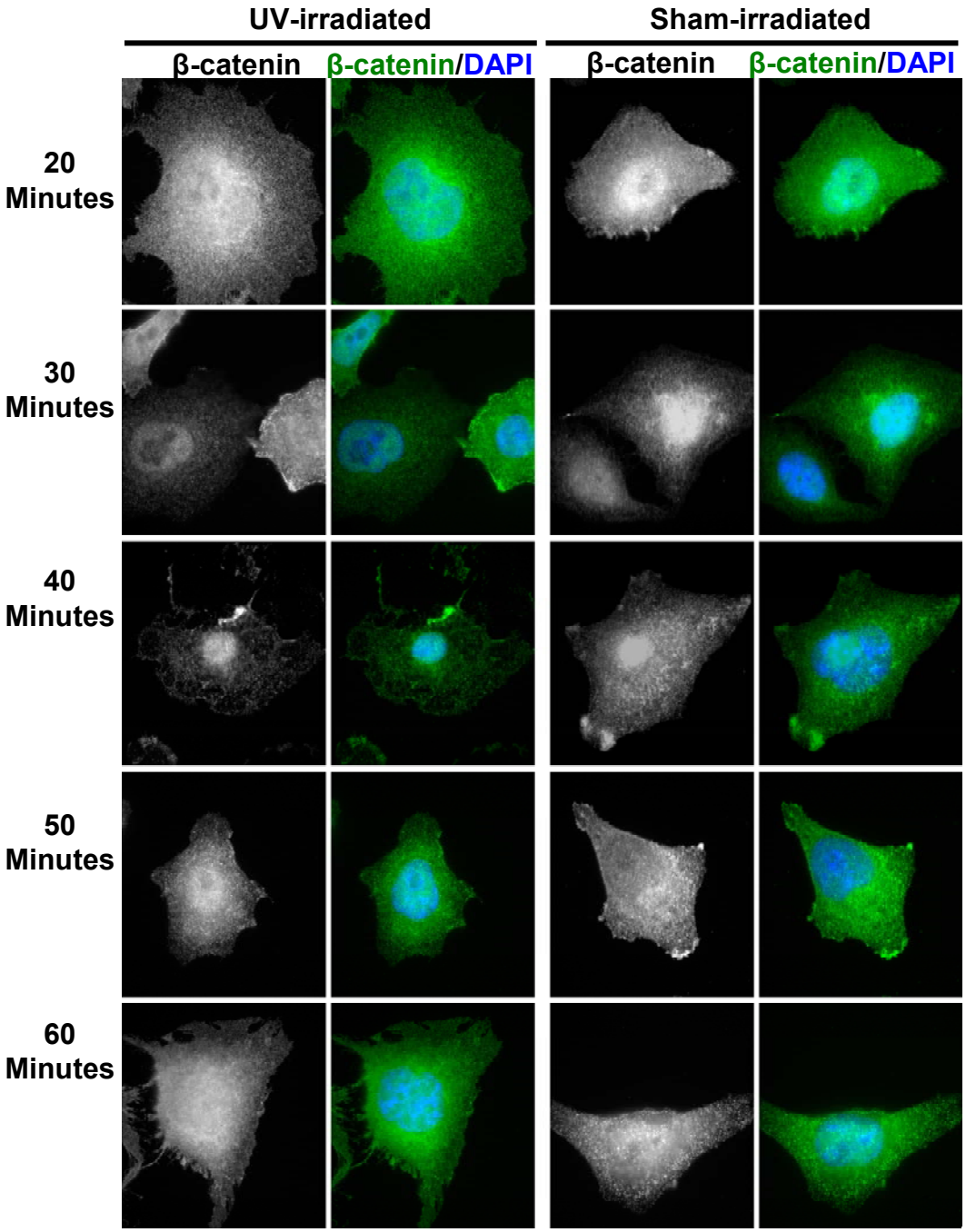

Figure 5.13
Analysis of β-catenin distribution in UV-irradiated and sham-irradiated cells at various points following irradiation. Cells were synchronized using aphidicolin block and released 4 hours before being UV/sham-irradiated. Cells for images were fixed the indicated amount of time following irradiation and stained with mouse anti-β-catenin antibody. DNA was visualized with DAPI. Images were captured on a Nikon TU2000 microscope equipped with a Letiga EXI camera (Q Imaging) and analyzed using *Phylum Live* software. Scale bar = 3μm.

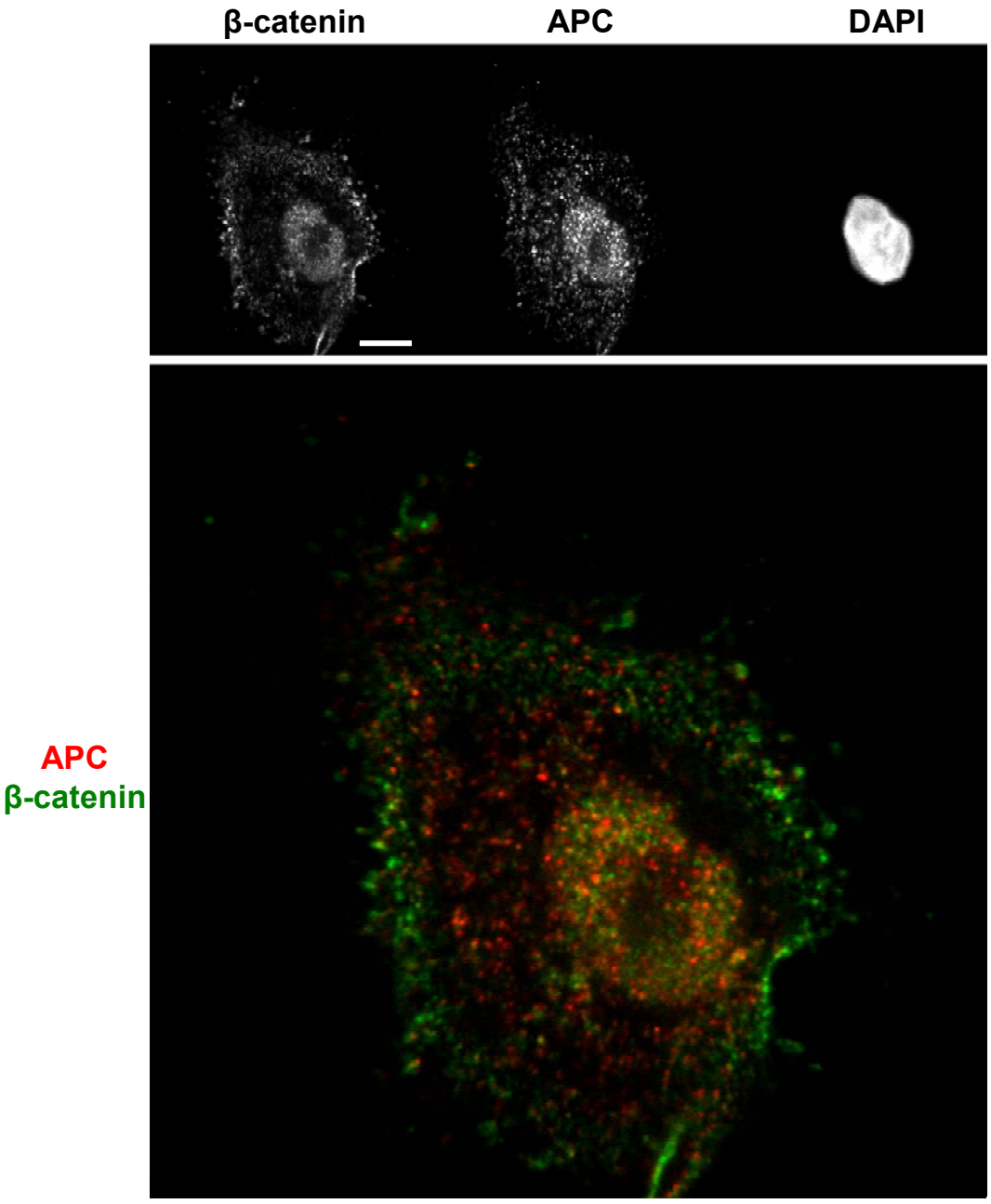

Figure 5.14
Optical slices of APC and β-catenin distribution in the nucleus of a UV-irradiated cell. Cells were synchronized using aphidicolin block and released for the indicated amount of time before being UV-irradiated. Cells were fixed 40 minutes after irradiation and stained with rabbit anti-APC M2 antibody and mouse anti-β-catenin. DNA was visualized with DAPI. Images were taken with an Olympus 3I spinning disc confocal TIRF inverted microscope and analyzed using *Slidebook* software. Scale bar = 3μm.

lysates (Figure 5.11) and optical slices through UV irradiated cells showed numerous distinct APC and β-catenin puncta within the nucleus (Figure 5.14).

Optimal nuclear localization of APC requires checkpoint kinase activity

Members of the phosphatidylinositol-3-kinase (PI-3-K) family of kinases are key initiators of the G_2/M checkpoint. These kinases, including DNA-dependent protein kinase (DNA-PK), Ataxia-Telangiectasia mutated (ATM) and Ataxia-Telangiectasia mutated and RAD3-related (ATR) are responsible for the activation and/or stabilization of many of the effector proteins responsible for NER repair of UV-induced lesions and the cellular response to double-strand DNA breaks (3, 39). To determine if the nuclear accumulation of APC was dependent on ATM/ATR kinase activity, synchronized HCT116βw cells were grown in the presence of wortmannin, a widely used G_2/M checkpoint kinase inhibitor (40, 41). In our experiments, wortmannin appeared to have no effect on APC localization in the non-irradiated control cells (Figure 5.15). However, the UV irradiated cells treated with wortmannin showed significantly less nuclear accumulation of APC when compared to cells treated with DMSO only (Figure 5.15). In some experiments wortmannin treatment also resulted in sub-nuclear APC foci in the UV-irradiated cells (Figure 5.15).

ATM and ATR initiate the checkpoint phosphorylation cascade through the signal transducer kinases Chk1 and Chk2 (3). Generally ATM is associated with signal transduction through Chk2 while ATR is associated with signal transduction

through Chk1; however, there is overlap between the functions of these proteins (3). Because wortmannin inhibits the kinase activity of both ATM and ATR, specific inhibitors for Chk1 and Chk2 were used in an attempt to further refine the signaling pathway leading to the nuclear accumulation of APC.

2-(4-(4-Chlorophenoxy)phenyl)-1H-benzimidole-5-carboxamide is a specific inhibitor of Chk2 (42). Cells treated with this Chk2 inhibitor displayed less nuclear accumulation of APC compared to the DMSO treated control cells following exposure to UV light (Figure 5.16). The ATM/Chk2 pathway is predominantly associated with the response to DNA double-strand breaks. This pathway may be responsible for some of the checkpoint response in UV irradiated cells due to some UV-induced double strand breaks as well as "cross-talk" between the two checkpoint kinase pathways. However the primary pathway expected to be induced by UV irradiation is the ATR/Chk1 signal transduction pathway. SB-218078 is a specific inhibitor that blocks the *in vivo* function of Chk1 (43). Surprisingly, when synchronized cells were treated with Chk1 inhibitor they displayed nuclear targeted APC following UV irradiation. Because the ATR/Chk1 pathway responds by initiating NER repair of thymidine dimers, it would be expected that Chk1 would be the primary transducer kinase activated upon detection of UV-induced DNA damage. However, unlike the wortmannin treatment, treatment with Chk1 inhibitor did not appear to inhibit the nuclear accumulation of APC (Figure 5.17).

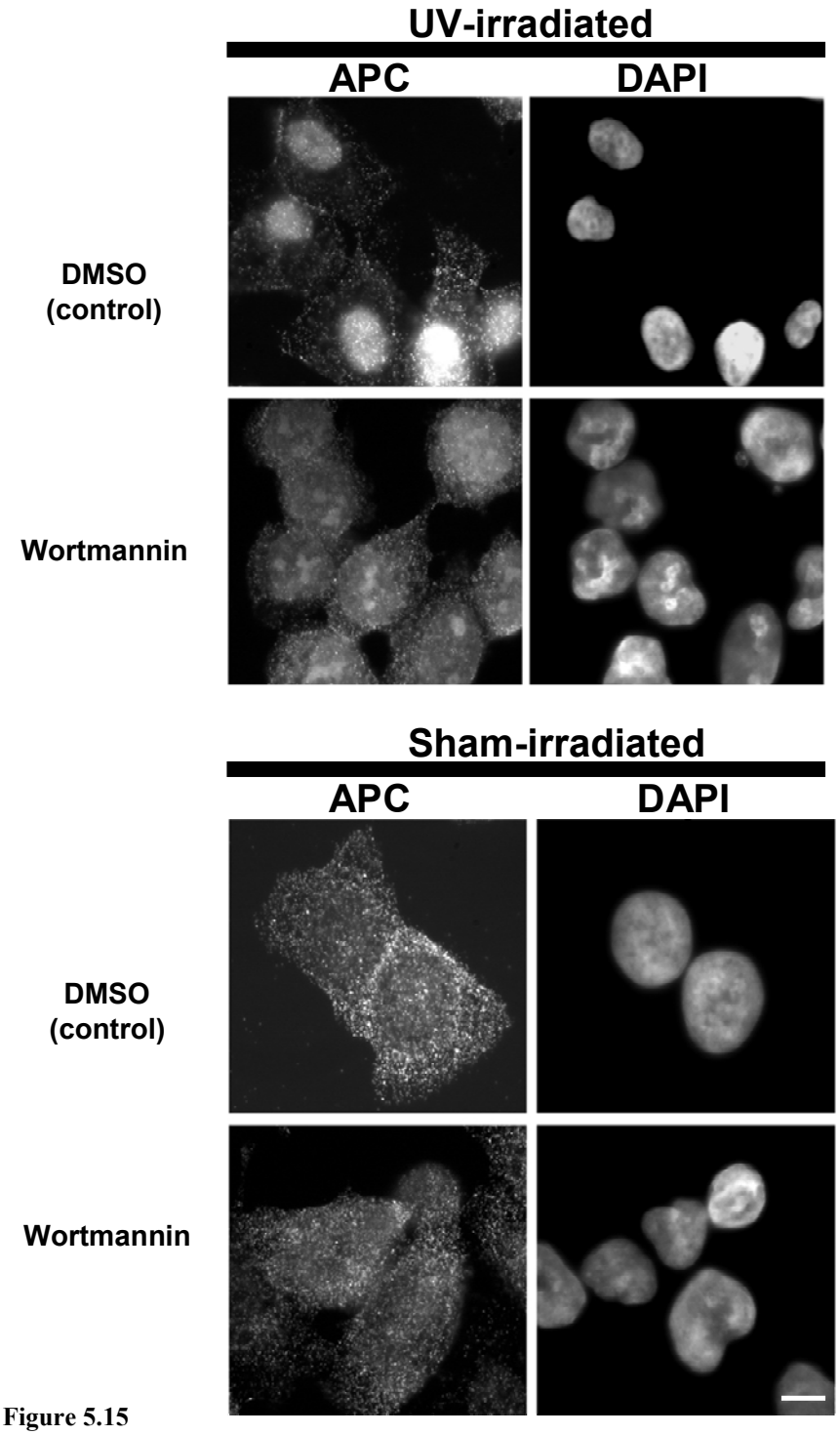

Figure 5.15
Wortmannin (Calbiochem) was used at a final concentration of 20μM to inhibit PI-3-kinases in synchronized HCT116βw cells UV-irradiated or sham-irradiated 4 hours after release from aphidiclolin block. Scale bar = 3μm.

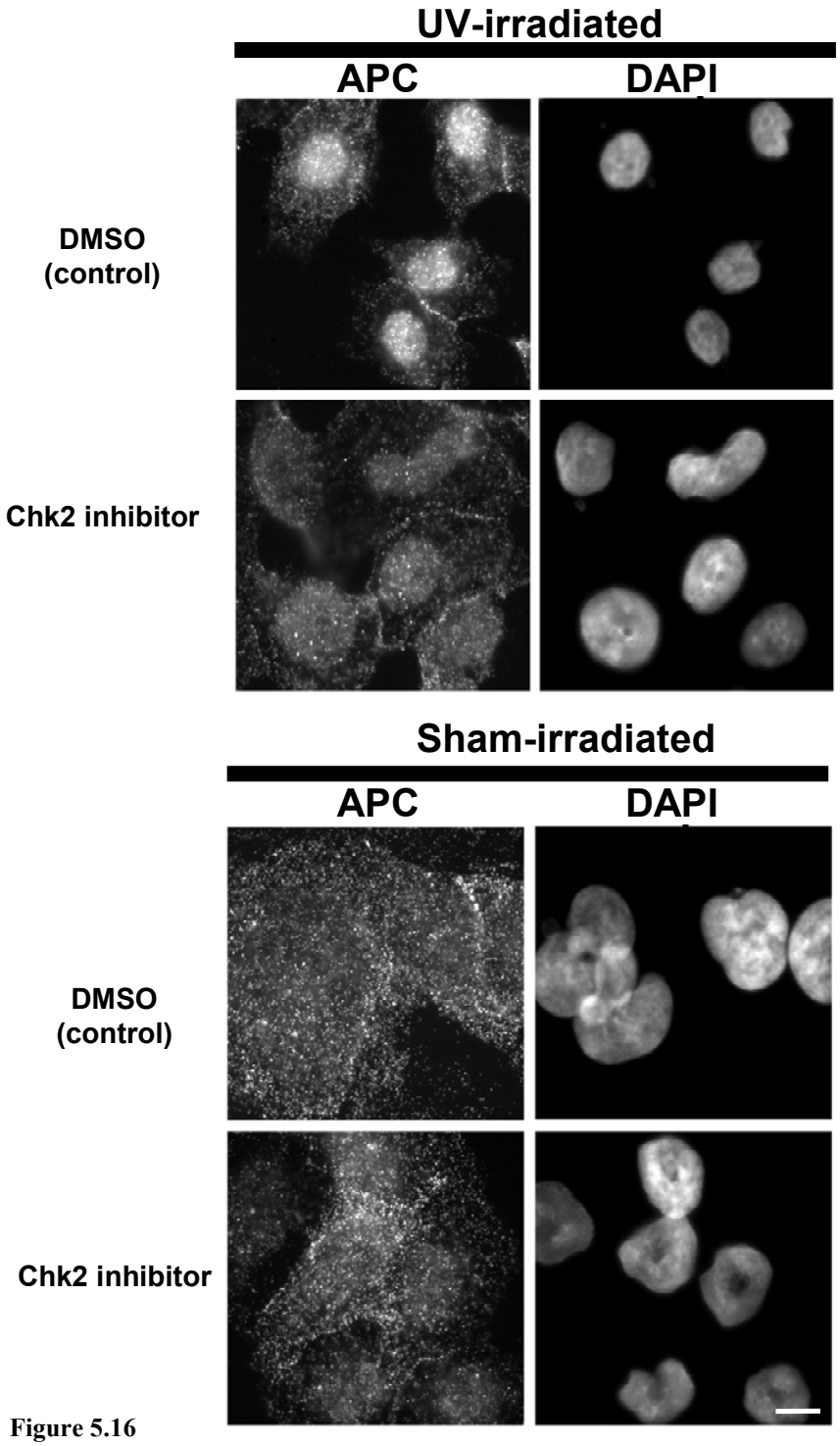

Figure 5.16
Chk 2 inhibitor [2-(4-(4-Chlorophenoxy)phenyl)-1H-benzimidole-5-carboxamide (Calbiochem) was used at 10μM to inhibit Chk 2 in synchronized HCT116βw cells UV-irradiated or sham-irradiated 4 hours after release from aphidicolin block. Scale bar = 3μm

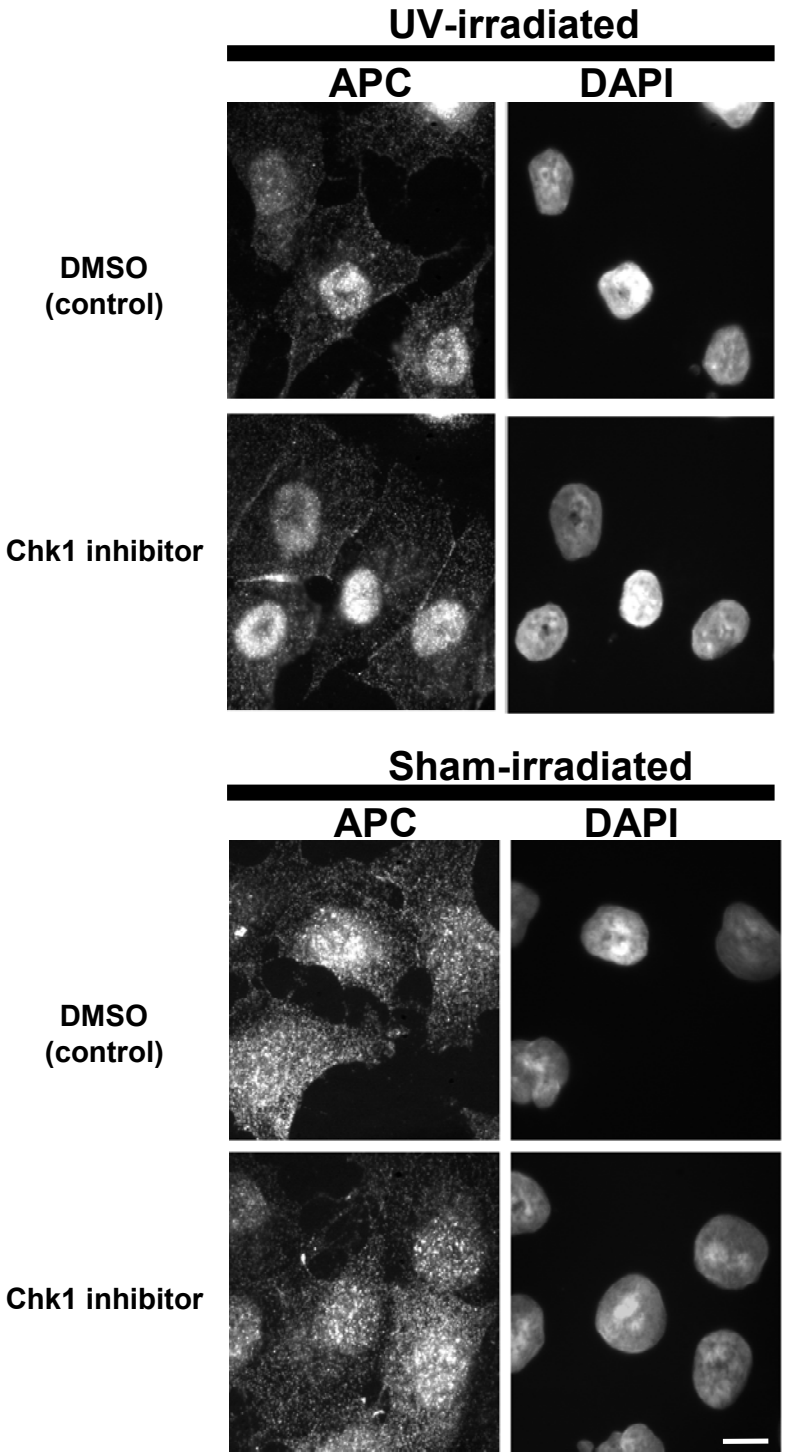

Figure 5.17
Chk 1 inhibitor [SB-218078 (Calbiochem)]was used at 5μM to inhibit Chk 1 in synchronized HCT116βw cells UV-irradiated or sham-irradiated 4 hours after release from aphidicolin block. Scale bar = 3μm.

Discussion

We observed that APC was transiently targeted to the nucleus in what appeared to be a cell cycle specific response to UV irradiation. APC was observed to translocate to the nucleus in response to UV light exposure in both primary mouse fibroblast cells and the human colon cancer cell line HCT116βw. Further evaluation of this phenomenon in the HCT116βw cell line revealed that APC was selectively targeted to the nucleus during the late S and G_2/M phases of the cell cycle, a time point that appeared to roughly correlate with the G_2/M cell cycle checkpoint. The stabilization of endogenous APC in HCT116 cells in response to $ZnCl_2$ has been reported to result in increased arrest at the G_2/M phase of the cell cycle (13). A fragment of APC (amino acids 1000-1326) containing no characterized NLS sequences was observed to localize to the nucleus in HCT116βw cells and over expression of this fragment induced cell cycle arrest at G_2 (14). This evidence suggests a role for APC in cell cycle control and G_2/M transition. It is possible that APC is selectively targeted to the nucleus during this phase of the cell cycle to halt cell cycle progression in response to the detection of DNA damage or the initiation of NER.

The nuclear targeting of APC appears to be dependent on the checkpoint kinases. Inhibition of DNA-PK, ATM and ATR by treatment with wortmannin reduced the nuclear accumulation of APC. Treatment with a specific inhibitor of Chk1 resulted in no visible reduction in nuclear APC following UV-irradiation. Inhibition of Chk2 resulted in some inhibition of the nuclear accumulation of APC,

though not the same degree as treatment with wortmannin. This might suggest that APC is not downstream of Chk1 or Chk2, but instead receives a nuclear targeting signal more directly from the ATM/ATR initiator kinases. The inability of either Chk1 or Chk2 inhibition to fully repress the nuclear accumulation of APC could also mean that there is redundancy between the two pathways and that either Chk1 or Chk2 alone can lead to the nuclear accumulation of APC. Wortmannin would be expected be more effective than either of the specific inhibitors alone because wortmannin is able to repress the upstream activation of both ATM and ATR. Finally, it is the possible that neither ATM nor ATR is upstream of APC, but the more broad-based inhibitor wortmannin prevents the nuclear accumulation of APC through repression of a separate pathway.

The exact nature of APC's role in the G_2/M checkpoint is unclear. It seems likely that APC is acting as a signal transduction molecule rather than an effector molecule based on the transient nature of APC's nuclear translocation. The DNA repair protein xeroderma pigmentosum group A (XPA) is involved in DNA repair after UV irradiation (3). Similar to the observed time course for APC, XPA begins to accumulate in the nucleus approximately 30 minutes after exposure to UV light. However, for XPA, the peak level of nuclear accumulation is reached 8 hours after the initial DNA damage (39). APC was observed to reach its peak level of nuclear accumulation approximately 40 minutes after exposure to UV light and redistributed to the cytoplasm in approximately one hour, suggesting that APC does not directly

participate in the process of sustained DNA repair or in the continued maintenance of the cell cycle block.

Interestingly, β-catenin was also observed to accumulate in the nucleus following UV irradiation with a time table that mirrored those of APC. This was unexpected because β-catenin is considered to be an oncogene. When up-regulated either at the protein level or the level of transcriptional activity, β-catenin is associated with increased cellular proliferation and neoplastic transformation (44). Proteins that are involved in the cellular response to DNA damage are typically tumor suppressors because a loss of function results in a decreased ability to respond to DNA damage and increased tumorigenesis (44). It was surprising to see such a striking β-catenin response to UV irradiation. The nuclear localization of β-catenin has previously been associated with an increase in transcriptional activity from the Wnt target genes and the promotion of cellular proliferation (45). It seemed counterintuitive that β-catenin would be targeted to the nucleus at a time when the cell cycle should be arrested.

The interaction of APC with β-catenin and other members of the Wnt signaling pathway is one of the most investigated areas of APC research. APC is known to directly interact with β-catenin and has been shown to be important for β-catenin degradation (44, 45). APC and β-catenin have been shown to interact at the promoter of Wnt target genes (46) and the nuclear shuttling of APC is suspected to play a role in determining the level of nuclear β-catenin (47-49). Remarkably, despite the observation that APC and β-catenin respond in nearly the same manner to UV-

irradiation, exposure to UV light did not appear to increase interaction between these two proteins (Figure 5.11) nor do they co-localize significantly within the nucleus suggesting that they are both targeted to the nucleus independently.

References

1. Hanahan, D., and Weinberg, R. A. (2000) The hallmarks of cancer. *Cell* 100, 57-70
2. Loeb, L. A. (1991) Mutator phenotype may be required for multistage carcinogenesis. *Cancer Res* 51, 3075-3079
3. Sancar, A., Lindsey-Boltz, L. A., Unsal-Kacmaz, K., and Linn, S. (2004) Molecular mechanisms of mammalian DNA repair and the DNA damage checkpoints. *Annu Rev Biochem* 73, 39-85
4. Alberts, B., Bray, D., Lewis, J., Raff, M., Roberts, K., and Watson, J. D. (1994) *Molecular Biology of the Cell*, Garland Publishing Inc., New York
5. Weinert, T. A., and Hartwell, L. H. (1988) The RAD9 gene controls the cell cycle response to DNA damage in Saccharomyces cerevisiae. *Science* 241, 317-322
6. Schmitt, E., Paquet, C., Beauchemin, M., and Bertrand, R. (2007) DNA-damage response network at the crossroads of cell-cycle checkpoints, cellular senescence and apoptosis. *J Zhejiang Univ Sci B* 8, 377-397
7. Kinsella, T. J., Little, J. B., Nove, J., Weichselbaum, R. R., Li, F. P., Meyer, R. J., Marchetto, D. J., and Patterson, W. B. (1982) Heterogeneous response to X-ray and ultraviolet light irradiations of cultured skin fibroblasts in two families with Gardner's Syndrome. *J Natl Cancer Inst* 68, 697-701
8. Luongo, C., and Dove, W. F. (1996) Somatic genetic events linked to the Apc locus in intestinal adenomas of the Min mouse. *Genes Chromosomes Cancer* 17, 194-198
9. Narayan, S., Jaiswal, A. S., and Balusu, R. (2005) Tumor suppressor APC blocks DNA polymerase beta-dependent strand displacement synthesis during long patch but not short patch base excision repair and increases sensitivity to methylmethane sulfonate. *J Biol Chem* 280, 6942-6949
10. Jaiswal, A. S., Balusu, R., Armas, M. L., Kundu, C. N., and Narayan, S. (2006) Mechanism of Adenomatous Polyposis Coli (APC)-Mediated Blockage of Long-Patch Base Excision Repair. *Biochemistry* 45, 15903-15914
11. Narayan, S., and Jaiswal, A. S. (1997) Activation of adenomatous polyposis coli (APC) gene expression by the DNA-alkylating agent N-methyl-N'-nitro-N-nitrosoguanidine requires p53. *J Biol Chem* 272, 30619-30622

12. Jaiswal, A. S., and Narayan, S. (2001) p53-dependent transcriptional regulation of the APC promoter in colon cancer cells treated with DNA alkylating agents. *J Biol Chem* 276, 18193-18199
13. Jaiswal, A. S., and Narayan, S. (2004) Zinc stabilizes adenomatous polyposis coli (APC) protein levels and induces cell cycle arrest in colon cancer cells. *J Cell Biochem* 93, 345-357
14. Wang, Y., Moore, D., Azuma, Y., and Neufeld, K. L. (Manuscript submitted) Tumor Suppressor APC interacts with Topoisomerase IIα PCNA: Implications for G2/M Transition.
15. Chan, T. A., Wang, Z., Dang, L. H., Vogelstein, B., and Kinzler, K. W. (2002) Targeted inactivation of CTNNB1 reveals unexpected effects of beta-catenin mutation. *Proc Natl Acad Sci U S A* 99, 8265-8270
16. Neufeld, K. L., and White, R. L. (1997) Nuclear and cytoplasmic localizations of the adenomatous polyposis coli protein. *Proc Natl Acad Sci U S A* 94, 3034-3039
17. Ausubel, F. M., Brent, R., Kingston, R. E., Moore, D. D., Seidman, J. G., Smith, J. A., and Struhl, K., eds (1988) *Current Protocols in Molecular Biology* Vol. 1, John Wiley and Sons
18. Sambrook, J., E.F.Fritsch, and Maniatis, T. (1989) *Molecular Cloning: A laboratory manual* Vol. 3, Cold Spring Harbor Laboratory Press, Plainview, NY
19. vom Brocke, J., Schmeiser, H. H., Reinbold, M., and Hollstein, M. (2006) MEF immortalization to investigate the ins and outs of mutagenesis. *Carcinogenesis* 27, 2141-2147
20. Brattain, M. G., Fine, W. D., Khaled, F. M., Thompson, J., and Brattain, D. E. (1981) Heterogeneity of malignant cells from a human colonic carcinoma. *Cancer Res* 41, 1751-1756
21. Kutchera, W., Jones, D. A., Matsunami, N., Groden, J., McIntyre, T. M., Zimmerman, G. A., White, R. L., and Prescott, S. M. (1996) Prostaglandin H synthase 2 is expressed abnormally in human colon cancer: evidence for a transcriptional effect. *Proc Natl Acad Sci U S A* 93, 4816-4820
22. Morin, P. J., Sparks, A. B., Korinek, V., Barker, N., Clevers, H., Vogelstein, B., and Kinzler, K. W. (1997) Activation of beta-catenin-Tcf signaling in colon cancer by mutations in beta-catenin or APC. *Science* 275, 1787-1790
23. Cahill, D. P., Lengauer, C., Yu, J., Riggins, G. J., Willson, J. K., Markowitz, S. D., Kinzler, K. W., and Vogelstein, B. (1998) Mutations of mitotic checkpoint genes in human cancers. *Nature* 392, 300-303
24. Parsons, R., Li, G. M., Longley, M. J., Fang, W. H., Papadopoulos, N., Jen, J., de la Chapelle, A., Kinzler, K. W., Vogelstein, B., and Modrich, P. (1993) Hypermutability and mismatch repair deficiency in RER+ tumor cells. *Cell* 75, 1227-1236
25. Spadari, S., Focher, F., Sala, F., Ciarrocchi, G., Koch, G., Falaschi, A., and Pedrali-Noy, G. (1985) Control of cell division by aphidicolin without adverse effects upon resting cells. *Arzneimittelforschung* 35, 1108-1116

26. Nathke, I. S., Adams, C. L., Polakis, P., Sellin, J. H., and Nelson, W. J. (1996) The adenomatous polyposis coli tumor suppressor protein localizes to plasma membrane sites involved in active cell migration. *J Cell Biol* 134, 165-179
27. Crissman, H. A., and Steinkamp, J. A. (1973) Rapid, simultaneous measurement of DNA, protein, and cell volume in single cells from large mammalian cell populations. *J Cell Biol* 59, 766-771
28. Sharpiro, H. M. (2002) *Practical Flow Cytometry*, John Wiley and Sons, Hoboken, New Jersey
29. Schlenstedt, G. (1996) Protein import into the nucleus. *FEBS Lett* 389, 75-79
30. Neufeld, K. L., Nix, D. A., Bogerd, H., Kang, Y., Beckerle, M. C., Cullen, B. R., and White, R. L. (2000) Adenomatous polyposis coli protein contains two nuclear export signals and shuttles between the nucleus and cytoplasm. *Proc Natl Acad Sci U S A* 97, 12085-12090
31. Zhang, F., White, R. L., and Neufeld, K. L. (2000) Phosphorylation near nuclear localization signal regulates nuclear import of adenomatous polyposis coli protein. *Proc Natl Acad Sci U S A* 97, 12577-12582
32. Miyamoto, Y., Saiwaki, T., Yamashita, J., Yasuda, Y., Kotera, I., Shibata, S., Shigeta, M., Hiraoka, Y., Haraguchi, T., and Yoneda, Y. (2004) Cellular stresses induce the nuclear accumulation of importin alpha and cause a conventional nuclear import block. *J Cell Biol* 165, 617-623
33. Stochaj, U., Rassadi, R., and Chiu, J. (2000) Stress-mediated inhibition of the classical nuclear protein import pathway and nuclear accumulation of the small GTPase Gsp1p. *Faseb J* 14, 2130-2132
34. Chu, A., Matusiewicz, N., and Stochaj, U. (2001) Heat-induced nuclear accumulation of hsc70s is regulated by phosphorylation and inhibited in confluent cells. *Faseb J* 15, 1478-1480
35. Lamian, V., Small, G. M., and Feldherr, C. M. (1996) Evidence for the existence of a novel mechanism for the nuclear import of Hsc70. *Exp Cell Res* 228, 84-91
36. Osborn, A. J., Elledge, S. J., and Zou, L. (2002) Checking on the fork: the DNA-replication stress-response pathway. *Trends Cell Biol* 12, 509-516
37. Fillingham, J., Keogh, M. C., and Krogan, N. J. (2006) GammaH2AX and its role in DNA double-strand break repair. *Biochem Cell Biol* 84, 568-577
38. Zhang, F., White, R. L., and Neufeld, K. L. (2001) Cell density and phosphorylation control the subcellular localization of adenomatous polyposis coli protein. *Mol Cell Biol* 21, 8143-8156
39. Wu, X., Shell, S. M., Liu, Y., and Zou, Y. (2007) ATR-dependent checkpoint modulates XPA nuclear import in response to UV irradiation. *Oncogene* 26, 757-764
40. Collis, S. J., DeWeese, T. L., Jeggo, P. A., and Parker, A. R. (2005) The life and death of DNA-PK. *Oncogene* 24, 949-961
41. Rosenzweig, K. E., Youmell, M. B., Palayoor, S. T., and Price, B. D. (1997) Radiosensitization of human tumor cells by the phosphatidylinositol3-kinase inhibitors wortmannin and LY294002 correlates with inhibition of DNA-

dependent protein kinase and prolonged G2-M delay. *Clin Cancer Res* 3, 1149-1156
42. Arienti, K. L., Brunmark, A., Axe, F. U., McClure, K., Lee, A., Blevitt, J., Neff, D. K., Huang, L., Crawford, S., Pandit, C. R., Karlsson, L., and Breitenbucher, J. G. (2005) Checkpoint kinase inhibitors: SAR and radioprotective properties of a series of 2-arylbenzimidazoles. *J Med Chem* 48, 1873-1885
43. Leung-Pineda, V., Ryan, C. E., and Piwnica-Worms, H. (2006) Phosphorylation of Chk1 by ATR is antagonized by a Chk1-regulated protein phosphatase 2A circuit. *Mol Cell Biol* 26, 7529-7538
44. Giles, R. H., van Es, J. H., and Clevers, H. (2003) Caught up in a Wnt storm: Wnt signaling in cancer. *Biochim Biophys Acta* 1653, 1-24
45. Kolligs, F. T., Bommer, G., and Goke, B. (2002) Wnt/beta-catenin/tcf signaling: a critical pathway in gastrointestinal tumorigenesis. *Digestion* 66, 131-144
46. Sierra, J., Yoshida, T., Joazeiro, C. A., and Jones, K. A. (2006) The APC tumor suppressor counteracts beta-catenin activation and H3K4 methylation at Wnt target genes. *Genes Dev* 20, 586-600
47. Neufeld, K. L., Zhang, F., Cullen, B. R., and White, R. L. (2000) APC-mediated downregulation of beta-catenin activity involves nuclear sequestration and nuclear export. *EMBO Rep* 1, 519-523
48. Henderson, B. R. (2000) Nuclear-cytoplasmic shuttling of APC regulates beta-catenin subcellular localization and turnover. *Nat Cell Biol* 2, 653-660
49. Rosin-Arbesfeld, R., Townsley, F., and Bienz, M. (2000) The APC tumour suppressor has a nuclear export function. *Nature* 406, 1009-1012

CHAPTER 6

DISCUSSION AND FUTURE DIRECTIONS

Numerous reports in the literature suggest that APC can shuttle in and out of the nucleus (1, 2) interact with a variety of nuclear proteins (3, 4), both facilitate and impede DNA repair (5-8), regulate transcription (9), participate in the cell cycle checkpoints (3, 10) and directly interact with DNA itself (11). Taken together these data result in a considerable number of proposed nuclear functions for APC. A great deal more study is required to elucidate the mechanisms by which APC is able to accomplish the current suggested functions and to evaluate how those cellular functions contribute to its role as a tumor suppressor in whole tissue.

To further clarify the role of nuclear APC in tissue, we generated a mouse model lacking the characterized APC NLSs. Multiple existing APC mouse models have demonstrated that both truncation and decreased expression of APC are associated with the development of intestinal adenomas (12-19). However, mutations resulting in altered protein levels or the deletion of substantial regions of APC make it difficult to examine how the various functions of APC are contributing to overall tumor suppression. The APC mNLS mouse model is unique in that a specific aspect of APC was altered, nuclear import through the NLS/importin pathway, while preserving the domains required for APC's other functions.

Targeted mutations were introduced into both NLSs of endogenous *Apc* in mouse ES cells using standard techniques (20-22). These mutations alter a total of 6

amino acids in full length APC and disrupt binding to importin-α (23). Because interaction with importin-α mediates translocation through the nuclear pore, these mutations inhibit the nuclear import of APC (24). Following the identification of an ES cell line with the correct incorporation of the knock-in mutations, an APC mNLS mouse line was generated. Normal levels of full length APC were detected in tissue from the mutant mice, confirming that the introduction of the APC mNLS mutations did not alter normal *Apc* expression. Because genetic background can influence phenotype (25, 26), we are in the process of generating a congenic mouse line. In the interim we began a preliminary analysis on cells carrying the APC mNLS mutations as well as the pre-congenic animals. In addition to variable defects in APC targeting, we also observed subtle defects in β-catenin regulation and immune function in the mutant mice. Further analysis of APC nuclear import in cells carrying mutant and WT APC also revealed a previously uncharacterized response to DNA damage, which resulted in the nuclear accumulation of APC through an unknown import mechanism.

The nuclear import of APC in NLS deficient cells

Surprisingly, our observations revealed that APC was not excluded from the nucleus in APC mNLS$^{-/-}$ cells or in tissue from the APC mNLS$^{-/-}$ mice. Some amount of nuclear APC was observed, regardless of the type of cells being examined. However, the degree of cellular differentiation appeared to influence the extent to which APC targeting was affected. Confocal microscopy of frozen tissue sections revealed that APC distribution in the undifferentiated cells at the base of the crypts in

both the colon and small intestine was nearly identical in the APC mNLS$^{-/-}$, APC mNLS $^{+/-}$ and APC mNLS$^{+/+}$ mice. Similarly the localization of APC in the APC mNLS$^{+/-}$ ES cells was indistinguishable from WT R1 ES cells. In contrast, the APC mNLS MEF cell lines displayed a noticeably decreased level of nuclear APC in the APC mNLS$^{+/-}$, and APC mNLS$^{-/-}$ cells when compared to APC mNLS$^{+/+}$ control cells. A similar observation was made in the intestines of the mNLS mice. The most differentiated cells, located at the luminal surface, displayed a reduced level of nuclear APC in tissue from APC mNLS$^{+/-}$ and APC mNLS$^{-/-}$ mice when compared to tissue from their APC mNLS$^{+/+}$ littermates.

The observation that mutations to the APC mNLSs resulted in a more apparent phenotype in differentiated cells implied that APC targeting may not be regulated in the same manner in differentiated and undifferentiated cells. It is known that APC participates in a number of cellular pathways (27-29). It is probable that APC performs different functions in different cell types. The more surprising observation was that some of APC's nuclear functions, particularly in stem cells, appeared to allow nuclear import of full length APC in the absence of the characterized NLSs.

Regulation of β-catenin in APC mNLS cells

Western immunoblot analysis of β-catenin levels in the intestinal epithelia of the APC mNLS mice revealed an increased level of β-catenin in the APC mNLS$^{+/-}$ and APC mNLS$^{-/-}$ mice compared to their APC mNLS$^{+/+}$ littermates. The observation

that mutation to APC resulted in increased β-catenin levels was not surprising. APC has been previously shown to be important in the regulation of β-catenin (30, 31). While the ability of the NLS-deficient APC to participate in β-catenin down-regulation in the cytoplasm should be unaltered, APC and β-catenin have also been observed to associate in the nucleus (2, 31, 32). Altered nuclear targeting of APC would therefore be expected to impact its interaction with β-catenin. Surprisingly, the observed increase in β-catenin level was not associated with an alteration in the cellular localization of β-catenin. In both the tissue of the APC mNLS mice and in the APC mNLS MEF cell lines, the pattern of β-catenin staining appeared to be identical in the APC mNLS$^{+/+}$, APC mNLS$^{+/-}$ and APC mNLS$^{-/-}$ cells. Traditional dogma assumes that increased β-catenin in the cell results in increased translocation of β-catenin to the nucleus (33). This correlation between total β-catenin levels and localization of β-catenin has also been observed in the previous APC mouse models (16, 34, 35). Our observations suggest that the NLS-deficient APC leads to both an increase in cellular β-catenin levels and a decrease in β-catenin nuclear import.

The obvious initial conclusion would be a role for APC in the nuclear import of β-catenin; however, this explanation contradicts much of the established ideas in the field (33). Another possibility is that APC is targeted to the nucleus to interact with β-catenin via the NLS/importin pathway in differentiated cells. In cells expressing NLS-deficient APC, translocation fails to occur and results in increased APC interacting with β-catenin in the cytoplasm. The number of β-catenin destruction complexes in the cytoplasm is restricted not only by the presence of APC,

but also by the availability of the other members of the protein complex, therefore excess APC in the cytoplasm may not be equivalent to increased β-catenin down-regulation. It is possible that interacting with free APC may prevent β-catenin proteolysis by competing with APC in the β-catenin degradation complexes for cellular β-catenin. The observation that APC shows increased localization to the lateral junctions in cells with reduced nuclear APC seems to support the idea that APC is associating with but not degrading cytoplasmic β-catenin in these cells. Thus the increased levels of β-catenin may result from the presence of excess APC in the cytoplasm rather than from a deficient level of APC in the nucleus.

Immune function in APC mutant mice

The observation that APC mNLS$^{+/-}$ mice display intestinal hyperplastic lymphoid nodules with an increased frequency compared to their APC mNLS$^{+/+}$ littermates suggests that APC may play a role in immune regulation in the intestine. There have also been reports of immune system phenotypes in previous mouse models that express APC mutations (36-39).

The APC 1638N mouse carries a WT *Apc* allele and a truncated *Apc* allele that expresses at only 2% of the WT level (34). Mice that carry the APC 1638N mutation essentially express APC at half the level of a WT mouse. APC 1638N mice display a decreased immune response to *Helicobacter* infection when compared to WT mice (38). Not only did the intestinal tissue of the APC 1638N mice lack the normal local inflammatory and proliferative responses to the bacterial infection, but

the APC mutant animals displayed a decreased systemic antibody response despite demonstrating higher bacterial loads than the WT mice (38).

APC's effect on polyposis and local immune response has also been explored in the APC Min mouse (36, 37, 39). The APC Min mouse displays an extensive polyposis phenotype with numerous intestinal lesions occurring early in the life of the mouse (12). This has made the Min mouse a popular model in which to study the effect of chemotherapeutics, diet and exercise on the process of polyposis in the intestine (40). In two separate reports, diets that stimulate immune function in the intestine also led to decrease in polyp number in the APC Min mice (36, 37).

The observation that the stimulation of an intestinal immune response in the APC Min mice leads to a decrease in polyp number while APC 1638N mutant mice appear to be deficient in their ability to mount a normal immune response in the intestine may initially seem incongruent. It is possible that the dissimilar results stem from the type of *Apc* mutation, and that a reduced level of total APC protein (APC 1638N) affects immune function differently than a truncation of the APC protein (APC Min). However, other factors may also play a role in the divergence of phenotypes, including the timescale of the experiments. APC Min mice begin developing intestinal polyps within 5 weeks of birth and have short lifespans, averaging only 120 days (12). Therefore, the analysis of diet in the APC Min mice takes place within the first 100 days, with mice sacrificed for analysis at 91 (39) and 110 (36) days. The APC 1639N mice do not begin developing polyps until nearly 10 weeks of age and have an average lifespan of over 1 year (13). In the analysis of

Helicobacter infection, the APC 1638N mice were sacrificed at 135, 180 and 225 days of age (38). In the heterozygous APC mNLS we saw an age dependent increase on hyperplastic lymphoid nodules in mice between 294 and 434 days of age.

Observations in the APC 1638N mouse suggest that decreased APC results in decreased immune function both in the intestine and systemically (38). Observations in the APC Min mouse suggest that immune stimulation represses intestinal polyposis (36, 37, 39). There was no polyposis phenotype observed in the APC mNLS mouse; however, an increase in immune tissue was detected in the older mice. This could suggest that the inhibition of the nuclear targeting of APC enhances immune stimulation. Alternatively, the presence of the correct level of full length APC may allow for normal immune function in the APC mNLS mice and the increase in localized immune tissue could be in response to the need to prevent the growth of pre-neoplastic cells in the mutant mice. It will be interesting to see if the APC mNLS mice displayed an enhanced polyposis phenotype in immune-deficient mice.

The nuclear accumulation of APC in response to UV light

A transient nuclear accumulation of APC was observed in cells exposed to UV light, suggesting a previously uncharacterized role for APC in the cellular response to DNA damage. Previous reports indicate that cell stress, including UV irradiation, induced the blockage of classic nuclear import by sequestering importin-α (41). These data led to the suggestion that the UV-dependent nuclear targeting of APC occurs through an NLS/importin-α-independent pathway. The observation that

UV irradiation induced the nuclear accumulation of APC in APC mNLS$^{-/-}$ MEF cells lends further support to an alternative pathway for APC nuclear import.

Cell-stress induced block of nuclear import has been observed in response to starvation, heat shock, ethanol, oxidative stress, and UV irradiation (41-43). Different cellular stresses also induce the nuclear localization of specific stress-response proteins including heat shock proteins and cognate proteins, transcription factors and DNA repair proteins (42-46). While the mechanism of import has not been evaluated in all cases, there is evidence for NLS/importin-independent nuclear import of several proteins characterized to have vital nuclear functions (46-48). The pathway by which this import occurs is currently unknown (47, 49).

Our evidence suggests that APC is also able to achieve nuclear import through an unknown importin-α-independent pathway. APC nuclear import is specific to cell cycle stage and time following UV irradiation, suggesting that post-translational modification to APC is contributing to this nuclear import. Because inhibition of the PI-3-K family of serine/threonine kinases is able to repress nuclear accumulation of APC, it is likely that the signal cascade initiated by DNA damage is responsible for APC re-localization following UV irradiation. Further study is needed to elucidate the mechanism underlying nuclear import of APC and the role for nuclear APC following UV irradiation

Future directions

We have provided evidence for nuclear import of APC through at least two independent pathways. It is possible that more pathways exist, since undifferentiated cells were able to import full length APC under normal cellular conditions in the absence of the endogenous APC NLSs. While the NLS-independent mechanism(s) that allow for nuclear import are currently uncharacterized, it is probable that both NLS- dependent and NLS-independent nuclear import are required for tumor suppression. APC has been observed to shuttle in and out of the nucleus in cancer cell lines containing a truncated APC lacking the NLSs (50), suggesting the presence of an alternative nuclear import pathway mediated by an N-terminal domain of APC. However, the function of the APC NLSs has also been characterized in cancer cell lines (23). Nuclear exclusion of full-length exogenous APC with mutant NLSs was observed in the SW480 human colon cancer cell line while WT APC appeared to shuttle normally (31). These observations suggest that NLS-dependent nuclear import is also required in these cells. Because the nuclear functions of APC are not yet defined, it is unknown if these independent nuclear import mechanisms serve a redundant function or if they represent separate cellular pathways leading to discrete nuclear tasks. The APC mNLS mouse was generated to allow the further evaluation of the role of nuclear APC in tissue development, maintenance and tumor suppression. The APC mNLS mouse model may also be useful in the evaluation of alternative import mechanisms required for proper APC shuttling.

References

1. Neufeld, K. L., and White, R. L. (1997) Nuclear and cytoplasmic localizations of the adenomatous polyposis coli protein. *Proc Natl Acad Sci U S A* 94, 3034-3039
2. Henderson, B. R. (2000) Nuclear-cytoplasmic shuttling of APC regulates beta-catenin subcellular localization and turnover. *Nat Cell Biol* 2, 653-660
3. Wang, Y., Moore, D., Azuma, Y., and Neufeld, K. L. (Manuscript submitted) Tumor Suppressor APC interacts with Topoisomerase IIα PCNA: Implications for G2/M Transition.
4. Catimel, B., Rothacker, J., Catimel, J., Faux, M., Ross, J., Connolly, L., Clippingdale, A., Burgess, A. W., and Nice, E. (2005) Biosensor-based micro-affinity purification for the proteomic analysis of protein complexes. *J Proteome Res* 4, 1646-1656
5. Kinsella, T. J., Little, J. B., Nove, J., Weichselbaum, R. R., Li, F. P., Meyer, R. J., Marchetto, D. J., and Patterson, W. B. (1982) Heterogeneous response to X-ray and ultraviolet light irradiations of cultured skin fibroblasts in two families with Gardner's Syndrome. *J Natl Cancer Inst* 68, 697-701
6. Luongo, C., and Dove, W. F. (1996) Somatic genetic events linked to the Apc locus in intestinal adenomas of the Min mouse. *Genes Chromosomes Cancer* 17, 194-198
7. Narayan, S., Jaiswal, A. S., and Balusu, R. (2005) Tumor suppressor APC blocks DNA polymerase beta-dependent strand displacement synthesis during long patch but not short patch base excision repair and increases sensitivity to methylmethane sulfonate. *J Biol Chem* 280, 6942-6949
8. Jaiswal, A. S., Balusu, R., Armas, M. L., Kundu, C. N., and Narayan, S. (2006) Mechanism of Adenomatous Polyposis Coli (APC)-Mediated Blockage of Long-Patch Base Excision Repair. *Biochemistry* 45, 15903-15914
9. Sierra, J., Yoshida, T., Joazeiro, C. A., and Jones, K. A. (2006) The APC tumor suppressor counteracts beta-catenin activation and H3K4 methylation at Wnt target genes. *Genes Dev* 20, 586-600
10. Jaiswal, A. S., and Narayan, S. (2004) Zinc stabilizes adenomatous polyposis coli (APC) protein levels and induces cell cycle arrest in colon cancer cells. *J Cell Biochem* 93, 345-357
11. Deka, J., Herter, P., Sprenger-Haussels, M., Koosch, S., Franz, D., Muller, K. M., Kuhnen, C., Hoffmann, I., and Muller, O. (1999) The APC protein binds to A/T rich DNA sequences. *Oncogene* 18, 5654-5661
12. Moser, A. R., Pitot, H. C., and Dove, W. F. (1990) A dominant mutation that predisposes to multiple intestinal neoplasia in the mouse. *Science* 247, 322-324
13. Fodde, R., Edelmann, W., Yang, K., van Leeuwen, C., Carlson, C., Renault, B., Breukel, C., Alt, E., Lipkin, M., Khan, P. M., and et al. (1994) A targeted chain-termination mutation in the mouse Apc gene results in multiple intestinal tumors. *Proc Natl Acad Sci U S A* 91, 8969-8973

14. Oshima, M., Oshima, H., Kitagawa, K., Kobayashi, M., Itakura, C., and Taketo, M. (1995) Loss of Apc heterozygosity and abnormal tissue building in nascent intestinal polyps in mice carrying a truncated Apc gene. *Proc Natl Acad Sci U S A* 92, 4482-4486
15. Itoh, M., Maeno, A., Tari, A., Itoh, S., Kawakami, A., Sawada, M., Ohno, T., and Noda, T. (2000) Genetic Analysis of Modifier Genes which Influence the Tumor Multiplicity in FAP Model Mice. In The 14th International Mouse Genome Confrence
16. Colnot, S., Niwa-Kawakita, M., Hamard, G., Godard, C., Le Plenier, S., Houbron, C., Romagnolo, B., Berrebi, D., Giovannini, M., and Perret, C. (2004) Colorectal cancers in a new mouse model of familial adenomatous polyposis: influence of genetic and environmental modifiers. *Lab Invest* 84, 1619-1630
17. Sasai, H., Masaki, M., and Wakitani, K. (2000) Suppression of polypogenesis in a new mouse strain with a truncated Apc(Delta474) by a novel COX-2 inhibitor, JTE-522. *Carcinogenesis* 21, 953-958
18. Ishikawa, T. O., Tamai, Y., Li, Q., Oshima, M., and Taketo, M. M. (2003) Requirement for tumor suppressor Apc in the morphogenesis of anterior and ventral mouse embryo. *Dev Biol* 253, 230-246
19. Li, Q., Ishikawa, T. O., Oshima, M., and Taketo, M. M. (2005) The threshold level of adenomatous polyposis coli protein for mouse intestinal tumorigenesis. *Cancer Res* 65, 8622-8627
20. Thomas, K. R., and Capecchi, M. R. (1987) Site-directed mutagenesis by gene targeting in mouse embryo-derived stem cells. *Cell* 51, 503-512
21. Mansour, S. L., Thomas, K. R., and Capecchi, M. R. (1988) Disruption of the proto-oncogene int-2 in mouse embryo-derived stem cells: a general strategy for targeting mutations to non-selectable genes. *Nature* 336, 348-352
22. Bunting, M., Bernstein, K. E., Greer, J. M., Capecchi, M. R., and Thomas, K. R. (1999) Targeting genes for self-excision in the germ line. *Genes Dev* 13, 1524-1528
23. Zhang, F., White, R. L., and Neufeld, K. L. (2000) Phosphorylation near nuclear localization signal regulates nuclear import of adenomatous polyposis coli protein. *Proc Natl Acad Sci U S A* 97, 12577-12582
24. Schlenstedt, G. (1996) Protein import into the nucleus. *FEBS Lett* 389, 75-79
25. Papaioannou, V. E., and Behringer, R. R. (2005) *Mouse Phenotypes: A handbook of mutation analysis*, Cold Spring Harbor Laboratory Press, New York
26. Shoemaker, A. R., Moser, A. R., Midgley, C. A., Clipson, L., Newton, M. A., and Dove, W. F. (1998) A resistant genetic background leading to incomplete penetrance of intestinal neoplasia and reduced loss of heterozygosity in ApcMin/+ mice. *Proc Natl Acad Sci U S A* 95, 10826-10831
27. Senda, T., Iizuka-Kogo, A., Onouchi, T., and Shimomura, A. (2007) Adenomatous polyposis coli (APC) plays multiple roles in the intestinal and colorectal epithelia. *Med Mol Morphol* 40, 68-81

28. Aoki, K., and Taketo, M. M. (2007) Adenomatous polyposis coli (APC): a multi-functional tumor suppressor gene. *J Cell Sci* 120, 3327-3335
29. Hanson, C. A., and Miller, J. R. (2005) Non-traditional roles for the Adenomatous Polyposis Coli (APC) tumor suppressor protein. *Gene* 361, 1-12
30. Behrens, J., Jerchow, B. A., Wurtele, M., Grimm, J., Asbrand, C., Wirtz, R., Kuhl, M., Wedlich, D., and Birchmeier, W. (1998) Functional interaction of an axin homolog, conductin, with beta-catenin, APC, and GSK3beta. *Science* 280, 596-599
31. Neufeld, K. L., Zhang, F., Cullen, B. R., and White, R. L. (2000) APC-mediated downregulation of beta-catenin activity involves nuclear sequestration and nuclear export. *EMBO Rep* 1, 519-523
32. Rosin-Arbesfeld, R., Townsley, F., and Bienz, M. (2000) The APC tumour suppressor has a nuclear export function. *Nature* 406, 1009-1012
33. Kolligs, F. T., Bommer, G., and Goke, B. (2002) Wnt/beta-catenin/tcf signaling: a critical pathway in gastrointestinal tumorigenesis. *Digestion* 66, 131-144
34. Kielman, M. F., Rindapaa, M., Gaspar, C., van Poppel, N., Breukel, C., van Leeuwen, S., Taketo, M. M., Roberts, S., Smits, R., and Fodde, R. (2002) Apc modulates embryonic stem-cell differentiation by controlling the dosage of beta-catenin signaling. *Nat Genet* 32, 594-605
35. Sansom, O. J., Reed, K. R., Hayes, A. J., Ireland, H., Brinkmann, H., Newton, I. P., Batlle, E., Simon-Assmann, P., Clevers, H., Nathke, I. S., Clarke, A. R., and Winton, D. J. (2004) Loss of Apc in vivo immediately perturbs Wnt signaling, differentiation, and migration. *Genes Dev* 18, 1385-1390
36. Churchill, M., Chadburn, A., Bilinski, R. T., and Bertagnolli, M. M. (2000) Inhibition of intestinal tumors by curcumin is associated with changes in the intestinal immune cell profile. *J Surg Res* 89, 169-175
37. Pierre, F., Perrin, P., Bassonga, E., Bornet, F., Meflah, K., and Menanteau, J. (1999) T cell status influences colon tumor occurrence in min mice fed short chain fructo-oligosaccharides as a diet supplement. *Carcinogenesis* 20, 1953-1956
38. Fox, J. G., Dangler, C. A., Whary, M. T., Edelman, W., Kucherlapati, R., and Wang, T. C. (1997) Mice carrying a truncated Apc gene have diminished gastric epithelial proliferation, gastric inflammation, and humoral immunity in response to Helicobacter felis infection. *Cancer Res* 57, 3972-3978
39. Pierre, F., Perrin, P., Champ, M., Bornet, F., Meflah, K., and Menanteau, J. (1997) Short-chain fructo-oligosaccharides reduce the occurrence of colon tumors and develop gut-associated lymphoid tissue in Min mice. *Cancer Res* 57, 225-228
40. Corpet, D. E., and Pierre, F. (2003) Point: From animal models to prevention of colon cancer. Systematic review of chemoprevention in min mice and choice of the model system. *Cancer Epidemiol Biomarkers Prev* 12, 391-400
41. Miyamoto, Y., Saiwaki, T., Yamashita, J., Yasuda, Y., Kotera, I., Shibata, S., Shigeta, M., Hiraoka, Y., Haraguchi, T., and Yoneda, Y. (2004) Cellular

stresses induce the nuclear accumulation of importin alpha and cause a conventional nuclear import block. *J Cell Biol* 165, 617-623
42. Gorner, W., Durchschlag, E., Martinez-Pastor, M. T., Estruch, F., Ammerer, G., Hamilton, B., Ruis, H., and Schuller, C. (1998) Nuclear localization of the C2H2 zinc finger protein Msn2p is regulated by stress and protein kinase A activity. *Genes Dev* 12, 586-597
43. Stochaj, U., Rassadi, R., and Chiu, J. (2000) Stress-mediated inhibition of the classical nuclear protein import pathway and nuclear accumulation of the small GTPase Gsp1p. *Faseb J* 14, 2130-2132
44. Wu, X., Shell, S. M., Liu, Y., and Zou, Y. (2007) ATR-dependent checkpoint modulates XPA nuclear import in response to UV irradiation. *Oncogene* 26, 757-764
45. Kuge, S., Jones, N., and Nomoto, A. (1997) Regulation of yAP-1 nuclear localization in response to oxidative stress. *Embo J* 16, 1710-1720
46. Lamian, V., Small, G. M., and Feldherr, C. M. (1996) Evidence for the existence of a novel mechanism for the nuclear import of Hsc70. *Exp Cell Res* 228, 84-91
47. Siomi, H., and Dreyfuss, G. (1995) A nuclear localization domain in the hnRNP A1 protein. *J Cell Biol* 129, 551-560
48. Smith, M. R., and Greene, W. C. (1992) Characterization of a novel nuclear localization signal in the HTLV-I tax transactivator protein. *Virology* 187, 316-320
49. Tsukahara, F., and Maru, Y. (2004) Identification of novel nuclear export and nuclear localization-related signals in human heat shock cognate protein 70. *J Biol Chem* 279, 8867-8872
50. Fagman, H., Larsson, F., Arvidsson, Y., Meuller, J., Nordling, M., Martinsson, T., Helmbrecht, K., Brabant, G., and Nilsson, M. (2003) Nuclear accumulation of full-length and truncated adenomatous polyposis coli protein in tumor cells depends on proliferation. *Oncogene* 22, 6013-6022